Sadiq Abdullahi Yelwa
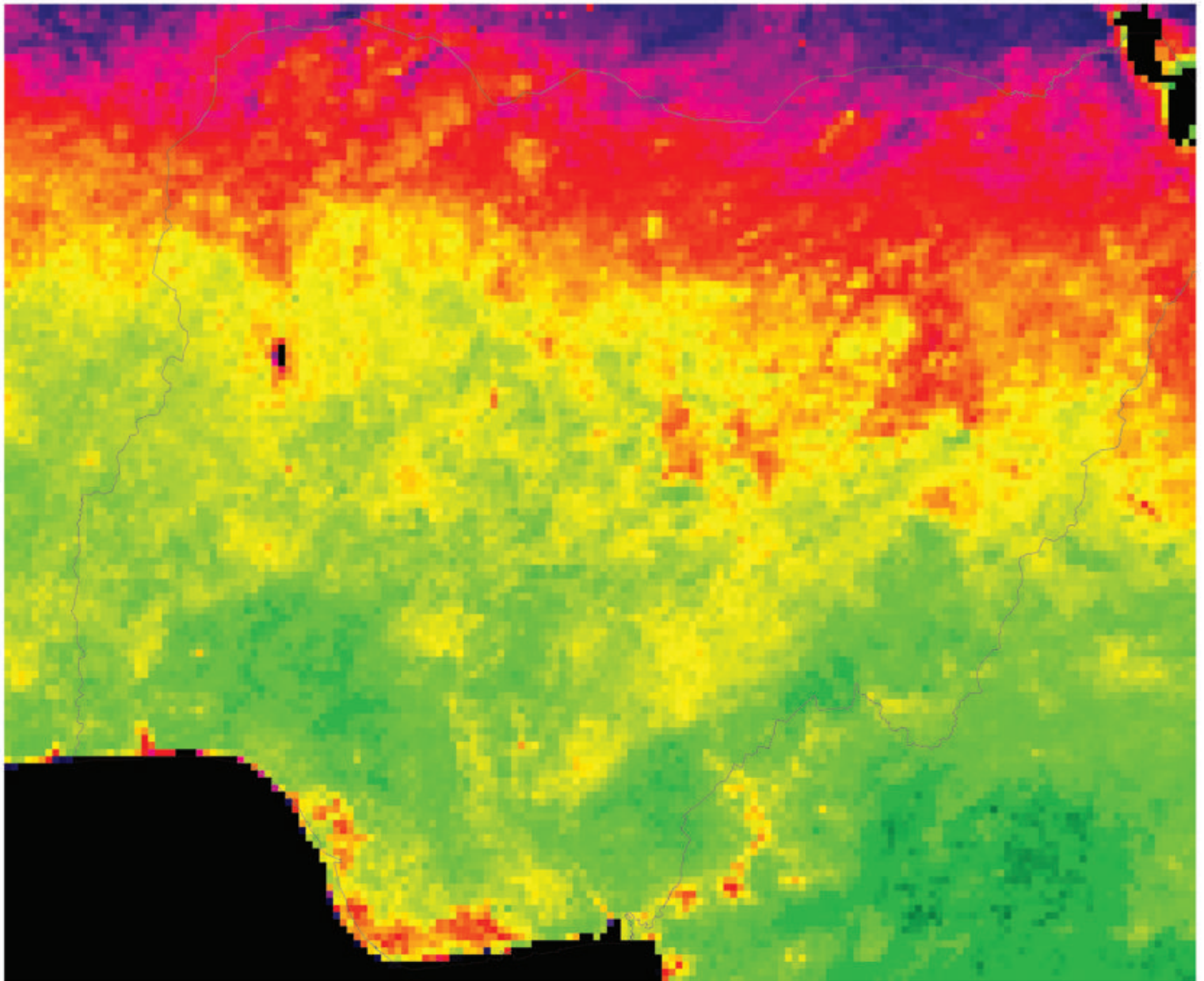
Broadscale Vegetation Change Assessment across Nigeria from Coarse Spatial and High Temporal Resolution AVHRR Data

Cuvillier Verlag Göttingen

Sadiq Abdullahi Yelwa

Broadscale Vegetation Change Assessment across Nigeria from Coarse Spatial and High Temporal Resolution AVHRR Data

Cuvillier Verlag Göttingen

SUPERVISORS AND EXAMINERS

Main Supervisor :   Dr. Patrick Osborne
Second Supervisor: Dr. Andrew Tyler

External Examiner: Prof. Andrew Millington
Internal Examiner: Sandra Winterbottom

DEDICATION

This Book is dedicated to all members of Alhaji Abdullahi Na-jijima family, living or deceased

ACKNOWLEDGMENTS

CONTENTS

INDEX TO FIGURES

INDEX TO TABLES

INDEX TO ACRONYMS

ASCII	American Standard Code for Information Interchange
AVHRR	Advanced Very High Resolution Radiometer
BIL	Band Interleave-by-Line
BISE	Best Index Slope Extraction
BSQ	Band Sequential
CBPP	Contagious Bovine Pleuropneumonia
CLAVR	Cloud Flag
CONCAT	Concatenation
CV	Coefficient of Variation
DAAC	Distributed Active Archive Center
DEM	Digital Elevation Model
DFRRI	Directorate of Food, Roads and Rural Infrastructure
EMS	Electromagnetic Spectrum
ENSO	El-Niňo /Southern Oscillations
ERDAS	Earth Resources Data Analysis System
EROS	Earth Resources Observation System
GAC	Global Area Coverage
GCP	Ground Control Point
GDP	Gross Domestic Product
GIMMS	Global Inventory Monitoring and Modelling Studies
GPS	Global Positional System
GIS	Geographical Information System
GNP	Gross National Product
GPCC	Global Precipitation and Climatology Centre
GSFC	Goddard Space Flight Center
GTOPO30	Global Topographic Database or Global Digital Elevation Model
GVI	Global Vegetation Index
HANTS	Harmonic Analysis of Time Series
HDF	Hierarchical Data Format
ISODATA	Iterative Self-Organising Data Analysis Technique
ITCZ	Inter Tropical Convergence Zone
LAC	Local Area Coverage
LAI	Leaf Area Index
MSS	Landsat Multi Spectral Scanner
MVC	Maximum Value Composite
NASA	National Aeronautics and Space Administration
NDVI	Normalised Difference Vegetation Index
NCDC	National Climatic Data Centre
NCP	National Climatology Center
NCSA	National Centre for Supercomputing Applications
NOAA	National Oceanic Atmospheric Administration
NPP	Net Primary Production
PAL	Pathfinder Land
PCA	Principal Component Analysis

RMSE	Root Mean Square Error
RS	Remote Sensing
SID	Simple Image Differencing
SCR	Slope of Change from Regression
SPOT	Systeme Pour l'Observation de la Terre
SEE	Standard Error of Estimate
SZA	Solar Zenith Angle
TM	Landsat Thematic Mapper
USGS	United States Geological Survey
UNCED	United Nations Conference on Environment and Development
WHO	World Health Organisation
WMOI	World Meteorological Organisation Information

ABSTRACT

Nigeria's vast land area is mostly covered with natural vegetation. The vegetation cover is wide-ranging and reflects past and present climatic variations. Nigeria's vegetation cover is rapidly changing due to natural and anthropogenic influences. Nigeria's population growth rate is one of the highest in the world, where a large proportion of this population are peasant farmers exploiting the rural environment. Previous studies have shown that vegetation cover in some parts of Nigeria is fast declining. The report on the implementation of Agenda 21 (UNCED, 1997) of the United Nations Commission Conference on Environment and Development (UNCED, 1992), which is a long-term global action plan for sustainable development, reported that there is still a persistent decline in the general vegetation cover across Nigeria due to population pressure, overgrazing and continuous exploitation of marginal lands for various purposes. It therefore suggests that periodic assessment and management of this vegetation cover for ecological sustainability would be highly desirable.

With barely $280 GNP per capita and accumulated foreign debts of over US$28 billion, a cost-effective approach to resource management and monitoring could be appropriate. This study employs the use of coarse spatial but high temporal resolution Advanced Very High Resolution Radiometer-Normalised Difference Vegetation Index (AVHRR-NDVI) data from the Pathfinder Land (PAL) dataset to identify and evaluate vegetation cover change. This data is administered by the National Oceanic Atmospheric Administration and National Aeronautics Space Administration (NOAA/NASA) and is, most importantly, freely available. The datasets used were recomposed into monthly Maximum Value (MVC) and annual mean composites in order to assess broadly the changes in vegetation cover across the whole of Nigeria. One hundred and twenty annual gridded point precipitation data for 12 years at 1° resolution covering the whole country were acquired from the Global Precipitation and Climatology Centre (GPCC), and were regressed linearly as a function of 13 other variables in order to create models for estimating spatial rainfall data for the whole country.

The estimated rainfall data was used together with the NDVI data to assess broad changes in vegetation cover across the country. Three change detection techniques were used in the investigation: Simple Image Differencing (SID), Slope of Change from Regression (SCR) and Principal Component Analysis (PCA). The results show that the simple image differencing technique can easily be used to identify broad areas of changes in vegetation cover attributable to climate or other influences in both absolute and relative terms, periodically across the country though they may be affected by the choice of start and end dates. The Slope of Change from Regression technique can be used firstly to isolate long term decline in vegetation cover and secondly the result can be used together with rainfall data to isolate areas that decline in vegetation cover across the country as a result of non-climatic influences. This approach was also useful in checking data quality. Problems in the PAL data set and image calibration were identified. The PCA, using the standardised principal components on the other hand, was able to identify spatial change patterns across the country as a result of seasonal trends. Other spatial change patterns detected by PCA are those that relate to the El-Niňo/Southern Oscillation (ENSO) phenomenon due to particular climatic processes and other artefacts that emanated from satellite and remote sensing mechanisms based on a complex decomposition of time series NDVI data.

This investigation has shown that there is great potential in using coarse spatial and high temporal resolutions NDVI data for consistent monitoring of vegetation cover across any country at regular intervals, especially for countries with very low economic standing like Nigeria. Results derived from the study can serve as a base for further study of vulnerable areas using high spatial resolution satellite imagery.

CHAPTER ONE

INTRODUCTION

1.1   An Overview of the Study

Nigeria has a vast land area covering 923,768 square kilometres. This land area contains a wide range of natural resources, and in particular, vegetation. The vegetation cover of Nigeria reflects past and present climatic variations (Areola, 1982) and is made up of secondary re-growths which over the years have been influenced by both natural and human activities (Badejo, 1998; Cline-Cole, 1998; Salami, 1999). From earlier studies (Soussan and Millington, 1982) it was shown that the general vegetation cover of Nigeria, particularly forest areas, had an annual deforestation rate of 5% per annum of its closed forests. This is one of the highest in the world. However, rapid population growth and demands for economic development on a relatively natural, and in some areas, undisturbed vegetation which is not properly managed can also lead to permanent conversion of most vegetated areas to other forms of landuse such as agriculture and housing in Nigeria.

The report on the implementation of Agenda 21 (UNCED, 1997) of the United Nations Commission Conference on Environment and Development (UNCED, 1992), which is a long-term global action plan for sustainable development, indicated that there is still a persistent decline in the general vegetation cover across Nigeria due to population pressure, overgrazing and continuous exploitation of marginal lands for various purposes. It therefore suggests that periodic assessment and management of vegetation cover for ecological sustainability would be highly desirable.

As a country with a population of over 88 million and a growth rate of 3 % per annum according to the 1990 census, where the majority of this population are peasant farmers, population pressure is most likely to have an impact on the general vegetation cover.

Koop and Tole (2001) assert that 'An important factor that influences a country's environment development trajectory is the extent to which economic expansion alleviates poverty pressures on the environment and promotes environmental awareness'. In the context of the degrading vegetal cover across Nigeria, poverty pressures on the environment are on the increase and the promotion of environmental awareness is not well established at present.

Mapping the distribution of landcover across large areas like Nigeria is said to be a prerequisite for informed natural resources management (Rogers *et al*, 1997). Vegetation is one such important natural resource which requires timely and effective monitoring for ecological sustainability. The coverage of topographic maps in Nigeria is very heterogeneous and mostly outdated (Balogun, 1985; Nsofor, 1998). If most of these topographical maps are produced regularly they can be used on a provisional basis to assess planimetrically where vegetation cover, particularly forest areas across the country, has changed.

Satellite data can be very useful in assessing any changes in vegetation cover across Nigeria because of its repetitive coverage. However, as a country with a GNP as low as US$280 and accumulated debts of over US$28 billion (World Bank, 1999) there are limits to what Nigeria can afford. Data acquired by the Advanced Very High Resolution Radiometer (AVHRR) on board the National Oceanic Atmospheric Administration's

(NOAA) Meteorological satellites can be obtained free (in contrast to other satellite data such as Systeme pour l'Observation de la Terre (SPOT), Landsat Multispectral Scanner (MSS) or Thematic Mapper (TM)) and it has high temporal resolution.

It is in the light of the Agenda 21 report regarding the persistent decline in vegetation cover across Nigeria (UNCED, 1997), the need for periodic monitoring and taking into account its economic status the feasibility of utilising the NOAA/NASA Pathfinder Land (PAL) dataset from AVHRR forms the basis of this investigation to assess changes in vegetation and land cover across the whole of Nigeria.

1.2   The Aim of the Study

This investigation is on the use of coarse spatial but high temporal resolutions AVHRR-NDVI data to assess temporal changes in vegetation cover across Nigeria with the following   objectives :

The Main Research Objectives

The objectives were to :

1.   Assess temporal changes in vegetation cover in absolute and relative terms across Nigeria from multi-temporal NDVI data.

2.   Develop a spatial model of precipitation for Nigeria based on coarse resolution rainfall estimates and other environmental variables.

3.   Use the modelled rainfall data and the NDVI data-set to identify and explain areas of change in vegetation and land-cover across Nigeria.

Because there is no systematic monitoring of vegetation cover across the whole of Nigeria this would provide provisional information for the potential use of the multi temporal NDVI PAL dataset periodically. Where necessary, further assessment can be undertaken based on the results obtained by using a small number of high spatial resolution satellite imageries covering specific areas.

1.3 Rationale for the Study

This study was undertaken against the background of different types of land cover changes across Nigeria by many studies that used high spatial resolution data such as aerial photographs, SPOT, Landsat imageries and environmental data (Adams, 1985; Adeniyi, 1980; Adeniyi, 1985; Schneider *et al,* 1985; Adejuwon and Adesina, 1988; Adams and Thomas, 1996; Badejo, 1998; Ite and Adams, 1998; Salami, 1999; Boele *et al,* 2001a; Boele *et al,* 2001b), and the report on Nigeria on the implementation of Agenda 21 by the United Nations (UNCED, 1997). This is to see if results from these investigations can further be verified or modified using very coarse spatial resolution data from AVHRR.

Studies which utilised NDVI data from AVHRR (eg Tucker *et al,* 1985; Justice *et al,* 1986; Townshend *et al,* 1987; Prince and Justice, 1991; Tucker *et al,* 1991a; Millington *et al,* 1994;) have shown that NDVI data can provide an effective measure of photosynthetically active biomass. This is because of the degree of absorption by chlorophyll in the visible red wavelengths, which is proportional to leaf chlorophyll density, and by the reflectance of near infrared wavelengths, which is proportional to green leaf density.

The study conducted by Malo and Nicholson (1990) on rainfall and vegetation dynamics in African sahel indicated that there is a strong linear relationship between NDVI and rainfall. Other studies (eg Eastman and Fulk, 1993) have shown that on a continental scale, Principal Component Analysis (PCA) has the potential for analysing time-series NDVI data of 10 minutes resolution from AVHRR, with the possibility of extracting and analysing climatic trends and other influences such as satellite anomalies from complex vegetation responses. Anyamba and Eastman (1996) have shown that there is a relationship between the interannual variability of NDVI and the El-Niňo/ Southern Oscillation (ENSO) over the whole of Africa using a 30 km resolution NDVI data. Young and Wang (2001) have utilised the 8 km AVHRR NDVI data from the PAL dataset using a combination of simple image differencing and PCA techniques to assess vegetation dynamics successfully over the whole of China.

From studies with NDVI data derived from AVHRR (Rogers, 1991; Rogers *et al,* 1996; Hay *et al,* 1997; Linthicum *et al,* 1999), it was shown that such data can be used in epidemiological studies and mapping of vector diseases especially in Africa where the resources available to deal with disease problems are not readily available. From recent studies linked to climate variability, land use and global climatic change (Sutherst, 1998; Linthicum, *et al,* 1999; Patz *et al,* 2000; Anyamba *et al,* 2002), it was also shown that varying climatic conditions related to ENSO events are now becoming risks to both humans and animals.

Furthermore, Millington *et al,* (1994) have examined and shown the potential of imagery acquired by the AVHRR for land cover studies generally, but this has not been utilised fully by countries with low economic standing. Because of the value of NDVI

derived from AVHRR it is therefore being utilised in this investigation for the assessment of temporal changes in vegetation across Nigeria. While the data has a high temporal resolution, the spatial resolution is limited to 8 km, and the impact of this needs to be determined.

1.4   The Structure of the Book

The book is divided into eight chapters. Chapter One, the Introduction, has highlighted some of the socio-economic problems which may be responsible for exerting pressures on the vegetation cover across Nigeria and the need for periodic assessment using a very coarse spatial resolution AVHRR-NDVI data.

Chapter Two briefly reviews literature on studies conducted with AVHRR data generally from global to continental and regional scales with further emphasis on the use of AVHRR-NDVI data from the PAL dataset. This also includes other studies conducted on Nigeria using other remotely sensed data and ancillary information.

Chapter Three provides a general overview of Nigeria in terms of its political, social and physical setting which includes its topography, soils, climate, land-use and vegetation.

In Chapter Four the general methodology used in undertaking the study is presented. This includes data access, such as the NDVI PAL dataset, the GTOPO30 Digital Elevation Model (DEM) data and the Gridded Precipitation data from the Global Precipitation and Climatology Centre (GPCC). In addition to these, the procedure for recompositing the NDVI dataset, making a subset of the DEM of the study area from

the original acquired GTOPO30-DEM and creation of rainfall models is also presented. This is followed with the description of how the spatial rainfall data was generated from the models. One major problem encountered with the NDVI data from the PAL dataset as part of its uncertainties is also highlighted. At the end of this chapter, a highlight on the three different techniques employed in analysing this data for vegetation change assessment across Nigeria is presented.

Chapter Five reports a preliminary assessment of the data prior to conducting the assessment of vegetation changes across Nigeria. This was done by using the original data acquired from the PAL dataset archive, the recomposited and derived rainfall data on selected sites from different vegetation zones of the country.

In Chapter Six the three different change detection approaches used in assessment of changes in vegetation across Nigeria are presented. This includes a Simple Image Differencing (SID) technique, Slope of Change from Regression (SCR) and Principal Component Analysis (PCA) using standardised principal components. Detailed results and brief discussion which includes the advantages and disadvantages of each technique for using it in vegetation change assessment are presented. A summary is then given at the end of the discussion about each technique.

Chapter Seven forms the general discussions chapter where the results of the three change detection techniques presented in Chapter Six are discussed in the context of other studies that used AVHRR data for vegetation studies, and the implications in the context of the country's ecological sustainability. Potential use of the data for studies in developing countries like Nigeria is highlighted, where the use of high spatial resolution

satellite data such as SPOT, Landsat MSS or TM may not be possible on a frequent basis due to economic and other factors.

In Chapter Eight the final conclusions are presented with a summary and recommendations based on the findings from the study.

CHAPTER TWO

LITERATURE REVIEW

2.1   Introduction

This chapter outlines and reviews published materials from the literature regarding the use of NOAA coarse resolution AVHRR data in vegetation research, with particular emphasis on vegetation change assessment using the NOAA/NASA PAL dataset. The chapter is divided into three sections. The first focuses briefly on the general steps in project formulation process for remote sensing change studies. The second section reviews the literature on general analytical procedures in Remote Sensing (RS) and Geographical Information Systems (GIS) change assessment using NOAA AHVRR data. The third section presents an overview of the literature based on studies conducted on vegetation change studies using AVHRR-NDVI data and focuses on studies conducted using the PAL dataset as well as studies conducted with other satellite and ancillary data specifically on Nigeria. The advantages and disadvantages of using the dataset for vegetation studies are summarised at the end of the chapter.

2.2   Steps in Project Formulation Process for Remote Sensing Land Cover Change Assessment

Most projects involving change detection through remote sensing require a project formulation approach (Jensen, 1996; Wilkie and Finn, 1996; Lunetta, 1998). Such an approach, according to Lunetta (1998), includes problem definition, data specifications, data requirements analysis, determination of data availability, calculation of data

9

acquisition costs and data analysis cost estimates. These are briefly described in turn below.

2.2.1   Data Specifications

An overview regarding this particular study covering Nigeria was highlighted in Chapter One. However, specifying the type of data to be used after defining the problem to be addressed is very important if the targeted aim is to be achieved. Different types of data in the form of hard copy materials such as maps, aerial photographs or satellite pictures are used in natural resources assessment depending on availability, affordability and choice. However, analogue and digital aerial photos or satellite data are often used in such studies because they are versatile.

2.2.2   Data Requirements

Four main criteria are used in choosing the type of remote sensing data for general environmental studies which includes natural resource assessment (Jensen, 1996; Wilkie and Finn, 1996; Lunetta, 1998) :

1.   Spatial resolution of the data

2.   Spectral resolution of the data

3.   Radiometric resolution of the data

4.   Temporal resolution of the data

These are briefly described below.

Spatial resolution of the remotely sensed data

Spatial resolution of remotely sensed data (depending on the size of the sensor) is defined as the size of the environmental feature that can be noticeable from the background or whose dimensions can be measured on the remotely acquired data (Wilkie and Finn, 1996).

Spectral resolution of the remotely sensed data

The spectral resolution of remotely sensed data is the length and number of wavelength sections in the Electromagnetic Spectrum (EMS) to which the sensing mechanism is sensitive. For example, the red in the visible spectrum (Channel 1) of the Advanced Very High Resolution Radiometer (AVHRR) has a broad spectral resolution sensitive to all reflected blue and green light between 0.4μm and 0.7μm while its near infrared spectrum (Channel 2) has a broad spectral resolution sensitive to red and near infrared light between 0.7μm and 1.1μm. These two spectral bands from AVHRR sensors are normally utilised in calculating the Normalised Difference Vegetation Index (NDVI). This vegetation index is used as one of the primary information sources for monitoring vegetation conditions and mapping land cover change (Teillet *et al,* 1997). Studies (eg Justice *et al,* 1985; Justice and Hienaux, 1986; Townshend *et al,* 1987; Millington *et al,* 1994; Mayaux and Lambin, 1995**)** utilised NDVI values of range between ± 1 (0- 255 for scaled NDVI). The scaled NDVI are used in this study which range from 0-255. However, in order to inter-convert, Scaled_NDVI = float_NDVI*125+128 (See Appendix 4). Healthy vegetation normally was shown to have highest positive NDVI values, while surfaces that contain very little or no vegetation at all such as soil, rock, water, snow, ice or clouds have NDVI values close to zero or slightly negative. NDVI from AVHRR imagery is calculated as:

$$NDVI = \frac{CH2 - CH1}{CH2 + CH1} \qquad (2:1)$$

The general sensitivity of typical remote sensing systems for bare soil, vegetation and water is illustrated in Figure 2.1

Although there are some overlaps in the spectral signatures of environmental features for satellite sensors from SPOT, Landsat MSS and TM and AVHRR, the more capacity a particular remote sensor will have in measuring the flow of radiation (radiometric resolution) that is reflected or emitted from environmental features, the more likely it will increase the chances of detecting and differentiating certain environmental features under investigation (Wilkie and Finn, 1996). For example, although both the spatial and spectral resolution of an image from AVHRR is able to offer enough information to detect forest patches within a large area, its radiometric resolution may be too coarse to fully differentiate between vegetation types of the savanna and that of a forest area especially when a much coarser dataset of the AVHRR such as an 8 km NDVI is utilised.
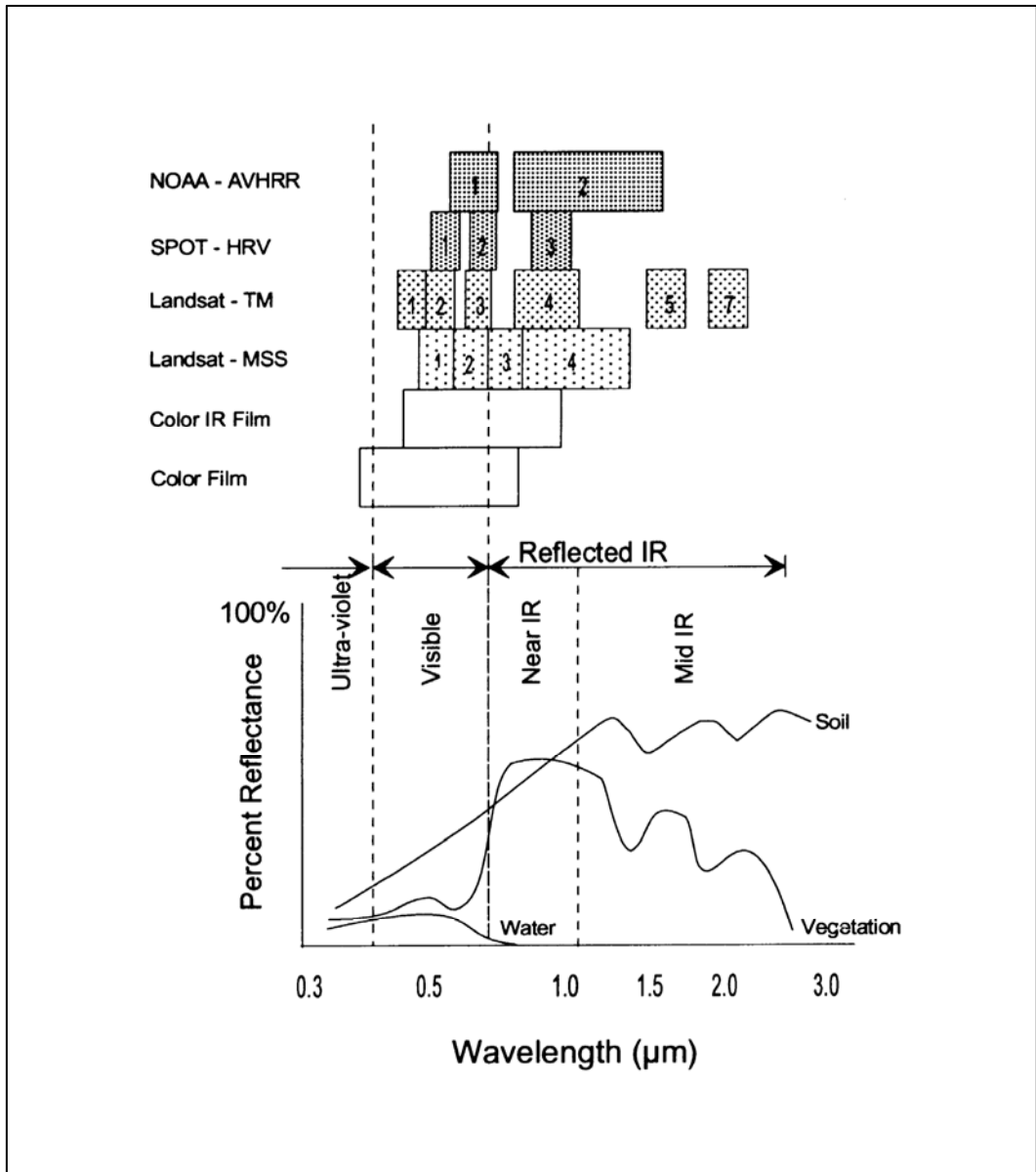
(Adapted from Wilkie and Finn, 1996)

Figure 2.1 An illustration of the General Spectral Sensitivity of typical remote sensing systems for bare soil, vegetation and water.

Radiometric resolution of the remotely sensed data

The radiometric resolution of remotely acquired data is defined as the ability of the sensor to differentiate the flow of radiation that is reflected or emitted by the terrain. For example, when the radiation sensitive to red and near infrared light between 0.7μm and 1.1μm reaches the Channel 2 of AVHRR sensor from terrain features a voltage is generated for that channel for a particular terrain feature. This voltage is then converted into digital reflectances (brightness values) also called Digital Numbers (DN). Conversion of these DN to absolute radiance values is very necessary in order to compare different images taken by different sensors because each sensor has its own different calibration parameters that are used in recording the DN values (Eastman, 1999b). However, although the same DN values in two images taken by two different sensors may actually represent two different radiance values, most commonly, the digital satellite data are distributed in 8-bit format corresponding to 256 DN levels (Eastman, 1999b). The radiometric resolution of the AVHRR sensor brightness values, for example, is rescaled from 0 to 255 (8-bit integer) brightness values.

Temporal resolution of satellite remotely sensed data

The temporal resolution of remotely acquired data is the measure of how frequently a particular satellite sensor acquires the imagery for a particular locality or area or how frequently the area is visited by the satellite sensor. Temporal resolution of data for global, continental or regional studies particularly relating to vegetation, for example, is based mainly on the annual phenological cycles of vegetation (eg Justice *et al,*1985; Townshend and Justice, 1990; Justice *et al,* 1991a; Tucker *et al,* 1994).

Table 2.1   Summary of characteristics of some Satellite Remote Sensing Systems

(a) Characteristics of the SPOT Satellite System

Band or Channel	Nominal Spectral Location	Sensitivity (μm)	Spatial resolution	Temporal resolution	Swath width (km)
1	Green	0.50 - 0.59	10 – 20m	5 – 26 days	60 km
2	Red/NIR	0.61 - 0.68	10 – 20m	5 – 26 days	60 km
3	Mid IR	0.79 - 0.89	10 – 20m	5 – 26 days	60 km
Panchromatic	Thermal	0.50 - 0.74	10 – 20m	5 – 26 days	60 km

Summarised from Campbell (1996), Mather (1999a) and Wilkie and Finn (1996)

(b) Characteristics of the Landsat Thematic Mapper (TM) System

Band or Channel	Nominal Spectral Location	Sensitivity (μm)	Spatial resolution	Temporal Resolution	Swath width (km)
1	Blue	0.45 - 0.52	30m	16 days	185 km
2	Green	0.52 - 0.60	30m	16 days	185 km
3	Red	0.63 - 0.69	30m	16 days	185 km
4	Near IR	0.74 - 0.91	30m	16 days	185 km
5	Mid IR	1.55 - 1.75	30m	16 days	185 km
6	Thermal	10.4 - 12. 5	30m	16 days	185 km
7	Reflected Mid IR	2.08 - 2.35	30m	16 days	185 km

Summarised from Campbell (1996), Wilkie and Finn (1996)

(c) Characteristics of the Landsat Multi Spectral Scanner (MSS) System

Band or Channel	Nominal Spectral Location	Sensitivity (μm)	Spatial resolution	Temporal resolution	Swath width (km)
1	Green	0.50 - 0.60	79m	16 – 18 days	185 km
2	Red	0.61 - 0.70	79m	16 – 18 days	185 km
3	Near IR	0.70 - 0.80	79m	16 – 18 days	185 km
4	Mid IR	0.80 - 1.1	79m	16 – 18 days	185 km

Summarised from Campbell (1996), Mather (1999a) and Wilkie and Finn (1996)

(d)   Characteristics of the NOAA AVHRR System

Band or Channel	Nominal Spectral Location	Sensitivity (μm)	Spatial Resolution Local Area Coverage (LAC)	Temporal resolution	Swath width (km)
1	Green	0.58 - 0.68	1100m	12 hours	27000 km
2	Red/NIR	0.725 - 1.1	1100m	12 hours	27000 km
3	Mid IR	3.55 - 3.93	1100m	12 hours	27000 km
4	Thermal	10.5 - 11.5	1100m	12 hours	27000 km
5	Thermal	11.5 - 12.5	1100m	12 hours	27000 km

Summarised from Campbell (1996), Mather (1999a) and Wilkie and Finn (1996)

Examples of general characteristics relating to spatial, spectral and temporal resolutions of the four major satellite sensing systems used in acquiring digital imagery that are frequently utilised in environmental and ecological studies are shown in Table 2.1.

2.2.3   Data Availability

In most remote sensing change detection studies the digital data used are either requested to be acquired specifically or obtained from an existing vendor from existing archives. In general, data that exhibit similar phenological conditions have a greater potential in distinguishing changes in landcover than those that are acquired at different phenological conditions (Jensen, 1996; Wilkie and Finn, 1996; Lunetta, 1998). For example, this would apply to data of different years but of the same month, data of vegetation of similar pheneological cycle or historical data such as the AVHRR data that were acquired and processed in order to provide corresponding NDVI data at 1 km, 4 km and 8 km resolutions respectively (eg Eidenshink, 1992; James and Kalluri, 1994).

2.2.4   Data Acquisition Costs

Data cost is very important when deciding the type of imagery to be used for general landcover change assessment. However, imagery of better spatial resolution acquired from Landsat MSS (80 metres), TM (30 metres) or SPOT (10 – 20 metres) is often more expensive than coarse spatial resolution imagery acquired from AVHRR, even though the data from AVHRR has the advantage of being acquired more frequently than these three named types of satellite data. The choice of which data to use depends on affordability, the extent of areas covered by the study and the purpose of the study. For example, if only preliminary information about landcover productivity of a country with a large land area is required, then it is better to use cheaper coarse resolution imagery with a high temporal resolution such as AVHRR rather high spatial resolution imagery of low temporal resolution like SPOT, Landsat MSS or TM.

2.2.5   Data Analysis Costs

One of the important factors worth considering in the sequence of operations in the analysis of remotely sensed data such as satellite imagery is the time that will be spent in analysing a particular type of satellite data. This is because the better the spatial resolution of satellite data in terms of differentiating landcover types, the more the quantity of the data that has to be acquired, stored and analysed. For example, in order to undertake a broad-scale vegetation cover analysis across Nigeria using NDVI data, about 3.5 billion pixels of 20 metre resolution from SPOT imagery is required. If however, AVHRR NDVI from PAL dataset at a coarser resolution of 8 km is used in such analysis, this will require a total of only about 24,000 pixels. Thus, for a broad scale analysis of such a large area, it will cost less financially, require less space for

storage and less time in analysis than when SPOT, Landsat MSS or TM data are utilised.

2.3 General Analytical Procedures in Remote Sensing Change Assessment

Prior to analysing digitally acquired remotely sensed data for change detection studies it is important to consider some analytical procedures so as to avoid deriving inaccurate results. This is to ensure that errors introduced into the data during the acquisition process are removed and the data is radiometrically and geometrically normalised to represent the landscape as realistically as possible (Duggin and Robinove, 1990; Lunetta *et al*, 1991; Wilkie and Finn, 1996). Accordingly, Lunetta (1998) has broadly categorised these analytical procedures into three groups namely :

1.   Radiometric Corrections

2.   Geometric Corrections

3.   Change detection analysis

 and they are summarily reviewed in turn below.

2.3.1 Radiometric Corrections

In multispectral satellite data such as SPOT, Landsat MSS and TM or AVHRR, the main causes of radiometric distortions are by atmospheric problems or sensors (instruments) failure used in acquiring the data. The PAL dataset utilised in this study however, has been corrected for both the atmospheric and instrument errors (James and Kalluri, 1994). Three most commonly utilised atmospheric radiometric correction techniques (Lunetta, 1998) summarised below relates to :

1.   Pseudo-variant features (Schott *et al,* 1988).

2.   Dark-pixel subtraction (Gonima, 1993).

3.   Relative radiometric normalisation (Elvidge *et al,* 1995).

Pseudo-variant features correction method

Remotely sensed imagery of the same location obtained under different conditions and times will be difficult to compare because of changes due to atmospheric scattering of dust particles and molecules. When using the pseudo-variant features method to correct errors introduced to the data due to atmospheric effects, certain terrain features that are normally stable and do not change spectrally are utilised. For example, bright targets such as deserts areas or areas of sunglint are used to normalise the satellite derived data (Che and Price 1992; Kaufman and Holben 1993) used for calculating the NDVI from the Visible Channel (Channel 1) and the Infrared Channel (Channel 2). However, the problem with this method is that any changes in surface moisture of the area considered invariable will change the reflectivity of the area. This will in turn affect the correction applied to the data. Hence the invariable area being used as a target for correction due to atmospheric distortion has to be really stable.

Dark-pixel subtraction correction method

Atmospheric influences that affect data acquired by satellite remote sensors such as SPOT, MSS, TM and AVHRR are largely due to scattering from air molecules, scattering due to particles associated with smoke and dust, and water vapour from water droplets (Jensen, 1996; Wilkie and Finn, 1996).

Because of such atmospheric effects on a satellite image, the histogram of pixels on the image will appear shifted further away from zero. This increases the brightness in each pixel (pixel values) within a spectral channel. In order to correct these effects, the size of the 'shift' (in values) is subtracted from the amount of brightness level in the histogram of each channel (Gomina, 1993). However, it was shown in this method of correction that if the effect such as haze is only on a small patch over the image, for example, the correction applied will alter the non hazy areas (Campbell, 1996; Wilkie and Finn, 1996). This correction can also be done in IDRISI-32 by creating a mask for the hazy areas from the original image and, by using the created mask interactively with the original image, the effects can be removed (Eastman, 1999b).

Relative radiometric normalisation method

In the relative radiometric normalisation method of correction, one image is used as a reference to adjust the radiometric properties of the other images in order to match that of the reference image (Hall *et al,* 1991). In this method, either dark areas representing deep water pixels or bright areas on the land surface representing pixels for soils or concrete (which are considered as no-change pixels) determined on the reference image are utilised. The pixels of no change areas on the reference image are plotted against the subject images of the near infrared channels on a scattergram-controlled regression (Yuan and Elvidge, 1993). Pixels above and below the regression line of no change are then used to perform the normalisation for gains and offsets of each spectral band of the images. However, the disadvantage of this method is that the initial position of the axis of no change must be determined visually. Though there was an improvement of this simple method when an automatic controlled scattergram was developed that selects pixels of no-change areas directly from a reference image to normalise the rest of the

images (Elvidge *et al*, 1995), it does not necessarily reduce the computation time. However, it reduces the effects of cloud, shadow and snow effects compared with the simple method which uses a small percentage of the pixels in the reference image. In another preliminary study, Gutman and Ignatov (1996) have shown that the cloud flag (CLAVR) in the AVHRR PAL dataset can be utilised in a post-composite cloud screening procedure to filter the residual clouds in NDVI dataset using spatial and/or temporal correlation function where interpolation is used to fill and replace cloud-induced pixels. However, this method was a preliminary assessment which requires further verification and is also time consuming.

Radiometric Correction of the Visible and Near Infrared Channels of AVHRR

Different studies utilising AVHRR NDVI for monitoring vegetation condition and landcover over the years (eg Tucker *et al,* 1985; Townshend and Justice, 1990; Townshend *et al,* 1991) and other related studies (eg Justice and Townshend, 1994 ; Lambin and Strahler, 1994a; Lambin and Strahler, 1994b) have noted the radiometric effects of the NOAA satellites on the data (eg NOAA 7, -9 and -11 AVHRRs). Hence, different studies also introduced other methods of data corrections from such instruments. For example, Teillet (1986) categorised the different methods of image correction for radiometric effects on remotely sensed data generally. Other methods of applying radiometric corrections to satellite acquired data and particularly from AVHRR are also described in other literature (eg Teillet *et al,* 1990; Teillet and Holben, 1994; Rao and Chen, 1995; Vermote and Kaufman, 1995; Roderick *et al,* 1996b) and for atmospheric affects (eg Holben, 1986; Justice *et al*, 1991a; Hanan, *et al,* 1995). The two main absolute methods used in applying radiometric corrections to the first two AVHRR channels are calibration over the ocean (Vermote *et al,* 1992; Vermote and

Kaufman, 1995) and calibration over desert sites (Holben *et al,* 1990 ; Kaufman and Holben, 1993) although Che and Price (1992) have shown that ocean sites yield greater uncertainties than desert sites because the signal level is lower on the ocean. However, studies on the calibration results particularly on radiances (for calculating NDVI) from the AVHRR instruments onboard NOAA -7, -9 and -11 have shown that NOAA -9 has fewer errors and is more stable than the others (Teillet *et al*, 1990; Che and Price, 1992). NOAA -14 was also shown to have produced unrealistic global increase in both reflectances and vegetation indices (Gutman, 1999). The NOAA -9 calibration coefficients are therefore used as a baseline for normalising the radiance measurements of Channel 1 and 2 sensors used in NOAA -7, -11 and -14. Hence, it was adopted for the post-launch calibration corrections (eg Rao and Chen, 1994; Rao and Chen, 1995) for the Pathfinder PAL dataset because of the instrument's degradation over the years (James and Kalluri, 1994; Smith *et al*, 1997). Although the maximum value compositing (MVC) technique (Holben, 1986) was applied to PAL-NDVI time series data for minimising atmospheric effects such as clouds, it is still considered to have a legacy of noise. Hence, Viovy *et al,* (1992) proposed the Best Index Slope Extraction (BISE) method as an alternative to the MVC. This method is based on a smoothing algorithm which retains high NDVI values and eliminates only extremely low values. However, the problem with this method is that there is a possibility that a high NDVI retained during the procedure could also be contaminated with cloud, or the one eliminated is a true surface reflectance as represented by the NDVI.

Other later studies such as Roerink *et al*, (2000) and Lovell and Graetz, (2001) used different approaches. Roerink *et al*, (2000), for example, used an alternative analogue technique called Harmonic Analysis of Time Series (HANTS) based on Fourier Analysis of times series NDVI data from AVHRR. However, in addition to its time-

consuming procedure the technique is limited to environments where annual NDVI trajectories are regular and predictable. This may not be applicable in the semi-arid and sub Saharan Africa including Nigeria, where vegetation is very dynamic. Lovell and Graetz (2001) on the other hand used a modified version of the BISE so as to filter the cloud contaminated AVHRR data using the 10-day NDVI from the PAL dataset for a site over Australia. In the modified version of the BISE, an algorithm searches for a spike in the data (ie, an increase followed by a decrease in a temporal profile of the 10-day NDVI data utilised). However, unless this method is applicable to any environment with different climatic conditions then it is still lacking some merit.

2.3.2 Geometric Corrections

Geometric distortions are introduced into satellite acquired data because of certain factors such as the earth's rotation during the satellite movement, the curvature of the earth surface, the angle of view of the sensing system, the topography beneath the satellite, changes in altitude of the satellite during acquisition of the data and instability of the satellite platform (Lillesand and Kiefer, 1994; Campbell, 1996; Wilkie and Finn, 1996).

Distortions introduced into the data can be corrected using two main approaches. The first is by modelling the sources of the distortions and then proceeding to create a formula that corrects them (Mather, 1999a; Tanré *et al,* 1992). However, unless all the sources of the distortions are known and their effects are uniform in the image this approach will not solve the problem (Wilkie and Finn, 1996). The second approach uses geographic coordinates of terrain features identified on standard map projection system and their corresponding images used as Ground Control Points (GCPs) on a satellite

image. These are utilised to generate statistically a pair of functions which transforms the pixel locations of the terrain features on a map. In this second approach, the map analyst can correct geometric distortions without knowing either the sources or magnitude of such distortions and is one of the most widely adopted methods. Two main procedures are utilised in this method and they are briefly described below :

Image to Map Transformation using Control Points

In the image to map transformation method of geometric correction a map of the same area as the image is required. The geometric correction is performed by identifying a set of GCPs both on the map and on the satellite image. These GCPs include road junctions, edges of bridges or dams and corners of bridges. However, not all maps or images are suitable for finding the exact locations of the chosen GCPs due to differences in map scales or resolutions of images. This is because the actual location of a particular GCP on such maps or images may vary by several metres. For example, on small scale maps a line representing a road may be over 250 metres wide (depending on how small the scale of the map is). When this is used in such geometric correction and involves an image of high spatial resolution such as Landsat TM (30 metre) or SPOT (10 metre) the error will be in the range of hundreds of metres. If however, the correction involves an AVHRR image of either 1 km, 4 km or 8 km resolutions the error will be minimal.When there are no suitable maps for use in the image to map transformation, it is suggested that a Global Positioning System (GPS) be used in the field to determine the true geographic location of the terrain features suitable as GCPs. In such geometric correction it is assumed that the shapes of the two mapping functions are not known, hence they are represented by a first (linear), second (quadratic) or third (cubic) order of polynomial fit desired for the GCPs by means of least square regression

(Richards, 1986; Eastman, 1999a). The minimum number of GPCs that is required in order to solve the polynomials has to be equal to the number of the coefficients within the equation. For example, a minimum of three GPCs are required for linear, six for quadratic and ten for cubic (IDRISI-32, 1998). The accuracy of these transformations are later evaluated for each GCP by computing their Root Mean Square Error (RMSE) for their true geographic coordinates (x and y) in relation to their transformed positions (*rows* and *columns*) on the image. In general the allowable total root-mean-square error (RMSE) should be less than half of the resolution of the input image (IDRISI-32, 1998).

Image to Image Coregistration

Image to image coregistration involves registration of two satellite images of the same geometric and geographic location together such that all corresponding terrain features appear on the same location on the two images (Che and Lee, 1992). Here, the first image that has been corrected using GCP's from a standard map projection is used as the master image to correct the second or other uncorrected images normally referred to as slave image(s). Gupta (1992) also used this approach in agrometeorogical studies for crop growth cycle where an NDVI image computed from geometrically corrected radiances was used to geocorrect another NDVI image derived from raw data. The disadvantage of this method generally, is that any image that is registered or corrected using an already rectified image from an existing map will inherit all the geometric errors that exist in the reference image. However, Jensen *et al,* (1993) have shown that rectification errors are greatly minimised when a hybrid approach of geometric correction is applied to satellite images.

2.3.3   Change Detection Analysis

General landcover changes are said to be driven by five broad causes as enumerated by

Lambin and Strahler (1994b) namely :

1. Long term natural changes in climatic conditions.

2. Geomorphological and ecological processes such as soil erosion at geological (normal) rates and vegetation successions.

3. Human-induced alterations of vegetation cover and landscapes, such as deforestation and land degradation (eg soil erosion at accelerated rates).

4. Inter-annual climatic variability which affects primarily arid and semi-arid regions, and which may lead to recurrent periods of drought accompanied by modifications in the vegetation cover, annual primary production and the hydrologic cycle.

5. Hypothetically, human-induced climatic changes through an enhancement of the greenhouse effect.

Four main approaches used in the analysis of general landcover change with satellite

remotely sensed data as a result of these driven causes includes single-band raw image

algebra (Image differencing or Image rationing), Spectral Vector Analysis, Classified

Image Comparison and Principal Component Analysis (PCA). These change detection

strategies are summarily reviewed in turn below :

Single-Band Raw Image Algebra

This is also called Univariate Image differencing. This is performed by subtracting one

image of the same band from the other (Singh, 1983) or by band rationing where one

image of the same band is divided by another image of later date that has been

geometrically rectified from the same base map (Green *et al,* 1994). In image

differencing, the resulting residual image contains negative and positive values of radiance changes and areas of zero indicating areas of no change. The problem with this method is where to place the boundaries of change between pixels of change and those of no-change. However, a procedure called thresholding is used to categorise areas (pixels) of true changes in land cover and those that are considered unchanged (Fung and LeDrew, 1988; Singh, 1989). The threshold values are also determined from the histogram of the resulting residual image (Singh, 1989). The advantage of this is that it is a simple method of change detection, and when applied to multitemporal satellite data gives an absolute result. This is because pixels that have changed in brightness values can easily be identified between individual images in a dataset or between image years. However, there are no clear guidelines on how to set thresholds (Eastman, 2000); although standard deviations were used in other studies (eg Quarmby *et al,* 1987; Fung and LeDrew 1988) quartiles can also be used. Fung and LeDrew, (1988) however, suggested that if ground truth data are available they serve as better means of assessing different thresholds.

Spectral Vector Analysis

Because spectral appearance of landcover of an area that has changed over time is easily distinguishable on multi-spectral images of different dates, this method is used to indicate the direction and magnitude of change from a first to a second image of different dates. The change vector is measured as the difference between the successive images represented as a vector in a multidimensional scaling or measurement. Engvall *et al* (1977) first experimented with this method using the multi temporal trend of mean vectors from Landsat data to classify agricultural crops. It was also applied successfully for monitoring changes in mangrove and reef ecosystems (Michalek *et al,* 1993).

Although NDVI is a single band data, it can also be used in the context of multi image datasets for change vector analysis. For example, Kajirawa and Tateishi (1990) described the temporal response pattern of vegetation using 12 monthly NDVI images for two years. The length of the change vector is said to give an indication of the magnitude of change while its direction shows the nature of the change (Lambin and Strahler, 1994a). However, the technique is sensitive to spatial registration of corresponding pixels between images (Eastman, 2000).

Classified Image Comparison

Classified Image comparison or post classification comparison is the most common method of change detection applied to multi-temporal satellite data (Jensen *et al,* 1993). In this method, rectified remotely sensed data are classified and later compared pixel-by-pixel based on the different classes of land cover. The results of the changes are tabulated in change matrices showing the different classes of changes. The success of this method is that each image data must be classified as accurately as possible (Augenstein, *et al,* 1991). The advantage of the method is that it provides a 'from-to' change class information of the change analysis (Jensen, 1996). However, its main disadvantage is that, in addition to aiming at a high classification accuracy for each image, each individual image in the dataset has to be classified separately before comparison is made. Hence, for a dataset containing 12 monthly NDVI images for 12 years this method can prove very laborious. The classification of image dataset can be done using either supervised classification, where ground truth data is available as a guide to assign similar and categorise different landcover classes or unsupervised classification using an automated classification algorithm (which requires very little human input) to assign and categorise individual image pixels into landcover classes,

also referred to as the Iterative Self Organising Data Analysis Technique (ISODATA) routine (Ball and Hall, 1965), or by using a set of pixel class intervals derived from a histogram of the satellite imagery. However, vegetation cover generally can be classified in different ways depending on the ultimate use of the final product (Townshend *et al,* 1987).

Principal Component Analysis (PCA)

Principal Component Analysis (PCA) is a data transformation and information extraction technique in multitemporal satellite data. In PCA transformations raw or refined satellite data produces new sets of Principal Component Images which are normally as good as but more interpretable than the original data (Singh and Harrison, 1985; IDRISI-32, 1998). For example, a Landsat TM image with seven bands can be transformed into two or three principal component images or 144 monthly NDVI image datasets for 12 years can be transformed into just 12 annual principal component images using PCA. Two types of analysis using PCA can be undertaken: either Standardised PCA based on the computation of eigenvalues from correlation matrices or Unstandardised PCA computed from covariance matrices of the transformed datasets (Eastman and Fulk, 1993). However, Fung and LeDrew (1987) and Eastman and Fulk (1993) have all showed that PCA which utilises Standardised Principal Components is better than that which utilises unstandardised principal components when analysing multitemporal datasets. This is because each image data in the dataset used in standardised PCA is given equal weighting in the transformation. Hence although the first few component images obtained in standardised PCA will be able to explain more of the variations in the total dataset used as input in the procedure, the last components which explain very little variance in the information content of the total dataset but may

also contain valuable information that the first few components could not explain. However, without very good knowledge of the area under study and other supporting environmental and ancillary information of the study area it will be very difficult to explain the variations. The main disadvantage of PCA also is that the brightness values of the resulting component images are not directly related to the reflectance characteristics of terrain features. This is because we cannot use the information we know about terrain features in relation to their reflectance characteristics to interpret the features on component images. For example, when time-series NDVI datasets are used in PCA where standardised Principal Components are obtained, it is the component loadings together with their respective component images that are used together to interpret change patterns of terrain features observed on the component images (IDRISI-32 1998).

2.4 A General Overview from Literature concerning Vegetation and Related Studies Conducted with Data Derived from AVHRR

The utilisation of the AVHRR system over the years has demonstrated that it can be used as a tool to monitor seasonal dynamics of the world's vegetation at global, continental and regional scales. For example, the analysis of the phenology of global vegetation (Justice *et al*, 1985), monitoring of forest clearance and differentiation of vegetation types in the Amazonian region (Tucker *et al,* 1984a; Batista *et al,* 1997), the productivity of African grasslands (Justice and Hienaux, 1986), African landcover classification (Tucker *et al,* 1985) and landcover change analysis of China (Young and Wang, 2001).

However, one of the most widely used methods in mapping landcover, and in particular vegetation phenology over different geographical areas using satellite data is by applying the Normalised Difference Vegetation Index (NDVI) (see Section 2.2.2, Table 2.1*d* and Figure 2.1). The Channel 1 and 2 of AVHRR used to derive the NDVI are related to the proportion of photosynthetically absorbed radiation which are now widely used in studies related to green biomass. Although there are numerous vegetation and vegetation related studies conducted with AVHRR data across continents and regions, some of these studies found to be of relevance to this study are briefly reviewed below :

2.4.1   Global Vegetation Studies conducted with AVHRR data

Although AVHRR derived data was not originally designed for vegetation studies (Cracknell, 1997), one of the pioneering studies with the data particularly (Justice *et al,* 1985) indicated that the data could be used for global studies in vegetation. In that study, NDVI calculated from AVHRR between 1981 and 1983 were used to describe the seasonal dynamics of major vegetation types for the continents of Africa, South America and South-east Asia supplemented with ground data and other published information. From that study, it was shown that the major desert areas of Africa such as the Sahara have low vegetation indices. Other areas like the Sahel and the Kalahari desert showed fluctuations in the amount and presence of vegetation. In a comparison between NDVI images of May and September of 1983 from that study, it was discovered that the northern part of Nigeria and southern Niger Republic showed a marked northerly increase in green vegetation prior to the growing season across the sahel. However, the tropical rain-forests of Africa within the Guineo-Congolian region as defined by White, (1983) ie in the rain forest zone from Guinea, the Ivory Coast and Ghana to Nigeria, have high NDVI values throughout the year. On the other hand, the

interior swamp lands of Lake Chad as well as some areas in the Niger Delta indicated some mixture of low and high NDVI values in their surroundings (See Figure 5.7b). It was further indicated in that study that the peak period of vegetation biomass growth occurred in September followed by a marked decrease in November NDVI images. Accordingly, the annual average rainfall distribution in West Africa generally is described as unimodal. In a related study with AVHRR-NDVI data Norwine and Greegor (1983) have indicated that most major ecoregion and native vegetation region boundaries do represent climatic discontinuities. However, although the results from these studies provided useful information about the vegetation phenology of these continents, regions or areas based on NDVI, if the dataset utilised in those studies was processed with the errors itemised in Section 2.4.3, the information will, to some extent, produce an under or over estimation of the vegetation phenology of the studied areas.

As the use of the different resolutions AVHRR data in general landcover studies increased over the years, new approaches have been applied to the data that differ from the traditional landcover classifications based on either the ISODATA (unsupervised) or the supervised classification approaches. These new approaches used a system of hierarchical tree structure. However, these approaches varied from using spectral signatures supplemented with ancillary ground information in a supervised classification (De Fries and Townshend, 1994), to using the 10-day NDVI composite from the PAL dataset to derive metrics from temporal profiles (De Fries *et al,* 1995), to utilising several Landsat MSS scenes to identify land features (De Fries *et al,* 1998), to using the 1 degree by 1 degree resolution NDVI composites together with temperature data to determine the best metrics to discriminate vegetation types (Hansen *et al,* 1996), to using two separate years AVHRR data at 1 km resolution to compare land cover between continents where tropical vegetation can be differentiated from temperate

vegetation (Hansen *et al,* 2000), to adopting the hierarchical tree structure in addition to another complex sub-tree structure in order to differentiate tropical and sub-tropical vegetation types (Los *et al,* 1994) and to monitor seasonal dynamics of temperate mixed ecosystems (Duchemin *et al,* 1999). In most of these studies, either one to two years data was utilised or the AVHRR data was used together with temperature and other finer resolution data such as Landsat MSS or TM. In most of these studies, the major problem affecting results is the cloud contamination of NDVI data from AVHRR especially during the months of August and September particularly around the Gulf of Guinea and the sahel for studies which covered these areas. The general conclusions from some of these studies showed that areas that exhibited large inter-annual variability of NDVI based on the NDVI temporal profiles produced are located in the semi-arid areas especially in the sahel and around the coast. On the other hand, a study with the PAL dataset (Smith *et al,* 1997) has shown that hot spots of inter-annual NDVI variations are found mostly in tropical Africa. This is also verified in this investigation using inter-annual and inter-seasonal coefficients of variation images respectively, illustrated in Figure 5.7*b*. In the context of these approaches, the new classification approach tends to give better results than the traditional landcover classifications used alone despite cloud contamination in the AVHRR data. The final analysis from various studies that utilised AVHRR datasets in global, continental and regional studies (eg Goward, *et al,* 1993; Gutman and Ignatov, 1995; Leprieur, *et al,* 1996; Teillet *et al,* 2000) concluded that most of the significant inconsistencies of the data analysed are caused by persistent cloud cover, atmospheric perturbations, elimination of data with low surface temperature and solar zenith angle effects, either individually or collectively.The primary methods of correcting such errors have been described in Section 2.3. However, the errors caused by cloud contamination, atmospheric scattering

of particles and solar zenith angles can lead to underestimation of biophysical parameter values such as NDVI if no corrections are made to the data prior to making any analysis. Despite these problems, NDVI data from AVHRR is shown to be very valuable for vegetation studies.

2.4.2 Vegetation Studies conducted with AVHRR data covering the African Continent and other places

According to Prince and Justice (1991), the potential of the data provided by AVHRR for vegetation studies at regional level was first tested on the African continent, followed by other studies using single date and multiple date datasets. One of the pioneering studies with AVHRR data in Africa (Tucker *et al,* (1984b) tested the potential of the 1 km LAC AVHRR data in monitoring vegetation in the Nile Delta with data for only a few months growing season within a single year. Another study (Schneider *et al,* (1985) used the NOAA AVHRR data with Landsat MSS data together to track changes in the Lake Chad basin in Africa. In that study, high NDVI values observed around the lake were attributed to the growth of aquatic vegetation. However, because the magnitude and uncertainties relating to AVHRR data such as atmospheric and radiometric effects were not properly understood at that time (see Section 2.4.3), later studies (eg El-Raey *et al*, 1995*;* Lupo *et al,* 2001) were not in close agreement.

On landcover classifications specifically covering the African continent, Tucker *et al,* (1985) undertook a feasibility study using the NOAA-7 AVHRR data. It was shown in that study that there is correspondence between seasonal variations in the density and extent of green-leaf vegetation and the patterns of rainfall associated with the Intertropical Convergence Zone (ITCZ). Although a very coarse resolution (15 km) was used in that study, the regional variations of the 1983 drought in the West African Sahel

were still observed. Other studies that utilised AVHRR-NDVI data for general landcover classifications are varied, from using three different techniques PCA, temporal plots of NDVI values against time and multitemporal data classification to characterise the South American landcover types (Townshend *et al,* (1987), to determine forest cover and forest fragmentation (Ripple, 1994), to classify forest/landcover types and percentage cover from different physiographic zones (eg Stone *et al,* 1994; Zhu and Evans, 1994), to metrics derived from AVHRR data for determining percentage forest cover (De Fries *et al,* 1997) and to a hierarchical classification approach where summer peak vegetation was separated from NDVI response to spring peak vegetation (Lobo *et al,* (1997). In these studies either a few months or years of AVHRR data was utilised in a supervised classification approach supplemented with high spatial resolution satellite data or aerial photographs with ancillary information.

Another study that utilised AVHRR data for monitoring and explaining landcover dynamics in the drylands is Millington *et al,* (1994). In that study, when the relationship between AVHRR-NDVI and moisture availability was examined, it was shown that in many dryland areas, vegetation productivity is related to the supply of irrigation water rather than rainfall because the graph of temporal NDVI curves for irrigated and rainfed areas (forest) clearly showed marked differences (see Figure 5.5b). Other studies include the use of time-series 1-km resolution NDVI composites to examine the ISODATA clustering technique for three areas in the USA (Vanderzee and Ehrlich, 1995), broadscale classification of the whole African continent in a comparative approach between NDVI and surface temperature data at broad spatial scales (Lambin and Ehrlich, 1995; Lambin and Ehrlich, 1996), sub-African landcover changes using

AVHRRR and surface temperature (Lambin and Ehrlich, 1997a), the use of socio-economic data with AVHRR data to create models that will identify the driving forces and mechanisms of landcover changes (Lambin and Ehrlich, 1997b), and the use of NDVI from PAL dataset in conjunction with MSS data to determine changes in land cover around major East African wildlife reserves (Serneels *et al,* 2001). Although from the different approaches utilised only fairly good results were achieved at broad scales, a general consensus is that NDVI time-series data were shown to give better results if averaged over longer periods especially when determining periods of important vegetation productivity (Seney, and Elliot, 2000). Furthermore, Serneels *et al* (2001) indicated that when simple image differencing technique is applied on such coarse resolution NDVI data, residual images will indicate areas that are subject to changes rather than delineating exact boundaries of changed areas because small spots are often not detected.

Other studies demonstrating the potential of NDVI data from AVHRR in climatic studies are varied. Schmidt and Gitelson (2000) for example, used data to distinguish different vegetation zones and temporal variability of vegetation. Srivastava *et al.,* (1997) on the other hand, utilised the AVHRR-NDVI data to assess the sensitivity of NDVI to varying climatic and land-use activities. While Li *et al* (2002) used the data to determine the relationship between NDVI and two climatic parameters (growing degree-days and rainfall), Lee *et al* (2002) on the other hand, evaluated the phenological patterns of vegetation from NDVI derived from AVHRR. Conclusions from these studies showed that different variations in vegetation biomass depends on precipitation, type or intensity of irrigation practice and other environmental factors (See Table 7.1).

In tropical and non-tropical regions different studies attempted the characterisation of dense forest areas with different resolutions of NDVI data from AVHRR together with ancillary information so as to provide accurate forest maps (eg Nelson and Holben, 1986; Laporte *et al,* 1995; Laporte *et al,* (1998; Lucas *et al,* 2000). Although most of the studies were able to produce forest maps of the studied areas, cloud contamination in the data hindered accurate estimation of forest types. Another similar study which utilised such NDVI data (eg Townshend and Justice, 1986) showed that although when NDVI data were plotted against time for different forest cover types, they showed characteristics profiled closely to their phenology, atmospheric effects limited accurate estimation of vegetation productivity despite further compositing. On the other hand, Millington *et al,* (1992) successfully mapped the forests and savannas in sub-Saharan Africa using 8 km AVHRR Global Vegetation Index (GVI) imagery. However, significant variations in the distribution of vegetation, especially Savannah woodlands, were attributed to climatic and human disturbances. Based on similar studies with coarse resolution AVHRR data covering central Africa, it was shown that with such coarse resolution data it is not possible to identify or differentiate changes in vegetation that are due to anthropogenic influences without supplementing with a finer resolution data like Landsat MSS or TM (Laporte *et al,* 1995; Justice *et al,* 1997; Laporte *et al,* 1998).

In drought studies two separate but similar studies that used NDVI data from AVHRR to determine the spatial extent of the Sahara Desert (Tucker *et al,* 1991b; Tucker *et al,* 1994) attributed expansion of the Sahara partly to drought due to climatic variations and partly to land mismanagement. Both studies showed direct correlation between primary production and NDVI and between NDVI and rainfall.

In the grassland of the sahel, the potential of biomass production was tested using NDVI and daily rainfall data (Justice and Hienaux, 1986). Although only a single year of data was utilised, the study showed that the range of NDVI values generally increased in the growing season with decreasing latitude. In other studies relating to drought, Hielkema *et al* (1986a) used the NOAA-6 and NOAA-7 AVHRR GAC 4 km NDVI data to illustrate the effects of the drought years in relation to rainfall data in Africa. The study indicated that primary production is generally closely related to rainfall in tropical savannas that receive between 200 and 1000 millimetres of rainfall. Henrickson (1986a), on the other hand, used such data for reflections on changes in vegetation conditions during the Ethiopian drought. The study showed that such distribution and change patterns in vegetation and their condition over changing seasons are strongly influenced by changes in topography. Reed (1993), however, used AVHRR-NDVI data in conjunction with Landsat MSS scenes utilising a simple image differencing approach and visual interpretation to identify drought affected areas in the United States. Due to the spectral and low spatial resolution of the AVHRR data the results obtained were very poor because results showed very little or no resemblance to the reference map used for the training sites. Hence, the study concluded that classification of low spatial and high temporal data such as AVHRR that is only supplemented with visual interpretation of high spatial resolution data such as SPOT, Landsat MSS or TM, will only be effective if ground truth information from the high spatial resolution data is utilised.

There are several studies that utilised AVHRR-NDVI covering Africa or parts of it for establishing the relationship between NDVI and rainfall. However, these studies also varied. For example, Malo and Nicholson (1990) used the data to establish a direct relationship between NDVI and rainfall while Davenport and Nicholson (1993) used the

data to study relationship between rainfall and NDVI for diverse vegetation types. Both studies showed that there is a strong similarity between temporal and spatial patterns of NDVI when annual rainfall is below 1000 millimetres. NDVI was also shown to be a sensitive indicator of the interannual variability of rainfall.

Studies on the relationship between NDVI and soil moisture also varied, from examining the variability of NDVI in relation to rainfall (Nicholson and Farrar, 1994), to examining the relationship of NDVI and soil moisture (Farrar *et al*, 1994) and to understanding the spatial variability of species richness (Oindo and Skidmore 2002). While the first two studies showed that, although the ratio of NDVI to rainfall in the southern African state of Botswana is several times higher than in either East Africa or the West African Sahel, the highest productivity and efficiency occur on the clay-rich vertisols soils and the lowest on the sandy arenosols and solonchaks, the latter study attributed the variability in vegetation activity observed in that study to environmental factors indicated by Millington *et al* (1994) (See Table 7.1). Furthermore, from these studies, the use of time-series NDVI data was shown to minimise the effect of soil background especially when annual NDVI dataset is utilised. In a different study on the influence of the red and nearInfrared channels of the AVHRR, Huete and Tucker (1991) showed that soil effects on vegetation indices are divided into primary variation associated with the brightness of bare soil, secondary variations attributed to colour differences among bare soils and soil vegetation spectral mixing. The primary variations in vegetation according to the study are attributed to shifts in the soil line owing to atmospheric or soil composition, while the secondary variations are attributed to the artefact areas especially in the Sahara where there are increased vegetation index responses in the AVHRR-NDVI data. Other studies conducted in determining the relationship between NDVI and rainfall include using dekadal and monthly datasets

(Eklundh, 1998; Richard and Poccard, 1998). Although the studies were able to establish the relationship between NDVI and rainfall, the strongest relationship between NDVI and rainfall was obtained when monthly NDVI values were used in the equation and the weakest relationship was found with the 10-day datasets. Other approaches, such as the use of Coefficient of Variation (COV) images derived from AVHRR-NDVI data were also used in vegetation studies. For example, the use of COV images to determine NDVI sensitivity to seasonal and inter-annual rainfall variations (Milich and Weiss, 2000a) and for explaining the relationship between GAC NDVI and rainfall and potential evaporation (Milich and Weiss, 2000b). Others utilising Coefficient of Variation images derived from AVHRR-NDVI include, the characterisation of the Sahel (Milich and Weiss (1997), the assessment of the Saudi Arabian rangeland using linear regression (Weiss *et al,* 2001). Most of these studies indicated that islands of high Coefficient of Variations surrounded by lower interannual coefficient observed in the COV images is a sign of rapid, dynamic land degradation in the observed areas. This to a certain degree confirms this based on study of the Niger Delta in Nigeria and the impact of oil exploration activities on the environment (Boele *et al,* 2001a) (see Figure 5.5b). Furthermore, a highlight on the potentials of NDVI data from the PAL dataset (Smith *et al.,* 1997) showed that coefficient of variation images derived from AVHRR are very subtle in the measurement of vegetation variability, and can be used to compute vegetation amounts in different sets of sampled data (Milich and Weiss, 1997). In studies relating to crops and diseases, Maselli *et al* (1992) compared NDVI from AVHRR and ground data for the sahelian areas. Instead of using data accumulated during the rainy season, their study utilised NDVI data only in the first part of some rainy seasons but took into account the geographical variability in land resources and atmospheric conditions in the area. The study indicated that NDVI values estimated at

the end of July (mid rainy season) seem to be more useful for environmental monitoring and forecasting. However, Coefficient of Variation images derived from time series NDVI data may be more useful in areas like the northern savannah zone of Nigeria close to the Niger-Nigeria border or in the coastal and Niger delta areas because these are characterised by high variability in land cover (See Figure 5.5b). Other crop studies with AVHRR-NDVI data include environmental monitoring and crop forecasting in the sahel (Maselli *et al,* 1992), assessment of ecological conditions associated with the 1980/1981 desert locust plague upsurge (Hielkema *et al,* 1986b). Other such crop studies with AVHRR-NDVI from different environments include the investigation of the differences between the NOAA-AVHRR LAC and GAC NDVI images in relation to spatial variability in northern Tunisia (Rembold *et al,* 2001), and the use of the modelling approach to estimate large-scale maize production in the North American corn belt (Hayes and Decker, 1996). These crop studies showed that when using AVHRR GAC NDVI data in areas where the LAC data is not available, and especially over large areas, it is better to average the available GAC NDVI data because doing so will reduce the spatial variability of the NDVI and so give more satisfactory results. In studies relating to forest fires with AVHRR data in the boreal forest regions, these studies varied from utilising tree decision approach backed by ground truth information to classify fire affected areas (Leblon *et al,* 2001; Remmel and Parera, 2001), to using multiple NDVI composites data derived from AVHRR to estimate the areal extent of wild fires in Alaska (Kasischke and French, 1995) and to examining patterns of vegetation cover after fires (Kasischke and French, 1997). These indicated that fire studies with AVHRR data yield better results if the thermal channels of the AVHRR are combined with NDVI data. They noted that cloud and haze have distinct effects on the intra-seasonal AVHRR NDVI signatures, and hence, when an 8 km NDVI imagery is

utilised in such studies in places where there are heterogeneous patches of forests, there will be an over-generalisation in pixels for areas with very small vegetation surrounded by large areas of unvegetated surfaces. In demonstrating the spatial response of NDVI to precipitation and temperature, Wang *et al,* (2001) utilised nine years AVHRR-NDVI data. The study showed that precipitation is a strong predictor of regional spatial patterns of productivity based on NDVI. It also showed that the general spatial distribution of NDVI corresponds with the spatial pattern of average annual precipitation while the year-to-year variation of NDVI depends largely on the variation of precipitation. In measuring the effects of El Niňo/Southern Oscillations (ENSO) on ecosystems generally, Batista *et al* (1997) for example, utilised time-series NDVI data from AVHRR to ascertain if the dominant vegetation types in the Amazonian region could be differentiated with the inter-annual climatic variations due to changing environmental conditions. The study showed that monthly NDVI composites from AVHRR revealed seasonality in some vegetation types while in others the phenology varies little throughout the year. The study also showed that annual NDVI values showed a clear and significant reduction in warm ENSO periods with an increase in NDVI in the colder ENSO periods. Ochi *et al* (2000) on the other hand, reported significant reduction in World Net Primary Production (NPP) and crop production in the 1982-83, 1986-88 and the 1990-93 ENSO periods as a result of climatic variability (see Figure 2.2). McVicar and Bierwirth (2001), in the absence of meteorological data, used the NDVI data from AVHRR to assess the drought in Papua New Guinea during the worst ENSO period of 1997. In that study, McVicar and Bierwirth (2001) indicated that NDVI from AVHRR is a very efficient measure of ENSO-related effects. Other studies (eg Eastman and Fulk, 1993; Anyamba and Eastman, 1996; Kogan, 1998; Kogan and Wei 2000; Anyamba *et al,* 2001) demonstrated the potential of NDVI from

AVHRR in detecting the effects of climatic trends related to the ENSO phenomenon in time-series NDVI data that were analysed in PCA using standardised principal components. In disease-related studies using NDVI data from AVHRR over Africa and Europe, Green and Hay (2002) demonstrated the potential of AVHRR data from the PAL dataset for arthropod vector ecology and disease distribution. Data for monthly mean temperature and water vapour from selected ground meteorological stations that are considered to have adhered to the World Meteorological Organisation Instrumentation (WMOI) and collection standards were utilised in the study. Although the study achieved a high significant correlation between Maximum Value Composites (MVC), NDVI and monthly mean surface temperature observations, this is not an ideal comparison. The results of the study, however, showed that utilising monthly mean and maximum mean derived from the PAL dataset outperformed the MVCs derived from dekadal NDVI when analysing time-series PAL dataset.
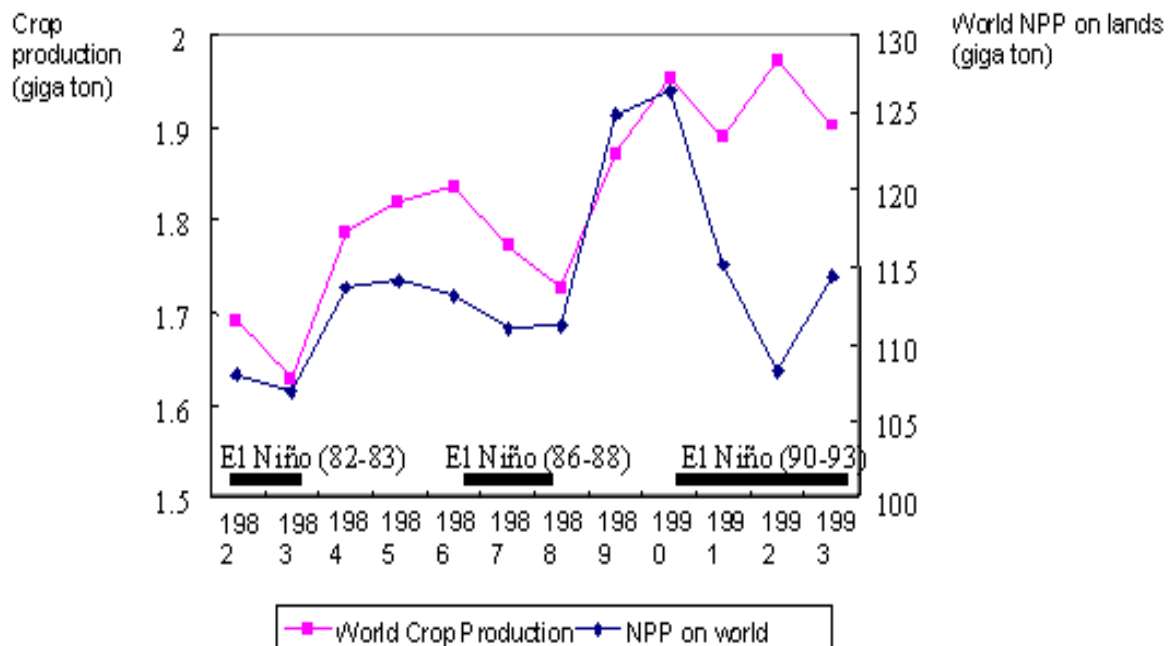
Figure 2.2 The effect of El-Nińo/Southern Oscillations on World Net Primary Production (NPP) and crop production (Adapted from Ochi *et al*, 2000).

On specific study with NDVI time-series data from the PAL dataset covering China, Young and Wang (2001) analysed changes in landcover with a simple image differencing technique supplemented by PCA. The study focused on changes in land-cover production rather than changes in landcover classifications which relied on ground truth information. It was shown from the study that yearly mean NDVI of end years utilised in simple image differencing approach can reduce further climatic contamination of the dataset when monitoring vegetation. Although absolute and relative areas of changes were discovered in that study, the results could not indicate seasonal or climatic changes such as drought or flood which may be related to the ENSO phenomenon.

2.4.3 An Overview of the NOAA-NASA Pathfinder Land (PAL) Dataset from AVHRR

Although there are number of coarse resolution datasets, particularly NDVI generated from the AVHRR instruments (see Section 4.3.2) and produced on different map projections, the Earth Science Committee jointly from NOAA and NASA were mandated to derive a consistently processed and calibrated global dataset from AVHRR that will include several parameters (James and Kalluri, 1994). This resulted in the generation of the Pathfinder Land (PAL) dataset. The PAL dataset contains 12 different parameters at 8 km resolution. It was generated from a very useful, scientific consensus algorithm which will enable the dataset to be used as a historical record for the study of global change (Smith *et al,* 1997). These parameters include calibrated radiances and brightness temperatures from the five channels of the AVHRR, the Normalised Difference Vegetation Index (NDVI) and the Sun and sensor geometry (Table 2. 2), and the NDVI data in the PAL dataset are scaled from -1 to 1. AVHRR sensors are normally

calibrated prior to launch, hence there is no proper on-board capability for assessing post-launch calibration for the visible and near infrared spectral Channels 1 and 2 respectively (Teillet *et al,* 1990). The use of NDVI, therefore, was intended to achieve the elimination of effects arising from differences of satellite scan angle, satellite azimuth angle with respect to the target, solar elevation and azimuth angles and variations in atmospheric conditions (Cracknell, 1997). However, all these normalisation factors do not get rid of the differences that arise from inherent differences between one AVHRR instrument and another. Earlier studies (eg Gallo and Eidenshink, 1988; Kindwell, 1991) have shown that NDVI calculated from pre-launch calibrations of the Channels 1 and 2 on board different AVHRRs yield fewer values and unreliable results than those calculated from post-launch calibrations. For these reasons, NDVI from the PAL dataset was generated in a consistent manner which included the post-flight sensor calibration and atmospheric corrections for scattering and ozone absorption (James and Kalluri, 1994). Although the temporal compositing method of NDVI (eg Holben, 1986) was applied to the PAL dataset so as to reduce further atmospheric effects such as cloud contamination, other studies conducted with AVHRR-NDVI data and particularly, the PAL NDVI data (eg Townshend and Justice, 1986; Maiden and Greco, 1994; Eklundh, 1998; Duchemin *et al,* 1999; Seaquist and Olsson, 1998; DeFries *et al.,* 2000; Liang, 2001; Young and Wang, 2001; Lee *et al,* 2002) however, indicated that there is still cloud contamination in the NDVI despite such methods of correction. Other studies (eg Viovy *et al,* 1992; Gutman and Ignatov, 1996; Roerink *et al,* 2000; Lovell and Graetz, 2001) therefore, devised other methods for minimising such atmospheric effects on the PAL NDVI data (See Section 2.3.1). However, studies conducted by Justice *et al* (1991a) have shown that the effects of

water vapour and aerosols from AVHRR although may vary spatially and temporally, are difficult to eliminate completely.

Table 2.2 The Pathfinder Land (PAL) AVHRR 8-km dataset parameters

Band/Parameter	Units	Geophysical Minimum Value	Geophysical Maximum value	Quantization
1.NDVI	Ndvi	-1	1	8bit
2.CLAVR Flag	-	0	31	8bit
3.QC Flag	-	0	31	8bit
4.Scan Angle	Radians	-1.0472	1.0472	16 bit
5.Solar Zenith	Radians	0	1.3963	16 bit
6.Relative Azimuth	Radians	0	6.2832	16 bit
7.Ch 1 Reflectance	% reflectance	0	100	16 bit
8.Ch 2 Reflectance	% reflectance	0	100	16 bit
9.Ch 3 btemp	Degrees (K)	160	340	16 bit
10. Ch 4 btemp	Degress (K)	160	340	16 bit
11. Ch 5 btemp	Degress (K)	160	340	16 bit
12. Days of Year	DDD.HH	001.00	366.23	16 bit

Adapted from James and Kalluri (1994) and Smith *et al* (1997).

Potential Applications

The main applications of the PAL dataset varies from studies in land science applications (eg Sellers *et al*, 1995; Justice *et al*, 1995), to studies conducted for land-cover classifications (eg Tucker *et al,* 1985; De Fries and Townshend, 1994; De Fries *et al,* 1998; Young and Wang, 2001), to studies in assessing crop conditions (eg Maselli *et al*, 1992; Quarmby *et al*, 1993; Hayes and Decker, 1996; Rasmussen, 1998a), to studies about Net Primary Production (NPP) (eg Tucker and Sellers, 1986; Diallo *et al,* 1991; Prince, 1991a; Prince and Goward, 1995; Rasmussen, 1998b; Reich *et al,* 1999) and to studies for deriving land surface parameters for climatic modelling (eg Prince, 1991b; Tucker *et al,* 1994; Hall *et al*, 1995; Dabrowska-Zielinska *et al,* 2002). However, there are other specific studies on continental Africa and other places that utilised the AVHRR data generally in addition to other studies specifically using the AVHRR-NDVI from the PAL dataset.

The problems with the PAL Dataset

As with any data meant for research, the PAL Dataset has its unique problems. According to Smith *et al* (1997) three problems were discovered with the PAL NDVI data although they were later rectified, namely :

1. The visible and near infrared reflectances were not normalised for the variations in the solar zenith angle (SZA).

2. An incomplete atmospheric correction was applied to the dataset.

3. There was an error in the computation of the SZA due to a software coding error that caused the SZA error to be seasonally dependent and increase in magnitude with increasing time.

The maximum SZA error was ± 7.5 degrees for the earliest data year in 1981. The error was removed using a post-processing code developed by the processing team. After removing the errors a test was conducted and it was found that the revised SZA is within ± 0.2 degrees of its correct value. Another analysis was also conducted later to determine the impact of the three errors discovered on the PAL dataset after all corrections were duly effected on the NDVI and the reflectance parameters. It was discovered that when the corrected SZA was used later to renormalize the data including complete atmospheric correction applied to the NDVI, a typical NDVI value changed from its uncorrected value by 0.02 NDVI units, while Channels 1 and 2 reflectances were changed by about 2% and 3% respectively. Other later problems (See Section 4.7 and Appendix 4) relate to incorrect calibration of Channel 1 and 2 of the AVHRR from the NOAA -14 satellite (Rao and Chen, 1996) used to compute the NDVI for the later years, for example, from 1995 to 1999. This problem partly necessitated the

re-computation of the NDVI data from 1995 to 2000 using new calibration coefficients (Rao and Chen, 1999), and the old data was replaced by the re-computed data in the NOAA/NASA archive (See Appendix 4).

2.5 Other vegetation-related studies conducted with remotely sensed data across Nigeria

Very few studies concerning vegetation were conducted specifically covering the whole of Nigeria using remote sensing after the political independence of Nigeria from Britain in 1960. This is partly due to the cost of high spatial resolution satellite data. However, there are studies covering certain parts of the country that used digital and analogue remotely sensed data. There are also other studies on Nigeria related to vegetation conducted with non-remote sensing techniques that were also found in the literature. One of the earliest studies using remote sensing in Nigeria was on vegetation mapping using radar. This was a project of the Federal Government of Nigeria in 1976 through the Federal Department of Forestry for the mapping of vegetation associations with emphasis on some specific forest reserves at a scale of 1: 250,000. The project was documented by Trevett (1978). Although radar imagery will be more relevant to geological studies rather than vegetation, among terrain features that were easily identified on that imagery are the aquatic grassland around Lake Chad due to its distinctive signature and because the boundary between the grassland and the shrub grassland follows the shoreline which suggests that there is a strong relationship between vegetation and geomorphic boundaries in the Lake Chad basin. Other land-cover identified are areas around Bendel State in the forest zone and also the coastal boundaries due to the distinctiveness of radar signatures of coastal dunes, older beach ridges, the saline coastal swamp and the river flood plains with mangroves. A study

conducted by Schneider *et al* (1985) using Landsat MSS and NOAA AVHRR data have also observed the changing patterns of both the water level and vegetation around Lake Chad basin due to increased agricultural activities around the lake. Lupo *et al* (2001) in monitoring landcover changes in West Africa with SPOT imagery observed changes around Lake Chad due to the anomalous rainfall that fell between June and August 1999 which caused flooding. This disaster was also said to have caused large human and ecological impacts because about 128,000 people were affected including 5,200 homes and about 165,000 hectares of agricultural land was submerged. According to Lupo *et al* (2001), the western part of Niger and Nigeria were also affected by heavy rains in September 1998 which led to flooding and which had direct economic impacts on over 20,000 people and resulted in cholera outbreaks and changes in the vegetation phenology of these areas. In another study on the identification of tropical deforestation fronts at broad scales, Lambin and Ehrlich (1997b) detected, on the basis of forest cover, the proportion and fragmentation of rural population increase. The study indicated that most of the deforestation hot spots in Nigeria are located in the western forest areas and the moist and lowland south-eastern forest parts of the country. On the other hand, deforestation red spots due to rural population increase and frequent forest fires were located around Kainji Lake and some parts of the north central areas of the country. Other more recent work with remote sensing data covering the whole of Nigeria was by Rogers *et al* (1997). Here, AVHRR data from the PAL dataset was utilised for a feasibility study in a supervised classification to investigate the potential for mapping landcover across large areas. Although the results achieved about 85 % accuracy in classification of the landcover the study only utilised a single year data from AVHRR. In the southern part of the country and particularly Nigeria's first capital Lagos, Adeniyi (1980) used sequential black-and-white aerial photographs for 1962 at

scale 1:40,000 and for 1974 at scale 1:20,000 to analyse the urban land-use change of Lagos city. Most of the changes identified were attributed to conversion of vacant and non-urban land to urban land with other intra-urban land-use changes. Ite and Adams (1998) undertook a study of the forest conversion in the Cross River state of Nigeria using 1967 aerial photographs, a landcover map for 1993 of the area and ancillary information. The study, which focused on the Mbe mountain complex close to the Adamawa plateau which is part of the Cross River National Park, indicated that the forest cover of that part of the country was being lost at an annual rate of 0.6 % per annum. The study further attributed the total loss of some forested areas and the accelerated rate of vegetation loss generally in this part of the country to human occupation and agriculture due to lapses in forest management and conservation policy implementation. The same view was held by Ite (1998) based on a study conducted about the reality of the tropical moist forest conservation in Nigeria. A similar land conversion which led to land degradation was observed in a study on the impacts on the natural and social environments of the Niger Delta area due to the activities of the Shell Petroleum Development Corporation (Boele *et al,* 2001b). In the western part of Nigeria, Salami (1999) used a combination of digital Landsat TM data of January 1991 and aerial photographs for January 1963 and December 1973 to assess the vegetation dynamics on the fringes of the lowland humid tropical forest of south-western Nigeria. This is an area where agricultural activities are advancing into the forested areas. According to the study, this annual practice by the cocoa farmers of western Nigeria is gradually depleting the forested lands. On a different study utilising multi-date aerial photographs and high resolution satellite imagery Salami *et al* (1999) detected some incursions in the forest reserves of south-western Nigeria mainly by farmers. This was also attributed to increasing population pressure and the need to feed this population. In

another study, Adepetu (1994) indicated that continuous cultivation in the forest zone of Nigeria has led to the decline in soil organic matter from 3.8 to 1.6 % within a period of seven years. The study undertaken by Badejo (1998) clearly stated that :

Due to human activities, the rain forest zone is shrinking in size as the savanna continues to extend to the south. In Nigeria, the forests of the northern part of the old Western and Eastern regions in the south have been replaced by savanna vegetation. These factors are inextricably linked with one another as they jointly influence the climate and agricultural potentials. For example, after deforestation and erosion have exposed the soil and organic matter loads have decreased, soil compaction as a result of grazing becomes intense. The little water remaining in the soil creeps up the fine capillary pores and evaporates.

This certainly will have some influence on the vegetation cover around those areas or even beyond. Based on another separate study regarding the causes of forest depletion in Nigeria generally, Osemeobo (1988), stated that :

There is plenty of evidence that the rate of forest depletion in the country may increase in relation to population increase, which is why, without adequate measures being taken, constraints in land-use could lead to shortened fallow periods, reduced crop-yields, overgrazing, indiscriminate burning of vegetation, extensive hunting, poor techniques of mineral exploitation and application of unconserving agro-technical practices for food production.

Boahene (1998) also highlighted some of the principal causes of deforestation in Tropical Africa generally. However, a coarse spatial resolution NDVI of 8 km from AVHRR can only indicate areas broadly, where such changes are probably happening and not necessarily caused by human activities. In the northern savanna zone of Nigeria, studies conducted with remotely sensed data includes Adeniyi (1985) who examined the possibilities and constraints of digital classification of landuse/landcover in the semi-arid area in the extreme northern part of the country. In that study, Adeniyi utilised a combination of Landsat MSS data on compatible tapes for November 1972, December 1975, June 1980, a radar mosaic of November 1976 at scale 1:250,000 and aerial photographs for November 1976 as well as other ancillary information in a supervised classification. The study was focused on the Bakolori irrigation project area within the Sokoto Rima basin in the semi-arid part of the country close to the Niger-Nigeria

border. The results of that study indicated that the differences in the density of tree canopy, mixed cropping of small farm plots, varying ground moisture conditions and atmospheric attenuation are the main factors hindering the classification of the remotely sensed data utilised in that study. This is because some landcover features were not classified accurately despite the different sets of high resolution of remotely sensed data utilised. In a different study, but also focused on the same area in the Bakolori irrigation project located in the Nigeria's northern sub-sahelian region, Pilon *et al* (1988) used an enhanced classification approach which combined image enhancement to isolate change with multi-spectral classification to identify change dynamics after the construction of the Bakolori Dam. The results showed that due to the construction of this large-scale reservoir, there was evidence of land degradation in flood plain areas downstream of the Bakolori Dam where flood plain cultivation had been reduced. In this part of north-western Nigeria, Mohammed *et al* (1996) also conducted a study to assess the vulnerability to desert conditions in an area within the Sokoto district using aerial photographs taken in 1972 and Landsat MSS imagery from 1976 and 1986 and other ancillary information in a GIS. The results indicated that there is an increase in sand accumulation, extensive erosion due to wind and water which have resulted in very low fertility and consistent decrease in crop yield, vegetation cover and livestock production in the area. In a similar study Ohamobi and Mohammed (1999) also observed similar conditions in this area when they used an aerial photograph taken in April 1972 and Landsat MSS imageries for February 1976 and February 1986 to monitor the degree and extent of land deterioration. However, based on the supervised classification results, it was shown that there was an increase in cultivated land in rainfed and irrigated areas, while shrublands used for grazing decreased due the encroachment of farmers into the grazing lands.

Other non-remote sensing studies in Nigeria include one undertaken by Thomas and Adams, (1997) in the north-eastern part of the country. This was focused on the flood-plain wetlands in the Hadejia-Jama'are river basin. The study indicated that the construction of dams around the area for irrigation and other purposes had a profound impact on the flood-plain ecology due to very poor performance of river basin planning. This view was also held by Adams (1985) in a study on the downstream impacts of dam construction at Bakolori on the River Sokoto in the north-western part of Nigeria. Based on a recommended policy programme in a study conducted by Silviconsult Ltd (1991) on fuelwood consumption for household energy in some states in the northern part of Nigeria, Cline-Cole (1997) undertook another study considering certain socio-economic factors and the dominant forms of land-use such as expansion of agricultural lands into woodlands and shublands and non-urban into urban areas in northern Nigeria. The study by Cline-Cole (1997) showed that the weak policy on land- use management including the close supervision of forestry institutions and their agents is the main factor contributing to the environment deterioration associated with forest resource depletion in this part of the country. A similar view was also maintained by Cline-Cole in 1998.

Jaiyeoba (1998) has shown that the absence of consistent sustainable soil is likely to have definite degradative effects on soil properties in the Nigerian savanna areas. Most studies found in the literature relate to general landcover changes, either in selected areas in the northern savanna or the southern forest areas and are never combined. Also most of the studies conducted utilised high spatial resolution satellite data in the form of aerial photographs and Landsat imageries of the selected areas for few years except one (ie Rogers *et al,* 1997) which utilised a single year AVHRR data for 1990 from the PAL dataset covering the whole country. The only study conducted with AVHRR-NDVI data

from the PAL dataset covering Nigeria (Rogers *et al* 1997) though broad in nature, is more likely to reveal the spatial patterns of NDVI relating to seasonal and annual variations across the whole country, in addition to a pattern of changes which may be shown to be due to localised events if such data for many years were utilised. However, despite the problems of the NDVI data from AVHRR as highlighted in the various studies reviewed, further assessments of the spatial variation of vegetation changes at very coarse scales by Townshend and Justice (1990) and Leprieur *et al* (2000) concluded that a substantial proportion of the changes detectable at finer spatial scale resolutions can also be detectable at coarser spatial resolutions.

2.6   Summary

This chapter highlighted the general sequence of operations in change detection procedures. The potential of this coarse resolution AVHRR-NDVI data for vegetation monitoring at global, continental and regional levels despite its radiometric and atmospheric effects was highlighted. NDVI data from the PAL dataset in particular, was also shown to have great potential for vegetation studies at a national level based on specific studies (eg Rogers *et al,* 1997; Young and Wang, 2001). It was recognised from this literature review that earlier studies conducted with AVHRR data relied on data from only one to two growing seasons. In later studies, more data are often utilised at global, continental and regional scales, and these studies, especially those conducted in Africa, highlighted the large inter-and intra-annual variations that occur in dryland vegetation cover. However, although the PAL NDVI data is of very coarse resolution, the degree of accuracy and results that will be achieved at national level will still serve as a provisional working document on which further or later studies can be based.

In Chapter Three the description of the main study area which is centred on Nigeria is presented. This includes its political trends after gaining political independence from Britain in 1960 until recently, the physical geography of the country including climate, soils, land-use and vegetation.

CHAPTER THREE

THE STUDY AREA

3.1   Introduction

This chapter aims to give an overview of the physical setting of the study area which is centred on the whole of Nigeria, but covers a rectangular area including parts of the Niger Republic in the north, Lake Chad in the north-east, Cameroon in the south-east, the Gulf of Guinea in the south and Republic of Benin in the west bounded within Latitude 04° 09' to 14° 00' N and Longitude 02° 00' to 14° 00' E (Figure 3.1). This area is covered by 138 rows and 174 columns of 8 km NDVI imageries from AVHRR used in this study. The main focus of this chapter is on the physical geography of the country which includes its climate, relief and drainage system, soils, land-use and vegetation. However, a very brief political history of the country is first given.

3.2   Brief political and administrative set up of Nigeria

According to Ijagbemi (1982), the political entity of what is now called Nigeria came into being in 1914. Initially, the country was composed of ethnic kingdoms and states of over 250 different tribes and different cultures until 1906 when it came under the control of British colonial rule. Its name was derived from the major river in the country, the Niger. The federal structure of Nigeria came into being after the London constitutional conference of 1953 and a subsequent conference in Lagos in 1954 which saw Nigeria as a federated unit of three regions, Northern, Eastern and Western, with a federal capital in Lagos. Nigeria was then given political independence by Britain on 1st October 1960.

Figure 3.1 Location of Nigeria covered by the AVHRR-NDVI data. The actual area covered by the data is 174 columns by 138 rows at 8 km resolution. This falls within Longitude 2° to 14° East and Latitude 4.15° to 14° North.

Due to persistent demand by the ethnic minorities in the Western region a third region was carved out from the Western region and the Mid-West Region was created. This brought the number of regions to four in 1963.

The first military coup in Nigeria in 1966 drove the country into a four-year civil war when the then Eastern region (renamed Biafra by the rebels) attempted to secede

57

from the federation. In 1970 when the war ended the then military leadership divided Nigeria into twelve administrative states. In 1975 there was another military coup, after which the country was reorganised into nineteen states on 3rd February 1976. The country returned to democratic rule in 1979, but by December 1983 the military took over power again. In 1989 two more states were created from the existing ones which brought the total number of states in Nigeria at that time to twenty-one. In 1991 the military leadership carved out nine new states from the existing twenty-one states bringing the total number to thirty. Although the then military leadership promised to hand over power to a democratically elected government in 1992, this was delayed until 1993. The military, however, cancelled the Presidential elections in June 1993, and the military leadership came under international pressure. The military leadership hand-picked a provisional civilian president who was deposed barely two months later. In 1996 the thirty states as at 1991 were reorganised and six more states were created to make the total number of states in Nigeria at present to thirty six (see Figure 3.2). The country once again returned to democratic rule in 1999 where a President, State Governors and other elected public officers were sworn-in on 29th May 1999.

3.2.1   Socio-Economic Characteristics of Nigeria

Although Nigeria is recognised as the most populous country in Africa, the exact size and distribution of its population have been a matter of great political controversy within the country. The 1963 census recorded 55,670,055 people; the results of a 1973 census were rejected by the government due to irregularities discovered. The UN, the World Bank, and the Nigerian government in the late 1980s estimated the country's population to be well above 100 million. However, the results of the 1991 census showed a total of only 88,514,501. In 2001 Nigeria's population was estimated at

126,635,630, giving an average density of 137 people per sq km (355 per sq miles). It was also estimated that around 43% of this population live in a urban areas while the greater proportion lived in rural areas. The population growth rate in 2001 was estimated at 2.61% (Encarta Encyclopedia 2002).

Nigeria was traditionally an agricultural country, providing the bulk of its own food needs and exporting a variety of agricultural goods, notably palm oil, cocoa, rubber and groundnuts (peanuts). By the 1970s oil had replaced cash crops as the major source of foreign exchange. After oil prices collapsed during the 1980s the federal and state governments embarked on ambitious development programmes aimed at diversifying the economy. Only some of these have proved sustainable and oil revenues remain the principal generator of economic activity in the country. However, the military leaders failed to make significant progress in moving the economy away from over-dependence on oil. The government of the day also failed to keep up with rapid population growth, and Nigeria, once a large net exporter of food, now has to import food and inflation is estimated to be around 60 % (Moser, 1995).

In 1999, Nigeria had a Gross National Product (GNP) of US$31,600 million (World Bank, 1999). This was influenced by the rising oil revenues. The Gross National Product (GDP) rose by an annual average of 6.9 % during 1965 to 1980. During 1980 to 1988, GDP receded by 1.1 % annually as oil prices and revenues dropped. In 1996, however, it grew by 3.25 %. By 1999 the GDP was estimated at US$35,045 million (US$280 per capita).
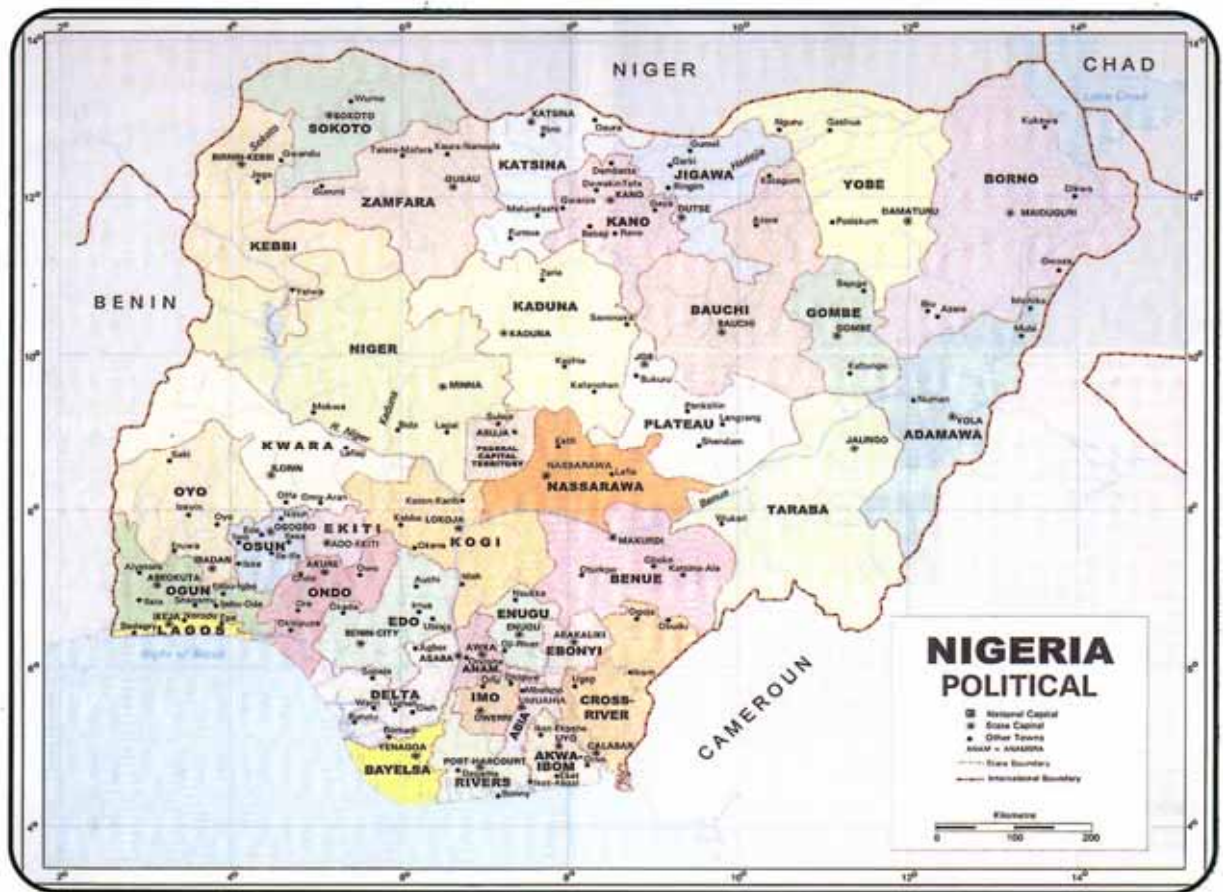
Figure 3.2   Political Map of Nigeria showing the existing 36 states of the Federation (Adapted from Mamman *et al,* 2000)

3.3   Climate

The location of Nigeria which is just a little north of the Equator benefit from two distinct climate, wet and dry seasons. However, according to Asangwe (1993), these wet and dry seasons are associated with the influence of the Inter Tropical Convergence Zone (ITCZ) from the moist maritime south-westerly monsoon from the Atlantic ocean and the dry continental north-easterly harmattan winds from the Sahara desert. The temperature varies considerably with the season as does the rainfall. The coldest month in Maiduguri the north can be between 20 and 8°C during the dry harmattan season around January and hottest can be over 40°C around April (before rain falls), while in the south the temperature can be between 30 and 17°C in

Warri (close to the Niger Delta). In January this can be between 30 and 19°C during the rainy season in August in the southern part of the country. The rainy season also varies, it can range from eight to ten months in the southern forest zones to less than four months in the extreme northern savanna (towards the sahel on the Nigeria-Niger border). However, the rainfall variation from the northern to the southern part is attributed to the fluctuation of ITCZ (Oguntoyinbo, 1982). The ITCZ reaches its northernmost position near the 19th parallel in mid-August, when sahel rainfall peaks, and after August, retreats rapidly southwards from June to September. This rapid movement affects the cumulative rainfall and crop production in west African countries and especially Nigeria (Ilesanmi, 1971). In Nigeria, the rains occur between April and October and the average rainfall ranges from about 2,495 mm (100 inches) around Port Harcourt on the Niger Delta to about 869 mm (35 inches) around Kano in the north (Figure 3.3). However, according to White (1983), the annual rainfall in the northern part of the study area (southern part of the Niger Republic and the extreme northern part of Nigeria) falling in the savanna vegetation zone of the country is not only (50 - 100mm) than in the rainforest and other parts of the southern forested areas of Nigeria, (ie the Niger Delta, the Cameroon southern part of Republic of Benin) but the distribution throughout the year is less even (Figure 3.3).
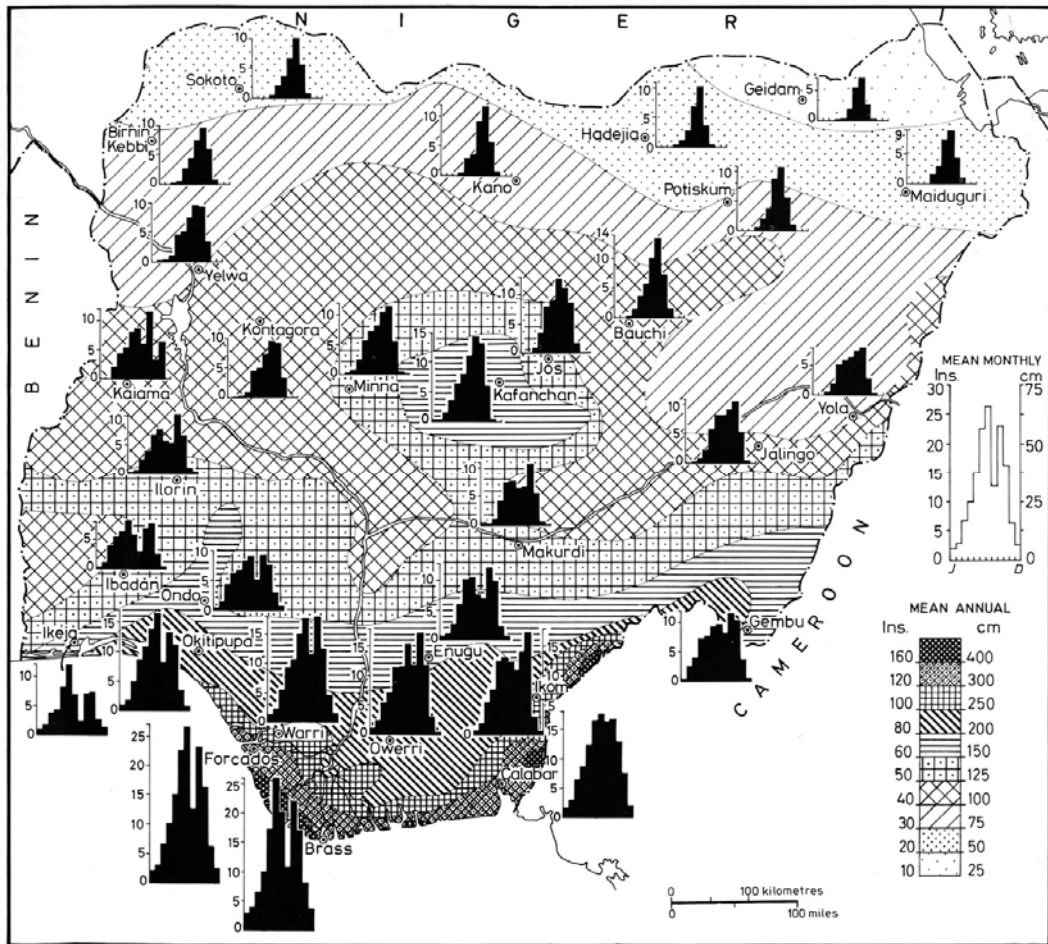
Figure 3.3   **Precipitation pattern across Nigeria** (Adapted from Oguntoyinbo, 1982**)**

3.4   Relief and Drainage System

The landscape of the country contains a variety of relief features, of lowlands which range from 150 metres in the Sokoto plains in the north-west to less than 20 metres in the coastal areas, and uplands of between 600 to over 1300 meters around the Jos plateau in the north central area and to over 3000 metres in the Adamawa and Cameroonian highlands in the south-east (see Figure 3.4). In his classification of Nigeria into zones, Akintola (1982) broadly split the country into seven divisions, and these are summarised in Table 3.1.

Table 3.1   A summary of the relief and drainage catchments of Nigeria (Summarised from Akintola, 1982 and Asangwe, 1993)

Broad physiographic division	Main relief features	Main rivers	Average elevation of relief features	Other remarks
The Creeks and the Lagoons	Mainly coastal shorelines and swamps	Yewa, Ogun, Oshun, Shasha, Osse, Benin and Imo rivers	Between 30 metres from the coast to about 50 metres inland	Relatively straight coastlines except areas around the Niger Delta which has indented lagoons
The Niger Delta	Mainly swamps and few islands of solid red earth	Andoni, Brass, Escravos, Forcados, Ramos, Bonny and Imo rivers	About 20 metres	One of the world's largest wetlands covering over 20,000 km^2 (Boele *et al*, 2001a). The area consists of rich biodiversity including many rare species (Ite, 1998), meandering creeks and river estuaries
The Coastal Plain	NW/SW trending scarps and cuestas with young sedimentary formations (Asangwe, 1993)	Benin, Imo, Ogun, Oshun, Shasha, Osse, Owenna and Yewa rivers	Between 30 to 250 metres	Gently undulating coastal plain with some swampy terrain
The River Basin Troughs	Udi-Nsukka plateau. rapids and falls, with a north-south scarp between Anambra and Cross River basins, and vale topography around the Gongola and Benue rivers	Anambra, Sokoto, Rima, Zamfara, Ka, Kontagora, Kaduna, Gaji, Katsina-ala, Shemanka, Gongola and Benue rivers	Between 100 to 350 metres	Streches from Sokoto in the north-west to Yola in the north-east. Dam constructions in the 1970s improved agricultural activities and provided good drinking water. Frequent soil erosion reported around rapids and scarp areas (Usoro,2000; Mbagwu, 2000)
The Inselbergs and North-central Plateau	Some sedimentary sandstone features and metamorphic rocks eg The Jos plateau, Kudaro hills, Kotoskoshi and Zaria inselbergs and Biu highlands	Kaduna, Sokoto, Rima, Zamfara, Ka, Mada, Gurara, Karami, Gongola, Hawal and Jama'are rivers	Between 300 to 650 metres and over 1000 metres around the Jos Plateau	Some volcanic hills with some crater lakes and ridge dykes
The Chad Basin	The Yobe Plains	Hadejia, Ngadda, Gana, Yobe, Yedseram, Katagum, Chalawa Shari, Mbuli, Goma and Jama'are rivers	Between 240 to 300 metres	Mostly uniform plain topography with some depressions extending from Gumel close to river Hadejia up to river Goma in the south of Lake Chad
The Eastern and South-eastern Highlands	Adamawa highlands, Bamenda and Mandara Hills	Taraba and Donga rivers	Over 1300 metres	Major surfaces are dissected with isolated hills and other metamorphic rocks
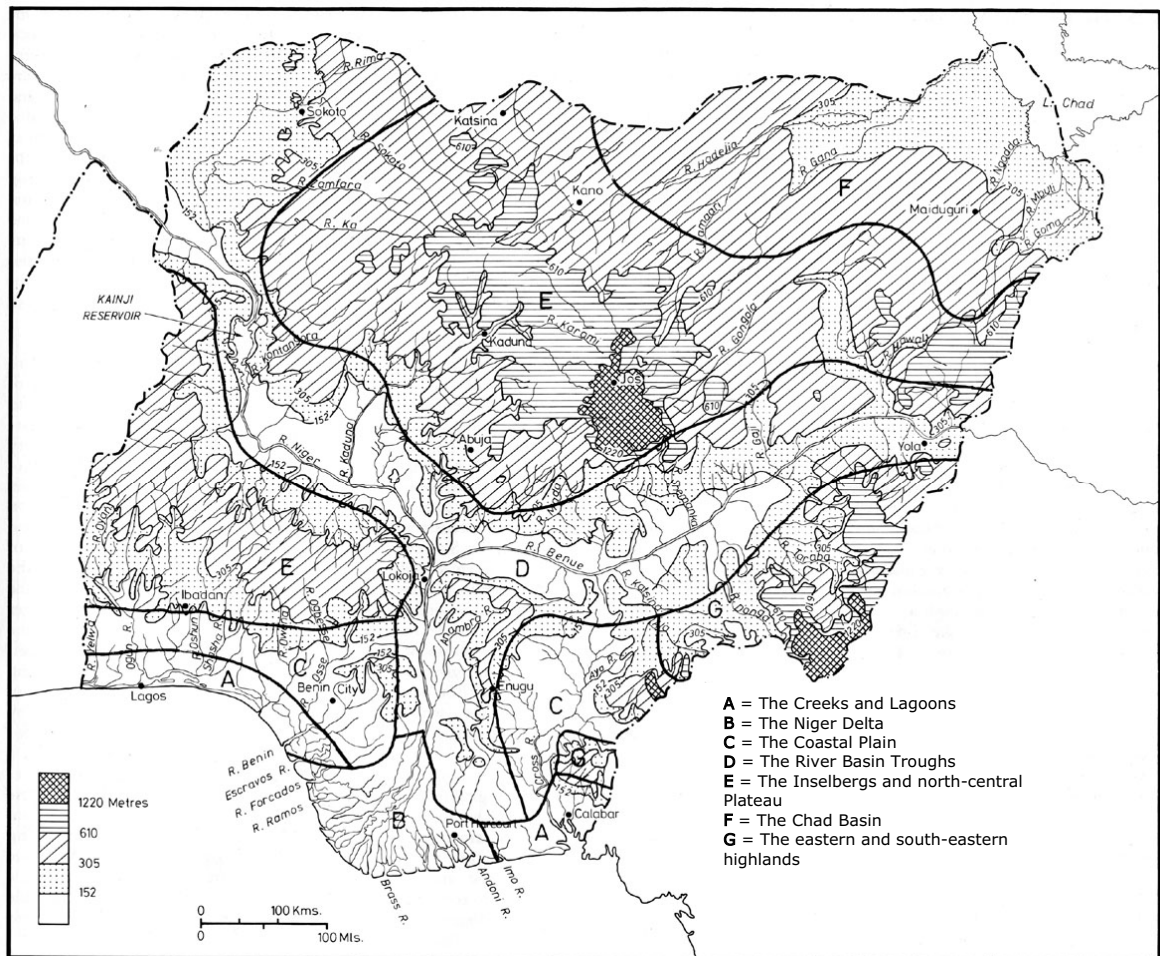
Figure 3.4 The Relief and River Catchments across Nigeria (Adapted and modified from Akintola, 1982)

3.5 Soils

Soils play important role in Nigeria's landscape because together with vegetation, they help in sustaining the environment. While the density of vegetation cover controls the moisture of the soil, the constituents of the soil matter assist in vegetation productivity. The distribution of soils types within the broad ecological zones of Nigeria is largely related to the parent rock which influences the soil depth, moisture condition, the texture and stoniness and the nutrient status as well as the weatherable minerals in the soil (Areola, 1982b). Accordingly, climatic factors particularly in Nigeria, affect the rate and depth of weathering of soils and their formation, taking into consideration the differences in climate between the humid southern part of the country and the sub-humid and arid north. Depending on the locality, the different soil types can be related to factors such as climate, vegetation lithology and topography. It is also possible to notice these relationships between soil types and vegetation as well as between soil and the local topography in areas of smooth relief. In some parts of the north-west of the country around Kebbi State or in some parts of the north-east around Maiduguri in Borno State where one can see examples of smooth relief, and the upper slopes mostly contain inactive soil, rather than the clayish type that can be seen in the immediate surroundings (Areola, 1982b), while soils on the lower slopes are formed by the washing down of material and are likely to be more stony and sandy.

In classifying soil types in Nigeria, Areola (1982b) broadly divided them into five classes. These are illustrated in Figure 3.5 and a summarised description of the broad classes is shown in Table 3.2.
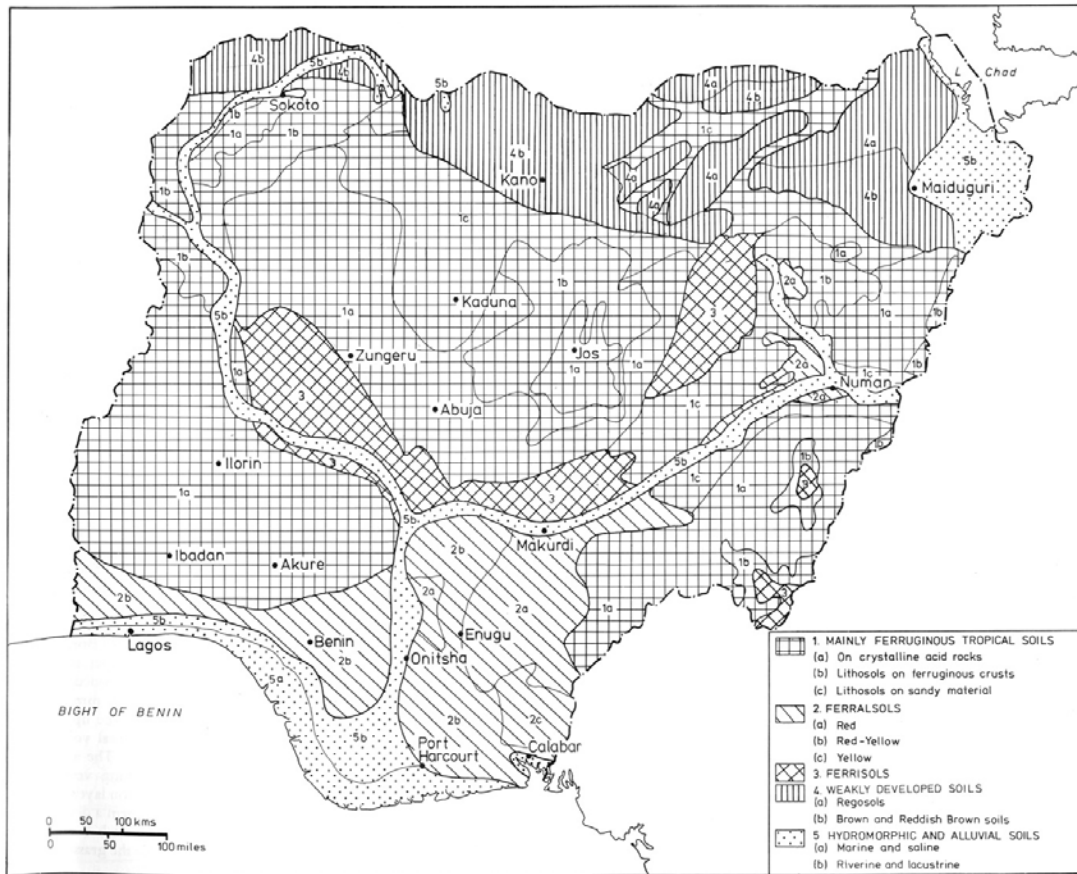
Figure 3.5   The main soil types across Nigeria   (Adapted from Areola, 1982b)

Table 3.2   A summary of the main soil types in Nigeria (Summarised from Areola, 1982b ; Adejewun and Adesina, 1992)

Broad Soil Type	Brief Soil Description	Predominant areas located	Other remarks
The Ferruginous tropical soils	Derived mostly from basement complex and old sedimentary rocks	Covers a large proportion of the country	This type of soils supports most of the food and cash crops produced in the country. Can be distinguished from the marked differentiation in horizons
The Ferralitic soils	Old , deep and highly weathered soils of the humid tropics	Mostly in some parts of the south-west and south-east of the southern forest zones of the country	The productivity of such soils depends on supply of litter from vegetation The clayish type of this soil is more fertile than the sandy ferralitic types. The sandy type soils are easily erodable when there is less vegetation cover (see effects of such erosion in Figure 3.6a).
The Ferrisol type soils	Soils of this type in the country are deep red and have a clay-enriched subsoil	Located mostly around the forest-savanna boundary of the country	Soil protected under dense woodland vegetation cover. High nutrient structure of the soil at boundary enables forest to flourish, and low nutrients permit the enclaves of savanna vegetation.
The weakly-developed soils	Regosols are the predominant of this type of soil and they are : were generally loose, drained and intensively leached	- mainly on the coastal sand ridge-barriers and in the Chad basin	Such soil types are productive with adequate water supply either from rainfall or irrigation as practised around the Sokoto river basins, Hadejia-Jama'are and Chad basin areas
	- desert type regosols of mainly brown and reddish-brown soils	- located around Kano and Jigawa, Sokoto, Kebbi and Zamfara as well as Kaduna and Katsina states.	Examples of the erosional effects on such weakly soils can be seen around Kebbi state in Figure 3.7 (*a* and *b*)
The Hydromorphic and alluvial soils	There are two types - organic	Located along the coastal creeks, valley depressions and enstuaries	- permanent by waterlogged
	- mineral	Located in river valleys and floodplains and Lake Chad basin	- seasonally waterlogged

67

(a)

(b)

Figure 3.6 Examples of gully erosion on ferralitic soils and lowland flooding on weakly developed soils in the savanna zones. Figure (a) is a site of gully erosion in Agulu-Anka in Anambra state, while Figure (b) is flooded millet crop around the lowland areas of Hadejia in Jigawa state. These seasonally affect the vegetation cover across Nigeria (After Mamman *et al,* 2000)

(a)

(b)

Figure 3.7 Examples of soil and gully erosion affecting vegetation cover in the Savanna zones.
Figure (a) shows a site around Zuru-Maga area in the south-east of Kebbi state, Latitude 11° 34.7' by Longitude 5° 10.10' (Magdelin 12 GPS), 27th December 1999. Note the advancing gully erosion towards the *Butyrospermum crassicaulis* (Kade) and *Parkia biglobosa* (Dorowa) trees and other shrubs. Figure (b) shows a site near Tungan-kawo village close to the Nigeria–Benin border in the south-west area of Kebbi state Latitude 11° 04.2´ by Longitude 4° 09.6´ (Magdelin 12 GPS). The gulley erosion here is at both sides of where the author was standing, 11th January 2000, and the eroded area is over 100 metres wide, with mixed vegetation dominated by *Combretum glutinosum* (Taramniya) and *Acacia Sieberiana* (Kaya) while in the foreground the vegetation consists of *Anogeissuds leiocarpus* (Marke) and *Buyrospermum crassicaulis* (Kade) trees (Photos by Sadiq Yelwa, 1999).

3.6 Land-use Categories

Land-use in Nigeria can be very complex due to the different cultural backgrounds of the people as well as their general attitude in relation to the environment. However, Nigeria was traditionally an agricultural country where its people practise a system of multiple cropping by growing different types of both food and cash crops within a particular vicinity. Although the land-use system across Nigeria is related to the different climatic zones as well as the types of soils occurring in different parts of the country, there are still certain types of crops that are specifically peculiar to certain parts of the country even though no clear-cut landuse system can be claimed to be in operation (Areola, 1982c). Based on these reasons therefore, Nigeria's land-use system based on the broad landuse classification map of Nigeria (Areola, 1982c) can be described as :

3.6.1 The Sokoto Fadamas

This is an extensive area covering the whole of the Sokoto Rima basin, an area of savanna lowlands with seasonal wind and soil erosion (see Figure 3.7). It also suffers largely from extensive grazing. These lowland areas called *fadamas* which cover most of the Sokoto plains are, however, very damp and fertile and are mainly used for growing things like rice, tomatoes, carrots and other vegetables immediately after the rains cease. The area covers most of the north-western part of the country including Kebbi and Zamfara states but also extends to Niger as well as Kaduna states in the north central region (Figure 3.8). The construction of dams such as Bakalori-Goronyo, Wurno, Gwai-gwaye and Mairuwa in the north-west, improved greatly the irrigation farming activities carried out within the basin especially in the *fadamas* (Adams, 1985). This is in addition to fishing by the locals in the reservoirs.
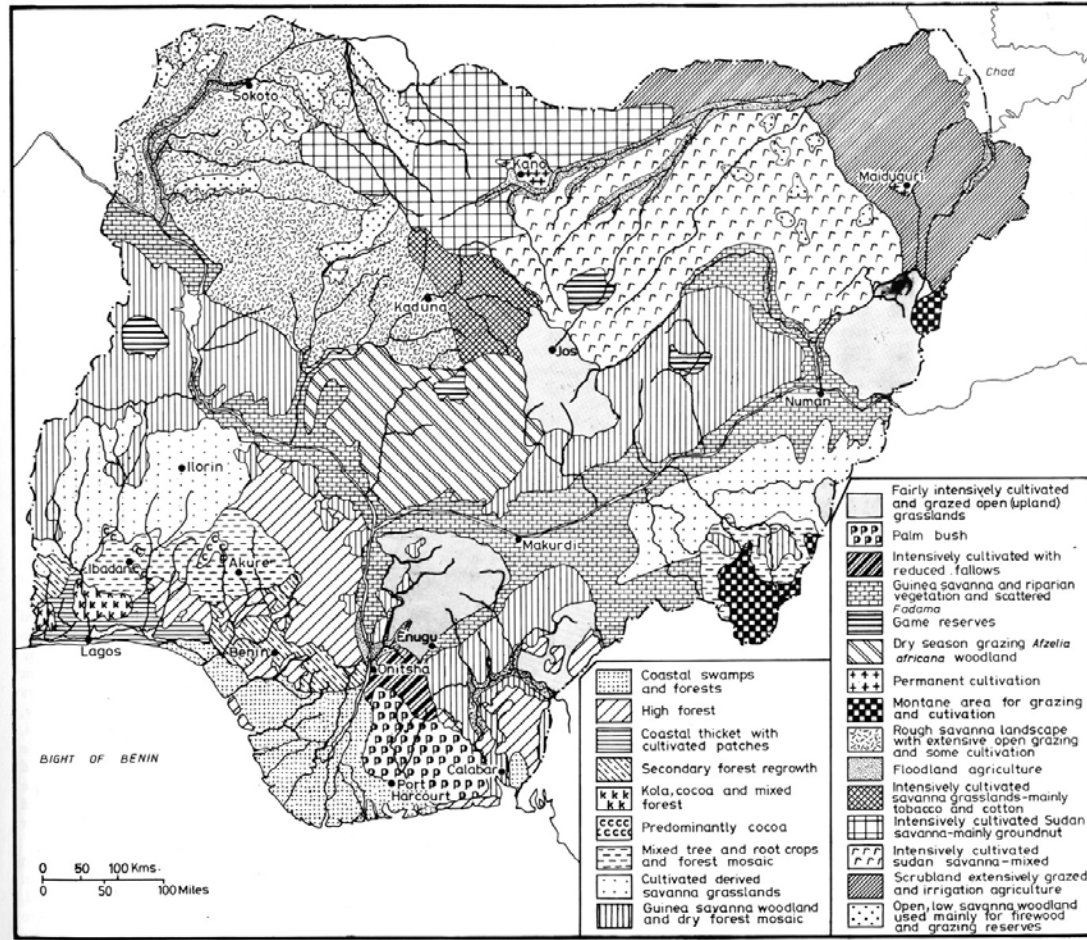
Figure 3.8   Land-use types across Nigeria (After Areola, 1982c)

During the dry season the types of crops cultivated by irrigation in these *fadamas* include rice, onion, wheat and vegetables (See Figure 3.9c). Other crops grown in these area include millet and sorghum (guinea corn), mostly in the rainy season. Due to the increasing population and the need to grow more food, parts of the regenerating woodland areas are increasingly cut down for farm extensions (see Figure 3.10a). In addition to some specific existing grazing reserves within this region, other parts of the region are also being heavily grazed especially after the rainy season (Figure 3. 10b) when there are fewer green plants.

71

3.6.2   The Groundnut Belt

The extreme northern part around Kano, which covers the whole of Kano, Katsina, and parts of Yobe, Bauchi and Kaduna states (see   Figure 3.2) is within the Sudan savanna zone and is referred to as the groundnut belt because the main crop cultivated around the area is groundnuts (peanuts), although cotton is also grown. Kano used to be the centre of groundnuts depot in Nigeria during the 1960s and early 70s when there this cash crop was a major export.

3.6.3   The intensively cultivated Sudan savanna and scrubland of Chad Basin

These areas comprise the extreme north-east of the country covering Borno states and parts of Yobe, Bauchi and Taraba states. Crops grown in these areas included cotton, tobacco, groundnuts and sorghum. However, in the 1970s the creation of river basin development areas such as the Lake Chad basin, the Hadejia-Jama'are river gave rise to the construction of dams such as Tiga and Challawa-Gorge (Adams and Thomas, 1996). This has made significant impacts on the environment and specifically, on the socio-economic status of the people, because intensive irrigation farming is practiced around these areas (see Figure 3.9b), and crops like rice, wheat and vegetables are grown. Fishing is also carried out in the lakes and reservoirs.

Accordingly, due to the changing land-use system along the canals and many of the smaller tributaries around the region, availability of rich wildlife especially in the Hadejia-Jama'are area has been reported. For example, the national and international importance of this area for Palaearctic and Afrotropical birds has been confirmed (Ash and Sharland, 1986). The area was also reported to be part of a wetland system in the Sahel which serves as an area of passage and wintering grounds for significant

numbers of Palaearctic migrant birds such as waterfowl, as well as important habitat for Afrotropical species (Stowe and Coulthard, 1990).

3.6.4   The permanently cultivated lands and the Montane areas

These areas comprise parts of Kano and Kaduna areas including other montane regions like the Jos plateau areas around Mubi in Adamawa State as well as the lower part of Taraba state. Land-use comprised crop rotation in some areas involving corn (maize), cowpea, sorghum and millet. The montane regions in Nigeria are known for growing tea and rice especially around the Mambila areas in Taraba state (see Figure 3.11b), as well as some form of crop rotation and terracing. The areas are often used for grazing by the normadic Fulani herders, while along the Benue and parts of the Niger rivers, in addition to fishing, the lowland *fadamas* are also utilised for growing seasonal crops like rice and vegetables.

3.6.5   The Woodlands of the Niger and Benure Troughs

In areas around the lowland middle belt region, the Niger and Benue troughs which are typically of riparian vegetation, the land-use system includes intensive cultivation of sorghum and beans. However, parts of the woodland areas have also been converted to arable farming where mixed farming and crop rotation is also practiced and large quantity of yams and cassava are produced. In recent times, areas mostly around the new Federal capital (Abuja) which includes parts of Plateau, Kaduna, Niger and Nassarawa states, most of the savanna woodland areas have been cleared for urban land-use. This must have affected the climatic pattern of the area and possibly, the energy flow especially around the Federal Capital Territory in Abuja, for example.

(a)

(b)

(c)

Figure 3.9 Examples of the dryland agricultural activities carried out in the *fadamas* and river basin sites within the sahel and sudan Savanna zones. Figure (a) is irrigated land in the sahel region of north-east Nigeria, Figure (b) is an irrigated field in the lowland area of Hadejia-Jama'are in Jigawa State while Figure (c) is an irrigated onion field inter cropped with corn (maize) and vegetables around Aliero in the north-western state of Kebbi, Nigeria (Adapted from Mamman *et al*, 2000).

(a)

(b)

Figure 3.10 Other examples of activities affecting the savanna zones. Figure (a) shows farm extension by cutting the regenerating *Piliostigma reticulatum* (Kalgo) shrubs while few *Parkia biglobolsa* (Dorowa) and *Diospyros mespiliformis* (Kanya) trees stand in the background. Figure (b) shows a typical overgrazing in the remaining sparse vegetation during the dry season in the north western part of Nigeria (Photo by Sadiq Yelwa, 1999).

(a)

(b)

Figure 3.11 Examples of some of the land-use activities carried out in the montane areas.
Figure (a) is a rice plantation in Batanje in Taraba state while Figure (b) is a tea plantation in the Mambila areas of Taraba state, Nigeria (Adapted from Mamman, *et al,* 2000).

The typical temperature of this area which was between 30 - 37° C and the two

seasons, rainy which was from April to October and dry, which was between

November and March (Abubakar and Mundi, 2000), have now changed to a

temperature of over 40° C while the two seasons vary between May to October for rainy and November to April for dry seasons respectively.

3.6.6   The cultivated derived savanna and sparsely cultivated woodlands

The land-use pattern of these areas which comprised part of Borgu in Niger state, south-western and   south-eastern Nigeria includes cultivation of crops like yams, cassava, tobacco and in some places, corn (maize). Areaola (1982b) described the soils of south-eastern part of this area (known as Yorubaland) as sandy loamy developed on crystalline rocks and very suitable for cultivating yams. Areas in Benue state mostly dominated by the Tiv tribe are also intensively cultivated with crops like yams and sorghum, while the areas around the Borgu game reserve close to Kainji Lake and areas around the shale vales of Cross-river state in the south-east which are sparsely populated, have similar vegetation cover due to low population (Areaola, 1982c). Similar crops are also cultivated with the exception of sorghum.

3.6.7   The palm bush and reduced fallow region

These areas are fairly densely populated and have serious soil erosion problems especially around Nsukka escarpments in Enugu state. However, areas of palm tree cultivation includes parts of Imo and Cross-river states. These are areas of arable farming with palm tree plantations (see Figure 3.12). Other cultivated crops include yams and cassava. Vegetables are also grown in some areas. However, the areas considered fallow around Onitsha in Anambra state have now been reduced due to the pressure on the land for more housing to accommodate the growing population as well as for more farmland to grow food (Okoye, 2000) for this increasing population.

3.6.8   The cocoa and kolanut growing areas

In the south-west and parts of the south-east which are the forest regions of Nigeria, different farm produce is being cultivated which includes cocoa, kolanut, yams and cassava. In the Abeokuta areas in Ogun state, for example, kolanut is the dominant farm produce and is inter cropped with yams and cassava. Around Ibadan and Ilesha in Oyo and Osun states respectively, the dominant crop cultivated is cocoa. Within the mixed secondary forests in Ondo and Ekiti states, these areas consist of arable farmlands where cocoa, coffee, yams and cassava are also cultivated.

3.6.9   The cultivated coastal thickets and deltaic swamp areas

These areas are strictly in the southern parts of the country and cover parts of Lagos, southern parts of Ondo and Delta states as well as most parts of Bayelsa, Rivers, Akwa-Ibom and Cross-river states (see Figure 3.2). The deltaic swamp areas covering most of the Rivers and Bayelsa states consist of mud flats with many fewer areas under cultivation. Although these areas used to be an agricultural and fishing zones (Adeyemo, 2000), the operations of the oil companies in recent times have made significant impacts on the land-use of the entire region (Boele *et al,* 2001a) so that only pockets of farmlands are operational. The areas referred to as the coastal thickets by Areola, (1982c) comprised parts of Lagos and Edo states where patches of land, though more densely populated than the other areas in the deltaic swamp areas, are cultivated with tree palms. In areas like the south-east close to the Nigeria-Cameroon border, in addition to cultivation of crops like palm trees and rubber, lumbering is also practised (see Figure 3.13).

(a)

(b)

Figure 3.12 Examples of land-use around the coastal forested zones. Figure (a) shows the PRESCO oil palm plantation around Saplele in Delta state, while Figure (b) shows the PAMOL rubber plantation also in Sapele in Delta state, Nigeria (Adapted from Mamman *et al,* 2000).

(a)

(b)

Figure 3.13 Examples of land-use activities that accelerate the depletion of the woodlands and forested areas. Figure (a) picture shows a site in the rain forest area of Western Nigeria around Ado-Ekiti where timber logging affects the limited forest resources around that area (After Mamman *et al.,* 2000). Figure (b) shows a truck transporting this type of timber from the forest-savanna mosaic areas to the sawmills around Mokwa in Niger state (Photo by Sadiq Yelwa, 1999).

3.7 The Vegetation (Ecological) Zones

Vegetation cover zones across Nigeria are generally closely related to the broad climatic north-south divide of the country (Areola, 1982a; Asangwe, 1993). The long dry season which is between October to May affects most of the northern parts of the country with intense dusty harmatan winds from the Sahara desert due to the effects of the north-east trade winds during the time when the ITCZ retreats towards the equator (Ilesanmi, 1971). However, the wet season is very short in the northern part of the country and the effect of the harmattan winds is very slight in the south with a longer period of rain compared to the north. All these are related also to the position of the ITCZ which is much closer to the southern part of the country which is mostly forested and closer to the sea. Rainfall is therefore the most influential factor in the distribution of vegetation across the country and is also characterised by the transition of the vegetation zones. In a wider perspective, Nigeria has two vegetation zones, namely the savanna which are mostly in the north and forests which are mainly in the south. However, although these can be sub-divided into different groups according to Areola (1982c), they are grouped into seven broad ecological types (zones) for the purpose of this study (see Figure 3.14) and are briefly described as :

3.7.1 The zone comprising Coastal and Mangrove Swamp Forests

This zone consists of the saline and the coastal swamp forest areas which are mainly closer to the coast. The vegetation in this zone covers areas from Lagos through parts of Ondo, Edo, Delta, Rivers, Akwa-Ibom and Cross-river states. The dominant vegetation type in the mangrove regions is red mangrove (*Rhizophera racemosa*) (Areola, 1982a) with a variety of different species. Average heights of trees varies from between 2 to 50 metres from the inner moist coastal areas to the drier outer zones of the coast. However, due to human disturbance most of the vegetation in the

coastal areas relegated to mainly dense thickets consisting of raffia and palm trees (See Figure 3.15). In the deltaic swamp forest around the previously protected Ogun forest reserve, there is some undisturbed vegetation consisting of slim trees of about 30 to 50 metres high. Recent studies have shown that this area is now being infringed by local farmers (Salami , 1999). However, parts of the lowland deltaic swamps are often disturbed and most of what remains are raffia palm trees especially along the valley swamps (Areola, 1982a).
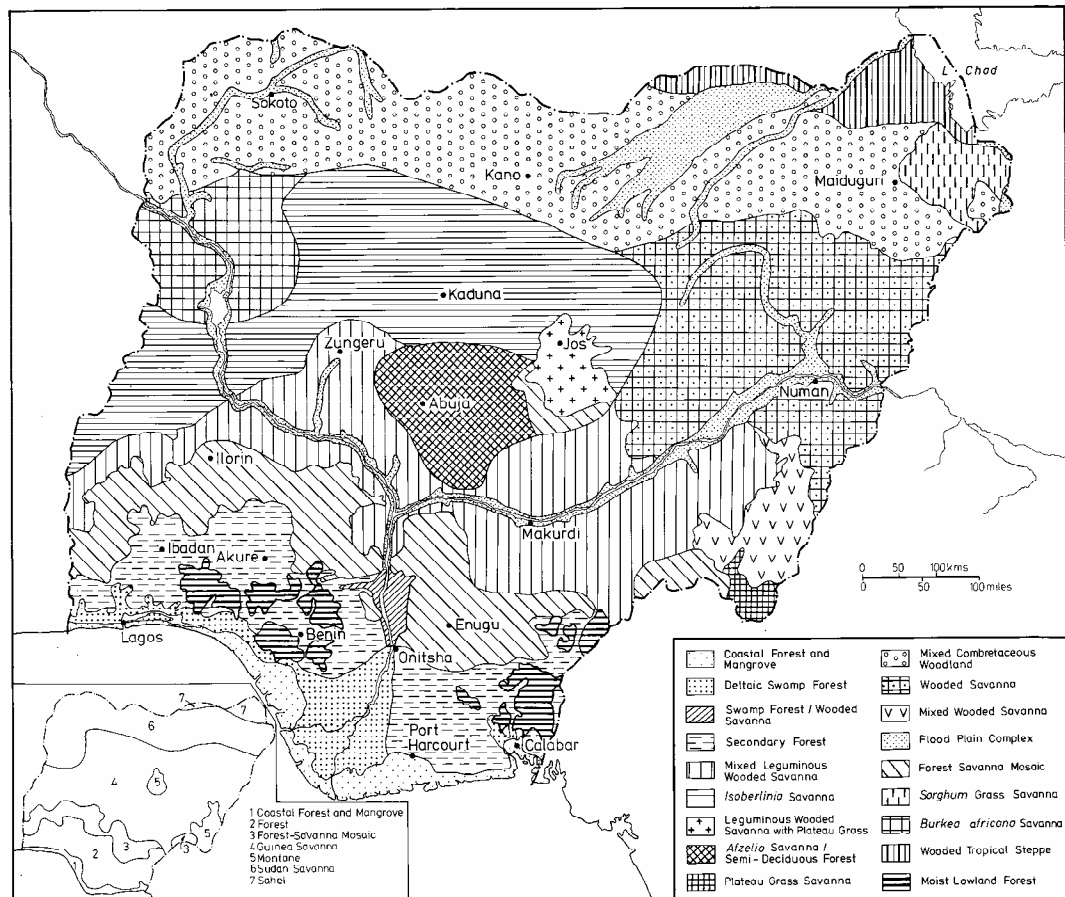
Figure 3.14 The Vegetation (Ecological) Zones of Nigeria (Adapted from Areola, 1982a)

3.7.2   The Forest Zone of Southern Nigeria

There seems to be an overlap between the coastal deltaic swamps and the main forest areas in Nigeria in terms of the constituent vegetation types. However, in this ecological zone which covers parts of the coastal states of Lagos, Ondo, Odun, Edo, Delta, Rivers, Ebonyi, Akwa-Ibom and Cross-river states (see Figure 3.2), most of the lower part of the forest areas consists of inaccessible swamps of green vegetation. This zone also extends from parts of Republic of Benin in the south-west to Cameroon Republic in the south-east. In addition to the common vegetation of bush thickets and tall grasses, the dominant species is raffia palm trees (Asangwe, 1983). In the upper part of this zone which is mostly tropical evergreen vegetation with secondary forests which extend to the lowland tropical rain forest covering some parts of Ondo, Edo and Rivers states the dominant vegetation consists of oil palm trees and mahogany including other varieties such as the Iroko, Obeche, Sapele wood and walnuts (Asangwe, 1993) (see Figure 3.16 and Figure 3.17). These are constantly being depleted (See Figure 3.13). Recent studies have shown that this area is experiencing rapid encroachment of savanna elements into the forest area (Salami, 1999) due to the intensification of agricultural activities especially by the cocoa farmers of the western states of Nigeria.

3.7.3   The Forest Savanna Mosaic Zone

In this zone, although most of the area consist of savanna vegetation mainly of woodlands, there is an element of overlap between the lower tropical lowland forest areas and this part of the savanna (Salami *et al,* 1991). Accordingly, Areola (1982a) referred to this area as having a characteristic vegetation pattern of a derived savanna due to the high rural population densities and the different types of shifting cultivation being practised. Due to the land-use activities in this zone which comprised shifting

cultivation and bush burning, most of the vegetation has been reduced from the patchy forest islands to derived savanna where fire-tender forest vegetation has been replaced by fire-tolerant savanna species (Areola, 1982a) in which the character of forest woodlands and savanna vegetation varies from place to place. However, in relatively undisturbed parts of this zone, tall grasses consisting of *Rennisetum, Andorpogon* and *Hyparrhenia* including trees of between 10 to 15 metres high, such as *Anogeisus leiocarpus, Daniellia oliveri, Afzelia Africana* (which can also be found in the tropical rain forest zones of the country)*, Parkia* and *Isoberlina doka* are found around in this zone (Aweto, 1993).

3.7.4   The Guinea Savanna Zone

This is the most extensive vegetation belt across Nigeria (Areola, 1982a; Asangwe, 1993). This ecological zone covers most of the middle belt region falling in parts of Benue, Kwara, Nassarawa, Kebbi, Niger, Plateau and Kogi States. It also extends to the upper parts of Anambra, Ondo, Edo and Oyo states. However, the dominant vegetation in the lower part of this ecological zone is secondary forest and mixed leguminous wooded savanna vegetation. Towards the upper portion of this belt at the boundary with the sudanean belt is the *Isoberlina* savanna vegetation (Areola, 1983) mostly covering parts of Kaduna and areas around the lower Kainji lake. In areas around the Federal Capital Territory in Abuja, the vegetation consists of semi-decidous forest and *Afzelia* savanna, while in the upper Jos plateau area in addition to plateau grass savanna, there are some patches of forest savanna mosaic and leguminous wooded savanna vegetation (see Figure 3.14). Examples of the savanna vegetation in some parts of these areas are shown in Figure 3.18.

(a)

(b)

Figure 3.15 Examples of the vegetation found in the Coastal and Mangrove Swamp Forest areas (Adapted from Asangwe, 1993). Figure (a) shows a site in the saline mangrove swamp forest around Calabar in Cross-river state. Figure (b) shows a site in the fresh water swamp forest at Oron in Akwa-Ibom state (Adopted from   Asangwe, 1993).

(a)

(b)

Figure 3.16   Examples of vegetation types in the Tropical Rainforest Region (Adapted from Asangwe, 1993 ; Mamman *et al,* 2000). Figure (a) shows a site in the tropical rain forest in the western state of Ondo. Figure (b) shows a site in the tropical rain forest area in Ikogosi, western Nigeria.
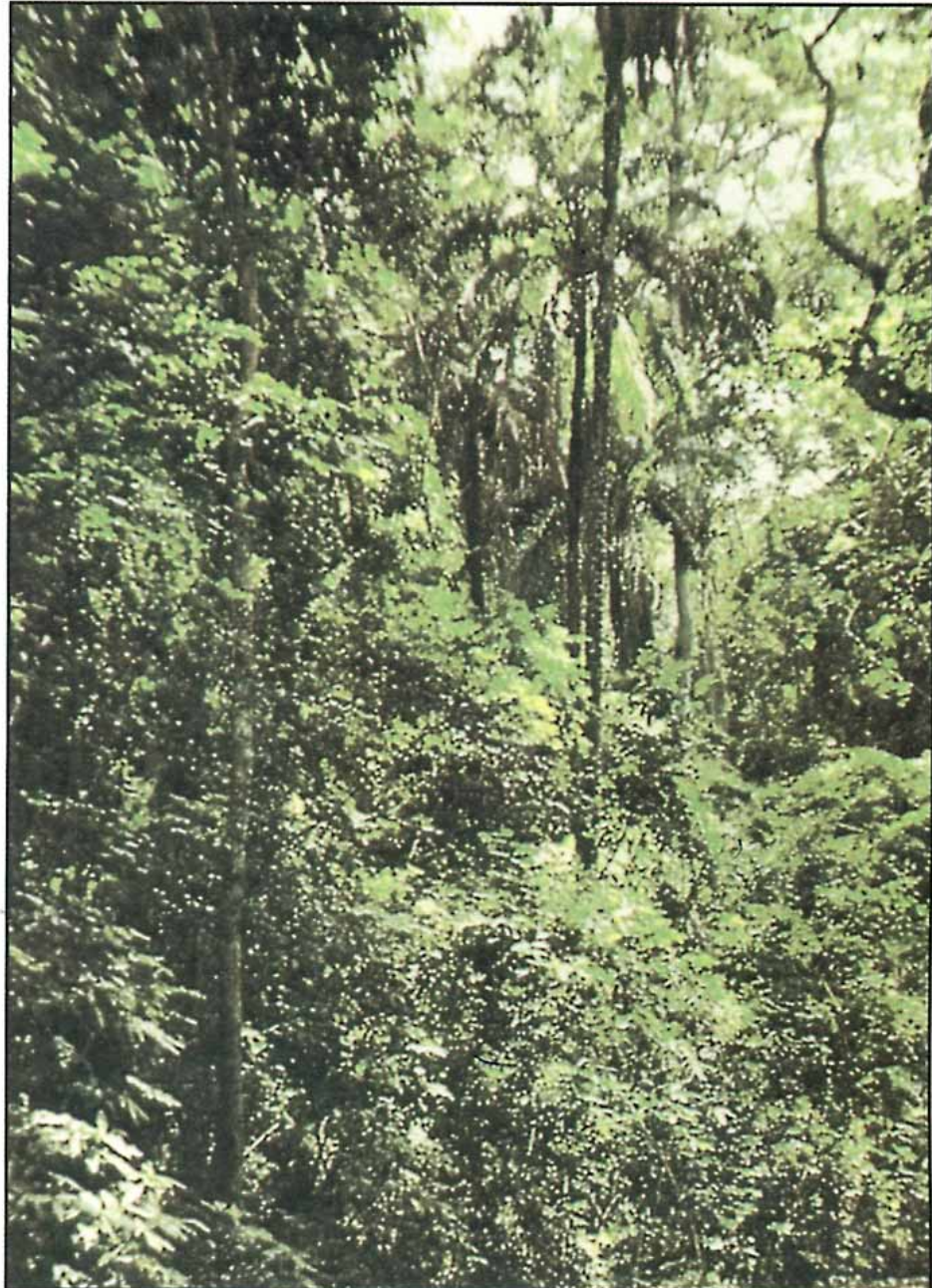
Figure 3.17 Example of a vegetated site in the coastal lowland forest zone (Adapted form Asangwe, 1993) . This part of the coastal lowlands around Eket in Akwa-Ibom state in Nigeria consists of palm trees and other plant species..

3.7.5   The Montane Zone

This zone covers a very small area in Nigeria and such montane regions consist of plateau grass and wooded savanna (mainly of *Isoberlinia spp.* species) with *Andropogon* and the *Ficus/Euphorbia* shrubland species found on rocky outcrops (Areola, 1982a). The two specific montane areas are found around the Jos plateau and the Mambila highlands in the north-east of the Adamawa plateau, over 1300 metres above sea level. Although no ground truth information is available for these areas, based on the altitude image (Figure 4.4) and the rainfall images (Figure 5.8) these sites are most likely to contain high photosynthetically active vegetation when compared with the vegetation of surrounding areas in the savanna zone across the country. It could be inferred that the vegetation variations of these areas when compared with all the vegetation zones across the country based on the coarse resolution 8 km NDVI imageries (Figure 5.5*b* and Figure 6.7) may be influenced by topography and soil moisture.
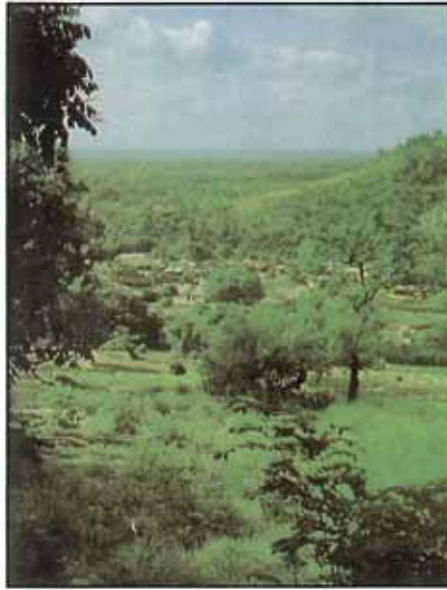
(a)

(b)

Figure 3.18 Examples of two sites in the Guinea savanna zone.   Figure (a) shows a site in the lower Guinea savannah region around Oturkpo in Benue state (Adapted from Asangwe, 1993) and Figure (b) shows part of the upper Guinea savannah region around Zuru area in Kebbi state (Photo by Sadiq Yelwa, 1999)

3.7.6   The Sudan Savanna Zone

In this zone, because of the much drier climate with an annual rainfall of between 400 to 100 millimetres as compared with the Guinea savanna with slightly over 1000 millimetres of average rainfall per annum (see Figure 3.3), the typical vegetation is mixed *combretaceous* woodland (Areola, 1982a). There are also other tree species like *Acacia* found in most places as well as pockets of woodlands. The Sudanean zone covers most parts of Sokoto, Katsina and Kano states as well as some parts of Kebbi, Zamfara, Niger, Bauchi, Taraba, Yobe and Borno states. There are other prominent types of tree species found in this zone especially in the lower part of the Sudanean zone. This includes *Butyrosperum parki, Andansonia digitata, Balanite aegyptiaca* as well as one of the most useful tree specie in this area the Acacia (*Faidebia albida*) which is in full foliage during the dry season when there is very little or no moisture around (Aweto, 1993) and serves as alternative fodder for the grazing animals. However, in recent times, due to the growing population there have been changes in the land-use systems (Dada, 1998). Most of the land-use activities are directed to the improvement of rural life through increased food production where farmlands are being extended and new ones was opened up by local farmers. There was also much road construction in the rural areas by the Directorate of Food, Roads and Rural Infrastructure (DFRRI) in Nigeria (Adalemo and Baba, 1993). Other activities include frequent bush fires and overgrazing by the nomadic cattle herders where the meagre vegetation cover in most of these areas is now threatened (see Figures 3.10, 3.19 and 3.20).

(a)

(b)

(c)
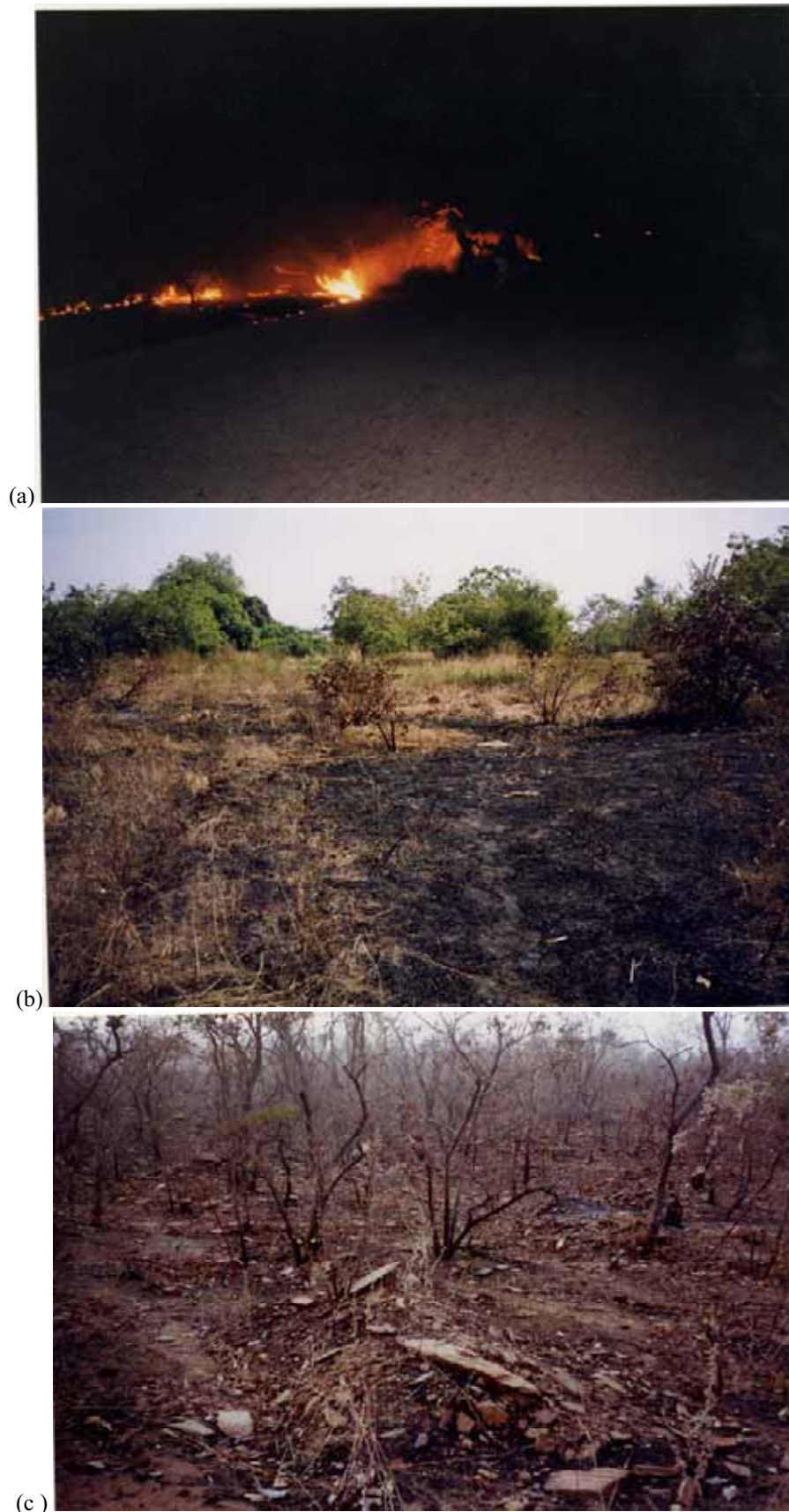
Figure 3.19 Examples of the indiscriminate bush fires that threaten the savanna vegetation.
Figure (*a)* is a burning site in the evening*, (*b*) is a partly burnt site and (*c*) is a burnt site of
regenerating mixed shrubs consisting mostly of *Detarium microcarpum* (Taura), *Ximenia americana*
(Tsada), C*ombretum glutinosum* (Taramniya) and *Annona Senegalensi* (Gwandar daji) within the
savanna vegetation zones (Photos by Sadiq Yelwa, 1999).

(a)

(b)

Figure 3.20 Further examples of activities partly affecting vegetation in the Savanna vegetation zones. Figures (*a*) and (*b*) are locations with few standing *Parkia biglobosa* (Dorowa) trees within the Guinea savanna zone around Riba and Dirin-Daji in the north-west part of Nigeria showing construction of rural roads (Photo by Sadiq Yelwa, 1999).

3.7.7   The Sahel Savanna

The sahel zone in Nigeria, the most arid part of the country, covers a small portion mostly in the north-eastern states of Borno and Yobe where average annual rainfall is below 500 millimetre, and there is a long dry season (see Figure 3.3). However, parts of the northern areas of Jigawa, Katsina and Sokoto states are becoming vulnerable. Studies on the expansion of the Sahara desert (Tucker *et al.,* 1994) have shown that more areas of the northern Sudan savanna are being engulfed by the sahel in Nigeria. Another study (Mohamed *et al,* (1996) also showed that the extreme northern part of the Sokoto plains in the north-western part of Nigeria is vulnerable to the sahel encroachment.

The construction of dams and reservoirs in some parts of the sahel areas which boosted irrigation farming in the dry season and some tree-planting activities, has improved the level of vegetation cover of these areas. In general though, the main vegetation in this zone is dominated by thorny and scattered *Acacia* trees and   shrubs such as *Commiphora Africana* and *Balanites aegyptiaca,* and   *sorghum* grasses mainly dominated by *Aristida stipoide* and *Choris prieurri* (Aweto, 1993). In some areas the land is bare with little or no vegetation (see Figures 3.21 and 3.22).

There is one other activity which is more socio-economic in character but relates to changes in vegetation cover in the savanna zones in Nigeria. Bulk collections of fuelwood from the woodland areas are being transported to the fuelwood depots/markets. These can be seen along roads linking towns and some cities and even within some townships (see Figure 3.23). While a greater proportion of the Nigerian population is concentrated in the rural areas, not every village or town in the country is provided with gas or electricity so that people can use them as alternative sources of energy.
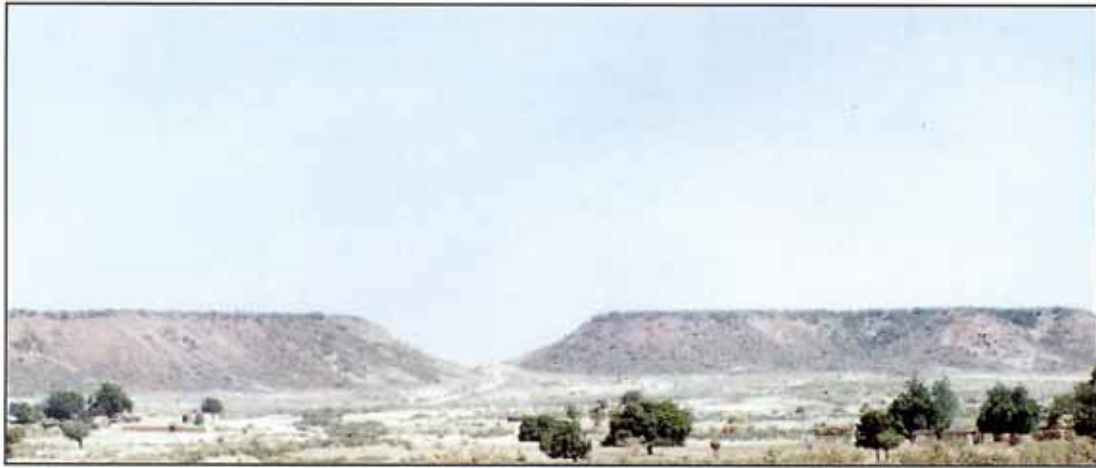
(a)

(b)

Figure 3.21 Examples showing types of vegetation found in the (wind eroded) north-western parts of the sahel zone. Figures (*a)* shows a location around Birinin-Kebbi with iselburgs and scattered trees and Figure (*b)* shows a site around Sokoto with the sand dunes in the background and few plants at the foreground. This is in the extreme north-west part of the Sudan savanna zone (Adapted from Asangwe, 1993).

94

(a)

(b)

Figure 3.22 Examples showing types of vegetation found in the north-eastern part of the sahel Zone. Figures (*a)* shows a location near Gwoza hills in Borno state. Note the scattered dry-looking shrubs around the hill. Figure (*b)* shows a site in the Yobe plains in Yobe state, north-east of Nigeria (Adapted from Asangwe, 1993).

(a)

(b)

(c)

Figure 3.23 Examples of other activities that can affect vegetation cover of the savanna zone.
Figures (*a)* shows a fuelwood market at Rijau in Niger state. Figure (*b*) is a fuelwood market along
Tambuwal-Sokoto road in Sokoto State and Figure (c*)* shows a pick-up van carrying fuelwood from
the woodlands around Kimo village in Yauri local government area to a selling depot in the townships
(Photos by Sadiq Yelwa , 1999).

In some places where these are provided, they are inadequate and the majority of the people cannot afford them due to their high cost. Accordingly, Cline-Cole, (1997), has shown that between 13.9 to 17.4 million tonnes of wood, 1.7 to 2.2 million tonnes of sorghum grass and about 112,000 tonnes of charcoal are used for domestic and non-domestic energy use in the drylands of the savanna region in Nigeria each year. This is an enormous amount of biomass consumption which certainly affects Nigeria's vegetation cover.

3.8 Summary

In this chapter, an overview of the study area centred on Nigeria covering the political trend of the country as well as its geography which included climate, physiograhic and drainage system, soils and land-use as well as its vegetation was presented.

From this overview, it was seen that the country after a period of political instability embarked on economic development on a relatively natural vegetation which is not properly managed. This is most likely to affect vegetation cover across the country. The different types of land-use in operation in different parts of the country, on different soil types and in different vegetation zones are also likely to have some impacts on the vegetation cover and in particular, the limited woodlands and forested areas. With its fast-growing population and people's general attitude to the environment, a gross GDP of barely $280 and a huge burden of foreign debts, it is unlikely that the vegetation resources of the country can be monitored systematically within short spans with high resolution satellite imageries which are expensive. However, with the provision of free coarse resolution NDVI data from the PAL dataset by NOAA/NASA it is possible to implement a periodic monitoring of the status of vegetation across the country so that vulnerable areas detected from the use

of coarse spatial resolution data can further be monitored using very few high spatial resolution satellite data. With this method, it is possible to create an inventory of the natural resources of the county which is not in existence at the moment.

In Chapter Four a general summary of the approach employed in conducting this study using the coarse resolution AVHRR-NDVI data from the PAL dataset is presented.

CHAPTER FOUR

GENERAL METHODOLOGY

4.1   Introduction

This chapter outlines the methodology and type of datasets employed in this investigation and encompasses issues of data availability, generation and manipulation. Whilst the research itself represents a methodological development, the primary methods required to underpin this are detailed in this chapter.

The methodology adapted in this study is divided into four sections. The first section outlines the methods used in selecting, acquiring and reorganisation of the satellite data used in the study. The second section outlines the procedures used in acquiring Digital Elevation Model (DEM) data, extracting a subset of the study area and deriving latitude and longitude images from it. The third section describes the methods used in acquiring rainfall data and subsequent creation of rainfall models. The models were used to estimate spatially and improvise complete annual rainfall data for 12 years from 1986 to 1999 (with the exception of 1989 and 1994 due to incomplete data) (see Section 4.3.3) covering the study area. This was done together with the subset DEM image data as well as the latitude and longitude images. The fourth section briefly describes the type of change detection techniques used in the investigation.

The subsequent methodological procedures after acquisition and reorganisation of the NDVI dataset, the DEM and rainfall data as well as their interrelationship in the assessment are summarised and presented in Figure 4.1.
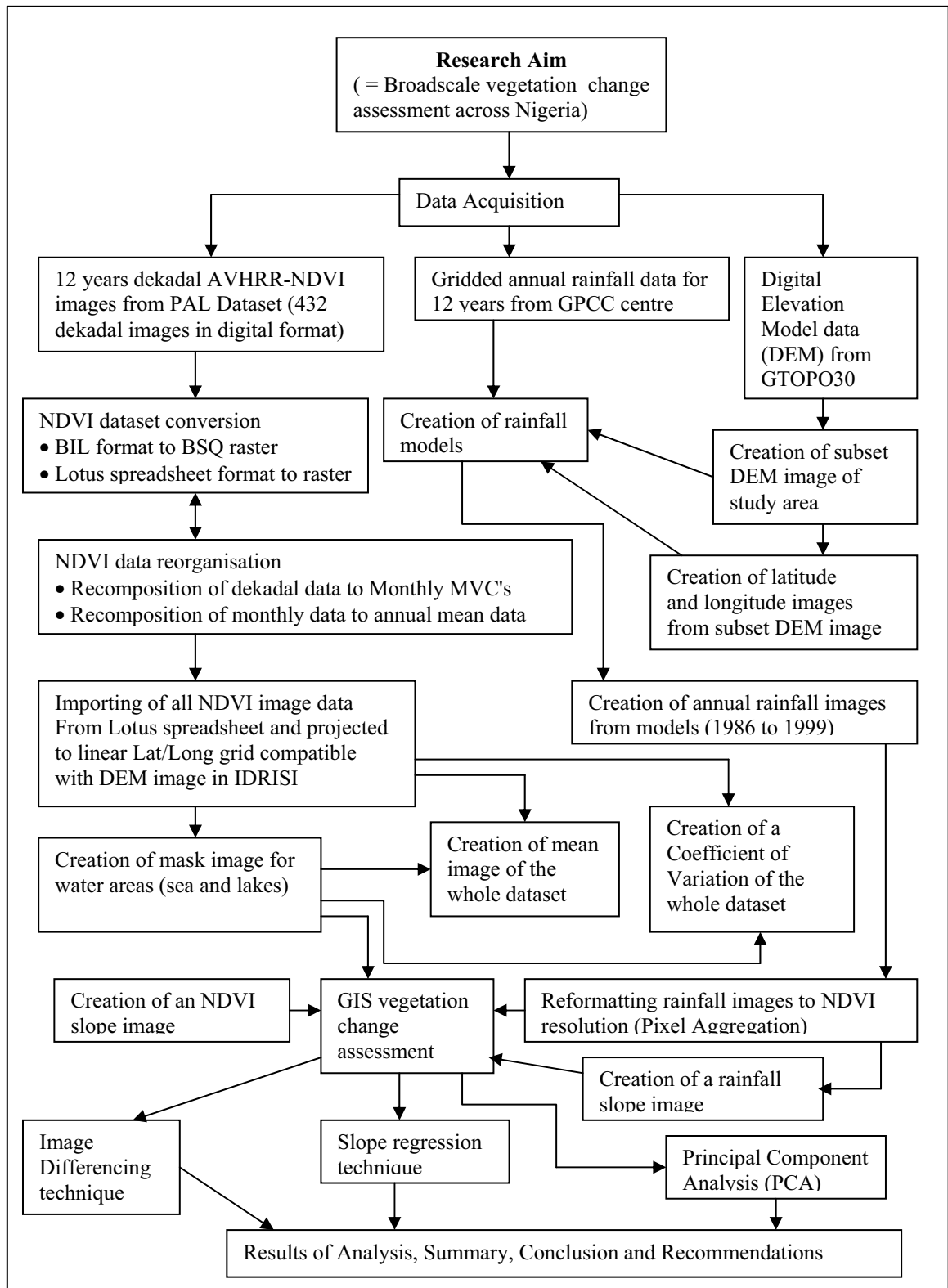
Figure 4.1 Flow diagram showing summary of the Methodological procedures

4.2   Software Packages

There were two remote sensing/GIS and two statistical software packages available for use in this investigation. The remote sensing/GIS software packages are ERDAS-Imagine Processing System version 8.3 (ERDAS, 1997) and IDRISI-32 Raster based Geographical Information Systems (GIS) (IDRISI, 1998). The two statistical software packages are SPSS and MINITAB.

4.2.1 Choice of Software

ERDAS-Imagine software has been used for data processing and analysis in many remote sensing studies (eg Stone *et al,* 1994; Senay and Elliott, 2000; Remmel and Perera, 2001) and can be used to perform more sophisticated remote sensing/GIS analysis but it is very expensive. IDRISI-32 software can also be used to perform all the analysis in this investigation, but it is cheaper and affordable by developing countries of low economic standing such as Nigeria as well as smaller organisations and educational institutions in most developing countries. IDRISI-32 was therefore the main remote sensing/GIS software used for the whole satellite and related data analysis. All the digital data accessibility ranging from satellite data, to precipitation (rainfall) to the GTOPO30 Digital Elevation Model (DEM) data was conducted via the World Wide Web (www), downloaded, saved and imported into the IDRISI-32 GIS software. The two types of statistical software available, each of which can be used to conduct the statistical analysis in this investigation, are SPSS and MINITAB. As matter of choice, MINTAB software was utilised in the statistical analysis. The final reorganisation, regeneration, as well as analysis of the whole dataset was conducted mostly in the Remote Sensing Laboratory, Department of Environmental Science, University of Stirling via an NT Operating system.

4.3   Satellite Imagery

For most successful change detection studies that involve remotely sensed imagery analysed within a GIS environment, it has been stressed that one should consider the spatial, spectral and temporal resolution of the remote sensing imagery (see Section 2.2.1) that covers the area being studied (Wilkie and Finn, 1996).

4.3.1   Imagery Requirements

Since this investigation is aimed at examining the potential use of coarse resolution NDVI data in providing a broad picture of changes in vegetation biomass across Nigeria, the use of expensive and better spatial resolution imagery such as Landsat Thematic Mapper (TM) and Multi-spectral Scanner (MSS) is not essential at the moment. Firstly, the temporally intensive time series analysis requires many data scenes, and there is the need to cover as a great a time period as possible to identify short/long-term changes in vegetation cover. Secondly, there is also the effect of weather/cloud cover which requires high frequency overpass to compensate for cloud cover etc, for which Landsat imagery is of less advantage compared with NOAA-AVHRR imagery. In terms of the cost of annual data from Landsat imagery, 4993 scenes at US$400 per scene are required for each year (assuming they are all available at 16-day repeat cycles over multiple seasons) to cover the whole of Nigeria at a total annual mean cost of US$2million (ie US$24million for the 12-year time series). This precludes the use of such expensive low temporal resolution imagery and favours the use of coarse spatial, but high temporal resolution imagery.

4.3.2   Image Selection

The identified satellite data considered most appropriate for this investigation therefore is the product from the Advanced Very High Resolution Radiometer carried on NOAA Meteorological satellites.

There are, however, different types of such coarse spatial but high temporal resolution datasets from this product. Most of them have to be purchased at minimal cost and reprocessed before being utilised in any investigation. Examples of such coarse resolution imageries that were used for continental and global studies are the Local Area Coverage (LAC) 1 km resolution AVHRR data (eg Loveland *et al,* 2000; Hansen *et al,* 2000), the Global Area Coverage (GAC) 4 km resolution data (eg Hielkema *et al,* 1986a; Hayes and Decker, 1996), the 8 km resolution dataset (eg Townshend and Justice, 1986; De Fries and Townshend, 1994; De Fries *et al,* 1995; De Fries *et al,* 1998; Defries *et al,* 2000), and a much coarser AVHRR data at 1 degree by 1 degree, 15-20 km and 64 km spatial resolutions in the global dataset known as the Global Vegetation Index (GVI) (eg Los *et al,* 1994; Hansen *et al,* 1996; Townshend *et al,* 1987; Townshend and Justice, 1990).

One of the main objectives of this investigation (see Section 1.2) is to use free and readily available coarse dataset from AVHRR, hence, the best choice of satellite data for this investigation would be the 8 km resolution AVHRR-NDVI data from the PAL dataset. This PAL dataset has been atmospherically and geometrically corrected and is made available free to the global research community (James and Kalluri, 1994; Smith *et al,* 1997).

The fact that this coarse spatial but high temporal resolution satellite data is obtainable free makes it very useful for developing countries with very low economic standing. Due to its versatility in terms of its high temporal resolution, it also became one of the

most frequently used satellite datasets in studies relating to climate, ecology and environment (eg Tucker *et al,* 1985; Townshend and Justice, 1986; Prince, 1991b; Millington *et al,* 1992; Eastman and Fulk, 1993; Millington *et al,* 1994; Laporte *et al,* 1995; Anyamba and Eastman, 1996; Lambin and Ehrlich, 1997a; Richard and Poccard, 1998; Senay and Elliott, 2000; Leblon *et al,* 2001; Young and Wang, 2001; Li *et al,* 2002). Hence, the final image data identified as suitable for this investigation was the free-of-charge 8 km coarse spatial resolution NDVI data from the PAL dataset.

4.3.3 Type of digital satellite data utilised

Based on the reasons stated in section 4.2 regarding choice of data, the main type of satellite data used in this investigation is the 8 km resolution dekadal Normalised Difference Vegetation Index (NDVI) in digital format. This is a product of NOAA/NASA Pathfinder Land (PAL) Advanced Very High Resolution (AVHRR) dataset. The PAL dataset contains 12 parameters including global and continental monthly and 10-day composites of Channels 1, 2, 3, 4 and 5 and the Normalised Difference Vegetation Index (NDVI) at 8km and 1 degree resolution (see Table 2.2). All these datasets are corrected for atmospheric and radiometric distortions (James and Kalluri, 1994) and are stored in the DAAC database in a physical file format called Hierarchical Data Format (HDF) (NCSA,1990). The NDVI data from 1986 to 1999 covering the study area (with the exception of 1989 and 1994 which have data gaps) was downloaded from the EOS Distributed Active Archive Centre (DAAC) between April and May 2000 and in March 2002.

This NDVI-PAL dataset is located at NASA Goddard Space Flight Centre's web site at

*http://daac.gsfc.nasa.gov/*CAMPAIGN_DOCS/LAND_BIO/GLBDST_main.html*).*

The original resolution of the NDVI data from AVHRR is 1 km referred to as Local Area Coverage (LAC). These are resampled to 4 km resolution called Global Area Coverage (GAC). There are also other much coarser NDVI dataset derived from AVHRR at different spatial resolutions (See Section 4.3.2) and utilised for general landcover classification for Africa (eg Tucker *et al*, 1985). However, it was the 4km GAC NDVI that was further resampled to 8 km resolution as contained in the PAL dataset that has been utilised here. These data were derived from the AVHRR 'afternoon' NOAA operational meteorological satellites (NOAA- 9, 11 and 14) ie covering the period from 1986 to 1999.

4.4   Acquisition of the NDVI PAL Dataset.

The downloading and subsequent processing of the NDVI data from PAL dataset is summarised in Figure 4.1 and detailed here. As part of the downloading procedure from the EOS DAAC website, the geographical coordinates for the subset area covering Nigeria (Longitude 2.00 to 14.00 degrees and Latitude 4.15 to 14.00 degrees), including the start month ie January and end month ie December, was entered for each year covered in the time series between 1986 and 1999. The NDVI dataset in digital format was then downloaded and saved in a directory created for each year.

There are three dekadal NDVI data layers for each month and 36 for each year. They are originally stored in the DAAC database in a compressed HDF format. For example, the whole dataset for 1986 is stored in one file as *avhrr_africa_ndvi_10_day_860101-861231*. After downloading all the dataset in HDF format covering the time series under investigation 1986 to 1999, they were uncompressed into Band Interleave-by-Line (BIL) format. For example, the dataset for 1986 in BIL format were uncompressed from *avhrr.ndvi.Intfaf.86101* to January 1-10, from *avhrr.ndvi.Intfaf.86111* to January 11-20,

and from *avhrr.ndvi.Intfaf.86121* to January 21-31 up to the last data in the 1986 folder

ie *avhrr.ndvi.Intfaf.861221* for December 21- 31, 1986. Each yearly folder was

similarly uncompressed up to the last dataset for 1999 (see Appendix 1a). All these

image data were originally produced in the Goode's Interrupted Homolosine equal-area

projection.

4.4.1 Importing and converting the uncompressed NDVI data to Raster Images

The uncompressed NDVI data from HDF format were first unzipped into Band

Interleave-by-Line (BIL) image files where they were saved in yearly folders. These

were subsequently converted into a series of dekadal raster images in IDRISI. This was

done by writing and executing a macro for each of the saved BIL image file folders (see

Appendix 1a) so as to import and convert each dataset stored in those yearly folders into

individual dekadal images. This procedure produced 36 dekadal NDVI images for each

year in each folder.

4.4.2 Re-composition of the NDVI dataset

In order to facilitate recomposition, extracting and subsequently interpreting the

information contained in the NDVI dataset in raster format, another macro was written

(see Appendix 1b) to convert all the 432 dekadal image data to American Standard

Code for Information Interchange (ASCII) format. These were imported into Microsoft

EXCEL to ease the process. Moody and Strahler (1994) showed that further

compositing of this type of dataset into monthly maximum NDVI images produces

dataset that will appear relatively cloud-free. For this reason, the Maximum Value

Compositing (MVC) method by Holben (1986) to reduce cloud contamination in the

data was adopted so that, for each three dekadal image data for each month in the

individual year folders the maximum value for each pixel was chosen to represent that pixel for that month. 12 MVC image data were generated for each month reducing the total number from 432 dekadal images to 144 monthly MVCs covering the time series. Lambin and Ehrlich (1996) have also shown that by using averages of long time series of coarse resolution data such as the NDVI derived from AVHRR, there is a possibility of reducing some minor inter-annual climatic fluctuations drop out, and the possibility of more long term climatic or other induced changes being discerned. For this reason a mean of the 12 monthly MVCs for each year was further generated to represent an annual mean NDVI image for that year in the time series. All these were saved as Lotus Spreadsheet files (in ASCII format) and subsequently imported into IDRISI as raster images in Latitude/Longitude grid so as to be consistent with the DEM image that was later used together with the NDVI dataset. Another macro was also written and run to aid the process (see Appendix 1c). A summary of the descriptive statistics of the dekadal, monthly MVCs and annual mean images of the datasets are shown in Appendix 2 (a-c). Samples of four dekadal images of the study area selected from the original 432 dekadal NDVI dataset falling in the dry and rainy season for the start and end date of the time-series dataset are illustrated in Figure 4.2.

4.4.3 Creation of a mask for water bodies

Although in the PAL dataset all water bodies were masked and assigned a value of one, for the purpose of this investigation, and in order to facilitate the change detection procedures, a different mask was prepared for this purpose. An NDVI raster image was used and classified by assigning a zero value to all areas covered by water bodies that was originally assigned a value of one from the original PAL dataset, and a value one for all land areas. This mask image is illustrated in Figure 4.3.
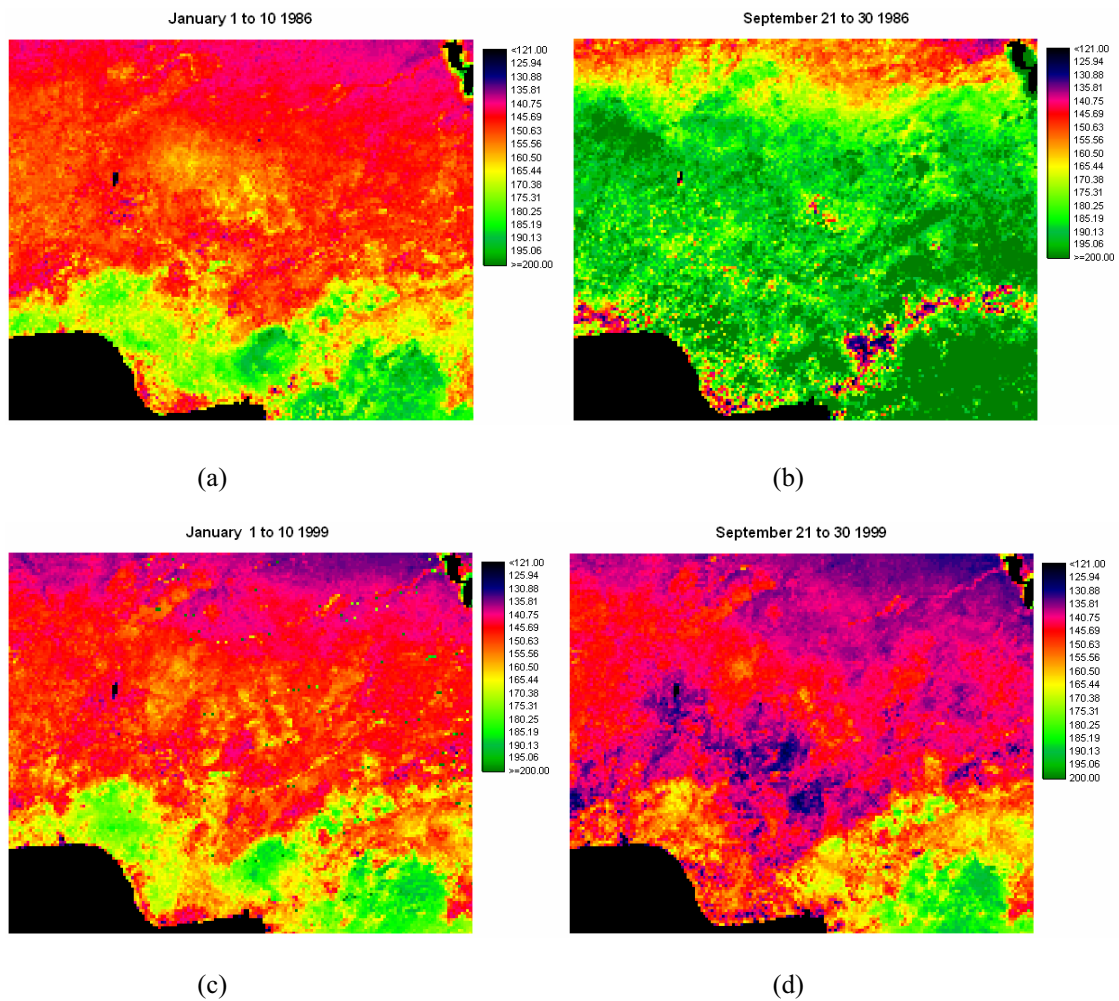
Figure 4.2 Samples of four original dekadal NDVI images of the study area. Image (a) is the first dekadal NDVI image in the timeseries covering the period from 1 to 10 January 1986 for the dry season period. Image (b) is the peak dekadal NDVI image in the first year of the timeseries covering the period from 21 to 30 September 1986 which falls in the rainy season. Image (c) is the first dekadal NDVI image of the last year in the timeseries covering the period from 1 to 10 January 1999 falling in the dry season, while image (d) is the peak dekadal NDVI image of the last year in the timeseries covering the period from 21 to 30 September 1999 falling in the rainy season. All these images were stretched for visual purposes. Note the differences between the two pairs of first dekadal and the peak period dekadal images each at the start and the last year in the timeseries. Note also the differences between the dry season images (January 1 to 10) and the rainy season images (September 21 to 30) of peak NDVI. In general, the images indicated that both the dry and rainy season images for 1986 contain more vegetation biomass compared with the 1999 dekadal images which showed a more stressed vegetation biomass (mostly in the savanna) both during the dry and the rainy seasons.

Figure 4.3 The mask image for water bodies area. This image was created for subsequent use with other images in the vegetation change analysis. 0 represents all the water bodies area ie Lake Chad in the north-east corner, Kainji Lake in the midnorth-west and the Gulf of Guinea in the south-west corner. 1 refers to land areas represented by NDVI values.

4.5 Acquisition of (Altitude) Digital Elevation Model (DEM) data

To facilitate the assessment in vegetation change of the study area together with the acquired NDVI dataset, Digital Elevation Model Data (DEM) was also acquired from the Global Topographic (GTOPO30) database created by the United States Geological Survey (USGS, 1998) at the EROS Data centre. The GTOPO30 dataset covers the world from Latitude 90° South to 90° North, and the Longitudinal extent is from Longitude 180° West to 180° East. The vertical units representing elevation above mean sea level are given in metres.

The data was produced at 30-arc seconds (about 1 kilometre resolution) with a horizontal coordinate system in degrees of longitude and latitude referenced to WGS84 Geographic Projection. This data was accessed via the USGS website *(http://www.edcftp.cr.usgs.gov)*.

Due to the physiographic information content of GTOPO30 digital elevation data and its value in geospatial applications, it has been utilised as an additional variable in the assessment of land cover changes (eg Wen and Tateishi, 2001), in the quantitative representation of mountain objects (eg Miliaresis and Argialas, 2002) and also in the delineation of drainage basins of the African continent (eg Danielson, 1996).

The GTOPO30 DEM data, however, has been divided into 33 zones called tiles to facilitate its regional and global distribution electronically. Because of this, it is not possible to input the geographical coordinates of the study area covering Nigeria as in section 4.4 for downloading the PAL NDVI dataset in order to download the DEM data of this area directly. The tile where the study area is located is in the north-west quadrant of Africa referred to as **W020N40** tile**.** This tile covers areas of the globe from -10 to 40° of Latitude and from -20 ° to 20° of Longitude. The tile was first downloaded, saved in a file and imported into IDRISI. The similar procedure outlined in

Section 4.4 in downloading the NDVI dataset using the geographical coordinates covering the study area was then adopted and a subset DEM data of the study area covering Nigeria was made from this tile. This subset DEM image (referred as altitude image in the remaining text) is illustrated in Figure 4.4.
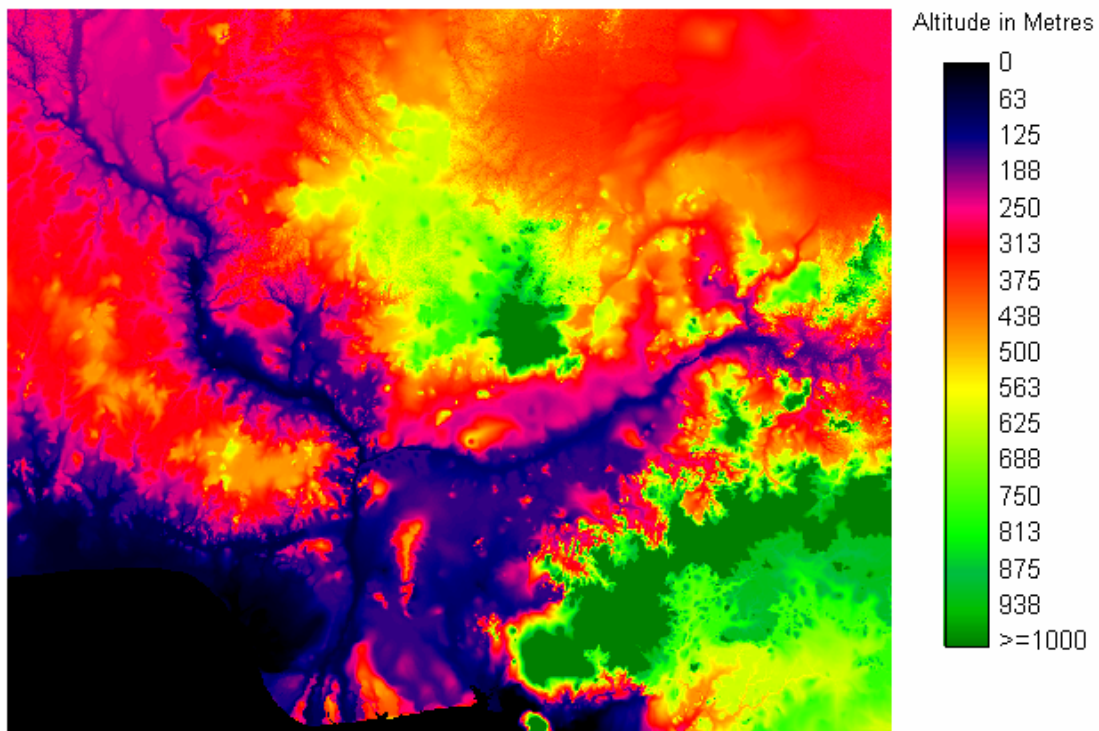
Figure 4.4 The Digital Elevation Model (DEM) image of the study area. The image is referred to as altitude image in the text. The image has been contrast stretched to allow more visual appreciation of the whole area. The black area in the south-west corner is the sea (Gulf of Guinea). River Niger in black and dark blue stretching from the north-west corner and River Benue from the north-east are very distinct. These two rivers meet around Lokoja in Kogi state and flow down to the Niger Delta in Rivers state, Nigeria. The Jos plateau is the dark green area in the central portion of the image. Adamawa Plateau in Nigeria and the southern Cameroonian mountains are the dark green areas in the south-eastern area of the image. Most of the dark green areas are equal to or over 1000 metres above sea level.

4.6 Acquisition of climatic (Rainfall) data

Due to the incompleteness of ancillary information such as climatic data in the form of rainfall figures from rain gauge stations across the whole of Nigeria, other sources of such data had to be sought. Ideally, NDVI should be correlated with the amount of water directly available for plant growth as opposed to estimated precipitation which even when accurate does not take into consideration surface run off and evaporation.

Two main sources of surrogate precipitation (rainfall) data covering the study area were identified via the world wide web (www). The first was the National Climatic Data Centre (NCDC) at NOAA (NCDC, 2000) and the second source was the Global Precipitation Climatology Centre (GPCC) in Germany (GPCC, 1998). The precipitation (rainfall) data in the NCDC archive was obtained from disparate sources dating as far back as the 1930s. Much of the rainfall data particularly for the African countries that has been collated by the then colonial masters were either not retained or their existence is unknown (NCDC, 2000). Accordingly, most of the rainfall data for Nigeria in the NCDC archive is inconsistent and has many gaps in most years. Their period range is limited to the 1970s and did not cover early or late 1980s. The GPCC, on the other hand, contained annual gridded point rainfall data in 1 degree and 2.5 degree resolutions in their database.

The rainfall data covering Nigeria in the GPCC archive has no data gaps but was only available from 1986 to 1999 at the time of sourcing. Although GPCC precipitation (rainfall) data is available in a gridded point format at a coarse resolution, it has been compiled from surfaced-based and satellite observations and has been tested on special studies such as the Oder river flooding in 1997 and the El Niño precipitation anomalies

in winter 1997/1998 (GPCC, 1998). Consequently, the GPCC rainfall data at 1° resolution was chosen as the primary climatic data to be used with the NDVI dataset for this investigation.

From the archive of the GPCC a similar procedure as described in Section 4.4 was used to subset and download 120 gridded points of annual rainfall figures covering the study area in ASCII format for each year in the time series under investigation. Because the rainfall data downloaded contained 120 gridded points in 1° resolution (in ASCII format) and not in two-dimensional map nature, it had to be converted into a spatial format. This should also be consistent with the NDVI dataset which has 24,012 points (pixels) at 8 km resolution. For this reason, the following procedure was adopted for the creation of yearly models to facilitate the production of complete rainfall data with 24,012 points (pixels) in 8 km resolution covering the study area for the same time period covered by the NDVI dataset.

4.6.1 Determining altitude values of the gridded rainfall points for spatial estimation of annual rainfall data

The first stage in the preparation of the yearly rainfall models was to determine the altitude point values of the respective 120 gridded rainfall points from the subset altitude image of the study area. For each of the 120 rainfall points (each point being the intersection of 1° of latitude and longitude), the cursor was moved over the altitude map window at the X and Y of the rainfall coordinate position and clicked. The altitude figure in metres was indicated and recorded for that particular point. By using this procedure, all the altitude points for the respective rainfall points with their latitude and longitude coordinates point were then acquired. From the 120 acquired gridded rainfall

data points, 115 incidentally are on the land. The remaining five fell in the water area (sea or lake), and these areas were subsequently masked out after the generated rainfall images. The second stage was to determine what variables were to be used as input in a multiple linear regression equation for creating the yearly models. The latitude, longitude and altitude were chosen as the first three variables as they are considered to be factors of rainfall. Using the three main variables (longitude, latitude and altitude), ten other variables were derived from their products and the numerical values of these products were calculated (See Appendix 3). This brought the total number of input variables to 13. In the third stage, the 13 predictor variables were used in a multiple linear regression to create rainfall models for each year. These variables are presented in Table 4.1 .

Table 4.1 Variables used for creation of yearly rainfall models

Serial No.	Predictor Variables
1	Longitude
2	Latitude
3	Altitude
4	$Longitude^2$
5	$Latitude^2$
6	$Altitude^2$
7	$Longitude^3$
8	$Latitude^3$
9	$Altitude^3$
10	Longitude*Latitude
11	Longitude*Altitude
12	Latitude*Altitude
13	Longitude*Latitude*Altitude

(Note that Latitude and Longitude utilised are in decimal degrees)

4.6.2 Creation of Longitude and Latitude base images

Longitude and latitude images are part of the input parameters required for the creation of rainfall models that will facilitate the production of complete annual rainfall data for analysis with the NDVI dataset. For this reason, the subset DEM image covering the study area was used as the primary data source for the creation of these two images using the geographical coordinates surrounding it. The subset DEM image covering the study area at 1 km resolution contains 1441 columns by 1138 rows. It was used as an opaque reference image for manual placement of the 1441 individual columns using the IDRISI CONCAT module. The longitude image with east to west coordinates (columns) was first created. Initially, the west-east extent representing the longitude (columns) area covering the opaque reference sheet was divided into six strips based on the range of the longitudinal coordinates. There are five equal strips of 250 individual 1° degree columns and the sixth strip contains 191 individual 1° columns. Secondly, the first strip of 250 columns was first placed on the opaque reference image and saved as a temporary file. This procedure was repeated until all the six strips were covered on the opaque reference image and the final image was saved as the longitude image. This image is illustrated on Figure 4.5(a). The next image to be created was the latitude image. However, instead of repeating a similar procedure used in the creation of the longitude image to create the latitude image, the longitude image was merely transposed 90 degrees counter-clockwise. This produced the latitude image and is illustrated in Figure 4.5 (b).

4.6.3 Creation of Rainfall Models from the best subsets of predictor variables

Having calculated the values of the 13 predictor variables for the 120 gridded rainfall points, the rainfall figures for these 120 points for each year were used as the dependent variables in one column and the 13 independent variables in each column were entered into Minitab Statistical software and analysed using multiple linear regression. For each year in the time series a run was first made to determine the best subsets of the equations that would give a good predictive model for estimating appropriate spatial rainfall data for that year. From the result of each output, the best appropriate model was chosen from the highest R^2 (Coefficient of Determination) which had as few predictors as possible, and excluding any additional variable which contributed little or nothing to the prediction. Finally the rainfall model for each year was derived, based on the regression equation describing the model. Out of the 12-year individual models, six had an R^2 of over 90% at $p < 0.05$ significant level. 1990 had the highest R^2 of 93.9 % from nine variables of best subset. 1992 had the lowest R^2 of 78.9% from eight variables of best subset. However, 1988 with an R^2 of 87.4% and 1991 with an R^2 of 90.5% had seven variables from the best subset used to create their models, and these two years had fewer predictor variables than all the other remaining years. The linear regression equations describing individual yearly models used to generate complete spatial rainfall data for the study area are shown in Table 4.2.

4.6.4 Spatial Estimation of Annual Rainfall images from model equations

Having created yearly models from multiple linear regression equations, rainfall image data was generated for each year. From the regression models detailed in Table 4.2 rainfall images were subsequently created for each year in the time series.

(a)

(b)
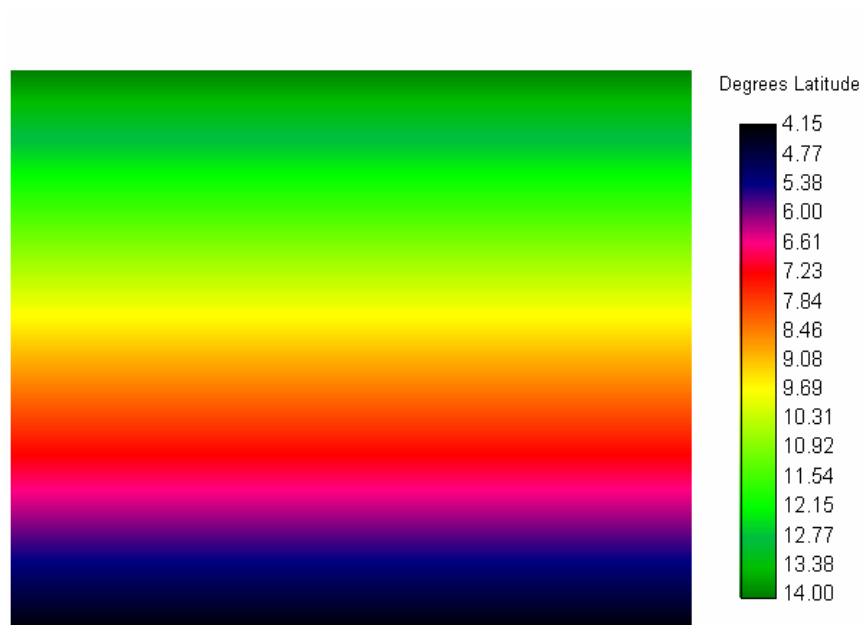
Figure 4.5 The Longitude and Latitude Images. Image (a) is the longitude image and (b) is the latitude image The longitude image was first created by CONCAT operation in Idrisi-32 using the (DEM) altitude image as an opaque base sheet referenced to its longitudinal coordinates. The latitude image was created by transposing the longitude image 90° counter-clockwise. Both the longitude and latitude images were created for the purpose of using them as input variables for the creation of rainfall models. The rainfall models were later used to recreate complete annual rainfall data covering the study area for the same time period as the NDVI image dataset.

4.6.5 Contracting of Rainfall Images to NDVI image resolution

To be consistent with the NDVI images for subsequent vegetation change analysis, the predicted rainfall images in 1 km resolution were reformatted using image contraction. From 1441 columns by 1183 rows of pixels at 1 km resolution each predicted rainfall image was contracted with an aggregation factor of 8 pixels in the X and Y direction. This procedure resulted in decreasing the cell resolution and reproduced rainfall images of 174 columns by 138 rows at 8 km resolution projected to latitude-longitude grid.

4.6.6 The quality of the Primary and derived Rainfall data

In Section 4.6 it was shown that unavailability of complete rainfall data from rain gauge stations across the whole of Nigeria was the reason why the data would have to be sourced from the GPCC. The annual rainfall data was available only in a gridded point. Hence, this necessitated the creation of models in order to generate complete data covering the study area. In order to validate the models, a comparison was made using correlation plots of the original GPCC data and the predicted rainfall data to demonstrate the quality of the output for each year.

The spatial rainfall data obtained from these models was based on multiple linear regression. In the subsequent procedure, the first derived rainfall data was aggregated so as to conform with the 8 km resolution of the NDVI data. Hence, the final aggregated rainfall data used in the investigation only indicates approximate rainfall figures of the area under study.

Table 4.2 Regression Equations for the Rainfall Models (1986 to 1999)

Year	Multiple Regression Equation used for the Models	Number of Variables of Best Subset used for equation	Coefficient of Determination (R^2) (adjusted)
1986	Rainfall = - 166 + 43.2 Longitude + 68.7 Latitude + 0.274 Altitude- 2.29 Long** - 7.58 Lat** + 0.0813 Long*** + 0.267 Lat***+0.0000001 Alt*** - 2.26 Long*Lat - 0.0448 Long*Alt - 0.0243 Lat*Alt + 0.00385 Long*Lat*Alt	12	92.3%
1987	Rainfall = 155 + 32.1 Longitude - 3.64 Long** - 2.52 Lat** +0.000063 Alt** + 0.140 Long*** + 0.112 Lat*** - 0.480 Long*Lat - 0.0162 Long*Alt + 0.00131 Long*Lat*Alt	9	93.3%
1988	Rainfall = 328 + 5.90 Longitude - 33.2 Latitude - 0.168 Altitude - 0.416 Long** + 0.769 Lat** +0.000061 Alt** + 0.0130 Lat*Alt	7	87.4%
1990	Rainfall = 50.1 + 36.1 Longitude + 0.405 Altitude - 0.581 Long** + 0.000078 Alt** + 0.0169 Lat*** - 2.65 Long*Lat - 0.0530 Long*Alt - 0.0493 Lat*Alt + 0.00526 Long*Lat*Alt	9	93.9%
1991	Rainfall = 187 + 49.0 Longitude - 18.8 Latitude - 6.58 Long** +0.000102 Alt** + 0.260 Long*** - 0.0169 Long*Alt +0.000914 Long*Lat*Alt	7	90.5%
1992	Rainfall = - 395 + 41.1 Longitude + 144 Latitude - 15.9 Lat** - 0.0649 Long*** + 0.552 Lat*** +0.0000001 Alt*** - 1.97 Long*Lat - 0.0169 Long*Alt	8	78.9%
1993	Rainfall = 75.9 + 32.7 Longitude + 0.392 Altitude - 0.591 Long** - 0.911 Lat** + 0.0559 Lat*** +0.00000005 Alt*** - 2.18 Long*Lat - 0.0523 Long*Alt - 0.0359 Lat*Alt + 0.00470 Long*Lat*Alt	10	93.8%
1995	Rainfall = - 369 + 58.6 Longitude + 128 Latitude + 1.08 Altitude - 14.0 Lat** - 0.0272 Long*** + 0.558 Lat*** +0.00000008 Alt*** - 4.99 Long*Lat - 0.125 Long*Alt - 0.114 Lat*Alt + 0.0122 Long*Lat*Alt	11	90.5%
1996	Rainfall = 9.4 + 48.9 Longitude + 0.925 Altitude + 0.0623 Lat*** +0.00000013 Alt*** - 4.39 Long*Lat - 0.117 Long*Alt - 0.0954 Lat*Alt + 0.0106 Long*Lat*Alt	8	87.4%
1997	Rainfall = - 120 + 46.9 Longitude + 86.4 Latitude + 0.694 Altitude - 12.1 Lat** - 0.0372 Long*** + 0.527 Lat*** +0.00000011 Alt*** - 3.70 Long*Lat - 0.0966 Long*Alt - 0.0784 Lat*Alt + 0.00937 Long*Lat*Alt	11	88.0%
1998	Rainfall = 27.1 + 39.6 Longitude + 0.734 Altitude - 0.490 Long** -0.000342 Alt** + 0.0389 Lat*** +0.00000023 Alt*** - 3.37 Long*Lat - 0.0707 Long*Alt - 0.0652 Lat*Alt + 0.00748 Long*Lat*Alt	10	86.7%
1999	Rainfall = - 301 + 56.6 Longitude + 118 Latitude + 1.15 Altitude - 13.8 Lat** - 0.0248 Long*** + 0.574 Lat*** +0.00000002 Alt*** - 4.92 Long*Lat - 0.138 Long*Alt - 0.123 Lat*Alt + 0.0134 Long*Lat*Alt	11	89.6%

4.7.   Data Quality

4.7.1 Other uncertainties with NDVI data from the PAL dataset

The AVHRR-NDVI from the PAL dataset has been used successfully for global, continental and regional studies over the years (eg Justice *et al,* 1985) Townshend and Justice, 1986; Tucker *et al,* 1985; Justice *et al,* 1991b; Millington *et al,* 1992; Eastman and Fulk, 1993; Anyamba and Eastman, 1996; Young and Wang, 2001). However, although it has been generated in a consistent manner which includes post-flight sensor calibration and atmospheric corrections for rayleigh scattering and ozone absorption (James and Kalluri, 1994), the dataset has its own problems (see Section 2.4.3) which necessitated later revisions. For example, due to the mistakes made in calculating the post-launch calibration coefficients of the visible and infrared channels of the AVHRR (Rao and Chen, 1996), a revised version of such calibration coefficients were later provided (Rao and Chen, 1999) (See Appendix 4). As a direct result, there was a setback in the initial analysis of the data. The NDVI data from 1995 to 1999 acquired from the NOAA-14 satellite was affected by this correction. The NDVI data from 1986 to 1999 from the PAL dataset was initially downloaded between March and May 2000 and analysis almost half way in February 2002.
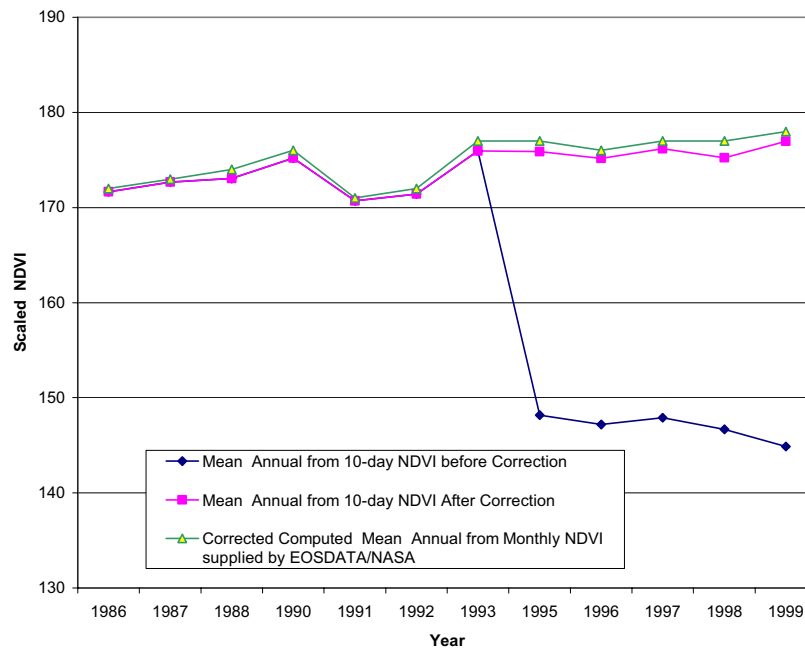
Figure 4.6   Illustration of a major problem encountered with the PAL NDVI dataset. This graph illustrates the problem encountered with data after one year into the analysis when the first data was downloaded from the PAL dataset archive. Three temporal plots of the annual mean NDVI dataset were plotted. Blue line represents original data (uncorrected) downloaded in 2000 before the data was corrected and replaced in the PAL dataset archive. Green line represents corrected and replaced data by NOAA/NASA using annual mean of the maximum monthly NDVI data. Red line represents corrected data re-downloaded in March 2002 showing annual mean NDVI derived from the 10-day composite data. The temporal plot blue line indicates very low NDVI values due to errors in calculating the Calibration Coefficients for Channels 1 and 2 of AVHRR onboard NOAA-14 which affected all the data from 1995 to 1999 and consequently affected the initial analysis.

Due to certain trends observed during the initial analysis of the data, the mean of each annual dataset (initial downloaded data) were determined and plotted (See Figure 4.6). The general trend indicated that from 1995 to 1999 the NDVI decreased drastically. This plot including a summary of the initial analysis was sent to NOAA/NASA for comments. The reply received (See Appendix 4) shows that because of the reasons highlighted in Section 2.3.6 and as mentioned above, the whole of the data from 1995 to 1999 had to be re-downloaded and re-analysed. Without this verification, the results obtained from the analysis of such data would be misleading.

4.8. Summary

This chapter presents the key methodologies utilised and their necessity to underpin the investigation of vegetation biomass changes across Nigeria.

The detailed methodology included the acquisition of the primary satellite data downloaded from the PAL dataset archive at NOAA/NASA. This is followed by reorganising and recompositing the dataset into monthly MVCs as well as annual mean data. A tile containing DEM data of the north-west quadrant of Africa from the GTOPO30 global digital elevation data was also acquired from the USGS website and a subset DEM of the study area covering Nigeria made out of it. This was followed by extracting the latitude and longitude coordinates of the study area and subsequent creation of latitude and longitude images. Gridded point rainfall data covering the study area was also downloaded from the GPCC website and subsequently used together with the latitude, longitude and DEM data to derive models for creating spatial annual rainfall images covering the study area. The derived rainfall data were later reformatted from 1 km resolution and contracted with an aggregated factor of 8 pixels in X and Y direction to 8 km resolution so as to be consistent with the primary NDVI dataset.

In Chapter Five, a preliminary assessment of the primary dekadal and derived NDVI as well as the estimated rainfall datasets covering Nigeria was made. This is to provide some demonstrations of the data quality and reliability prior to using the datasets for vegetation change assessment.

CHAPTER FIVE

A PRELIMINARY INTERPRETATION OF THE NDVI AND RAINFALL IMAGERIES

5.1 Introduction

Prior to the application of time series analysis techniques, it is important to interrogate the datasets for vegetation change assessment across Nigeria. This chapter presents the NDVI data from the PAL dataset, the derived NDVI data and the rainfall maps generated from the methods described in Chapter 4. It aims to provide a check on the data quality, identify possible outliers or influences on the data which might affect the overall results. It is also aimed at providing useful information to help identify optimum approaches to time series analysis and aid the interpretation of the results as well as gain an overall appreciation of the datasets. The preliminary analysis is undertaken on the data sets as a whole and for specific locations.

5.2 The Primary NDVI data from the PAL dataset

From the 12-year dekadal NDVI data in the time series a mean was determined for each dekad. These were plotted and grouped into four sets of plots (for convenience) in order to examine the nature of the dekadal and monthly datasets (See Figure 5.1). In these temporal plots for each year, there are many fluctuations in the graphs showing very low peaks between January and March, between June and August and between November and December. The January to March and November to December low peaks can be attributed to the dry season. Dusty winds during this dry harmattan season may also have affected the
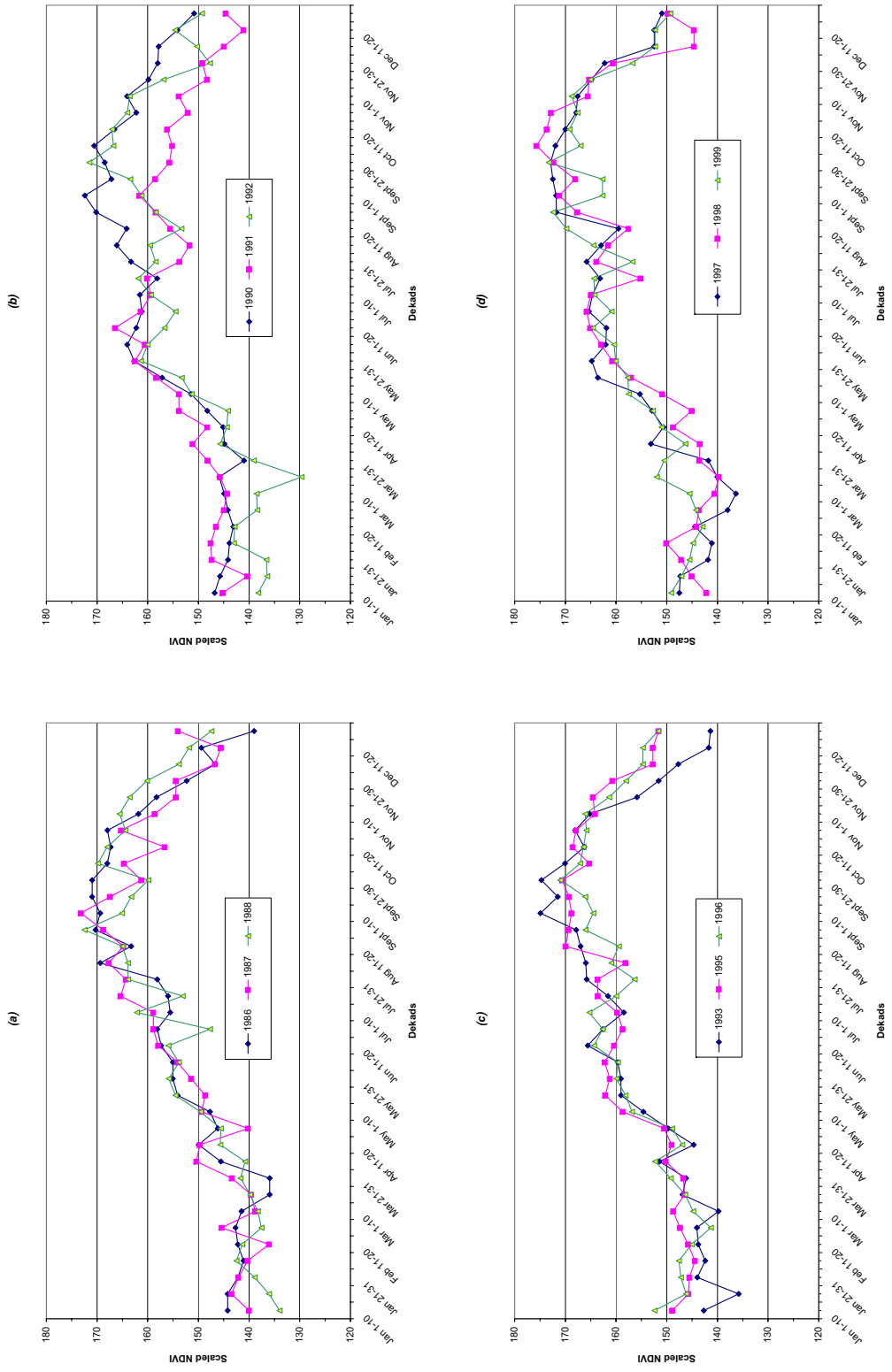
Figure 5.1 Temporal Plots of dekadal NDVI dataset. Plot (a) contains plots for 1986 to 1988, (b) represents plots for 1990 to 1992, (c) represents plots for 1993,1995 and 1996 and (c) represents plots for 1997 to 1999. These plots were based on the mean dekadal dataset which are scaled from 0-255. (To inter-convert, scaled_ndvi = float_ndvi*125+128).

data. The June to August low peaks, on the other hand, may be due to persistent cloud cover during the rainy season which the whole study area experienced during these times. For example, dust, soil effects and cloud cover are the major factors influencing AVHRR-NDVI data in the northern savanna areas (Heute and Tucker, 1991; Tucker *et al,* 1991; Tucker *et al,* 1994) while in southern parts of Nigeria which incidentally falls in the tropical rain forest region, atmospheric water vapour, haze and cloud cover tends to affect NDVI data (Tucker *et al.,* 1985; Prince and Justice, 1991). This suggests that the dataset is generally affected by cloud contamination despite the maximum compositing method (Holben, 1986) applied to the daily data. This explains the low NDVI values recorded which caused those very irregular peaks. From the dekadal temporal profiles in Figure 5.1, 1991 and 1992 appeared to be more affected with atmospheric effects in the dataset (see also Figures 5.2b, 5.3b, 5.8a and 6.13) because of the very steep peaks in the profiles. The lowest peak in the profiles in Figure 5.1 occurred in the second dekad for March 1992. From the graphs it can be seen that despite the maximum value compositing method applied to the daily NDVI data, there are still signs of atmospheric effects in the dataset for each year due to these very low peaks representing low NDVI values. Generally, 1992 data appears to be more affected with low NDVI troughs in the profile while 1995 appears less affected compared with the rest of the years. This suggests that the data derived from the dekadal NDVI datasets needs to avoid the influences from cloud cover variation which may contaminate the results.

5.3. The derived data from the dekadal NDVI datasets

To remove the influence of cloud contamination from the dekadal NDVI data, further manipulation was required, as outlined in Section 4.4.2. From the three images for each month, the maximum pixel value was chosen to represent the NDVI data for that month. Whilst this removed some of the temporal resolution, the advantage it provides is to further remove the possible influence from cloud cover (Moody and Strahler, 1994). The approach was used to derive new monthly Maximum Value Composites (MVCs) from which the mean annual data were derived for each year studied. Temporal plots of the dekadal, monthly NDVI-MVCs and the mean annual datasets as well as for other selected points were plotted to determine their characteristics.

The profiles presented in Figure 5.2 indicated that the recomposed dekadal datasets to monthly MVCs provided a smoother time series profile suggesting that a relatively cloud-free dataset had emerged to enable a meaningful analysis. However, there are still signs of cloud or atmospheric effects because of sudden drops in the profiles of some years. For example, the graph for 1992 and 1996 indicated sudden drops in NDVI in the month of August. This is the period of peak rainfall in most of the areas in Nigeria, suggesting greater cloud cover is inevitable and the reason why the NDVI recorded for this month have such low values.

From most of the graphs in Figure 5.2, the month of March appears to be the period when vegetation in most of these areas starts growing after the dry season. This is also the beginning of rainfall season in the southern forest areas. In general though, the graph pattern indicates that there is a steady growth in vegetation for all the years from February
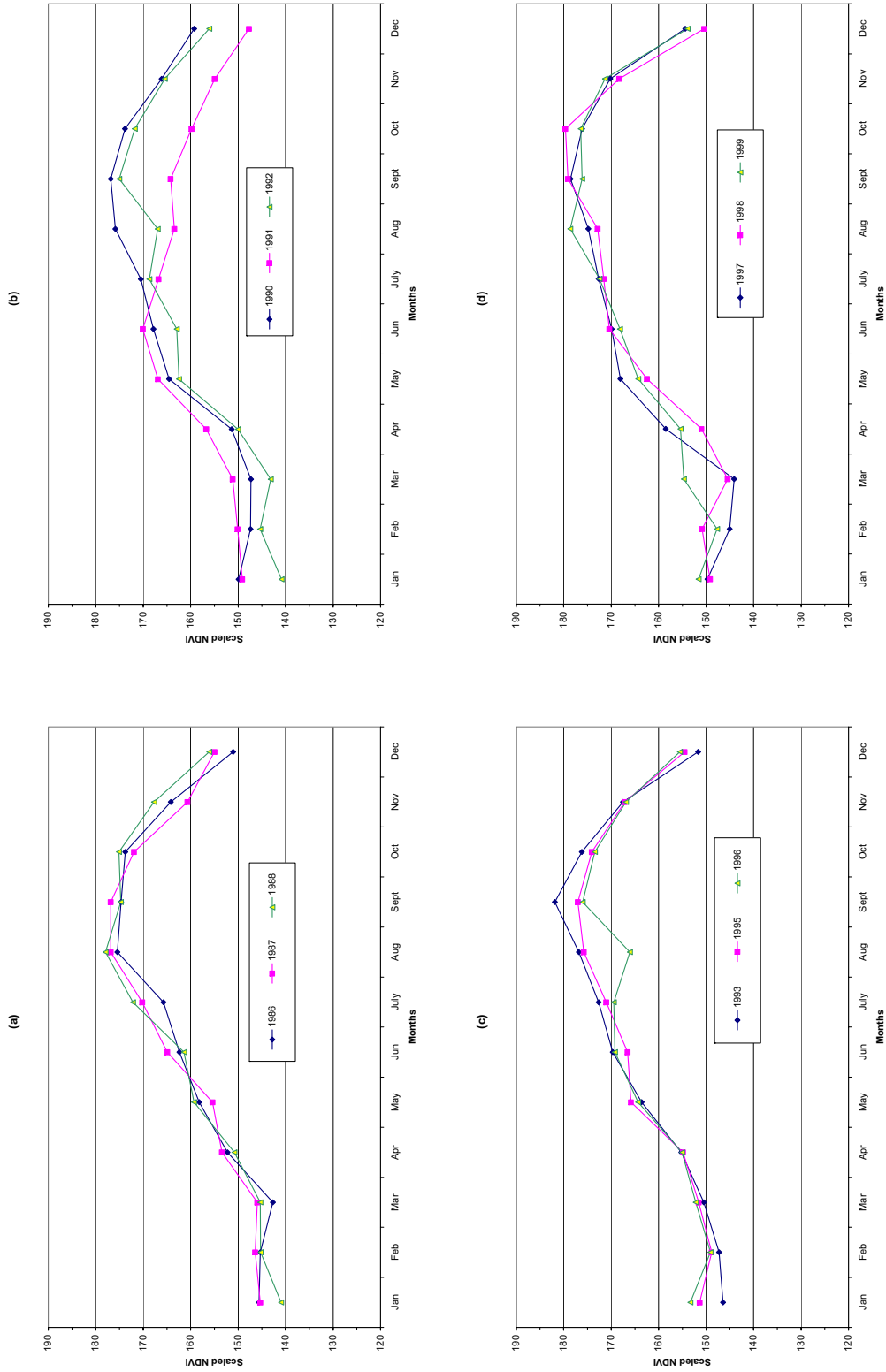
Figure 5.2 Temporal plots of the recomposed Mean Monthly MVCs dataset. Figure (a) represents plots for 1986 to 1988, (b) represents plots for 1990 to 1992, (c) represents plots for 1993, 1995 and 1996 and (c) represents plots for 1997 to 1999. From these graphs it can be seen that the recomposition had smoothed the dekadal dataset by reducing the atmospheric effects to a minimum and produced a much less contaminated dataset for the analysis. The NDVI here are scaled from 0-255. (To inter-convert, scaled_ndvi = float_ndvi*125+128).

(a)

(b)
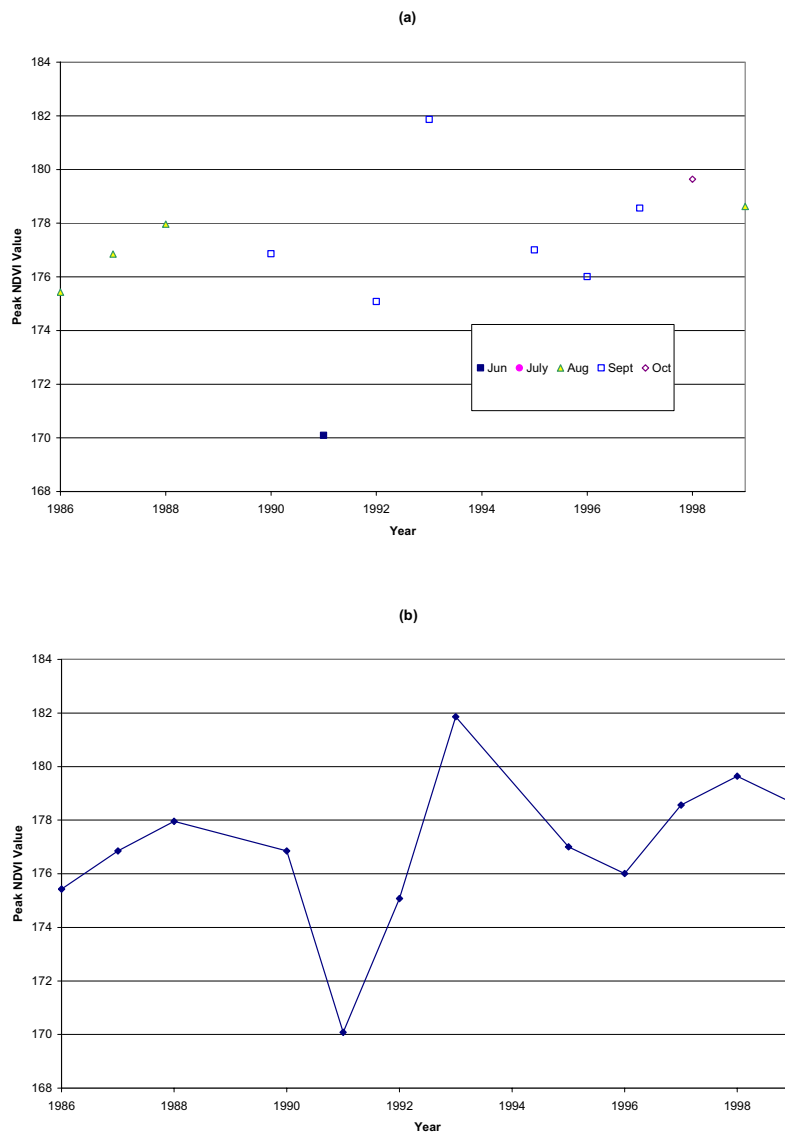
Figure 5.3 Graph of Peak NDVI with Month and Year. **Graph (a) shows the peak NDVI values with month while graph (b) shows the peak NDVI values with year. Most of the peak NDVI fell in the month of September. The lowest NDVI peak is in June 1991 while the highest NDVI peak in the time series is in September 1993.** . NDVI are scaled from 0-255. (To inter-convert, scaled_ndvi = float_ndvi*125+128).

or March based on the NDVI trajectory. This reaches a peak mostly in September (Figure

5.3a) and then decreases to December and January. The lowest NDVI peak in the time

series fell in the month of June 1991 while the highest NDVI peak is in September 1993

(Figure 5.3b). While there was no NDVI peak in the month of July, there was only one NDVI peak in the month of October 1998 in the time series. The general trend indicated that the peak NDVI month is always getting later in the year suggesting that the northern savannah is getting greener later and contributing to the overall blooming of the whole country.

5.4. The Derived Monthly MVCs and Annual Mean Composites

Studies conducted with AVHRR-NDVI from PAL dataset have shown that by using the mean of long time-series NDVI data there are possibilities of reducing some minor inter-annual variations as well enabling the long term climatic or other induced changes to be discerned (Lambin and Ehrlich, 1996; Young and Wang, 2001). Meyer *et al* (1995) on the other hand, showed that averaging also reduces the bias introduced by the selection of high monthly NDVI values especially towards the end of the compositing period in the growing season and also reduces the negative effect of most of the unvegetated surfaces. Hence, the recomposed Monthly MVCs were further recomposed into annual mean NDVI composites as described in Section 4.4.2. The production of the annual mean images therefore provides good information of the amount of, and variation in, annual vegetation productivity. These annual mean NDVI images derived from the monthly MVCs are illustrated in Figure 5.4.

From the annual mean NDVI composites in Figure 5.4 it can be observed that the area around Lake Chad is getting greener, with more spatially extensive NDVI values. The coastal area (the Niger Delta) on the other hand, increases in aridity with the lowest mean NDVI values in 1991/1992.
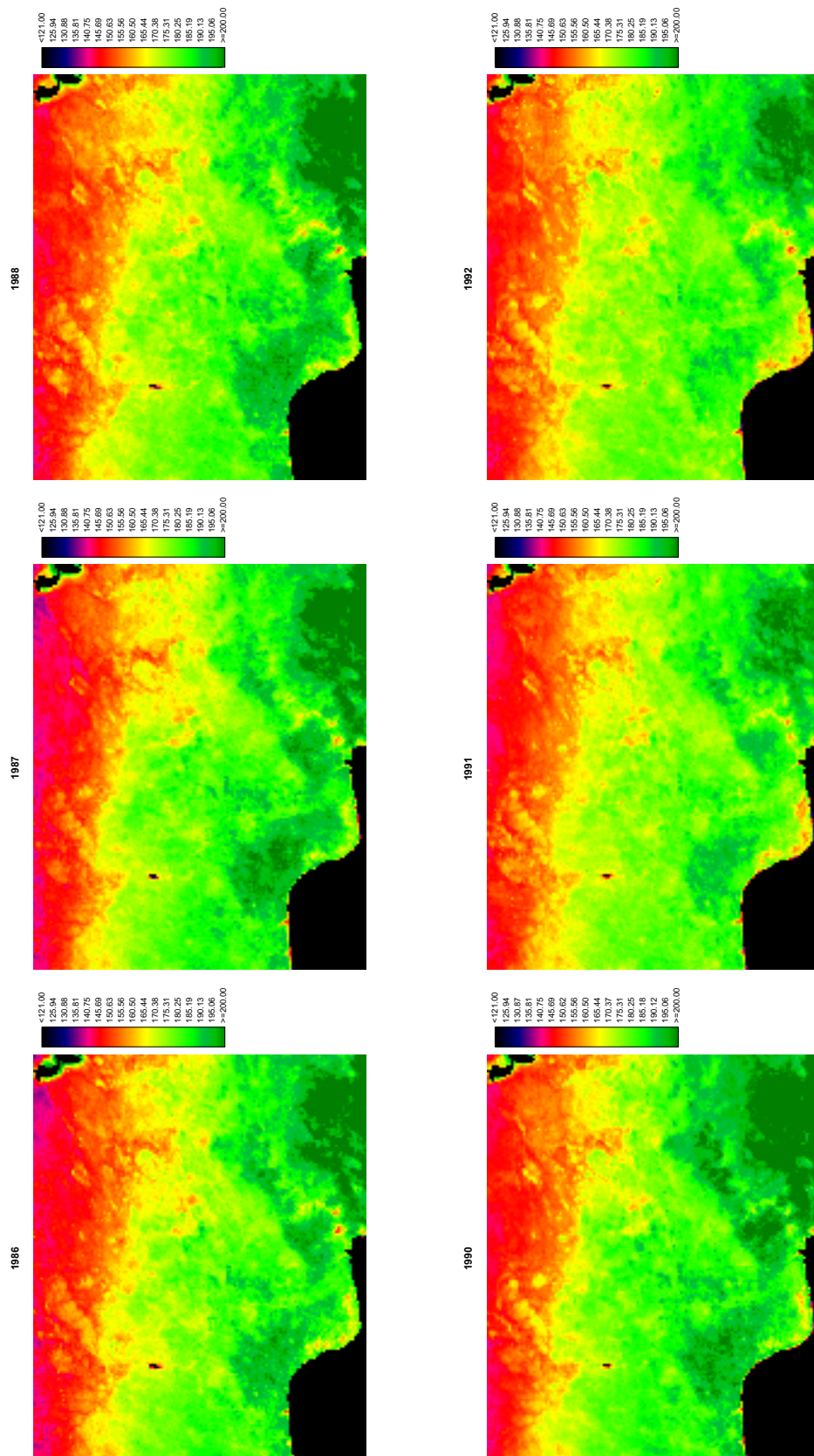
Figure 5.4 Annual mean NDVI images for the 12-year timeseries (1986 to 1999). These images were produced using Idrisi colour palette and were stretched for visual purposes. Note the similarities of the images especially the less vegetated areas and the general variation in the density of vegetation vigour from blue to red in the northern sahel and savanna to green and dark green in the southern tropical rain forests and coastal mangrove areas. The NDVI values were scaled from 0-255. (To inter-convert, scaled_ndvi = float_ndvi*125+128).
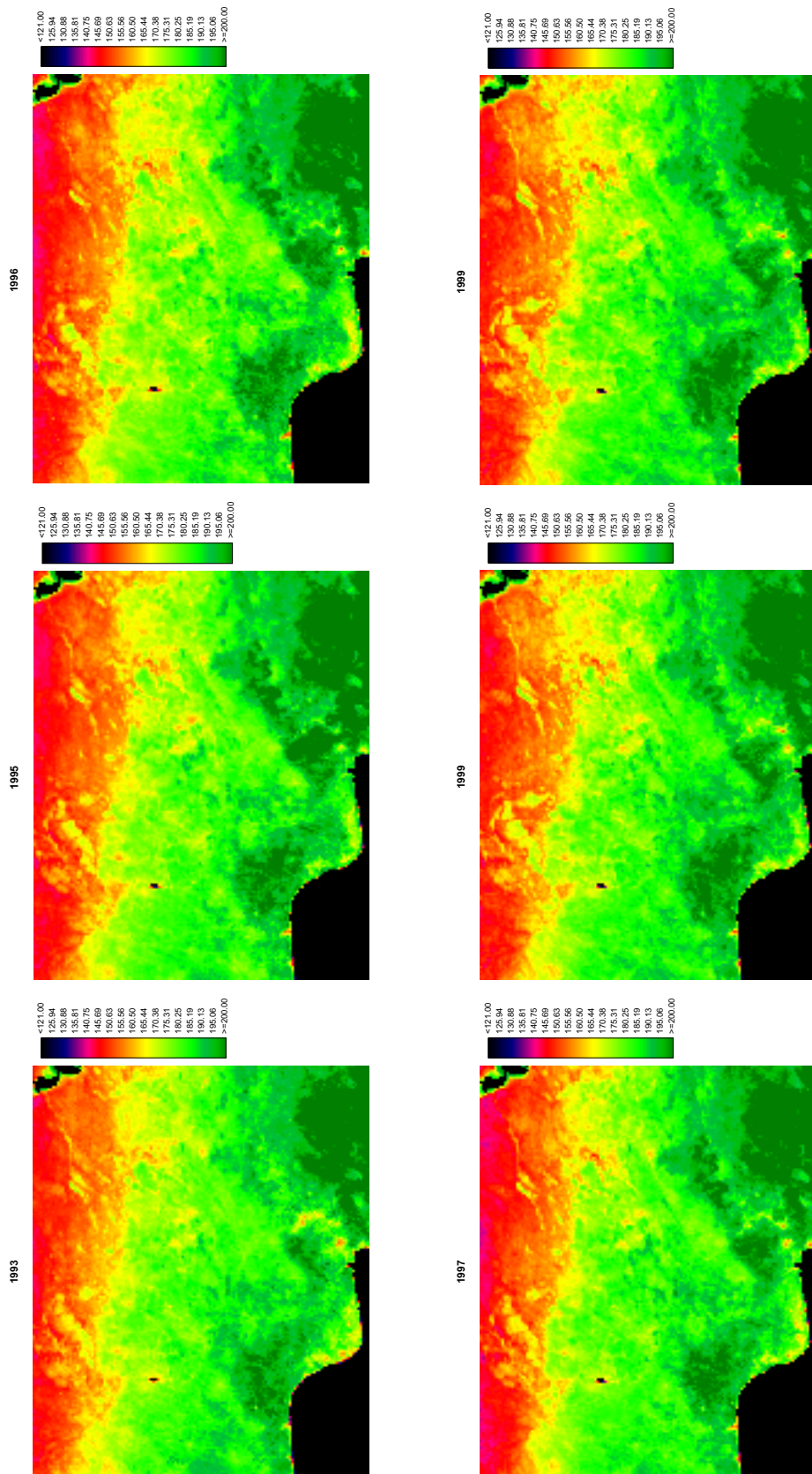
Figure 5.4 (Cont.) Annual mean NDVI Composite images.

5.5.   Examining the NDVI data using Selected Sites

5.5.1   Site Selection

In order to demonstrate further the benefit of recomposing the NDVI data acquired from the PAL dataset before analysis is undertaken, six sites (Figure 5.5a) were selected to examine the influence of atmospheric effects on the dekadal and the monthly MVCs. The dekadal data for 1995 considered less affected by atmospheric effects (based on Figure 5.1) was chosen and used to examine the data for these selected sites and was plotted on graphs. This selection of sites was based on the Nigerian vegetation zones (Areola, 1982) (see Figure 3.14) which are areas with obvious vegetation changes, and which incidentally fall very close to Nigerian rain gauge stations (at 8 kilometre spatial resolution). For each site, the dekadal NDVI value of the site was chosen using the geographical coordinates location of the closest rain gauge station and plotted. This represents one pixel per site which is approximately 64 square km.

The first two sites are in the Sahel region falling in the northern Sudan savanna area of Nigeria. One of these sites is an area close to Lake Chad (supposedly a lowland area where there is intensive dryland irrigation farming) and the second site is an area close to the Niger-Nigeria boarder in the north-east. The third site is an area considered to be in the Sudan savanna region. The fourth is a site in the Guinea savanna near the north-west part of Kainji Lake and the fifth is a site in the tropical forest region around Nigeria/Cameroon border in the south-east. The sixth site is in the coastal and mangrove swamp forest in the Niger Delta where the changing land use particularly due to petroleum exploration activities by the SHELL company is reported to have some environmental impacts on the area (Boele *et al,* 2001a). These temporal plots are illustrated on Figures 5.5b and 5.6.

(a)
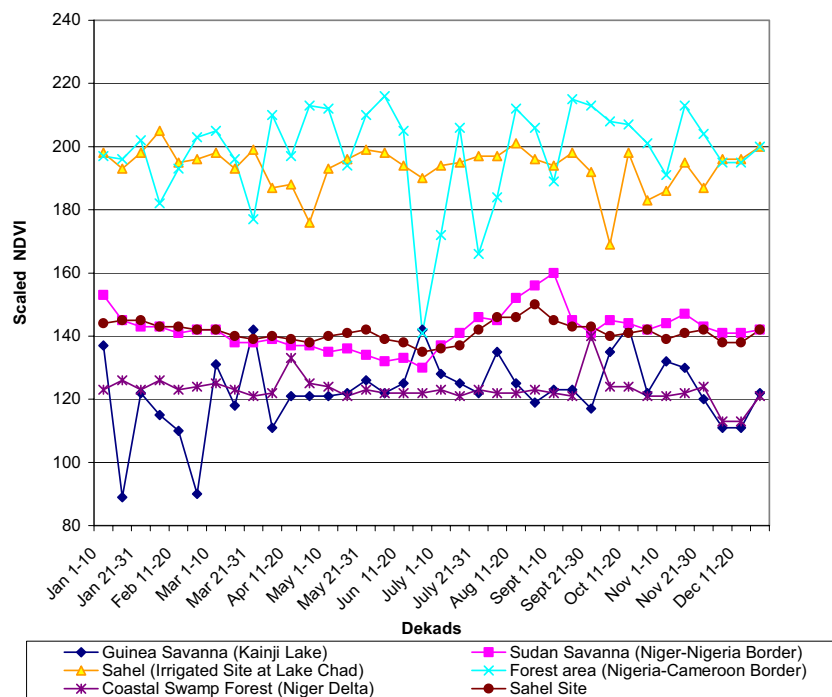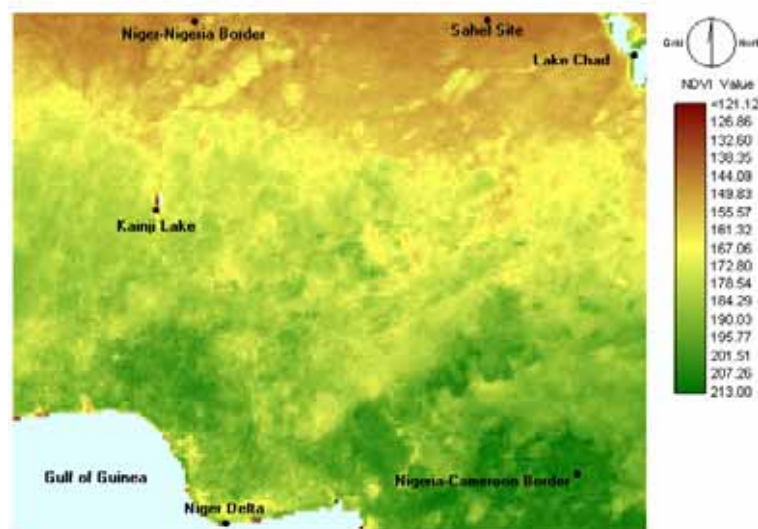
(b)

Figure 5.5 Temporal dekadal NDVI plots of selected sites from different vegetation zones based on 1995 NDVI Image. Figure (a) using a stretched NDVI palette, indicates the selected sites based on 1995 dekadal NDVI data which is considered less affected by atmospheric effects as in Figure 5.1. One site was selected from six of the seven Nigerian vegetation zones in Figure 3.14 (Areola, 1982a). Figure (b) shows the temporal plots of the dekadal data for these selected sites. The plots suggests that, despite the maximum value compositing of the NDVI data, there are still signs of atmospheric and cloud effects in the data because of sudden low peaks in the profile. The forest region, with consistent high NDVI values for example, still recorded a very low peak in the last dekad in June. The selected site within the Guinea savanna shows many fluctuations with sudden low peaks. The coastal lowland swamp forest site shows consistent low NDVI values which may be due to the changing land use activities in the area. NDVI are scaled from 0-255. (To inter-convert, scaled_ndvi = float_ndvi*125+128).

5.5.2   Temporal dekadal plots of selected sites

From the temporal plots of the selected sites in Figure 5.5b, except the Sudan savannah area which indicated a stable pattern of vegetation biomass based on the mean NDVI, each of the other sites still indicated an element of atmospheric or cloud effects in the data due to the sudden drops and low peaks in the profile. The Guinea savanna area close to Kainji Lake, for example, shows the lowest NDVI trough of less than 100 for the second dekad in January and the third dekad in February 1995.

The first Sahel site shows consistently low NDVI values except in August which increased because this was in the middle of rainy season in this area. The consistent low NDVI values may be related to the frequent forest fires around this region as indicated by Lambin and Ehrlich (1997b).

The second Sahel site (supposedly in an irrigated area close to Lake Chad) indicated high NDVI values which may be due to the high growth of water weeds (Schneider *et al*, 1985) or the dry season agriculture (Adams and Thomas, 1996) reported around the lake. In dryland areas such as the Sahel, it was shown that vegetation productivity is related to irrigation water rather than rainfall (Millington *et al,* 1994), hence the markedly high values unexpected of the Sahel area. However, there are still some signs of atmospheric effects in the last dekad in April and the first dekad in October of 1995 because of very low peaks. The April low peak may be due to the dusty wind at the beginning of the rainy and the harmattan seasons while the October low peak could be attributed to misty clouds of the late rains.

The coastal swamp forests on the other hand have a consistent average NDVI of slightly above 120 in most dekads except for the second dekad in April and the last dekad in September. Although there may be seasonal variations in NDVI, studies by Boele *et al,* (2001a) have shown that the Niger Delta area had suffered significant negative impacts due to the activities of the SHELL petroleum company. This may be another reason for the consistent low NDVI values for this site. When compared with the sahel region (close to Lake Chad) that has high mean NDVI values due to the all-year agricultural activities around Lake Chad, cloud atmospheric effects partly due to water vapour are likely to be part of the reason for that consistent low NDVI values in such a mangrove swamp forest area (Eck and Kalb, 1991; Justice *et al,* 1991a).

The forest area at the Nigeria-Cameroon border though with consistent high average NDVI values compared with the other sites, also shows signs of atmospheric effects due to the sudden drops in the profile, with an extremely low trough in the last dekad of April. This type of atmospheric effect was also reported in studies conducted on the tropical forest areas of Cameroon (Lucas *et al,* 2000).

5.5.3   Further verifications using the dekadal plots of selected sites

The assertions that recomposing the dekadal data into monthly and annual dataset further reduces atmospheric contamination in the dataset (Lambin and Ehrlich, (1996; Young and Wang, 2001; Meyer *et al,* 1995) was proved a little further. The site close to Kainji Lake in the Guinea savannah area shown in Figure 5.5a, and which indicated lower NDVI values between January and April than the Sahel sites illustrated in Figure 5.5 was used as an example. First, the 1999 dekadal data for this site close to Kainji Lake was

(a)
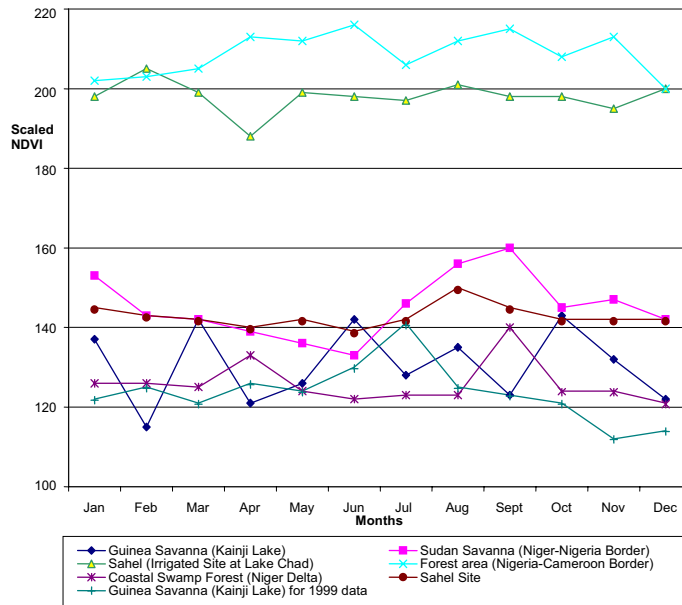
(b)
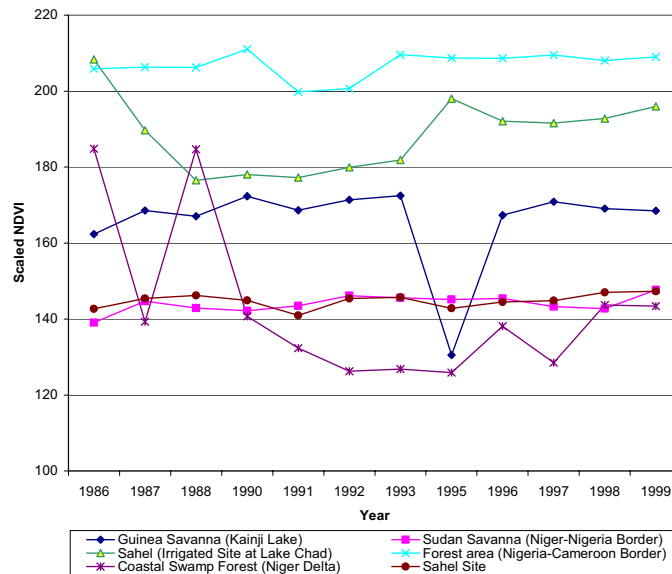
Figure 5.6 Profile of the recomposed monthly MVCs, and annual mean NDVI dataset for the selected sites. The graphs indicated that further recomposition into monthly MVCs and annual mean composites gives an opportunity to clearly find areas of long-term climatic or other induced changes. Figure (a) shows the profile for monthly MVC's and Figure (b) shows the annual mean composite data. The Kainji Lake site in the Guinea savanna area for 1999 data included in Figure (a) for example, indicated a smoother profile for this site compared with the profile on the 1995 data. The profiles for the selected sites using the monthly MVCs are generally smoother than that in Figure 5.2 except for the Kainji Lake site in the Guinea savanna which shows irregular peaks throughout the profile and the site in the coastal swamp forest area. These two sites give a clearer picture of the atmospheric and cloud effects on the annual mean composite data. NDVI are scaled from 0-255. (To inter-convert, scaled_ndvi = float_ndvi*125+128).

further recomposed into monthly MVCs and plotted along side the 1995 monthly MVCs of the other selected sites. These are illustrated in Figure 5.6a. Secondly, all the 1995 monthly MVCs for all the selected sites in Figure 5.5a were recomposed into annual mean composites and their means plotted. These are illustrated in Figure 5.6b.

The result shows that the profiles have smoothed except for areas with serious problems of atmospheric effects which are likely to be the cause of those sudden drops in the profile despite their further recomposition. In particular, the profile for 1999 monthly MVCs for the site close to Kainji Lake on Figure 5.6a, shows a smoother profile compared with the profile of 1995 monthly MVCs of the same site.

However, the profiles of all the sampled sites for the annual mean data showed a clearer picture of the atmospheric and cloud effects in the dataset (Figure 5.6b) for the Guinea savanna site and the site in the coastal swamp forest. As for the two Sahel sites, these are more distinct. The site which is located in an irrigated area shows a higher NDVI values than that which is in the main Sahel area where no dryland irrigation activities are being carried out. The irrigated Sahel site close to Lake Chad on the other hand shows a clear difference from the site in the forest area. It can be noticed that the irrigated Sahel site close to Lake Chad has higher NDVI values than the other sites. This may be due to the year-round agricultural activities in the area. However, the NDVI values for this site are lower than those of the forest region which contains natural vegetation.

5.6 Generation of Mean Annual and Coefficient of Variation Composite images

Having recomposed the dekadal NDVI datasets and examined their characteristics using selected sites, an annual mean composite image of the whole dataset for the 12-year time period covering the whole study area was also generated so as to show the representative vegetation cover of this area for the entire time period. This image is illustrated in Figure 5.7a. The overall annual mean image is intended to provide a visual view of the amount of, and variation in, inter-annual vegetation productivity of the study area.

In an attempt to determine the extent of the Sahara desert and to document its inter-annual variation Tucker *et al* (1991a) used the coefficient of variation of the mean NDVI from AHVRR to highlight vegetation changes over the sahel region in Africa. Milich and Weiss (2000a) on the other hand, used the coefficient of variation of NDVI images from AVHRR to assess vegetation changes and ecosystem boundaries. These did not cover the area under study. In this study covering Nigeria, both the Mean and Coefficient of Variation composite images of the study area centred on Nigeria were generated. This image is illustrated in Figure 5.7.

The overall coefficient of variation image of the whole data set covering the study area will provide a spatial view of interannual variation of vegetation productivity. This image was generated from the 144 monthly MVCs that have been derived from the 432 dekadal NDVI images for the time period under investigation (1986 to 1999).

(a)

(b)
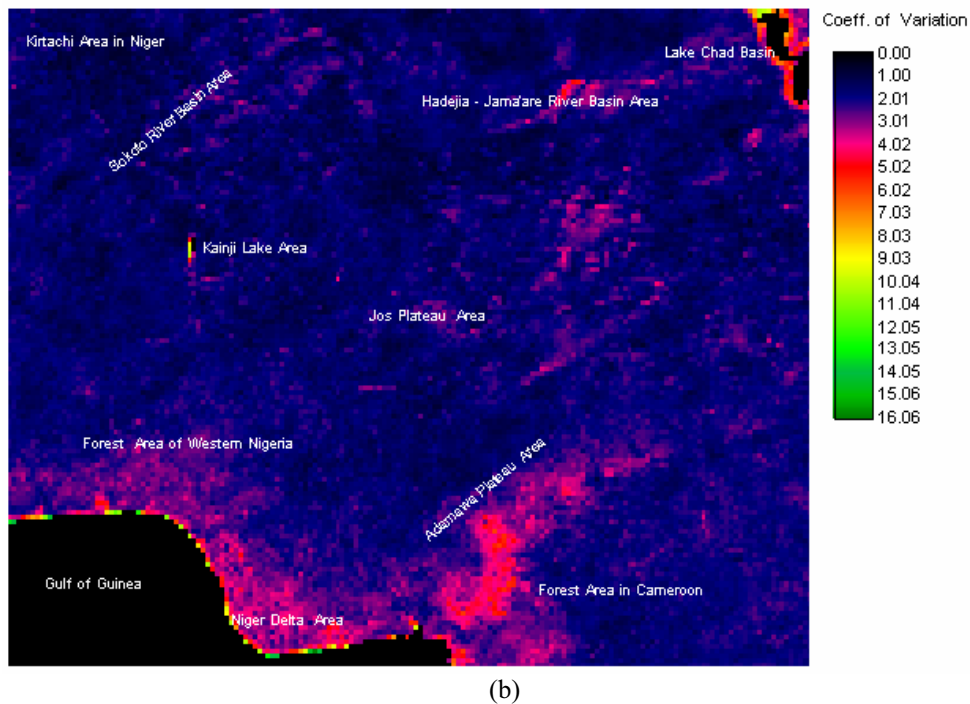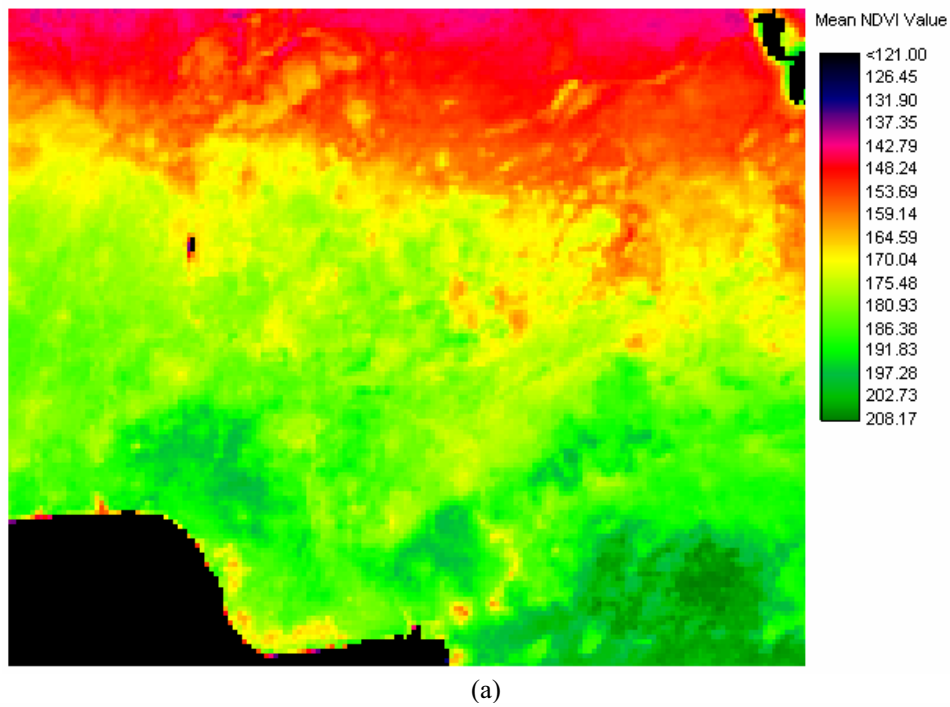
Figure 5.7 Annual Mean and Coefficient of Variation Image composites of the study area. Figure (a) is the Annual Mean NDVI Composite created from 144 Monthly MVCs that have been derived from the 432 dekadal NDVI image data for the whole time period 1986 to 1999. This image has been scaled from 0-255 and stretched for visual purposes like the yearly mean images in Figure 4.2. Figure (b) shows the Coefficient of Variation image created from 12 annual mean NDVI composites derived from the same 144 monthly MVCs. This last image highlights areas with maximum inter-annual variability. Areas of such high variability are located in the coastal areas and Niger Delta, around Kainji Lake in the north-west, in the north-eastern part around Lake Chad and Hadejia-Jama'are River basin and Adamawa Plateau (between Nigeria Cameroon borders). Areas of high inter-annual variability surrounded by lower inter-annual values as on the coefficient of variation image are signs of rapid dynamic land degradation (Ehrlich and Weiss, 2000). This can be seen around the Niger area in the extreme south around the coastal region.

5.6.1 The Mean Annual Image of the whole dataset

In the first procedure, the mean image of the whole 12 annual mean composites was calculated as:

$$\mu_{12} = \frac{\sum_i X_{12}}{N} \tag{5.1}$$

Where

μ_{12} denotes the mean composite image of the whole dataset for the 12-year period

X_{12} denotes the individual pixel values in their respective locations on the 12 annual mean composite images and

N denotes the time period (12 years).

Secondly, the standard deviation of the whole dataset was calculated as :

$$\delta_{12} = \sqrt{\left[\frac{\sum_i \left(X_{12} - \delta_{12}\right)^2}{N}\right]} \tag{5.2}$$

Where

X_{12} denotes the individual pixel values in their respective locations on the 12 annual mean composite images

δ_{12} denotes the standard deviation of each individual pixel value for its respective location on the 12 annual mean composite images and

N denotes the time period (12 years).

5.6.2   The Coefficient of Variation (CV) Image of the whole dataset

In the final process, the Coefficient of Variation image of the whole dataset expressed as a percentage, was calculated as :

$$CV_{12} \quad = \quad \frac{\delta_{12}}{\mu_{12}} \quad x \ 100 \qquad\qquad (5.3)$$

Where

CV_{12} denotes Coefficient of Variation of the whole dataset for the 12-year time period

δ_{12} denotes the Standard Deviation of the each individual pixel value for its respective location on the 12 annual mean composite images.

μ_{12} denotes the mean composite image of the whole dataset for the 12-year time period derived from the 144 monthly NDVI-MVCs.

The annual Coefficient of Variation (CV) image derived from the 144 monthly NDVI-MVCs for the time period 1986 to 1999 is illustrated in Figure 5.7b. The Coefficient of Variation calculated for each pixel in the entire time series data highlights areas with maximum inter-annual variability covering the time period from 1986 to 1999.

5.6.3   Summary

In general, although the NDVI data from the PAL dataset utilised in this study still contains some atmospheric and climatic effects, the methods used in recomposing the data seems to have overcome the problem to a certain degree to enable the data be used for the analysis of changes in vegetation cover across Nigeria. However, although no attempt was made in this investigation, it will be useful if the Best Index Slope Extraction (BISE) approach (Viovy *et al,* 1992) can be modified as an alternative to the

MVC method of cloud screening (Holben, 1986) where algorithms used in the BISE method can be applied to NDVI on any environment. Alternatively, since the MVC of the NDVI has the risk of selecting an outlier, averaging or clearer pixels can be used as another alternative to reduce the cloud gaps such that values can be filled by interpolation (Gutman, and Ignatov, 1995). This second alternative, though not applied in this investigation, can be applied to the 1989 and 1994 NDVI data which have many data gaps as result of non-satellite overpass across the study area. This will give a more consistent coverage of the whole dataset from 1986 to 1999.

5.7   The rainfall data

5.7.1   The estimated rainfall data from models

The generated (estimated) annual rainfall images resulting from the multiple regression equations in Table 4.2 are illustrated in Figure 5.8. According to these maps, areas of high rainfall (in red, yellow and green) are mostly located in the highlands and the forested regions as well as around the coastal areas of the southern part of the country. Areas of less rainfall on the other hand are mostly located in the savanna and the sahel areas in the northern part of the country. The annual (estimated) rainfall images are in 1 km resolution. All the maps to a certain extent compare with the rainfall map of Nigeria in Figure 3.3 where the southern and coastal areas have more rainfall than the northern savanna and sahel areas.

5.7.2   The reformatted rainfall data

As mentioned in Section 5.7, the annual reformatted (contracted) rainfall images at 8 km resolution were derived from the estimated 1 km resolution rainfall data by pixel aggregation (Idrisi-32, 1998). These reformatted rainfall maps are illustrated in Figure 5.9. The reformatted rainfall maps at 8 km spatial resolution resemble those in Figure

5.8 which are at 1 km spatial resolution. On both maps in Figures 5.8 and 5.9, the images were contrast stretched for visual purposes. In general, the amount of rainfall around the coastal areas were lower in the late 1980s than in the 1990s. This ties in with the more arid years in the early 1990s. However, the highlands areas in Jos plateau in the central area, Adamawa and Mambila highlands in the south-east, for example, have 1000 millimetres or above of rainfall annually. These are areas with more rainfall than the northern savanna and sahel regions.

5.7.3   Relationship between the Primary and derived Rainfall data

In Section 4.6, it was mentioned that 120 gridded points rainfall data was acquired from GPCC as the main rainfall data available for use in this investigation. Only 115 of these points incidentally fell on land while five fell on the sea or a lake. The relationship between the original values of these 120 gridded points rainfall data and the estimated rainfall data for the same points were evaluated on graphs. These graphs are illustrated on annual correlation plots in Figure 5.10.

From the correlation plots in Figure 5.10, all the predictive models are significant at $p <$ *0.05* level. However, there are few random dispersal points in some years. It can be seen from the plots that the year with best predictive model between the observed and predicted 120 gridded points is 1990. It has an adjusted R^2 of 94.3% followed by 1993 with an R^2 of 94.2%. The least, although good, is 1999 with an adjusted R^2 of 79.8%.

In comparison to the yearly predictive models (R^2) for the complete estimated dataset (Table 4.2) and the 120 gridded points indicated in Figure 5.10, both 1990 and 1993 are the best predictive models. In all the different coefficients of determinations (R^2) shown in Table 5.1 and Figure 5.10, 1993 still stood as the best predictive model. In general though, because the originally acquired 120 gridded rainfall points in Figure 5.10 are fewer in number they have better predictive powers (R^2s) for those locations.
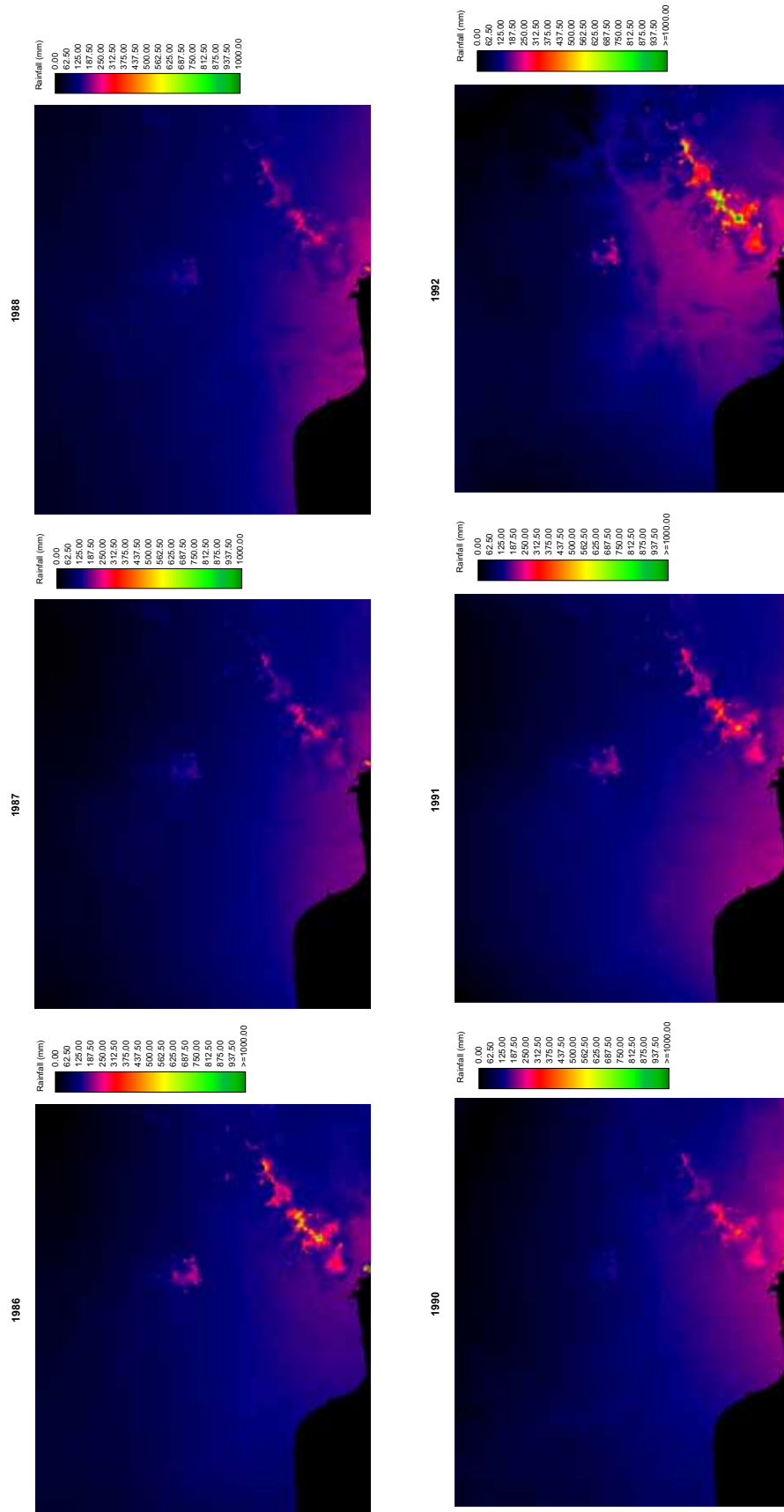
Figure 5.8 Estimated Annual Rainfall Images. These maps were produced from regression equations of each year using the Map Algebra in IDRISI-32. The images were contrast stretched to allow areas over 1000 millimetres of rainfall to be fairly visible. Areas of high rainfall are mostly around the highlands and forested regions as well as in the coastal areas. Areas of less rainfall are mostly located in the northern savanna and the sahel in the extreme north of the images.
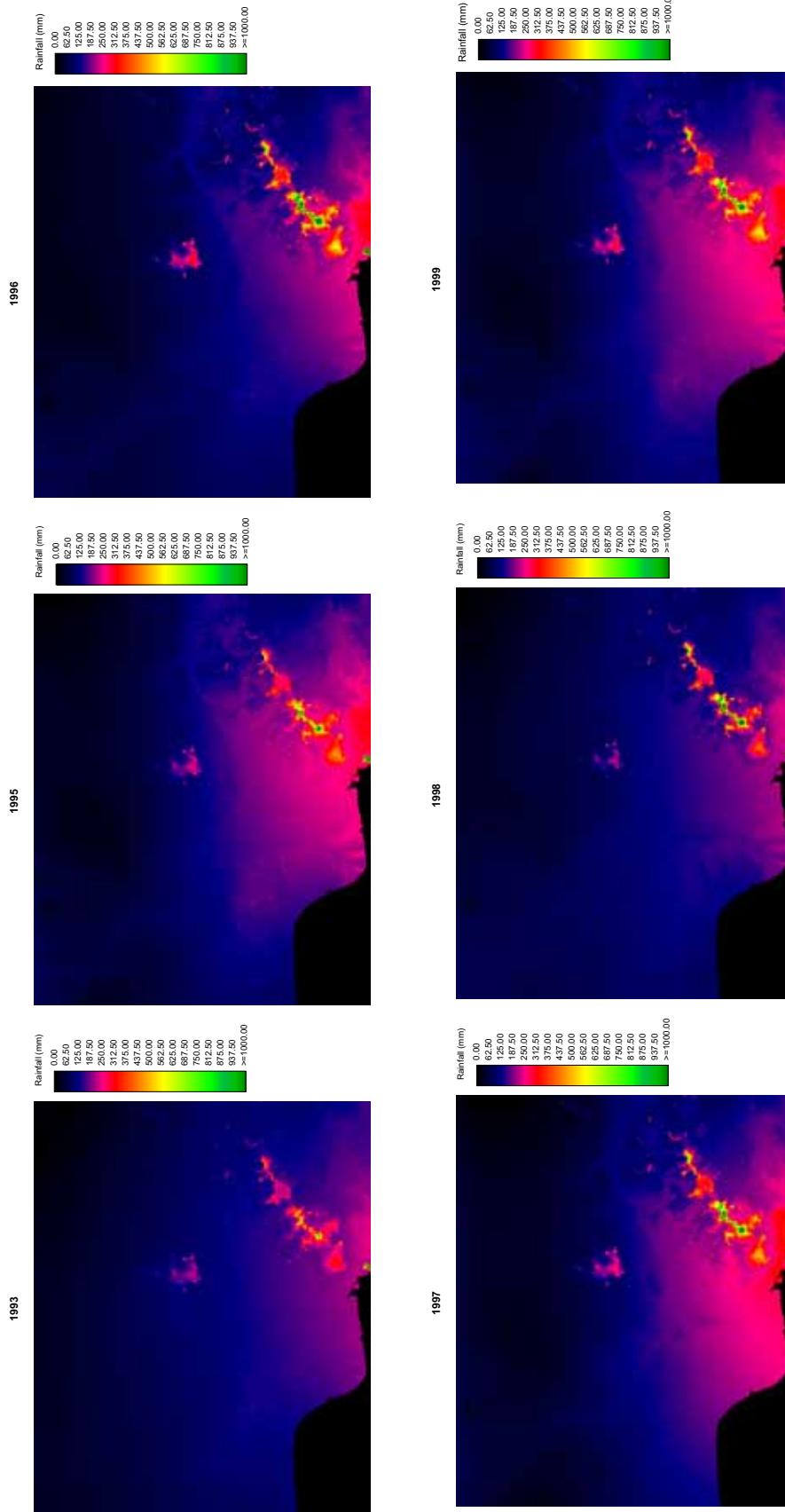
Figure 5.8 (Cont.) Estimated Annual Rainfall Images.
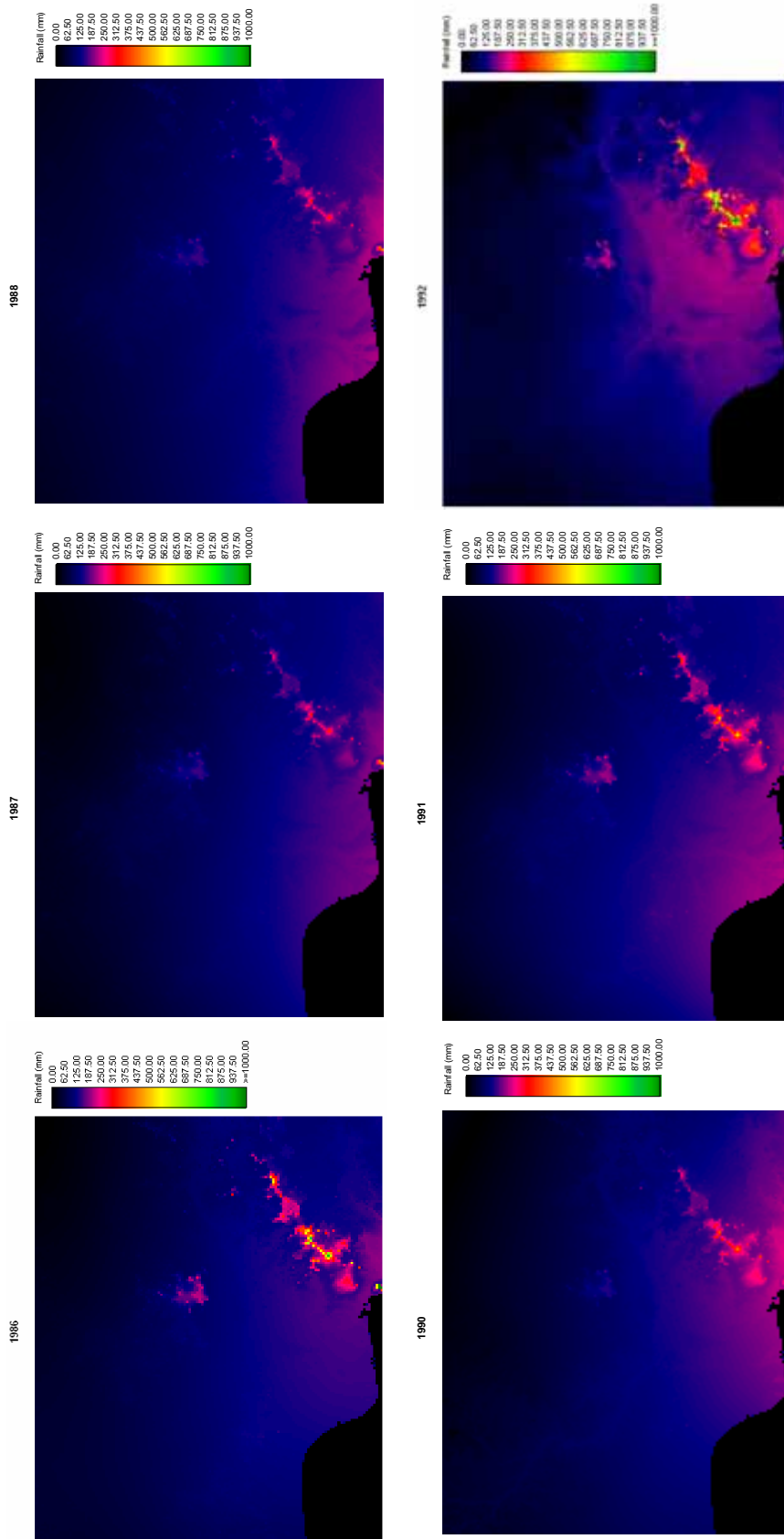
Figure 5.9 The reformatted Annual Rainfall Images. These images were derived from the main Annual Rainfall images that were produced from regression equations (illustrated in Figure 4.7). They were formatted by projecting them to the 8 km resolution of the NDVI images using pixel aggregation where the 1441 columns and 1183 rows on the original (predicted) were contracted to 174 columns by 138 rows. The images were contrast stretched for visual purposes only. Images with less than 1000 millimetres as maximum values were equally stretched. The images look similar to those in Figure 4.7 with the highlands areas in Jos plateau in the central area of the image and Adamawa and Mambila highlands in the south-east which have more rainfall, more highlighted than other places.
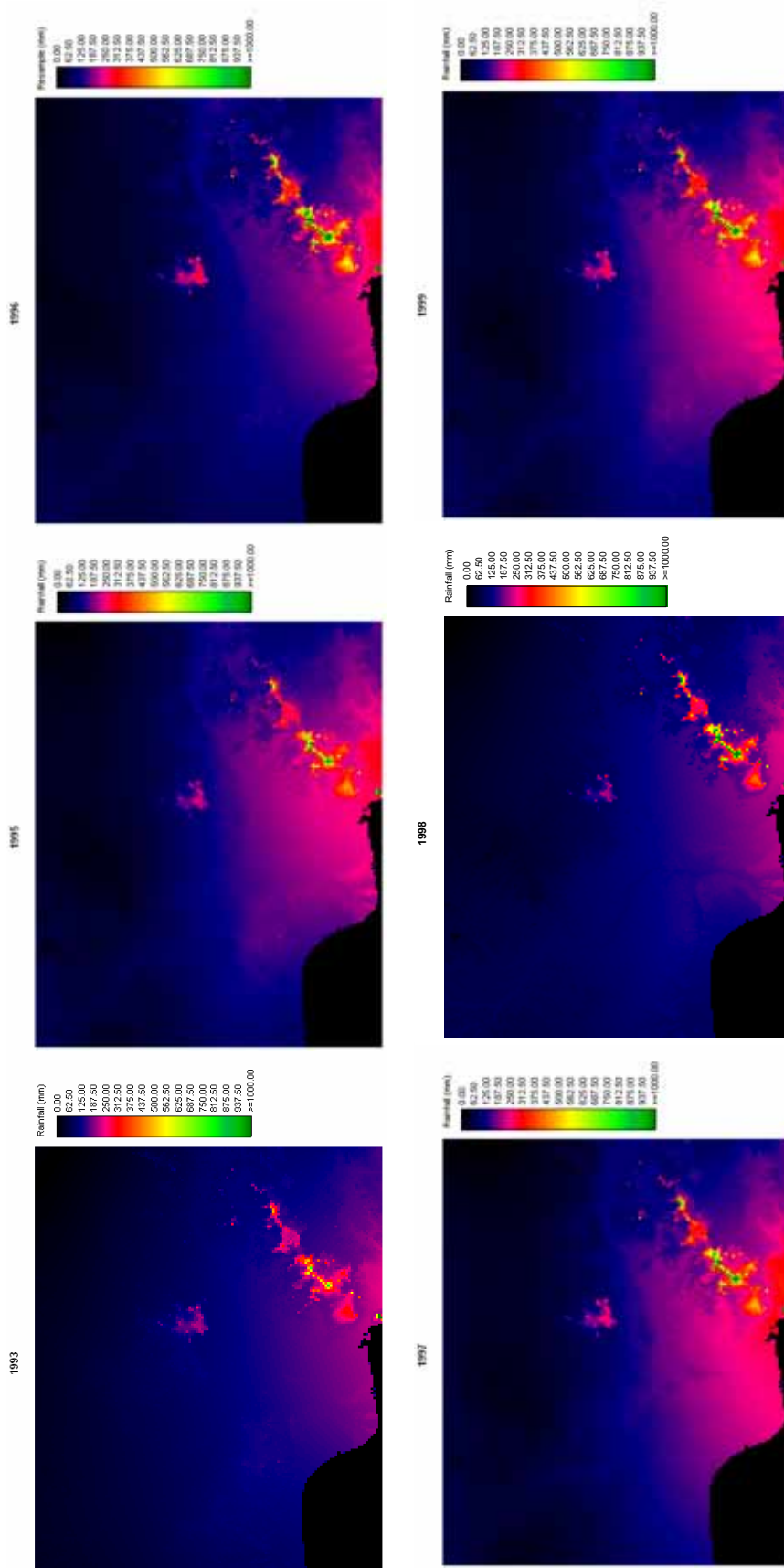
Figure 5.9 (Cont.) The Reformatted Annual Rainfall Images.

147
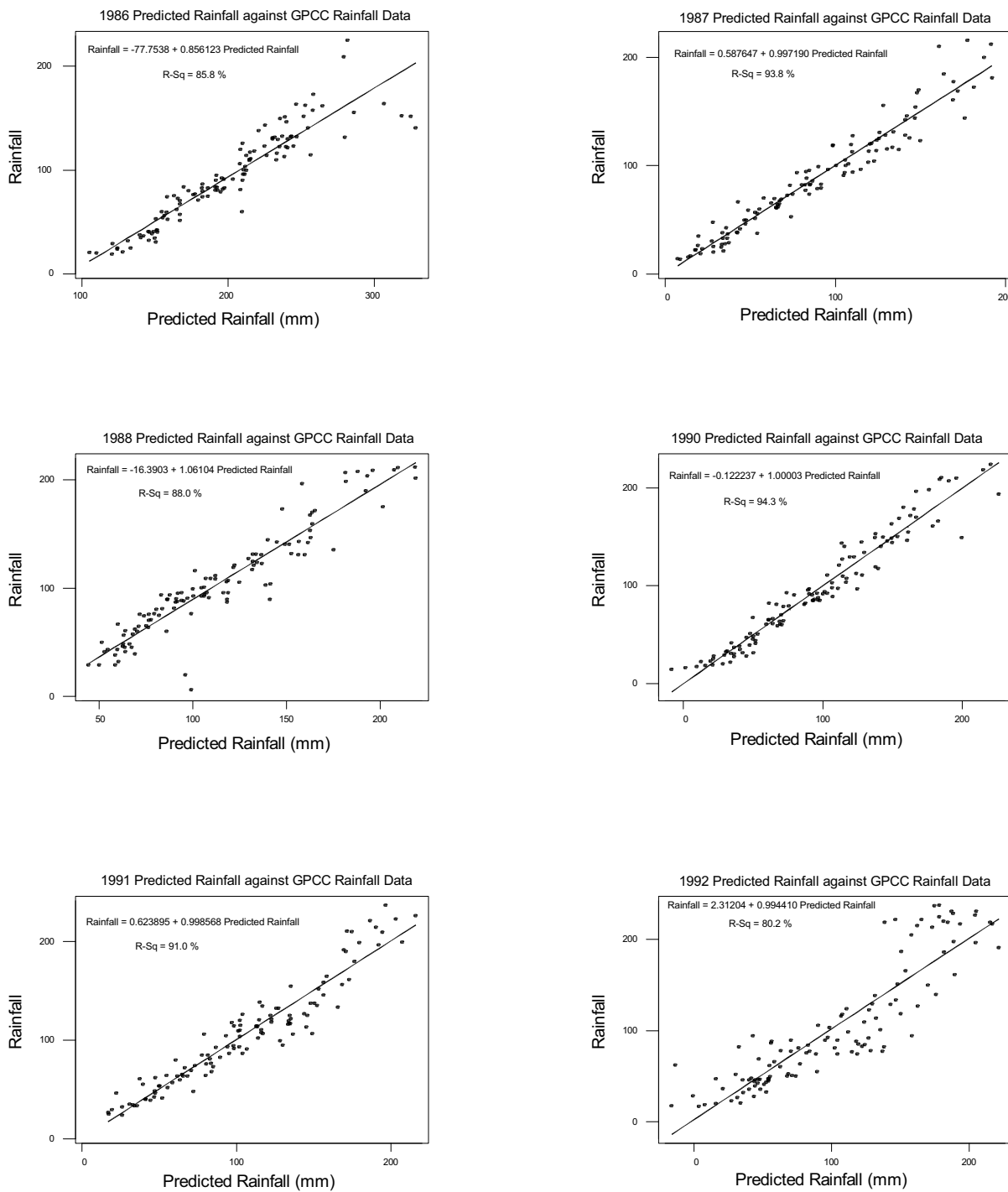
Figure 5.10 Correlation between the original GPCC and the predicted rainfall data. The different plots for each year indicates the relationship between the original 120 gridded point precipitation data from GPCC and the predicted rainfall for the same points for each year in the time series. All the plots showed a linear relationship with few random dispersal points between the original gridded data and the predicted rainfall data for the study area for all the years. The calculations were based on the multiple linear regression equations presented in Table 4.2. Using the adjusted R^2 values, all the plots indicated a linear correlation between the original GPCC rainfall and the predicted rainfall at $p = 0.05$ significant level.
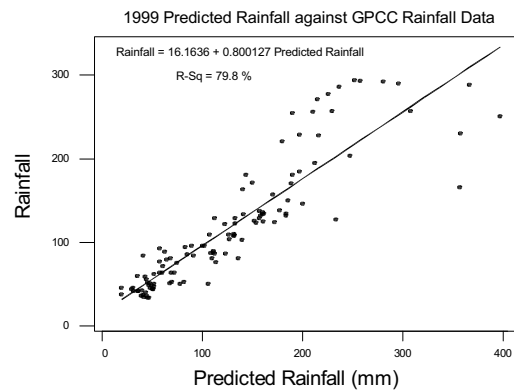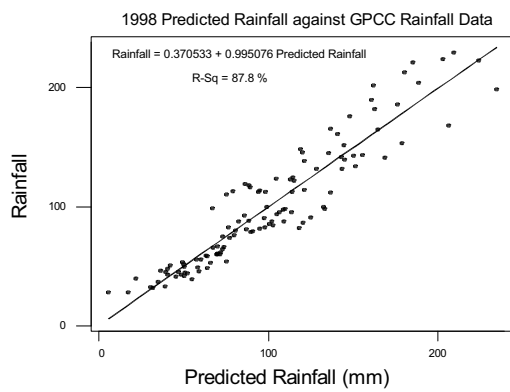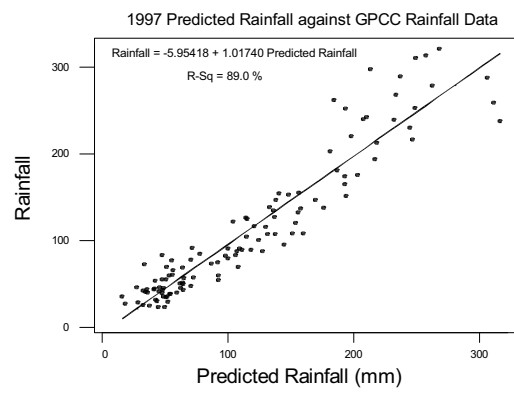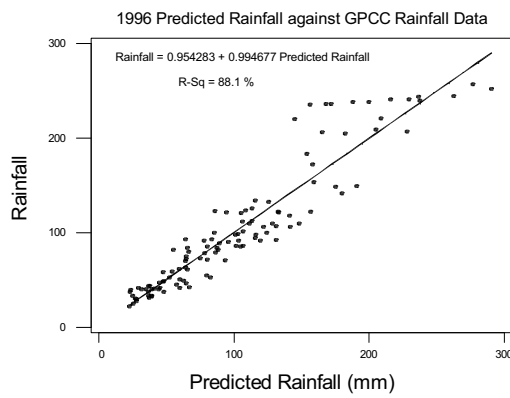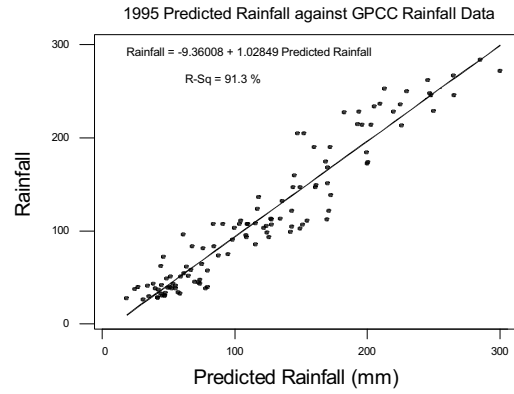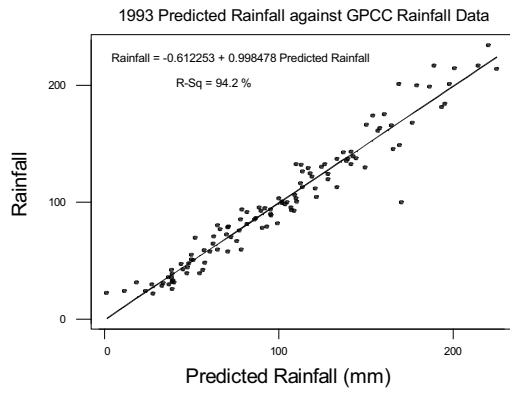
Figure 5.10 **(Cont.)** *Simple correlation plot between the original GPCC and the predicted rainfall*

5.8 Inter-annual variations of annual mean NDVI and rainfall for the whole study area

Inter-annual variations of the annual mean NDVI and rainfall for the complete datasets covering the study area is illustrated on a graph in Figure 5.11. From this graph, the general trend indicates that there is an increase in NDVI (green biomass) temporally over the years despite other climatic or atmospheric influences. However, 1986 to 1988 as well as 1991 and 1992, have an overall lower mean NDVI than all the other years. These years accordingly were detected to contain serious inter-annual variations of vegetation greenness over Africa due to climatic trends related to El-Nińo Southern Oscillations (Eastman and Fulk, 1993; Anyamba and Eastman, 1996).
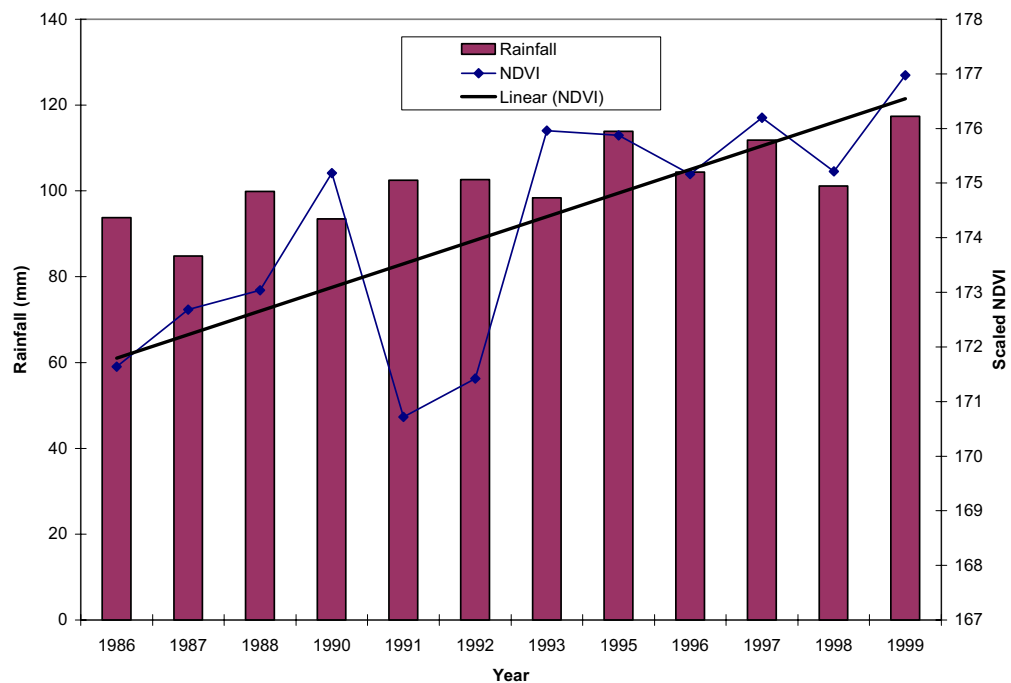
Figure 5.11 Graph of inter-annual variations in Annual Mean NDVI and rainfall of the study area. Annual mean datasets for NDVI and rainfall based on 8 km resolutions. The general trend indicates that there is increase in NDVI (green biomass) temporally despite climatic and other influences.

5.9   Inter-annual variations of annual mean NDVI and rainfall for the selected sites

In Section 5.8 the overall annual mean NDVI for the time-series covering this investigation (1986-1999) indicated that the earlier years contained inter-annual variations in vegetation greenness. The annual mean NDVI and rainfall data for the selected sites examined in Section 5.5 were also used to determine their inter-annual variations for the same time period (1986-1999). These are illustrated on graphs in Figure 5.12.

From these graphs in Figure 5.12, plots (a) and (c) representing the savanna sites indicated high NDVI for given rainfall input compared, for example, with graphs (e) and (f) representing the tropical rain forests. Graph (b) representing the sahel site around the irrigated areas close to Lake Chad indicated high NDVI with corresponding low rainfall, suggesting management implications.

The effects on the World Net Primary Production (NPP) which is probably related to the influence of El-Nińo Southern Oscillations shown in Figure 2.2 is reflected on the inter-annual variations of NDVI in Figure 5.12 on plot (e) representing the site at the Nigeria-Cameroon border and (f) representing the swamp forest. By implication, this suggests that areas of tropical forest region within the study area are more affected by these climatic trends.

In general, despite recomposition of the dataset into annual mean, the results suggest that possible inter-annual variations in the NDVI are likely to be caused by some climatic trends that may be related to El-Nińo/Southern Oscillations.
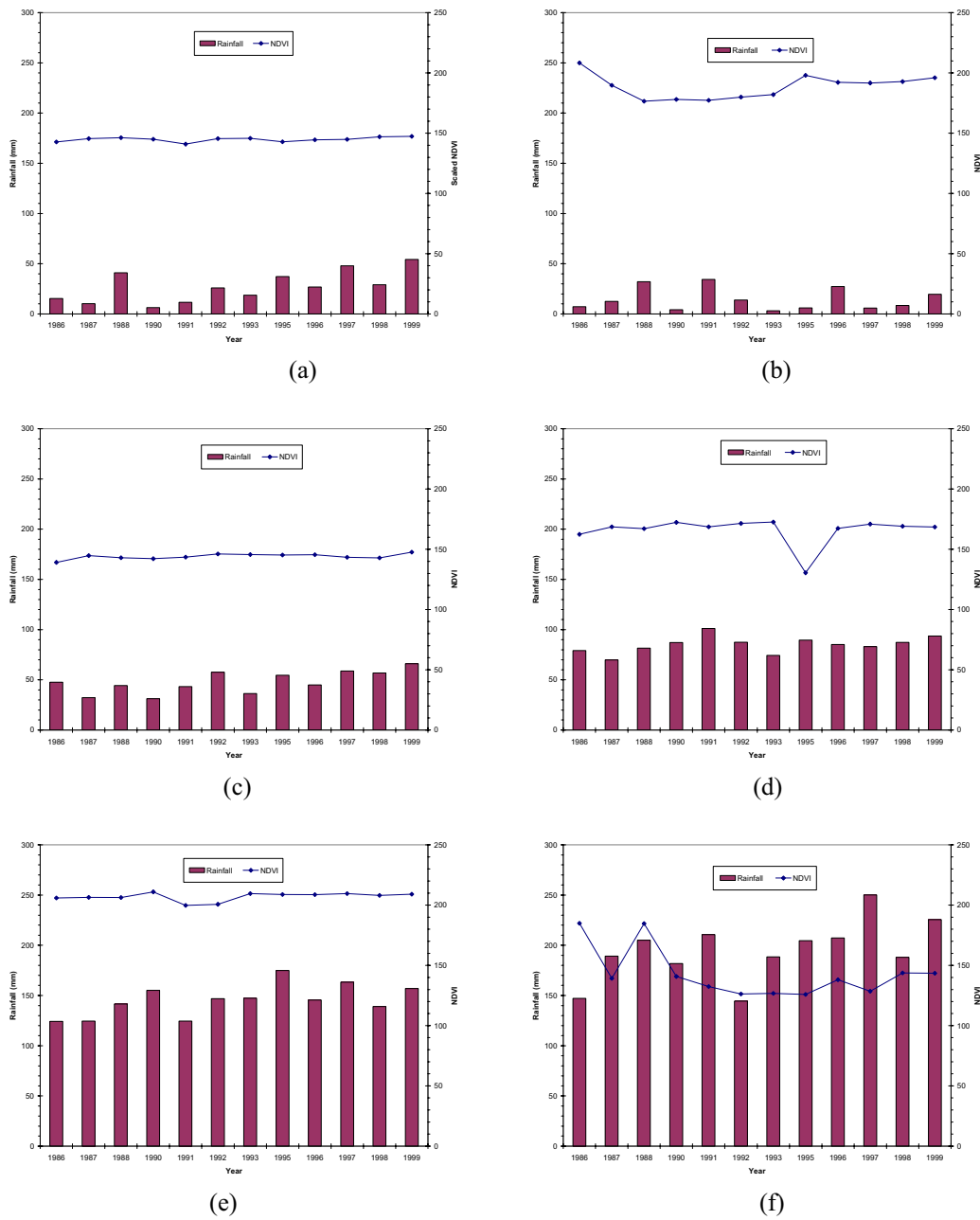
Figure 5.12 Graphs of inter-annual variations in annual mean NDVI and rainfall for the selected sites. Figure (a) shows the inter annual variation of the NDVI and rainfall for the main sahel site. Figure (b) shows the irrigated sahel site close to Lake Chad. Figure (c) shows the Sudan savanna site at the Niger-Nigeria border. Figure (d) shows the Guinea savanna site close to Kainji Lake in the north-west of Nigeria. Figure (e) shows the forest site at the Nigeria-Cameroon border while Figure (f) shows the coastal swamp forest around the Niger Delta. Despite recomposition of the dataset into annual mean, the results suggest that possible inter-annual variations in the NDVI are caused by some climatic effects and other factors. . NDVI are scaled from 0-255. (To inter-convert, scaled_ndvi = float_ndvi*125+128).

5.10 Summary

This chapter presents a preliminary assessment of the original dekadal and derived NDVI data, and the generated rainfall datasets. Selected sites from the vegetation zones of Nigeria were used with a view to providing some detailed observations on vegetation biomass change.

The key findings are :

- The original dekadal NDVI data from the PAL dataset still contains atmospheric and cloud contamination despite the maximum value compositing technique (Holben 1986) applied to it.

- By recomposing the dekadal NDVI data into monthly MVCs and annual mean datasets, the cloud contamination was greatly reduced to allow a meaningful assessment of the vegetation biomass change (based on NDVI) across Nigeria.

- The predicted (estimated) rainfall data validated with the primary gridded point rainfall data obtained from the GPCC for all the years are correlated at $p < 0.05$ significant level.

- Despite reformatting and aggregating the resolution of the rainfall data from 1 km to 8 km resolution, the data is still useful for analysis with the NDVI-PAL dataset.

- The annual Coefficient of Variation Image of the study area derived from 144 Monthly MVCs of the whole dataset covering the study area indicated areas of inter-annual variation in vegetation biomass across the country. It showed areas of rapid dynamic land degradation (eg the Niger Delta and coastal regions) which contain high inter-annual variability in NDVI that are surrounded by lower inter-

annual NDVI values. This corresponds with findings based on a study by Ehrlich and Weiss (2000).

- Preliminary analysis of the datasets indicated that the data, without further processing is not generally sensitive enough to identify confidently influences from, for example, climatic trends that are likely related to El-Nińo/Southern Oscillations.

- The trend of inter-annual variations in annual mean NDVI and rainfall datasets for the time period (1986-1999) covering the whole study area indicted that there was increase in green vegetation biomass despite climatic influences.

- Analysis of inter-annual variations in the annual mean NDVI and rainfall datasets for the selected sites within two distinct Nigerian vegetation zones (savanna and forest) indicated that NDVI varies with a given rainfall amount. However, serious inter-annual variations of NDVI which is likely to be related to the influence of El-Nińo Southern Oscillations are more evident in the tropical forest region.

- This free NDVI data from the PAL dataset is very useful for broadscale vegetation change analysis for developing countries with very low economic standing like Nigeria, after further processing.

In Chapter Six, three change detection approaches, Simple Image differencing (SID), Slope of Change from Regression (SCR) and Principal Component Analysis (PCA) were applied to the recomposed NDVI and generated rainfall dataset. This is with a view to assessing vegetation changes broadly across the country.

CHAPTER SIX

VEGETATION CHANGE DETECTION

6.1   Introduction

Having generated and optimised a reliable time series dataset from AVHRR-NDVI and rainfall across Nigeria as described in Chapter Five, this chapter presents the results of three separate change detection techniques applied to the dataset. Section 6.2 presents an introductory change detection approach using a simple image differencing technique (SID). The second technique uses slope of change from regression analysis and is presented in section 6.3. The third approach, using Principal Component Analysis (PCA), is presented in section 6.4. A short discussion on the techniques is presented at the end of each approach.

6.2 Vegetation Change Detection using Simple Image Differencing Technique

6.2.1   Aim and objectives

The main aim of this section is to use a Simple Image Differencing (SID) technique utilised by Young and Wang (2001), to identify broad temporal scale changes in vegetation biomass (based on NDVI) across Nigeria.

6.2.2   Methodology

This technique uses the annual mean NDVI recomposed from the monthly MVCs described in Chapter 5. Out of the total of 12 recomposed annual mean NDVI composite images, only eight (1986, 1987, 1991, 1992, 1996, 1997, 1998 and 1999) were utilised in the SID technique.

Determining Absolute change

To provide an overview of vegetation biomass change covering short and long time spans, the eight annual mean NDVI composite images were categorised into three sets based on a quasi five-year, quasi ten-year and 14-year time periods, as summarised in Table 6.1. Although the choice of the annual mean NDVI images used in this change detection approach were based entirely on detecting short and long term changes, the end-point years coincidentally fell within the different El-Niño/Southern Oscillations (ENSO) warm and cold phases which may have some implications on the results.

Table 6.1 Composition of residual datasets for the Annual Mean NDVI , the quasi five-year, quasi ten-year and 14-year periods used in the Image Differencing procedures

Annual Mean Images (End-point years)	Quasi 5-year Period (5 year period)	Quasi 10-year Period (10 year period)	14-year period
1986/87	1991/92 minus 1986/87	1996/97 minus 1986/87	1998/99 minus 986/87
1991/92			
1996/97	(1986 to 1991)	(1986 to 1996)	(1986 to 1999)
1998/99			

To further reduce the influence of climatic extremes and possible cloud contamination in the imagery, the mean NDVI of the end years of each comparison (the quasi time periods) was calculated (after Young and Wang, 2001) as illustrated in Table 6.1.

To aid the visual comparison of the images, the annual mean NDVI composites of the end-point years were then classified based on an interval of five NDVI units using the information from the minimum and maximum value range obtained from the descriptive statistics of these images.

The next process entailed the determination of the quasi five-year, quasi ten-year and 14-year changes between 1986 and 1999 (short-and long-term changes), using simple image subtraction to provide residual images for each change period.

The information showing the minimum and maximum NDVI value for each residual image were used to calculate a general ± 5 NDVI unit colour classification scheme for each image.

Determining Relative Change

To provide an overview of relative changes to the end-point years, for example, a change of 10 NDVI units in the savanna area of low NDVI (low biomass) might represent a big change compared to a change of 10 NDVI units in the forest area of high NDVI (high biomass). This might identify areas of significant change. To achieve this, the images derived from the absolute short- and long-term changes were used together with the end-point years of the annual mean images. The purpose is to calculate and derive proportionate change images (relative changes). The first process in this procedure is determining proportionate short-term change image. Hence, the original residual image for the quasi five-year change (1986 to 1991) was divided by the 1986/87 mean NDVI image to derive a 'per-pixel' change image (proportionate change) showing the relative changes between 1986 and 1991 for each pixel in the image data.   The same procedure was repeated for the other residual image sets so as to derive proportionate long-term relative change images for 1986 to 1996 and 1986 to 1999. The minimum and maximum range values from the summary statistics of the resulting proportionate change images were then used

to calculate a standard NDVI unit colour classification scheme, which was applied to each proportionate change image. In all the derived images from these procedures, only pixels covering land areas in all the classes were used in the analysis. For example, in the -1 to 4 class, the zero class which represents water bodies was masked out before the analysis and only land pixels were finally analysed.

6.2.3   Results

Classification of end-point years, absolute and relative change images

The results from the SID approach of change detection are illustrated in Figures 6.1 to Figure 6.9. However, because there is no clear-cut method for placing a threshold when classifying satellite images for areas of different land cover changes (Eastman, 2000), a simple classification using round number equal interval breaks was adopted (Monmonier, 1982).

The Classified Annual Mean NDVI Images

The classified annual mean NDVI images illustrated in Figure 6.1 shows 20 classes that were categorised into an interval of five NDVI units of increasing vegetation vigour. This is to give a visual view of an approximate vegetation map of Nigeria for the different end-point years chosen. The first class, 0 – 120, represents very sparse or un-vegetated areas including water bodies, while class 121 to 215 shows areas of increasing vegetation biomass cover. By simple comparisons, even though the classifications were not based on ground truth information, the classified images still showed a resemblance in patterns of vegetation boundaries with the annual mean NDVI images illustrated in Figure 5.4 and with the ecological zones on the vegetation map of Nigeria illustrated on Figure 3.14. The NDVI classes between 121 to 126 and 156 to 160 in

almost all the images tend to fall within the southern sahel and sudan savanna zones of Nigeria respectively. Classes between 161 and 165 and 186 to 190 mostly fall within the Guinea savanna. NDVI values ranging from 191 to 200 fall between the forest savanna mosaic and the coastal forest mangrove regions. The 201 to 215 NDVI classes fall within the densely forested and montane areas of the Guinea-Congolian vegetation zone (White, 1983).

The montane areas within the area under investigation, however, are areas that lie between 1400 and 3000 metres above sea level (White, 1983), and have more rainfall than any other parts in the savanna zones (ie the Jos plateau area in the north central part of Nigeria as well the Adamawa highland and the Cameroonian mountains in the south-east) (see Figure 5.8 and Figure 5.9). Based on these classified NDVI images, there are 1740 pixels covering those sparse or un-vegetated surfaces including water bodies (classes 0 - 120) and a total of 22,272 considered as land area containing average vegetation biomass (classes 121 – 215).

Table 6.2 Descriptive Statistics from the Annual Mean[1] NDVI Composite Images

Annual Mean Composite Images	Min	Max	Mean	SD
1986/87	127.29	208.25	172.16	16.30
1991/92	128.25	202.42	171.07	13.54
1996/97	123.38	212.63	175.68	16.71
1998/99	123.83	211.29	176.09	16.09

[1]Simple Image differencing images creating Annual Mean NDVI Images of end years {(1986+1987)÷2 , (1991+1992)÷2 , (1996+1997) ÷2 and (1998+1999) ÷2} in order to obtain the annual mean composites so as to further reduce climatic extremes in the data.

Table 6.3 Descriptive Statistics from the quasi five-year, ten-year and 14-year periods[2] showing absolute changes in NDVI

Quasi Year periods	Min	Max	Mean	SD
1986to1991 (5-year)	-41.63	34.29	-1.01	4.42
1986to1996 (10-year)	-37.96	43.46	3.27	3.43
1986to1999 (14-year)	-31.42	38.42	3.65	2.99

[2]Simple Image differencing images creating a quasi five-year change (1991/92 minus 1986/87) a quasi ten-year change (1996/97 minus 1986/87) and a 14-year change (1998/99 minus 1986/87).

Table 6.4 Descriptive Statistics from the derived relative changes showing proportion[3] of changes in annual mean NDVI

Trend periods	Min	Max	Mean	SD
1986to1991 (5-year)	-0.23	0.23	-0.004	0.026
1986to1996 (10-year)	-0.23	0.30	0.002	0.020
1986to1999 (14-year)	-0.19	0.26	0.022	0.019

[3]Simple Image differencing images creating the quasi five-year {(1991/92 minus 1986/87) ÷1986/87}, quasi ten-year {(1996/97 minus 1986/87) ÷ 1986/87} and the 14-year {(1998/99 minus 1986/87) ÷ 1986/87}   showing proportion of changes in NDVI.
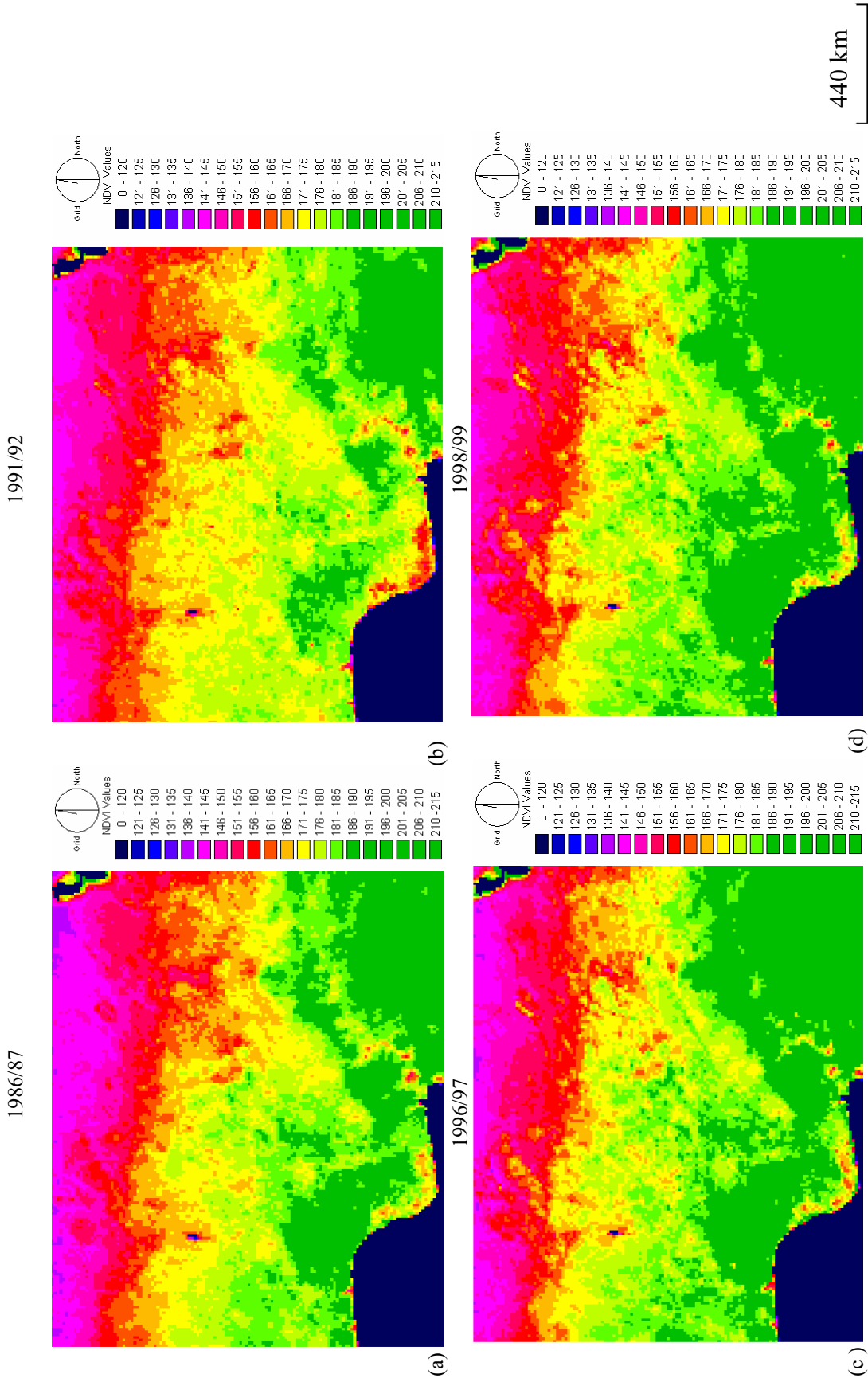
Figure 6.1 End-point years of annual mean NDVI Images (1986 to 1999). Simple Image differencing images was used to derive these end-years annual mean NDVI images in order to further reduce climatic extremes and other abnormalities in the data. Image (a) is the 1986/87 mean created by adding 1986 and 1987 images and their mean obtained, (b) is the 1991/92 mean, (c) is the 1996/97 mean, (d) is the 1998/99 mean images which were obtained by the same procedure as in creating the first mean image of 1986/87. Based on this classification Class 0-120 basically represents unvegetated surfaces including water bodies, Class 121-12 represents less vegetated surfaces, while from Class 126-130 up to Class 211-215 represents areas of increasing vegetation. (Note that NDVI values as indicated were scaled from 0-255. To inter-convert, scaled_ndvi = float_ndvi* 125+128).

The Classified Residual Images showing absolute short and long term changes

From the summary of the classified changed images (Figure 6.2), presented in Table 6.5, most of the absolute changes occur from the -21 to -16 up to 14 to 19 classes. However, majority of the negative changes from the -21 to -16 up to -11 to -6 are located in the southern forest areas, the montane and the Lake Chad areas. The remarkable negative changes, for example, the < -31 class in the short term period (Figure 6.2a) is mostly concentrated in southern coastal areas. In the long term (Figure 6.2b) periods, the negative changes are more in the -21 to -11 and -11 to -6 classes located in the southern coastal areas and around Lake Chad but the -6 to -1 change class during this period is spread across the whole country. In the much longer term period (Figure 6.2c), while the -11 to -6 change class are located more around the coastal and Lake Chad areas, the -6 to -1 change class are spread across the country. Class -1 to 4 generally are areas that either remained unchanged or have experienced minimal changes in vegetation biomass both in the short and long term periods across the country.

The majority of the positive change classes occur in the 4 to 9 class in both the short- and long-term periods across the country. However, these changes occurred more in the short-term period around the lowland areas of the river basins in the northern savanna than in the southern forest areas. Changes in the long-term period (Figure 6.2b) are concentrated more in the lowland areas of the northern savanna and the montane regions while in the much longer time period (Figure 6.2c) the changes in the 4 to 9 class are spread across the country.

The graph showing trends in NDVI change for the absolute change images are illustrated in Figure 6.3. Though most classes changed from one class to another, between the short and the longer term periods, there are few classes that still remained unchanged. For example, class 24 to 29 in the short term and >34 in long term periods. Although not very visible on the graph in Figure 6.3, the trends for classes <-31 and -26 to -21 for the short term from 1986/91 to 1986/96 to the longer term period 1986/91 to 1986/99 indicated that more positive changes in NDVI (increase in biomass) have taken place especially in the coastal areas, in the lowland forest region and in the savanna around Lake Chad area. Similar change also applies to -21 to -16, -16 to -11 and -11 to -6 change classes in these vegetation zones.

Conversely, the trends from -1 to 4 up to 29 to 34 classes both in the short term and longer term change periods indicated that there was a consistent increase in vegetation biomass across the country. The only exceptions in the trend are in the 24 to 29 class which indicated no change in the short term and the < 34 change class which indicated no change in longer term periods. Generally though, trends in the northern savanna areas indicated that more positive changes (increase in vegetation biomass) occurred in the longer term periods than in the short term. In the southern savanna, however, the trends showed that there are more negative changes (decrease in vegetation biomass) in the short term than in the longer term period.

(a)

(b)

(c)
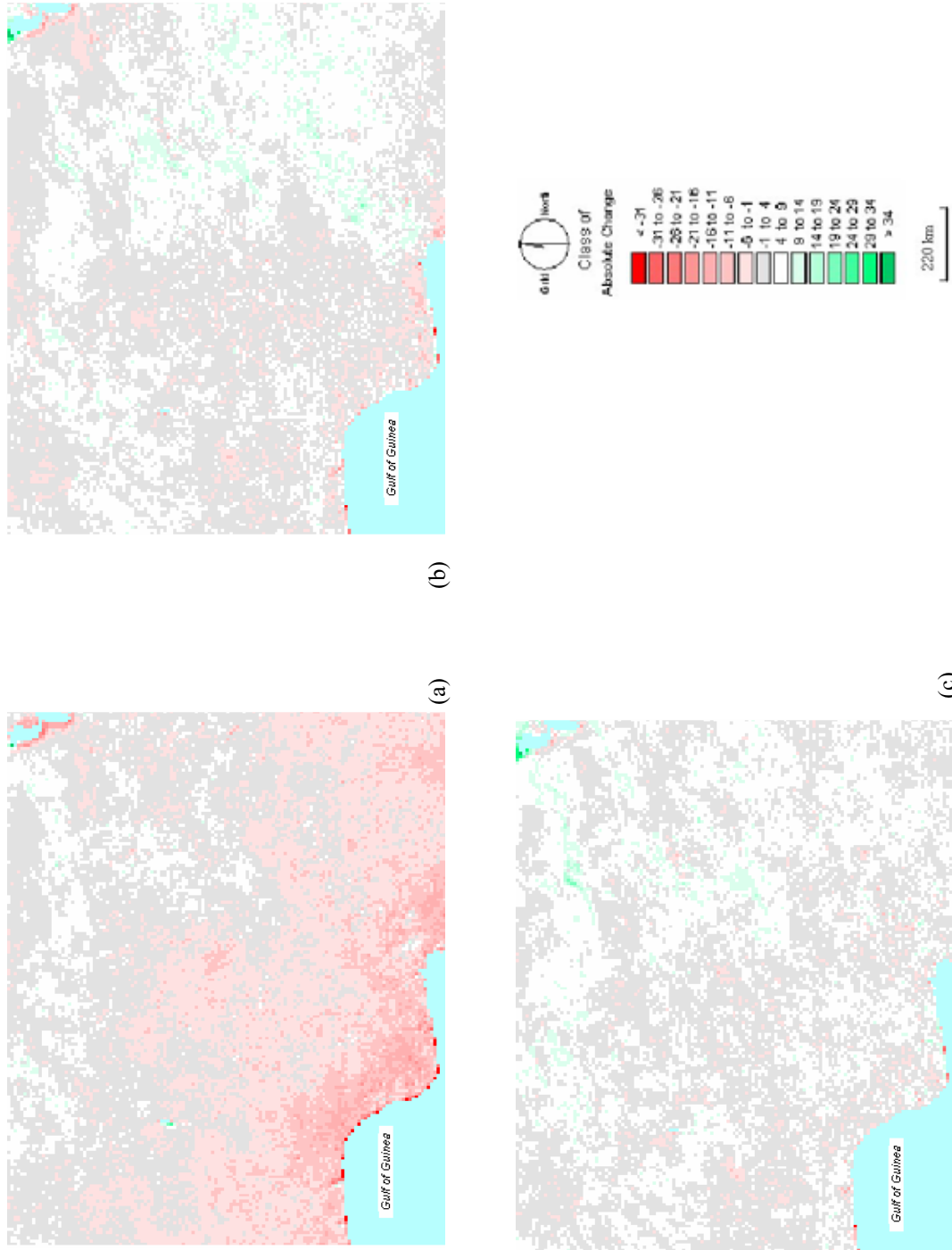
Figure 6.2 Classified Residual Images showing short- and long-term absolute changes in NDVI.   Simple Image differencing procedure was used to create these images. The first image (a) is a short-term absolute change (the quasi five-year change) in annual mean NDVI from 1986 to 1991 where the mean NDVI image for 1986/87 was subtracted from the mean image of 1991/92. Image (b) is a long-term absolute change (the quasi ten-year change) from 1986 to 1996 where the 1986/87 mean image was subtracted from the 1996/97 mean image while image (c) indicates a much longer term change (the 14-year absolute change) from 1986 to 1999 where the 1986/87 mean image was subtracted form the 1998/999 mean image. Broadly the short-term absolute change image shows more (negative) decrease in NDVI than the long-term changes. Both the long-term changes (ie the quasi ten-year and the 14-year change periods) tend to show areas of positive change in NDVI rather than negative changes

Table 6.5   Area covered by absolute change classes in the short- and long-term periods

Pixel Change Class	The Quasi Five-Year, Ten-Year and 14-Year Absolute Change Composite Images			% of Change between the Absolute short and long term changes in NDVI from 1986 to 1999	
	5-Year Absolute Change 1986 to 1991	10-Year Absolute Change 1986 to 1996	14-Year Absolute Change 1986 to 1999	86/91 to 91/96 (short term)	86/91 to 86/99 (long term)
	Number of 8 km NDVI pixels per change class				
< -31	18	2	1	-88.9	-94.4
-31 to –26	3	5	1	66.7	-66.7
-26 to –21	15	3	3	-80.0	-80.0
-21 to –16	55	5	2	-90.9	-96.4
-16 to –11	489	18	8	-96.3	-98.4
-11 to –6	2271	102	31	-95.5	-98.6
-6 to –1	7596	1316	642	-82.8	-91.5
-1 to 4*	9329	11121	10706	19.2	14.8
4 to 9	2423	8727	10101	260.2	316.9
9 to 14	68	929	722	1266.2	961.8
14 to 19	2	35	39	1650.0	1850.0
19 to 24	1	2	8	100.0	700.0
24 to 29	1	1	2	0.0	100.0
29 to 34	0	3	5	300.0	500.0
> 34	1	3	1	200.0	0.0
TOTAL	**22272**	**22272**	**22272**		

* The number of pixels in this category excludes the total number of pixels covering unvegetated
 surfaces including water bodies in each of the classified changed images = (1740)

The classified images showing short- and long-term relative changes

The summary and area of recorded changes in NDVI relative to the absolute changed
images illustrated in Figure 6.4 are shown in Table 6.6. Generally, there are similarities
in the areas that changed relative to the absolute changed images in Figure 6.2 which are
shown in Table 6.5. The greater part of these areas in the relative changes occurred in the
-0.16 to -0.11 and in the 0.09 to 0.14 change classes both in the short- and long-term
periods across the savanna and the forest areas.

Absolute
Decrease in biomass

Absolute
Increase in biomass
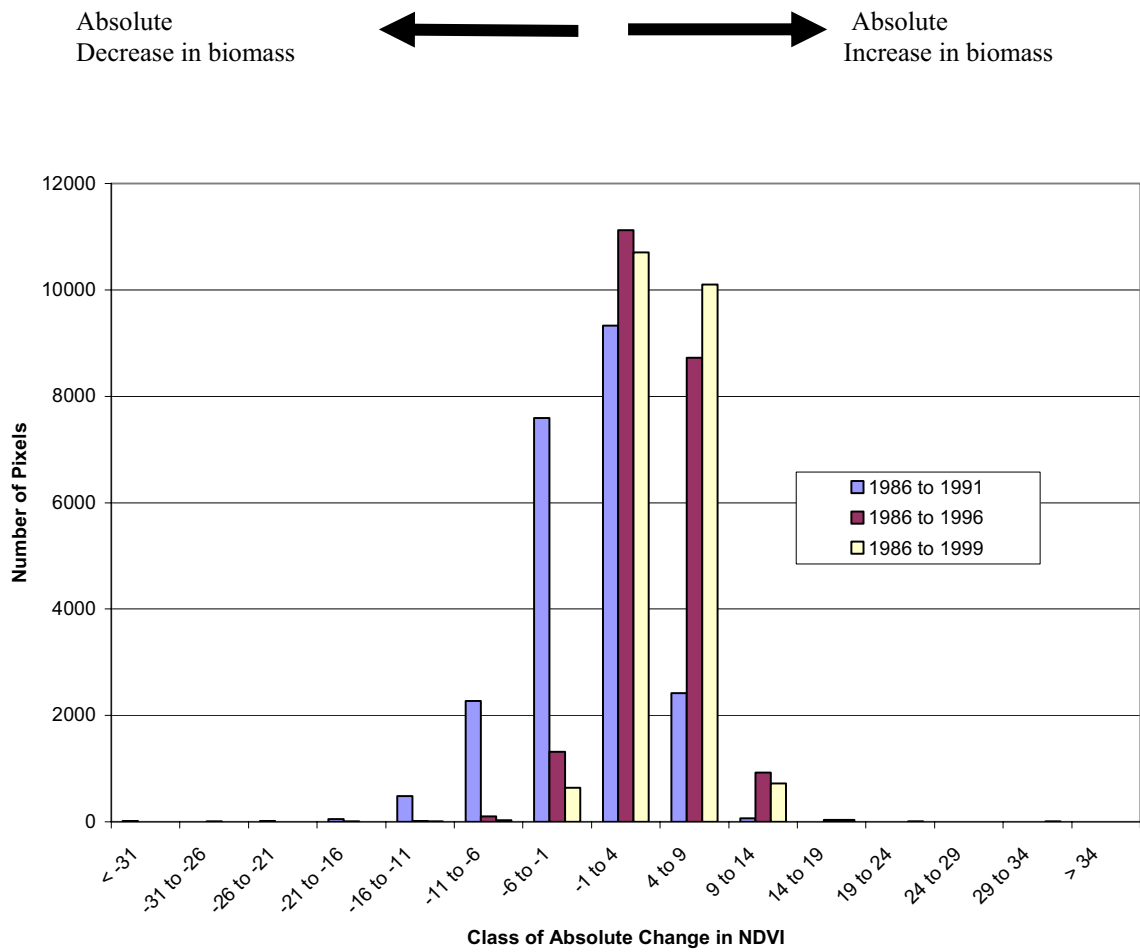
Figure 6.3   Trends in area covered by different classes of Absolute change in the short and long term periods

On the relative change images in Figure 6.4 there are also similar areas with trends in area covered by different change classes (short- and long-term change periods). These are later monitored using the annual mean NDVI and rainfall datasets for selected sites within these areas of observed changes in trends.
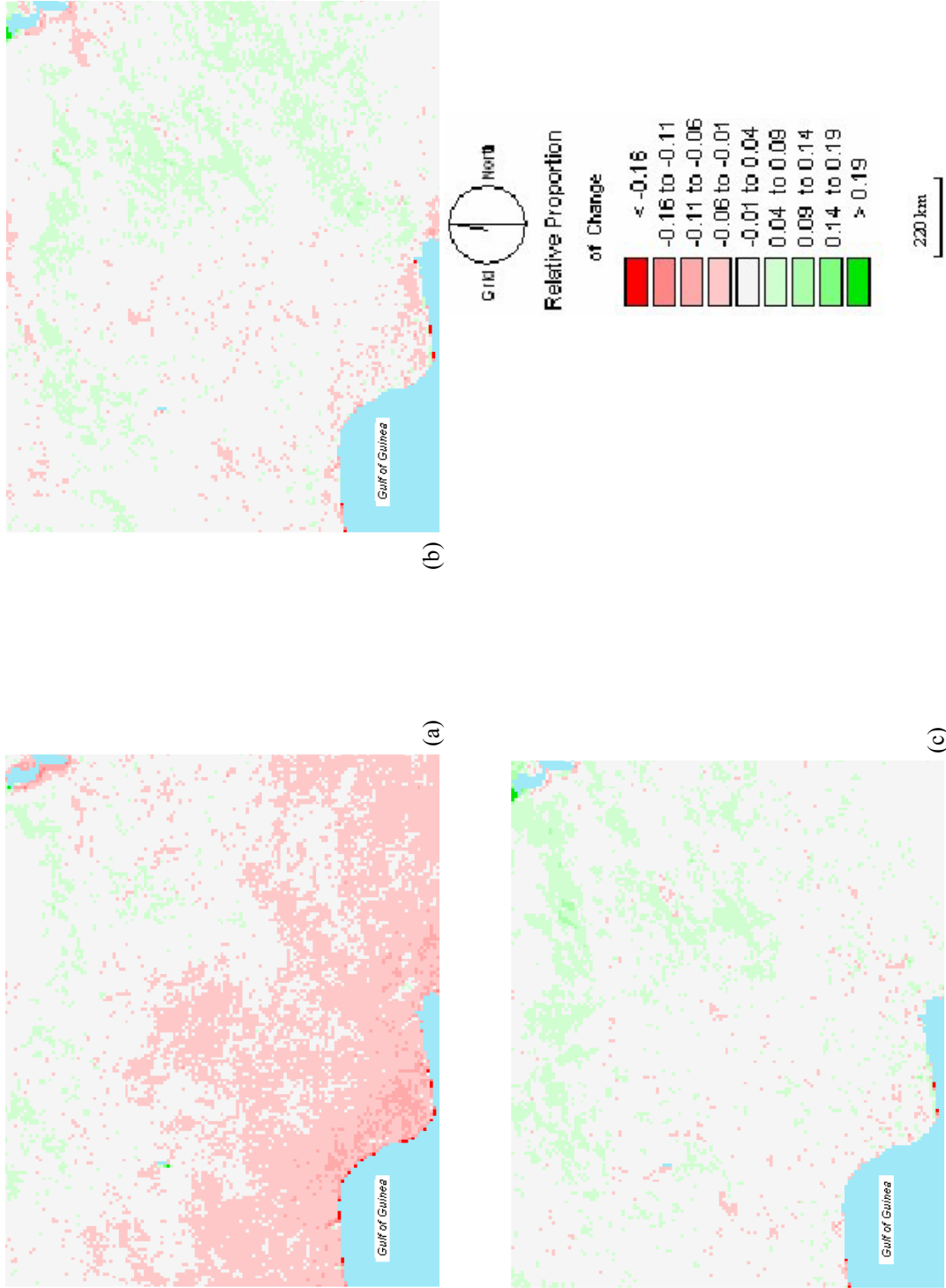
Figure 6.4 Classified Images showing short- and long-term relative changes in NDVI. Image (a) shows a short-term relative change (the quasi five-year change) in annual mean NDVI between 1986 and 1991 where the short-term absolute change image was divided by the annual mean NDVI image of 1986/87 to derive this image. Image (c) shows a long-term relative change (quasi ten-year change) from 1986 to 1996 where the absolute long-term image in Figure 6.4b was divided by the annual mean NDVI image of 1986/87 to derive this image. Image (c) shows a much longer term relative change (14-year change) in annual mean NDVI from 1986 to 1999 where the absolute change image in Figure 6.4c was divided by the annual mean NDVI image of 1986/87 to derive this image. In relative terms, there are similarities in the pattern of changes shown in the absolute change images for both the short- and long-term changes.

Table 6.6   Area covered by proportionate change classes in the short- and long-term periods

Pixel Change class	The Quasi Five-Year, Ten-Year and 14-Year Relative Change Images			% of change between the relative short- and long-term changes in NDVI from 1986 to 1999	
	Five-Year Relative Change 1986 to 1991	Ten-Year Relative Change 1986 to 1996	14-Year Relative Change 1986 to 1999	86/91 to 86/96 (Short-term)	86/91 to 86/99 (Long-term)
	Number of 8 km NDVI pixels per change class				
< -0.16	21	8	5	-61.9	-76.2
-0.16 to -0.11	23	2	2	-91.3	-91.3
-0.11 to -0.06	472	33	10	-93.0	-97.9
-0.06 to -0.01	8441	910	411	-89.2	-95.1
-0.01 to 0.04*	12625	18102	18765	43.4	48.6
0.04 to 0.09	684	3190	3021	366.4	341.7
0.09 to 0.14	3	19	49	533.3	1533.3
0.14 to 0.19	1	2	3	100.0	200.0
> 0.19	2	6	6	200.0	200.0
TOTAL	**22272**	**22272**	**22272**		

* The number of pixels in this category excludes the total number of pixels covering water bodies in each of the classified changed images = (1740)

6.2.4   Examination of inter-annual variations in vegetation biomass on selected sites of distinct NDVI trends

From areas with distinct NDVI trends observed on the classified absolute change images in Figure 6.2 and shown on Table 6.5, six sites (Figure 6.6) were chosen for examination. One pixel representing a site (64 square km) was selected within each of the six chosen areas in order to examine their inter-annual variations in vegetation biomass using the annual mean NDVI and derived rainfall datasets.

Relative
Decrease in biomass

Relative
Increase in biomass
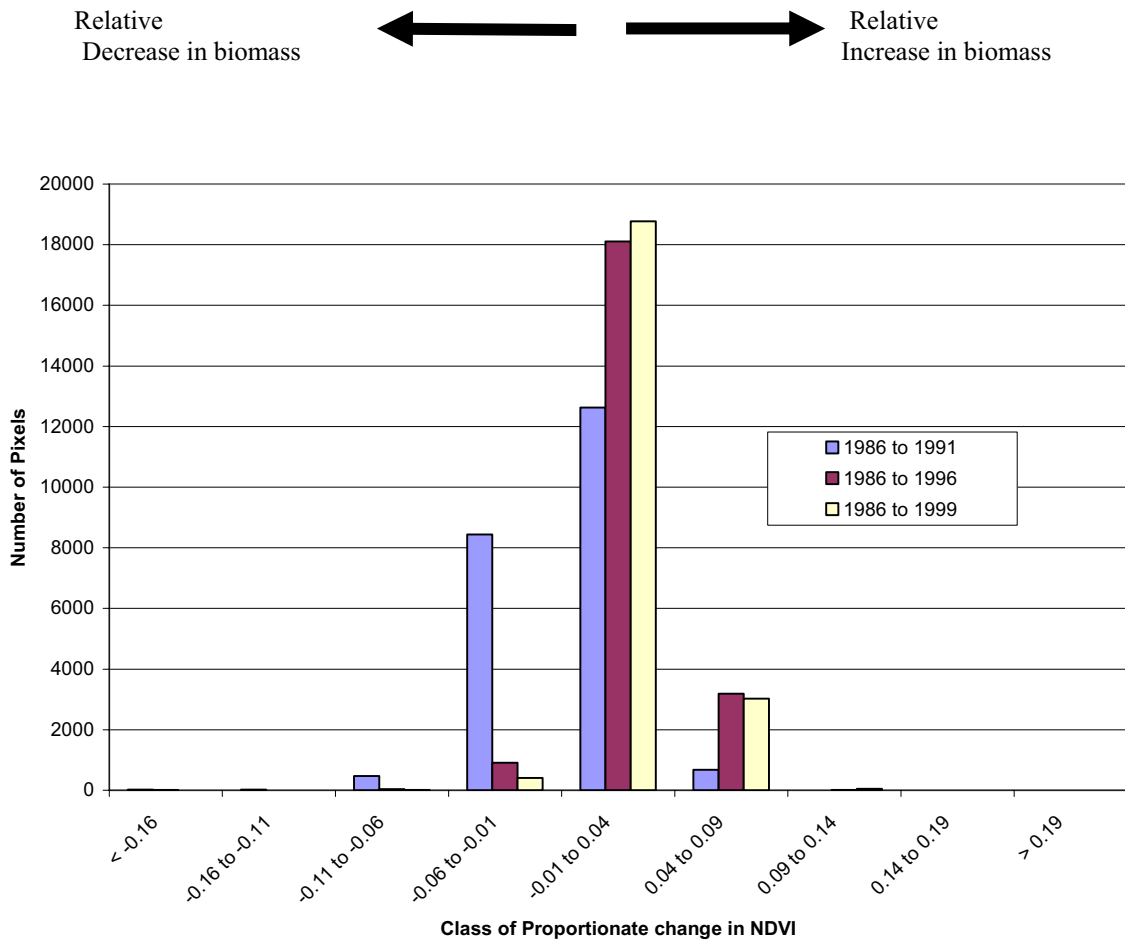
Figure 6.5 Trend in area covered by different classes of relative changes in the short- and long-term periods

Site Selection

The selection of sites was made within the Nigerian vegetation zones (Areola, 1982) (see Figure 3.14) of the observed areas of trends in NDVI covered by different classes (Tables 6.5 and 6.6). Using the geographical coordinates location closest to a rain gauge station within the observed areas of NDVI pixel change class, the annual NDVI and rainfall values were determined for each site (pixel) chosen.
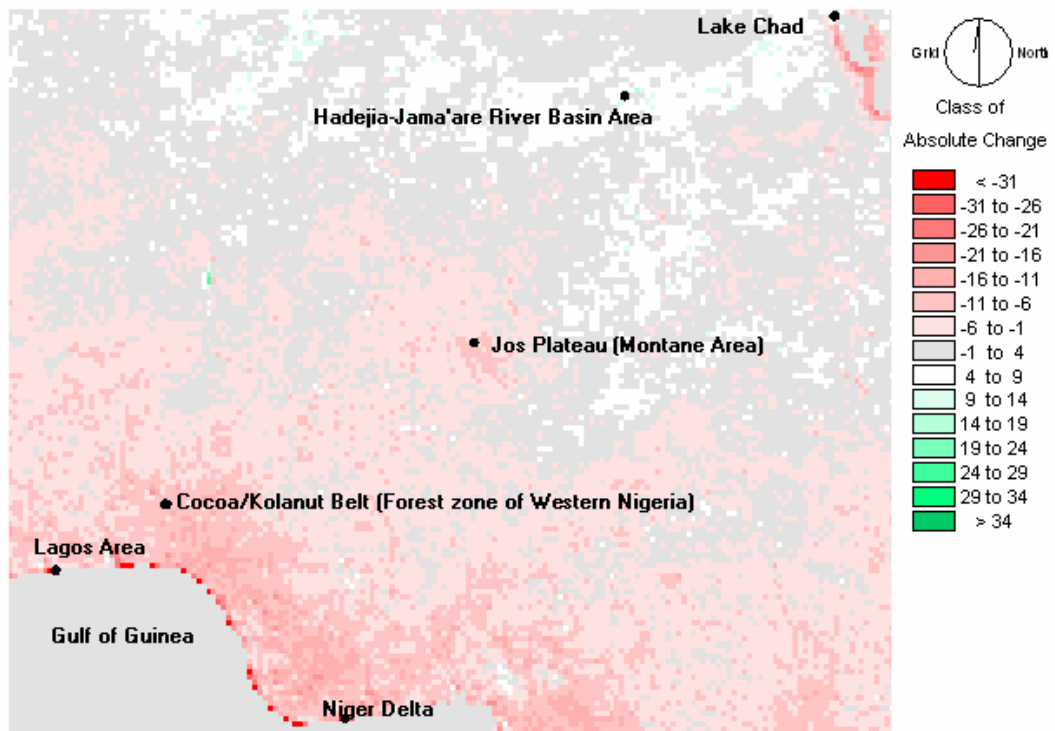
Figure 6.6 Selected sites with distinct trends in inter-annual variations in vegetation biomass cover and rainfall. The exact pixel positions shown in black dots (using the short-term changed image, 1986 to 1991) are chosen from areas of distinct NDVI trends on the absolute change images in Figure 6.2.

The individual sites selected fall around :

1.   The Niger Delta area. A pixel was selected from areas of highest negative change in NDVI (< -31) in the absolute change class (Figure 6.2), which also shows a relative negative change in NDVI in the < -16 class for both the short- and long-term periods. However, based on studies conducted on the Niger Delta (Boele *et al,* 2001b), the site (pixel) chosen within this change class falls in an area said to have experienced certain levels of environmental degradation as result of the activities of oil companies (see Section 6.3.9).

2.   Lagos area. A pixel was selected from areas of highest negative change in NDVI in the < -31 absolute change class (Figure 6.2), which has a relative change in the <-16 change class in NDVI both in the short- and long-term periods (see Figure 6.4). Based on studies regarding land-use/cover changes around Lagos and its environs (Adeniyi, 1980), a pixel falling in this area was chosen within this change class.

3.   The cocoa/kolanut belt in the forest region of the south-western part of Nigeria. A pixel was selected within area covered by the -11 to -6 NDVI change in the absolute change class (Figure 6.2) with a relative negative change in NDVI in the -0.06 to -0.01 class (see Figure 6.4). The pixel selected within this area of change class falls in an area where a study has shown that the intensity of agricultural activity around these areas has made it vulnerable to savanna incursion (Salami 1999).

4.   The montane area around Jos plateau in the central part of Nigeria. This site (pixel) was selected within area covered by the -11 to -6 NDVI change in the absolute change class (Figure 6.2). This same site (pixel) also falls within area covered by the -0.06 to -0.01 proportionate change class on the relative change maps (Figure 6.4) within the short- and long-term periods (1986 to 1999).

5.   The Hadejia-Jama'are River basin in the north-east part of Nigeria. This site was selected within area covered by the 4 to 9 NDVI change class (Figure 6.2). The same site (pixel) selected falls within an area in the -0.01 to 0.04 relative change in NDVI class (Figure 6.4). On the other hand the pixel selected within this area of change class falls within the Hadejia-Jama'are wetlands where a study has shown that there were both

positive and negative environmental and socio-economic impacts in the area due to dam

constructions (Adams and Thomas, 1996) (see Sections 3.4.3 and 6.6.3).

6.   Northern part of Lake Chad. A pixel was selected from areas of highest positive

change in NDVI (>34) in the absolute change class (Figure 6.2), which also falls within the

area covered by the relative positive change in NDVI in the > 0.19 class both in the short

and long term periods. However, the pixel selected in the area falling within this change

class also falls in an area where a study has shown that there was land-use transformation

due to dryland irrigation around the region (Adams and Thomas, 1996).

After determining the annual mean NDVI and rainfall values for each of the selected

locations (sites) within the observed areas of trends in NDVI covered by different classes,

they were plotted on graphs. These graphs show the inter-annual variations in annual mean

NDVI and rainfall for these selected sites and are illustrated in Figure 6.7.

From these graphs site (a) in the Niger Delta area suggests that except for 1986 and 1988,

which clearly showed an increase in NDVI, not much has changed positively over the

years, although there was very high rainfall with corresponding low NDVI values across

the time series.

Site (b) representing a site around the Lagos area shows a similar pattern of inter-annual

variations to site (a) despite the high annual rainfall as shown by the graph. There are,

however, low troughs in the profile in 1987 and 1990, otherwise not much has changed

positively in vegetation biomass.

(a)

(b)

(c)

(d)

(e)

(f)
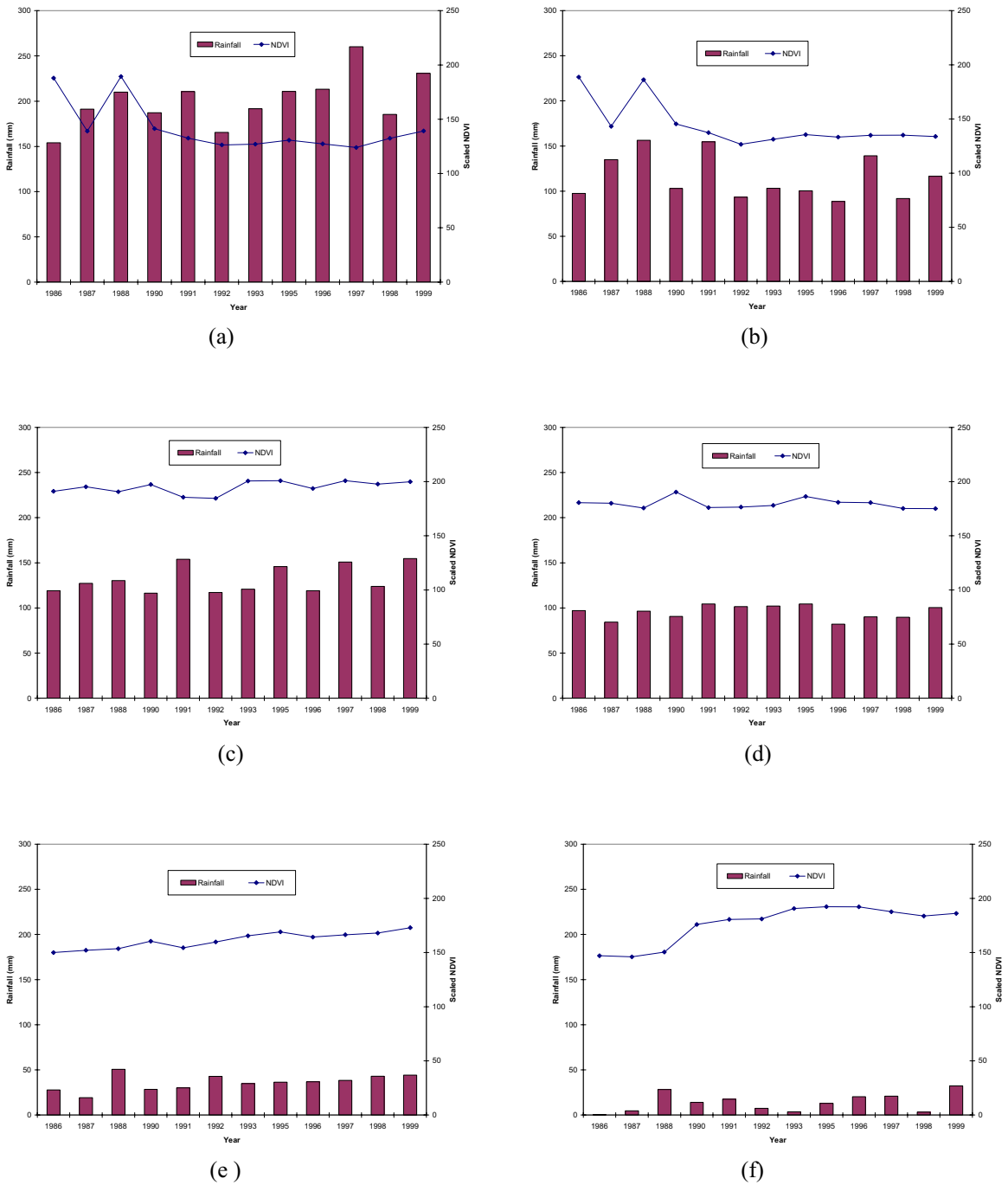
Figure 6.7 Inter-annual variations in annual NDVI for selected sites in areas with apparent trends in NDVI changes. These sites were based on the absolute change images in Figure 6.2. Figure (a) represents a site around Niger delta in change areas <-31, (b) represents a site around the Lagos area from change areas <-31, (c) represents a site in the cocoa belt in the forest region of south-western Nigeria from areas -11 to -6 , (d) represents a montane site around Jos Plateau from change areas -6 to -1, (e) represents the Hadejia-Jama'are site from change areas -1 to 4 and (f) represents a site north of Lake Chad from change areas >34.

Site (c) represents an area around the Cocoa belt in the south-west forest region of Nigeria. This site showed a fluctuation in the graph of the interannual variation of vegetation biomass. Although there are both high NDVI and rainfall values (above 100 mm) in this tropical forest area, the NDVI in 1991 and 1992 are much lower (below 190) than all the other years.

Site (d) representing a site in the montane area around Jos Plateau has high rainfall values (~100 mm) in most years. However, it has high NDVI values in all the years with the highest mean NDVI in 1990.

Site (e) represents a wetland area around the Hadejia-Jama'are river basin in the northern savanna area. Although with a low annual rainfall (below 50 mm) in most years, there is a slight increase with time which is reflected in a consistent increase in annual mean NDVI.

Site (f) represents a site in the northern part of Lake Chad basin. This site like site (e), both in the northern savanna area of Nigeria, has very low rainfall (below 40 mm) in all the years. However, the trend in annual mean NDVI is much higher when compared with site (e).

6.2.5 Discussion

Analysis of vegetation changes across Nigeria with PAL NDVI dataset using simple image differencing technique shows that this is feasible. However, one of the critical elements of Image Differencing Technique in remote sensing change detection is where to place a threshold between change classes (Singh, 1983; Jensen, 1996). Although standard deviations have been used in other studies (eg Quarmby *et al,* 1987; Fung and LeDrew, 1988), other authors (eg Fung and LeDrew, 1988; Eastman, 2000) further suggested the use of ground truth data as a means of assessing the accuracies of classified satellite data. In general, there are no clear guidelines on how to set thresholds when classifying satellite data used in change detection (Eastman, 2000). Although such classification by Fung and LeDrew (1988) could be adopted in this investigation, owing to the non-ground truth information covering the whole study area composed of savanna and forest vegetation, this becomes problematic. Hence, an alternative classification approach was adopted.

When showing spatial changes of varying classes on quantitative maps or satellite images simple classification approach can be applied to show such changes in absolute or relative terms. For example, the use of natural breaks, quartiles, standard deviations or equal class intervals of round numbers (Monmonier, 1982) was used in this technique. The advantage of the equal class interval adopted in this investigation is that one can choose any class breaks such as 4, 5, 10 etc for the class intervals and it is easy to interpret. On the other hand, choosing the optimum number of classes is also difficult especially if the data is evenly distributed. In the context of this investigation even if standard deviations are used as a way of placing threshold of change classes it is not

possible to check the accuracy of the classification since it was not based on actual landcover classes that were linked to groundtruth information. Hence, the results did not give the 'from-to' change classes of actual landcover information derived, rather, the number of pixels that changed from the different interval classes was one of the major changes obtained. So even the round number class intervals used require a very careful selection of class breaks.

With regard to the NDVI data utilised in this technique, this was selective because not all the annual mean NDVI data was used as input in the procedure. The selective use of the data must have hidden certain changes (positive or negative) that have taken place within the years of those images not included in the procedure. In addition to being selective in using the annual mean NDVI datasets in the procedure, the mean of the end-point years for the selected datasets were the only images used as input in the analysis. However, this procedure was shown to have an advantage of reducing serious climatic effects in the overall change results (Young and Wang, 1999). Although the overall changes determined within the short- and long-term periods in absolute terms were also shown to be useful in determining proportionate change in relative terms (Young and Wang, 2001), other underlying changes cannot be detected. For example, high negative or positive changes in NDVI as a result of serious drought or anomalous rainfall were not apparent. Hence, another disadvantage is that because only selective annual mean NDVI images from the time series were utilised in the procedure, the results obtained must have been under- or over-generalised. For example, this appears in the short-term change image in Figure 6.2a showing overall changes in NDVI between 1986-1991. This is because both the annual mean images in the image base

years (end-point years) ie 1986/87 and 1991/92 coincidentally fell in ENSO years affected by global changes in Net Primary Production (NPP) and crop production as a result of climatic variability (Ochie *et al,* 2000) (see Figure 2.2). Thus, it also affected the overall results across the whole country in the first five-year period.

It is more likely to achieve better results with this technique if the whole annual mean NDVI datasets were utilised in the procedure where a sequencial image differencing is applied from year to year in the time series. This would show varying changes in vegetation biomass between individual years across the time series.

Although not the main focus of this investigation, image deviation procedure was employed as a supplement in the analysis (See Appendix 5). In the supplementary procedure each annual mean NDVI was subtracted from a cumulative annual mean image of the whole NDVI dataset. The result gave individual residual images for each year. Hence, with image deviation, each area (pixel) was easily identified by contrast to a long-term characteristic condition, ie it showed how each image data deviated from the overall mean image of the time series. It also showed clearly, for example, that NDVI values were different for the three base years (1986, 1987 and 1988).

Despite the advantages and disadvantages of this technique, the overall change map in Figure 6.4c showing proportionate changes in vegetation biomass across Nigeria as captured by NDVI, suggests a positive trend (see Figure 5. 11 and Figure 6.2c) where vegetation biomass across Nigeria between 1986 to 1999 showed an increase. However, based on the temporal NDVI and rainfall plots (e) and (f) in Figure 6.7 there were more rapid changes in vegetation biomass within the savanna than in the montane or forest areas, given the rate of change in rainfall.

6.2.6   Summary

- This simple image differencing technique has shown that it is possible to isolate areas that experienced changes in NDVI over short- and long-term periods in both absolute and relative terms.

- Although the procedure utilised annual mean NDVI which captures average productivity over a single year, it reduces the problem of capturing vegetation at different times in a phenological cycle.

- Because only the broad picture is captured for a whole year as a result of utilising selective end-point years across the time series, the use of complete data rather than a few selective years would identify more areas of serious changes in NDVI due to drought or anomalous rainfall.

- There are similarities in the pattern of changes in NDVI on both the absolute and relative change maps in the short- and long-term periods in most areas.

- Positive changes in NDVI are more prominent in the northern savanna (particularly along river basins) than in the southern forest areas over long-term periods.

- Negative changes are more prominent in the short-term period in the southern forest zone and around the coastal areas as well as areas close to the Lake Chad in the sahel zone.

In the next section, the second change detection technique using slope of NDVI from regression is presented. This is aimed at evaluating areas of vegetation biomass change using a pairwise comparison of annual NDVI and rainfall dataset covering the whole study area.

6.3   Vegetation Change Detection using Slope from Regression

6.3.1 Introduction

This section presents the results of the second approach to vegetation change assessment across Nigeria using slope of change from regression. The 12 timeseries annual mean NDVI and rainfall images utilised in Section 6.2 were used to evaluate gradient of changes. Different techniques have been applied to time series NDVI data from the PAL dataset to assess spatial changes in vegetation. However, in this investigation the use of slope of change from time series of NDVI and rainfall in a pairwise comparison is, according to our knowledge, for the first time being presented. In change detection changes can either be positive or negative, but the main focus in this approach is on the negative aspect of the changes, especially in areas of increasing rainfall, to discover if anthropogenic influences can be detected.

6.3.2 Aim and Objectives

The aim of this approach is to assess spatial change information of a negative nature in vegetation biomass (based on NDVI) across the whole of Nigeria despite increase in rainfall.

(i)   To derive slope of change images, one each for NDVI and rainfall from time-series data from 1986 to 1999.

(ii)   To isolate areas of negative changes in NDVI from the main NDVI slope of change image.

(iii)   To isolate areas of positive changes in rainfall from the main rainfall slope of change image.

(iv)   Use the negative NDVI slope of change and the positive rainfall slope change images together in a cross-tabulation/classification in order to identify areas where there was decrease in vegetation biomass despite increase in rainfall.

(v)   Monitor the inter-annual variability of NDVI and rainfall dataset for those changed areas identified.

(vi)   Evaluate the relationship between the changes in NDVI and rainfall for selected sites within change areas of numerically comparable classes.

6.3.3 Methodology

As presented in sections 4.3.3 and 5.7.3, the original NDVI time-series data from the PAL dataset has been subjected to standardised normalisation procedure and has also been re-composed into mean annual data. On the other hand, the derived (estimated) rainfall was validated using the original rainfall data obtained from GPCC. Results of validation showed a 5% level of significance. On the basis of these, slope of change images were created both from the time series annual mean NDVI and rainfall datasets using the following procedure.

Creation of an NDVI slope of change image

In determining a slope of change for each pixel between the successive annual mean NDVI images, all the 12 annual mean NDVI images derived from the 144 monthly MVCs were used in this procedure. Firstly, all the images were converted to ASCII format and exported from IDRISI into EXCEL where they were laid into columns from 1986 to 1999. The *slope* function in EXCEL was used to determine the numerical slope of change for each individual pixel along each row in the time series. The numerical data (in positive and negative values) representing the slope of change for each NDVI

pixel from 1986 to 1999 was then imported back into IDRISI and converted into an NDVI slope of change image (1986 to 1999).

In order to utilise only the negative slope areas in a cross-classification with the rainfall slope image, all the positive NDVI slope areas were masked out. The resulting image produced negative slope of changes in NDVI. This image was later classified.

Creation of a rainfall slope of change image

As described in sections 4.6.5 and 5.7.2 the derived rainfall images at 1 km resolution were reformatted and aggregated to 8 km resolution to conform with the resolution of the NDVI dataset. A total of 12 annual rainfall image data products from 1986 to 1999 (with the exception of 1989 and 1994 due to non-data coverage) were utilised to create a rainfall slope image as had been done to create the NDVI slope image. This image was also used to mask out the negative rainfall slope values so that the final image showing only positive slope values in rainfall was produced. This positive slope of rainfall image was later classified.

Individual classification of negative NDVI slope of change and positive rainfall slope of change images

In order to use these two separate slope of change images in a pairwise comparison each image had to be classified separately. From the data on each slope of change image, therefore, the quartile range of each image was numerically determined. These were value-sliced into five classes indicating the different areas of change/no change.

Cross-classification of the classified negative NDVI slope and classified positive rainfall slope of change images

In order to determine the spatial associations of the two separate classified slope of change images, they were used together in a pairwise comparison where they were cross-classified/tabulated. In the final result, a cross-classified image with 26 possible associations (combinations) of classes was produced.

6.3.4 Results from the technique using slope of change from regression.

Images showing slope of changes from time-series NDVI images

Results derived from the creation of NDVI slope images are illustrated in Figure 6.8. The first image *(a)* shows the original slope of change for each pixel in the entire time series of the NDVI images from 1986 to 1999. On this image all NDVI pixels which have negative values (indicating decrease in vegetation biomass) are in black to blue to red colour. On the other hand, all pixels which have positive values (indicating vegetation increase) are in light yellow to dark green. Areas covered by water bodies are shown in dark yellow. Although not part of this analysis, this image has a pattern of positive change in areas similar to the long term relative change (1986 to 1996) image (Figure 6.4b) indicating areas of relative positive changes in NDVI around the river basin areas in the northern savanna zone of Nigeria. This is an area where mostly dry season irrigation farming is intensified. The negative areas of NDVI change on the other hand look a little closer to the first short term relative change image (Figure 6.4a). The similarities of the negative changes on these slope of change images to that on Figure 6.4a are mostly around the forest areas of the southern part of Nigeria as well as the coastal areas.

On the second image *(b)* the areas of negative change were isolated. Thus, it contains only pixels where the slope of change for each pixel in the entire time series of the NDVI images from 1986 to 1999 were negative. Areas with high decrease in NDVI are shown in dark brown to light brown, moderate areas of negative change in light brown to yellow while areas of slight negative change are indicated in light yellow to light green colours. Areas of positive change or covered by water bodies here are areas of zero value indicated in dark green. Although there are few areas of negative NDVI in the northern savanna and central areas, most areas of pronounced negative changes in NDVI (green biomass reduction) are located either in the south-west of Nigeria in the forested regions, the montane or around the coastal mangrove and swamp forest regions in the south-east of the country.

Images showing slope of changes from time-series rainfall images (1986 to 1999)

Results derived from creation of rainfall slope images are illustrated in Figures 6.9. The first image *(a)* indicates the slope of change for each rainfall pixel in the entire time series between 1986 to 1999. On the second image *(b)* all negative values were masked out leaving positive slope pixels. Although the two images were contrast stretched, the most prominent areas of positive rainfall changes in the second image (areas of rainfall increase over the years) are the central part of the country around Jos plateau and part of the southern Adamawa highlands around the Nigeria-Cameroon border. Other noticeable areas of increase in rainfall over the years are located at the extreme north-western corner of the image, a small portion of the sahel in Yobe state in the north-east and along lower Benue river. These areas of increase in rainfall are also located in the south-eastern part of the image (ie around Mbala Bodi and Oban hills as well as Awai peak in Nigeria and around the hilly areas of Bamenda in Cameroon).
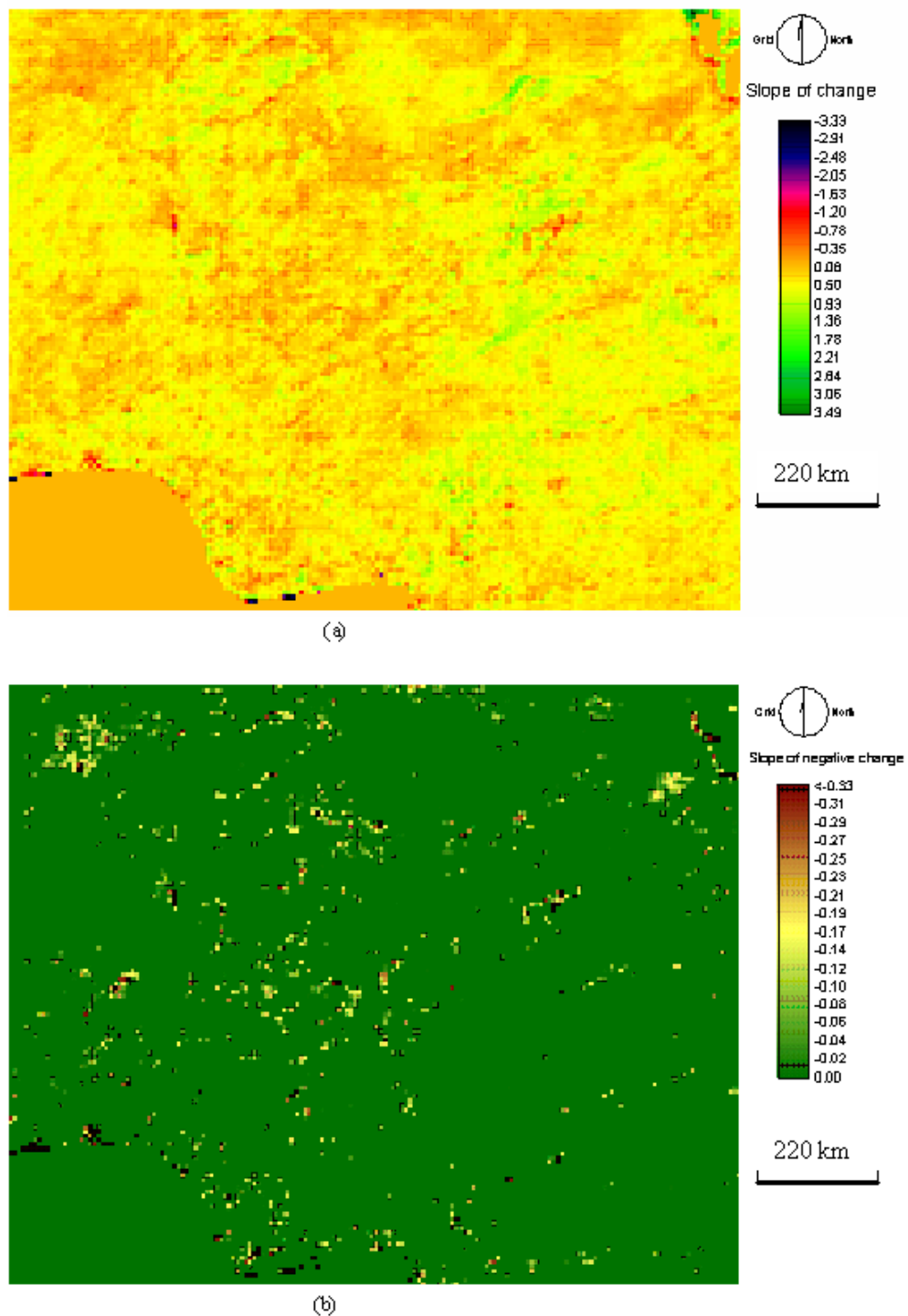
Figure 6.8 Annual Mean NDVI Slope of Changes across the time series 1986 to 1999. Image *(a)* was derived from the 12 annual mean NDVI images in the time series where all the 12 annual mean NDVI images were first converted to ASCII format and exported into EXCEL spreadsheet. Using the slope function in EXCEL the slope of change for each individual pixel along each row was numerically determined. This was later exported back to IDRISI and converted to an NDVI slope image. Image *(b)* is the slope of negative NDVI change. It was derived from the original NDVI slope of change image by isolating the areas of negative change from that of the positive change areas. The SCALAR function of IDRISI was used to create an NDVI boolean image (indicating a one for areas of negative NDVI and a zero for areas of positive NDVI). This was multiplied with the original NDVI slope image to isolate and use only areas of negative change in NDVI in the analysis. The image was contrast stretched to highlight negative change areas. Water bodies and areas of no change are the zero areas shown in dark green.
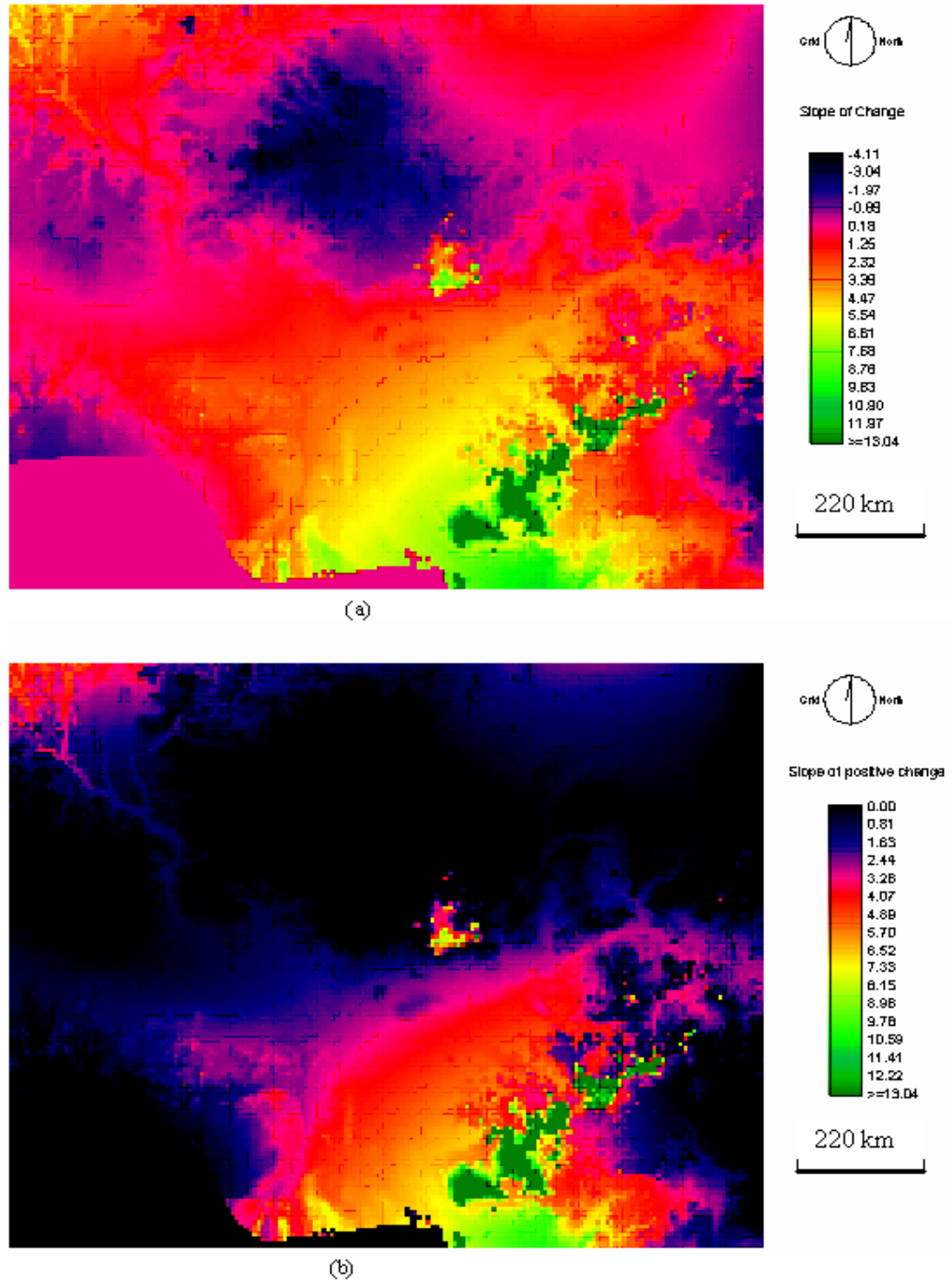
Figure 6.9 Annual Mean Rainfall Slope of Changes 1986 to 1999. The first image *(a)* was derived from the 12 annual mean rainfall images that were resampled to 8 km resolution from the original precipitation data obtained from the Global Precipitation and Climatology Centre (GPCC). All the 12 annual mean rainfall images were first converted to ASCII format and exported into EXCEL spreadsheet. Using the slope function in EXCEL the slope of change for each individual pixel along each row was numerically determined. This was later exported to IDRISI-32 software and converted to a full rainfall slope image. The second image *(b)* is the slope of positive rainfall change. This image was derived from the main rainfall slope of change image by isolating the areas of positive values from that of the negative value areas (using the SCALAR function of IDRISI) where a Boolean image of the slope of rainfall was multiplied with the original rainfall slope image in **(a)** to isolate and use only areas of positive change in rainfall in the analysis. Water bodies and areas of no change are the zero areas shown in black. The images were contrast stretched for visual purposes.

The classified negative NDVI and positive rainfall slope images

Results from individual classifications of the negative NDVI and positive rainfall slope images are illustrated in Figure 6.10. These were first value-sliced into five classes using the quartile range from the main slope of change images (see Table 6.7a and Table 6.7b). The summary statistics indicating areas covered by each class is presented in Table 6.8. The first image (Figure 6.10*a*) indicates the negative NDVI slope image which was value-sliced into classes based on quartiles. Although six classes are indicated, the first class indicates areas covered by water bodies and the sixth class indicates areas of positive or no change in NDVI. Although areas of negative NDVI changes on this image are scattered across the country, areas of high NDVI changes (in red) are more prominent around Lake Chad, Kainji Lake and in some parts of Bauchi and Jigawa states in the northern savanna while in the southern forest areas these can be seen around the coastal areas and the montane area in the south-east.

The second image (Figure 6.10*b*) shows the classified positive rainfall slope image which was also value-sliced into classes based on quartiles. On this image, areas of high rainfall increase (in dark red colour) are the extreme north-west areas and areas in the north-central part (around Jos plateau). Substantial areas covered by this category of high increase in rainfall are areas around the south-eastern part of the country and mostly falling around the Nigeria-Cameroon border.

Areas of moderate increase in rainfall are areas very close to the areas of high increase in rainfall. In general, the changes showed a pattern where the high change areas are followed by the moderate, followed by slight and then by very slight changes in most directions.

Table 6.7 *(a)* Quartile range for the negative NDVI and positive

rainfall slope images used for classifying the images into different

categories of change

Quartile	Negative NDVI Image	Positive Rainfall Image
Lower	- 0.031315	0.70000
Medium	- 0.080340	1.72000
Upper	- 0.153405	3.56000

Table 6.7.*(b)*. Classification of the various categories of changes based on the

quartile range from the negative NDVI and positive rainfall slope images

Class ID for Negative NDVI/Pos. Rainfall Slope Image	Slope Value range for Negative NDVI Image	Category of change for Negative NDVI Slope Image	Slope value range for Positive Rainfall Image	Category of change for Positive Rainfall Image
0	-	Water Bodies	-	Water Bodies
1	-3.33 to -0.15341	High negative	3.56000 to 238.89999	High positive
2	-0.153399 to - 0.0880340	Moderate negative	1.72000 to 3.55999	Moderate positive
3	-0.0803399 to - 0.031315	Slight negative	0.70000 to 1.71999	Slight positive
4	-0.03131499 to - 0.00015	Very slight negative	0.00001 to 0.69999	Very slight positive
5	- 0.0001499 to 0	Positive or no change	0 to 0.000099	Negative or no change

Class of change in NDVI

(a)

■	Water Bodies Area
■	High
■	Moderate
■	Slight
■	Very Slight
□	Positive or No Change

220 km

Class of change in Rainfall

(b)

■	Water Bodies Area
■	High
■	Moderate
■	Slight
■	Very Slight
□	Negative or No Change

220 km
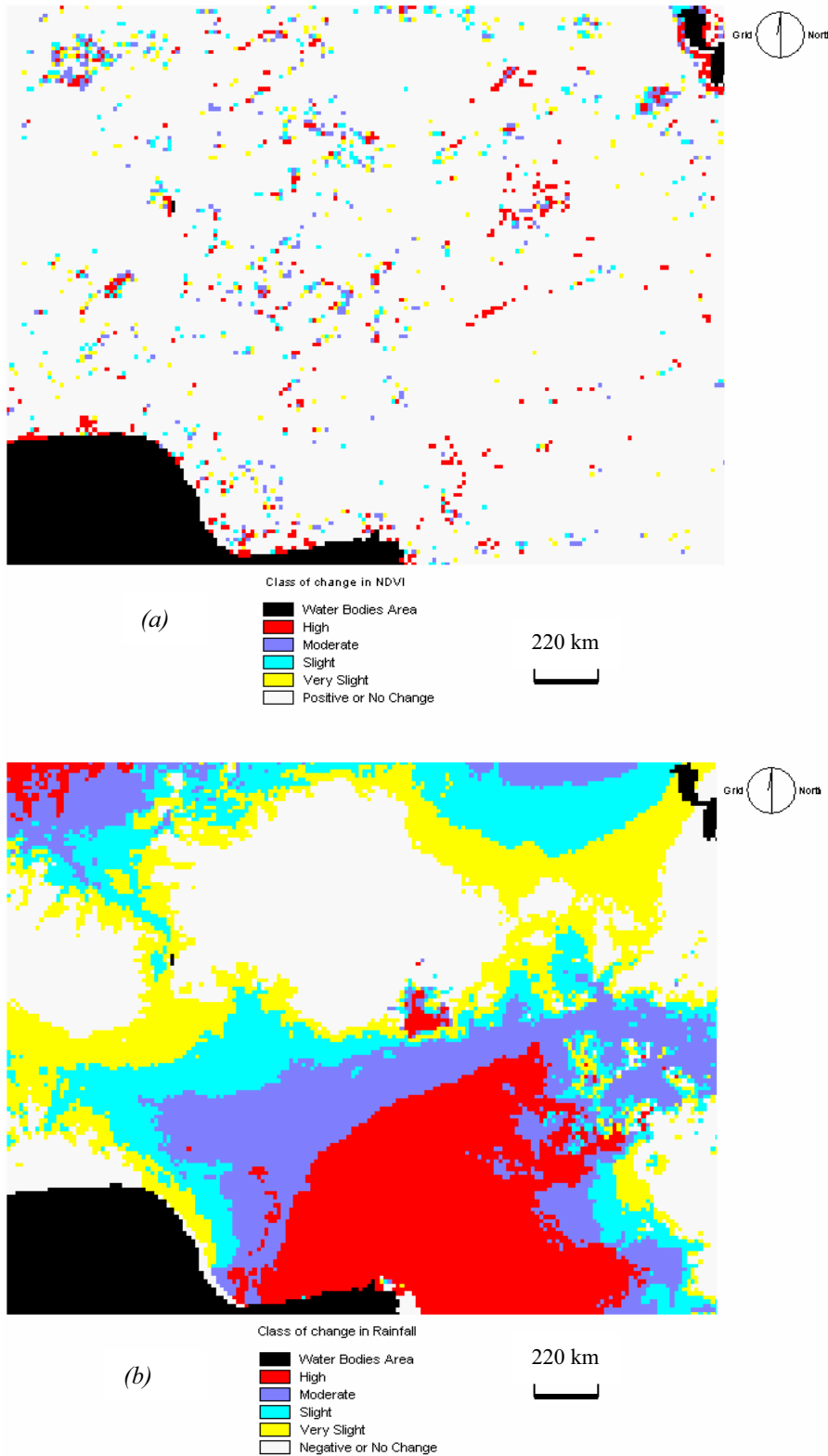
Figure 6.10   Classified Negative NDVI and Positive Rainfall Slope Images. *(a)* is the classified negative NDVI slope image indicating different classes of negative changes in NDVI (showing areas of decrease in vegetation biomass) in the entire time-series between 1986 to 1999. *(b)* is the classified positive rainfall slope image indicating the different classes of changes in rainfall in the entire time-series between 1986 to 1999. These two images were used in the cross-classification/tabulation.

188

Areas where rainfall appears to be steady or decreasing are shown in grey. Substantial areas covered by this class of steady or decreasing in rainfall are located in the north-central area occupying parts of Kano, Kaduna and Niger states as well as the Federal Capital territory area in Abuja. Areas of moderate and slight positive changes in rainfall are mostly in the north-west (along Sokoto Rima basin), north-east (close to Lake Chad basin) in the central part (around Gurara and Kaduna rivers) and around the southern coastal areas. Areas of very slight positive changes in rainfall are also located close to these areas.

Table 6.8   Area covered by each class of change from the individually classified NDVI and Rainfall slope images

Serial No.	Class Code	Category of Change	Number of Negative NDVI Slope Pixels	Number of Positive Rainfall Slope Pixels
1	0	Water Bodies	1740	1740
2	1	High	494	3942
3	2	Moderate	358	3990
4	3	Slight	351	3955
5	4	Very slight	341	3915
6	5	Positive or no change in NDVI/negative or no change in rainfall	20728	6470
-	-	TOTAL	24012	24012

The Cross-classified NDVI and Rainfall Slope Images

The result of the cross-classification of the two slope of change images showing areas of NDVI (vegetation biomass) decrease despite the increase in rainfall is illustrated in Figure 6.11.

Class of Change

0 = Water Bodies Area
1 = High
2 = Moderate
3 = Slight
4 = Very Slight
5 = Positive NDVI/Negtive Rainfall/No Change Areas

220 km
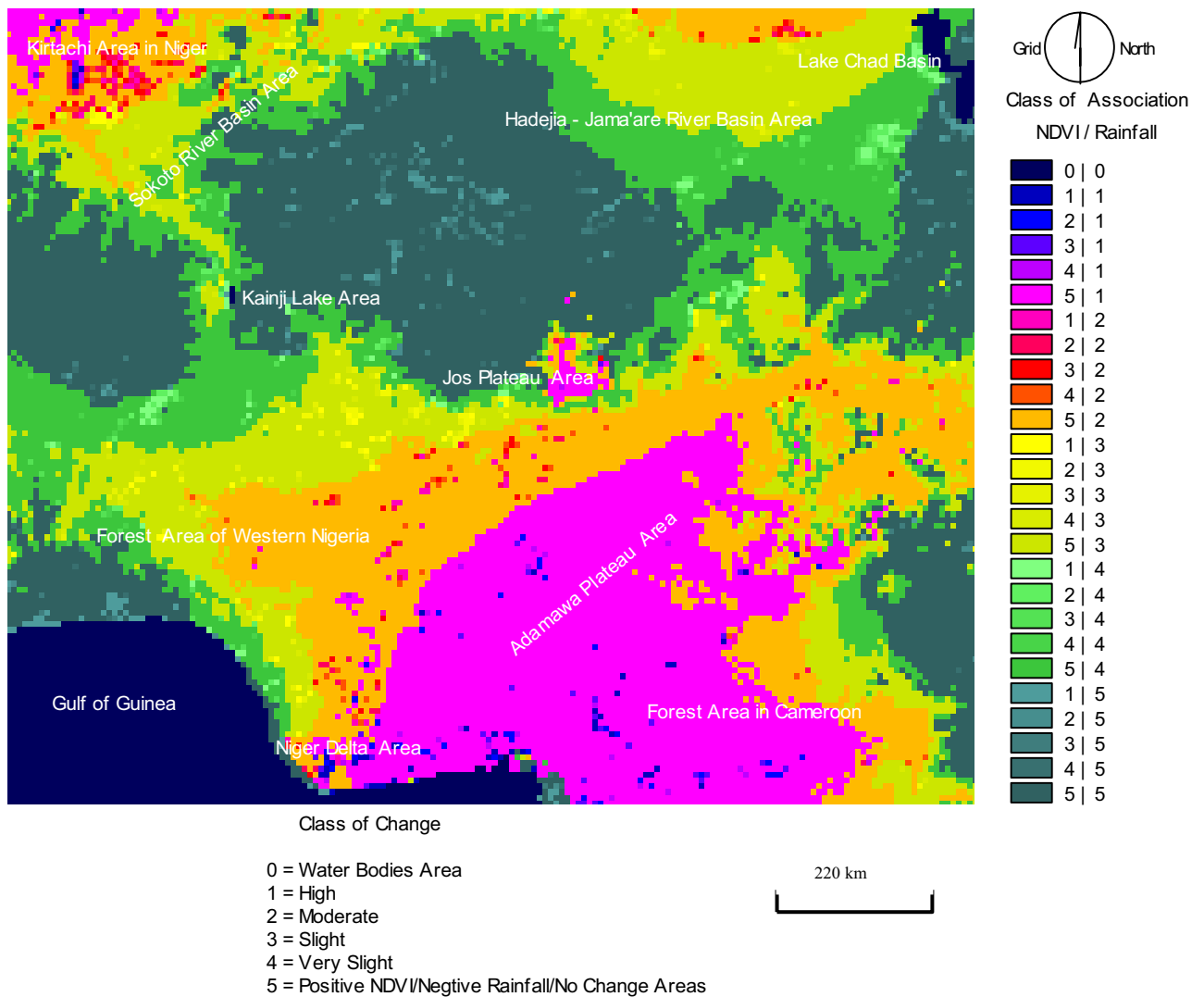
Figure 6.11 Cross-classified Images of Negative NDVI and Positive Rainfall Slope of Changes. This image was derived from cross-classification of the individually classified negative NDVI and positive rainfall slope images. Each individual slope image was initially classified into five categories of change excluding the water bodies area. The final result shows 26 possible combinations (association) of classes. These classes of associations were later monitored through temporal profiling of the time-series NDVI and rainfall dataset.

The image shows 26 possible (associations) combinations of classes based on the cross-classification. The *0:0* combination in black is the water bodies area on each classified

slope image (negative NDVI and positive rainfall). Areas of high negative NDVI (decrease in vegetation biomass) despite high increase in rainfall (class *1:1*) shown in dark blue fall within the areas of high increase in rainfall. These are the hilly or mountainous regions in the south-eastern part of the country which are also forested. The remaining few areas in this category are located in the extreme north-west at the Niger-Nigeria border (mostly around Kirtachi in the Niger Republic).

Most of the savanna areas in the northern part of the Nigeria show a pattern of slight and very slight decrease or no changes in vegetation biomass despite other different classes of increase in rainfall with few exceptions around the north-east. Part of the sahel area around the north-western side of Lake Chad, however, shows a mixture of positive and negative NDVI with moderate increase in rainfall. Within this same area there are spots where despite moderate increase in rainfall, there was also moderate decrease in NDVI over the years.

Towards the north-west of the country in areas around the Sokoto river basin, for example, there are mixed changes between slight to very slight decrease in NDVI and slight to very slight increase in rainfall over the years. In the extreme north-west area (around Niger-Nigeria border) there was a pronounced change of high increase in rainfall in areas of high decrease in NDVI over the years. In the far north-central areas, although there are few pixels showing high decrease in NDVI despite increase in rainfall, the area generally shows a circular zone where not much has changed in NDVI or in rainfall increase. In areas around the Kainji Lake there are few indications of serious changes in vegetation biomass or rainfall increase over the years.

Towards the montane area particularly around Jos in the central area of the county, it shows a high increase in rainfall with either little or no change in vegetation biomass over the years. In the forest areas of the south-west of Nigeria, there are mixed changes ranging from moderate to very slight decrease in vegetation biomass with slight to very slight increase in rainfall over the years. At the lower south-west of the forest areas (around Lagos and Ogun states), although the areas generally showed not much change in vegetation biomass and rainfall, there are some places particularly around the coasts that indicated a high decrease in NDVI despite little or no change in rainfall.

The Niger Delta area seems unique here because there are both indications ie high decrease in NDVI with high increase in rainfall, and high decrease in NDVI with no change in its high rainfall status (see Figure 3.3) over the years. The highlands areas in the Adamawa plateau in the south-east as well as the forest areas around the Cross River tropical lowland forests (along the Nigeria Cameroon border) shows a region of either slight or very slight decrease in NDVI with high increase in rainfall over the years. However, there are some spots within this wide zone where there is an indication of high decrease in vegetation biomass despite the high increase in rainfall.

The overall changes based on this result (Classes 1 to 4) in Table 6.9 show that only 6.9% of the total vegetated area experienced one class of decrease in vegetation biomass or other despite any class of increase in rainfall over the time period (1986 to 1999). With regard to rainfall, 70.9% of the total vegetated areas experienced one class of increase in rainfall or other within this time period.

The temporal profiles of NDVI and rainfall for the cross-classified classes of change

The time series NDVI and rainfall datasets for the 26 combined classes of associations derived from the classified negative NDVI and positive rainfall slope images were monitored on graphs. These are illustrated on temporal profiles showing these different possible combinations in Figure 6.12.

Based on these possible combinations, only 1,544 pixels out of the total 22,272 pixels covering vegetated areas experienced one class of decrease or the other despite increase in rainfall. From their respective graphs, most of the sites or areas profiled indicated an average annual rainfall of below 100 mm except in a few of the sites which indicated over 100 mm of rainfall with high decrease in vegetation biomass.

Profile (a) representing class 1:1 for example, shows a unique trend of high decrease in vegetation biomass over the years with very high increase in rainfall as compared with profile (b) for class 2:1 which shows moderate decrease in NDVI with high increase in rainfall. Both the combined change classes 1:1 and 2:1 are located in small areas at the extreme north-west of the study area, as well as the Niger Delta and the highland areas in the south-east.

Profile (c) representing class 3:1 on the other hand, indicated areas where there was a slight decrease in NDVI with high increase in rainfall. These are in small places located around the montane area of Jos plateau, at the extreme north-west of the study area, the Niger Delta and the highland areas in the south-east and part of the forest area in the Nigeria-Cameroon border.

Table 6.9 Area covered by possible associations of cross-classified NDVI and rainfall slope of change images.

Serial Number	Class of Association (NDVI | Rainfall)	Number of 8km pixels	% of total land pixels
1	0 | 0	1740	7.8125
2	1 | 1	84	0.377155
3	2 | 1	42	0.188578
4	3 | 1	33	0.148168
5	4 | 1	30	0.134698
6	5 | 1	3753	16.85075
7	1 | 2	64	0.287356
8	2 | 2	78	0.350216
9	3 | 2	67	0.300826
10	4 | 2	83	0.372665
11	5 | 2	3698	16.60381
12	1 | 3	80	0.359195
13	2 | 3	78	0.350216
14	3 | 3	82	0.368175
15	4 | 3	68	0.305316
16	5 | 3	3647	16.37482
17	1 | 4	116	0.520833
18	2 | 4	82	0.368175
19	3 | 4	76	0.341236
20	4 | 4	69	0.309806
21	5 | 4	3572	16.03807
22	1 | 5	150	0.673491
23	2 | 5	78	0.350216
24	3 | 5	93	0.417565
25	4 | 5	91	0.408585
26	5 | 5	6058	27.20007

Where :

Class 0 = Water Bodies and unvegetated areas
Class 1 = High
Class 2 = Moderate
Class 3 = Slight
Class 4 = Very slight
Class 5 = Positive or no change in NDVI/ negative or no change in rainfall

Profile (d) representing class 4:1 shows areas of very slight decrease in vegetation biomass with high increase in rainfall over the years, and these are areas found in small portions in the same zone as 1:1, 2:1 and 3:1 classes. The temporal profile (e) representing class 5:1, however, shows average areas where there was increase or no change in vegetation biomass with high increase in rainfall throughout the time-series. These areas cover almost entirely the highlands in the south-east, the montane areas in the central part of the country as well as a larger portion of the extreme north-west corner of the study area (around the Niger-Nigeria border).

Profile (f) representing class 1:2 indicated a combination of change classes where there was high decrease in NDVI with moderate increase in rainfall. These areas can be seen in spots in the north-eastern sahel part of the country, ie., around the Sokoto and Rima rivers as well as along River Benue. Profile (g) representing class 2:2 shows areas where there was moderate decrease in vegetation biomass and moderate increase in rainfall over the years. These areas are located in the sahel area in the north-east, the area at the Niger-Nigeria border in the north-west, a small portion of the Jos plateau in the central area, the Niger Delta and few spots in the moist lowland forest area of the south-east of the country.

Temporal profile (h) representing class 3:2 indicates areas of slight decrease in vegetation biomass with a moderate increase in rainfall. These areas are located at the sahel area in the north-east, the Niger-Nigeria border in the north-west and along Benue river down to the Niger Delta. On profile (i) representing class 4:2, this shows areas of very slight decrease in vegetation biomass but with moderate increase in rainfall. These areas are found in similar locations as in the site for class 2:2. Temporal profile (j) representing class 5:2 shows areas

where there was either no change or an increase in NDVI with no change or decrease in rainfall over the years. These areas cover large parts of the sahel region in the north-east, the north-west, the transect along the Benue river, parts of the forest area in the south-west and moist lowland forest areas of the south-east of the country. In temporal profile (k) representing class 1:3, this indicates areas where there was high decrease in NDVI with slight increase in rainfall over the entire time period from 1986 to 1999. This class covers areas around the Sokoto Rima basin, forest areas in the western region, parts of Delta State and most parts of Kogi State at the confluence of Niger and Benue rivers in the north-central part of the country.

Profile (l) representing class 2:3 shows areas where there was moderate decrease in NDVI with slight increase in rainfall. These are areas located along a strip from the Sokoto Rima basin cutting across to the north-east and from the south-west forest areas across to the southern part of Lake Chad. Profile (m) representing class 3:3 shows areas where there was slight decrease in NDVI with slight increase in rainfall. These areas are located around the north-west, the south-east of Kwara State and parts of Edo State in the south-west. In temporal profile (n) representing class 4:3, this shows areas where there was very slight decrease in NDVI with slight increase in rainfall over the time period under investigation. These are areas located along the River Niger and the Sokoto River basin. It also covers parts of Edo state as well as some parts of the moist lowland forest area of the south-east.

(a) (b)

(c) (d)

(e) (f)

(g) (h)
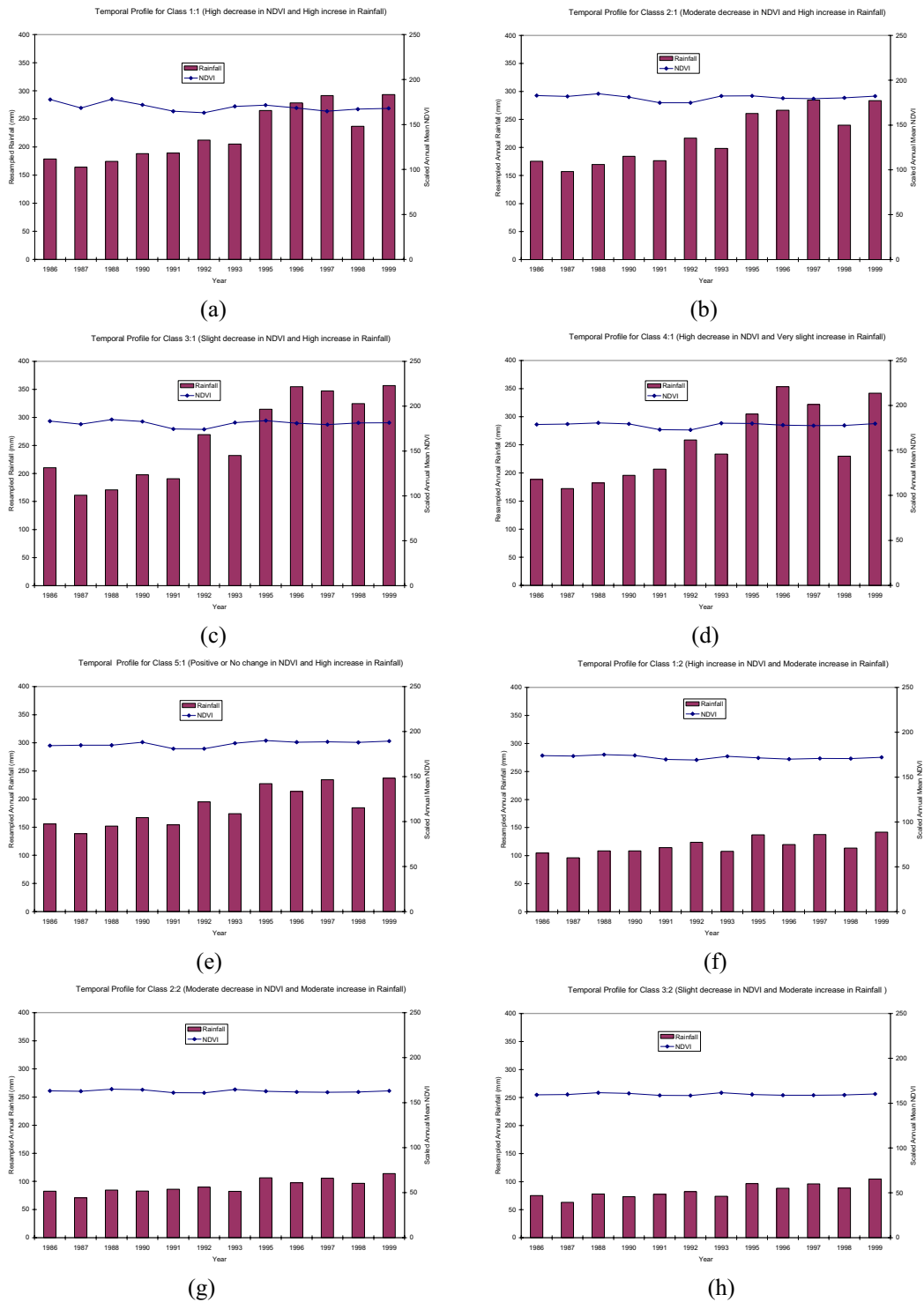
Figure 6.12 Temporal profiles for the different class of combinations from the cross-classified NDVI and rainfall slope change images. All the class of combinations were derived from the cross-classification of the classified image of negative NDVI slope and a classified image of positive rainfall slope. The graph plots indicate the mean of the classified areas (in annual mean NDVI and rainfall) which were determined through profiles of the time-series NDVI and rainfall datasets for the different classes (sites). (Note that NDVI values as indicated were scaled from 0-255. To inter-convert, scaled_ndvi = float_ndvi*125+128).
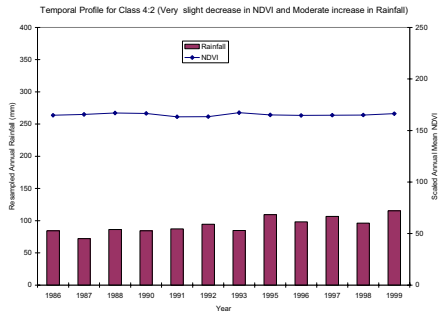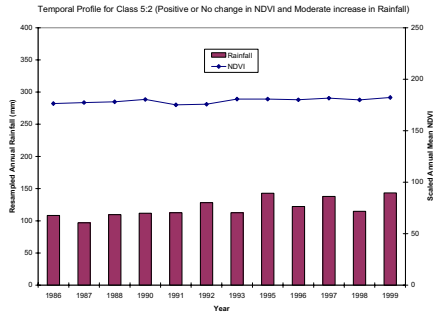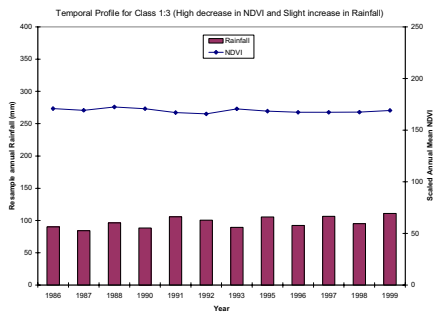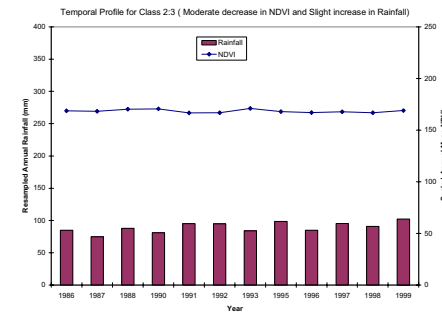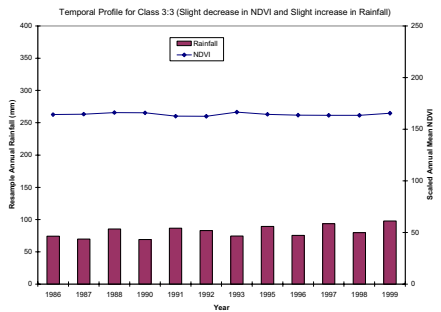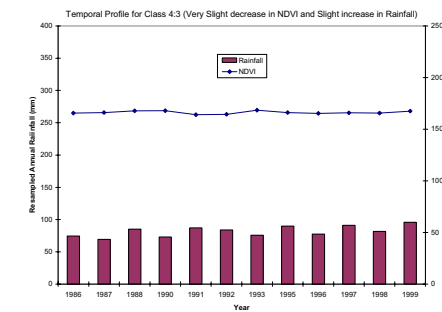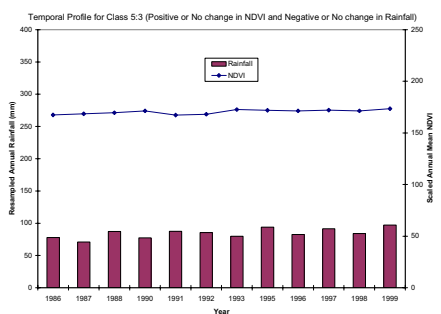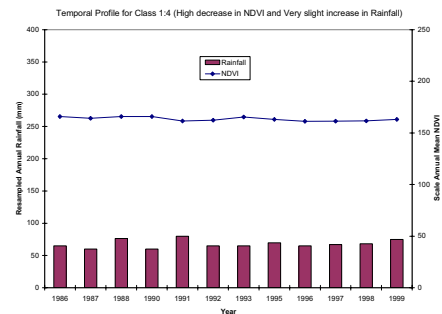
Figure 6.12 (cont.) Temporal profiles for the different classes of combinations
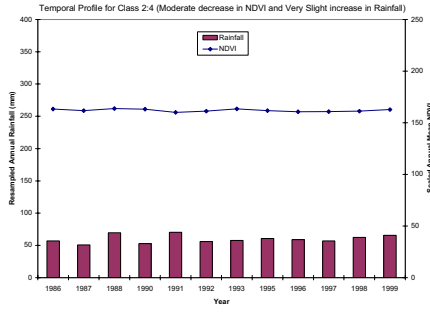
(q)
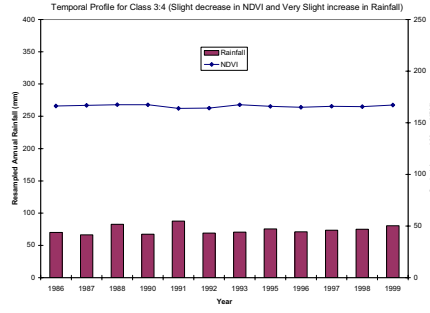
(r)
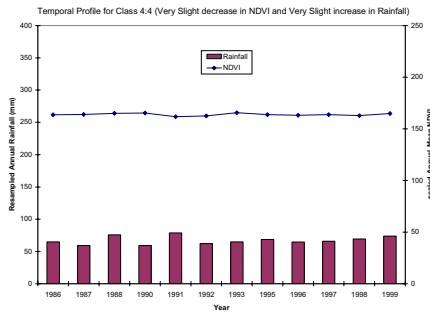
(s)
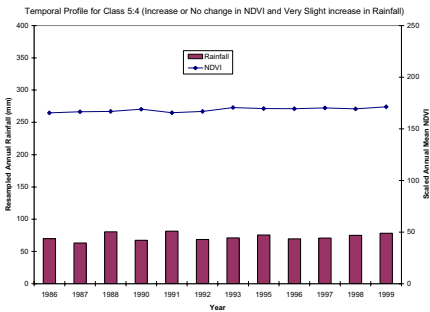
(t)
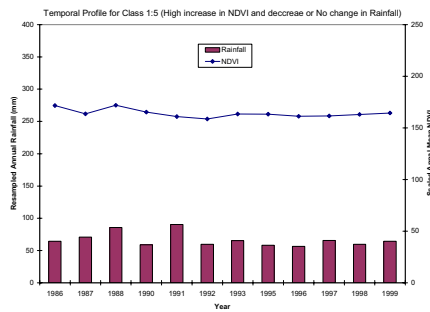
(u)
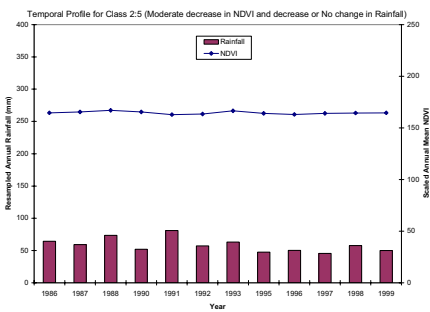
(v)
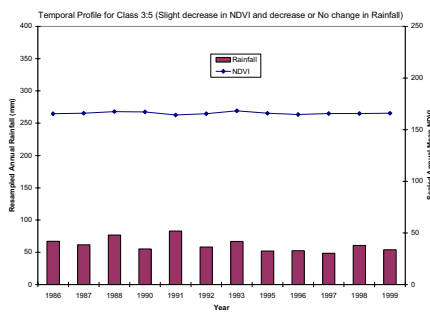
(w)
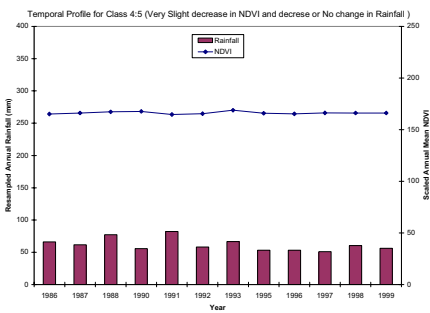
(x)

Figure 6.12 (cont.) Temporal profiles for the different classes of combinations
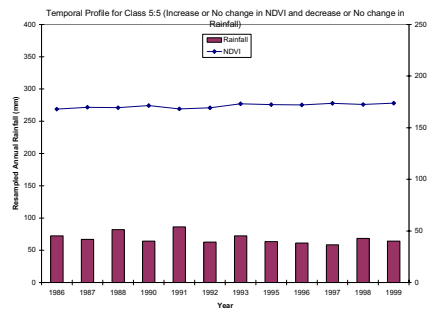
(y)

Figure 6.12 (cont.) Temporal profiles for the different classes of combinations

In profile (o) representing class 5:3, this is an area where over the years, there was either no change or increase in vegetation biomass despite slight increase in rainfall. These areas covered almost the whole of the Sokoto Rima basin, the lower part of the sahel area in the north-east, and parts of the forest region in the Nigeria-Cameroon border in the south-east. Profile (p) representing class 1:4 indicates areas where there was high decrease in vegetation biomass with very slight increase in rainfall. These areas are located around Lake Chad, parts of Katsina state in the north, around the capital territory in Abuja in the central region, the south-western part of Kwara State and along the coastal areas of Ondo and Delta states in the south-west. In profile (q) which represents class 2:4, these are areas where there was moderate decrease in vegetation biomass with very slight increase in rainfall. These areas are located around northern part of Katsina state, parts of the lowland areas of the Hadejia-Jama'are river basin, the Kainji Lake, the capital territory Abuja and some areas in the forest zone on the south-west of Nigeria. Profile (r) representing class 3:4

shows areas where there was slight decrease in vegetation biomass with very slight increase in rainfall. These areas area mostly located in very small areas of Borno and Gombe states in the north-east, in the southern part of Kwara state as well as in some parts of Ondo, Edo and Delta states in the southwest. Temporal profile (s) representing class 4:4 is shows areas where there was very slight decrease in vegetation biomass with very slight increase in rainfall. These areas, however, are in scattered locations in Kebbi, Zamfara and Katsina states in the north-west, in Borno, Gombe and Bauchi states in the north-east and around Oyo state in the south-west of the country.

Temporal profile (t) represents class 5:4 showing areas where there was either no change or increase in vegetation biomass with very slight increase in rainfall over the years. These areas located almost cover substantial parts of Katsina, Jigawa, Kwara, and Gombe states in the savanna region as well as the southern portions of Ogun, Ondo, Osun, Edo and Delta states in the south-west forest region. In profile (u) representing class 1:5 shows areas where there was high decrease in vegetation biomass with either no change or decrease in rainfall over the time period under investigation ie 1986 to 1999. These are areas located around the central northern savanna zone, in the southern part of Lake Chad and around Lagos state area in the south-west.

Temporal profile (v) representing class 2:5 shows areas where there was moderate decrease in vegetation biomass with either no change or decrease in rainfall. These are also areas located in the central part of the northern savanna and the southern part of Lake Chad in the north-east. Profile (w) representing class 3:5 shows areas where there was slight decrease in vegetation biomass with either no change or decrease in rainfall. These areas are found in

scattered locations in the central part of the northern savanna, part of the Republic of Benin in the north-west and some areas in the extreme south-west. The temporal profile (x) representing class 4:5 shows areas where there was very slight decrease in vegetation biomass with either no change or decrease in rainfall. These areas are also located in the central zone of the northern savanna, some parts of the forest zone of the south-west and in small spots in the moist lowland forest area of the southeast. The last profile (y) represents class 5:5. This shows areas where there was either no change or increase in vegetation biomass with either no change or decrease in rainfall during the period between 1986 and 1999. These areas covered a large area portion of the central zone of the savanna region, the north and southern part of the Republic of Benin, a strip in the coastal areas around Ondo, Edo and Delta states in the south-west, an area stretching to the southern part of Lake Chad and parts of the south-east forest zone mostly falling in Cameroon.

Temporal profiles of selected sites from changed areas of numerically comparable classes

The temporal profiles of changed areas (classes $a - y$) in Figure 6.12 were based on average figures of large areas from different vegetation zones. These graphs may not necessarily show a true representation of the changes for a particular site within a particular cross-classified change class. To demonstrate this, five sites were chosen (a pixel per site) from each area of numerically comparable change classes (ie Class 1:1, 2:2, 3:3, 4:4 and 5:5) for examination. These individual pixels (sites) were chosen as close as possible to a raingauge station. The five chosen sites from these numerically comparable classes of change are :

1. From class 1:1 - a site supposedly in the Sudan savanna in the north-west corner (Niger-Nigeria border) of the image in Figure 6.11. This savanna site falls in an area where despite high increase in rainfall within the area, it had high decrease in vegetation biomass.

2. From class 2:2 – a site in the northern sahel savanna zone of Nigeria falling in the north-eastern state of Yobe. This Sahel area normally has less rainfall. However, the change map in Figure 6.11 indicated that this site falls in an area of moderate negative change (decrease) in vegetation biomass despite moderate increase in rainfall over the time period 1986 to 1999.

3. From class 3:3 – a site in the forest zone of the south-western part of Nigeria. The temporal profile in Figure 6.12(m) represented areas in which this class belongs. It showed that this class had slight negative change (decrease) in vegetation biomass despite the slight increase in rainfall.

4. From class 4:4 - a site in the montane area of Jos plateau in the central savanna zone. This site normally has more rainfall than the surrounding savanna areas. Based on the changes illustrated in Figure 6.11, this site falls in an area where, despite slight increase in rainfall over the time period under investigation, it had slight decrease in vegetation biomass.

5.   From class 5:5 – a site chosen from a site represented in the temporal profile in Figure 6.12. This site falls in the tropical dense humid forest zone of Cameroon. This is an evergreen forest area which normally has high rainfall. From the change results in Figure 6.11 it falls in an area where there was either no change or increase in vegetation biomass despite also falling in areas where there was no change or decrease in rainfall.

The annual NDVI and rainfall datasets for these selected sites for the period 1986 to 1999 were determined and plotted on graphs. These are illustrated on temporal profiles in Figure 6.13.

From this demonstration, it shows that the spatial changes of each individual site observed on the changed map illustrated in Figure 6.11 in most of the sites, are highly generalised in their respective temporal profiles represented in Figure 6.12.

The temporal profiles in Figure 6.13 representing each individual site (pixel) from its cross-classified class, suggests that, for each site in each class of association, the changes in vegetation observed may be closely related to the types of land use in operation in those particular vegetation zones. All the other three profiles *a – c* in Figure 6.13 showed a different pattern compared with the profiles they were represented in Figure 6.12 except for site (d) in the montane area and site (e) in the humid dense forest region in the south-east of the study area which closely show similar patterns in their profiles in Figure 6.12.
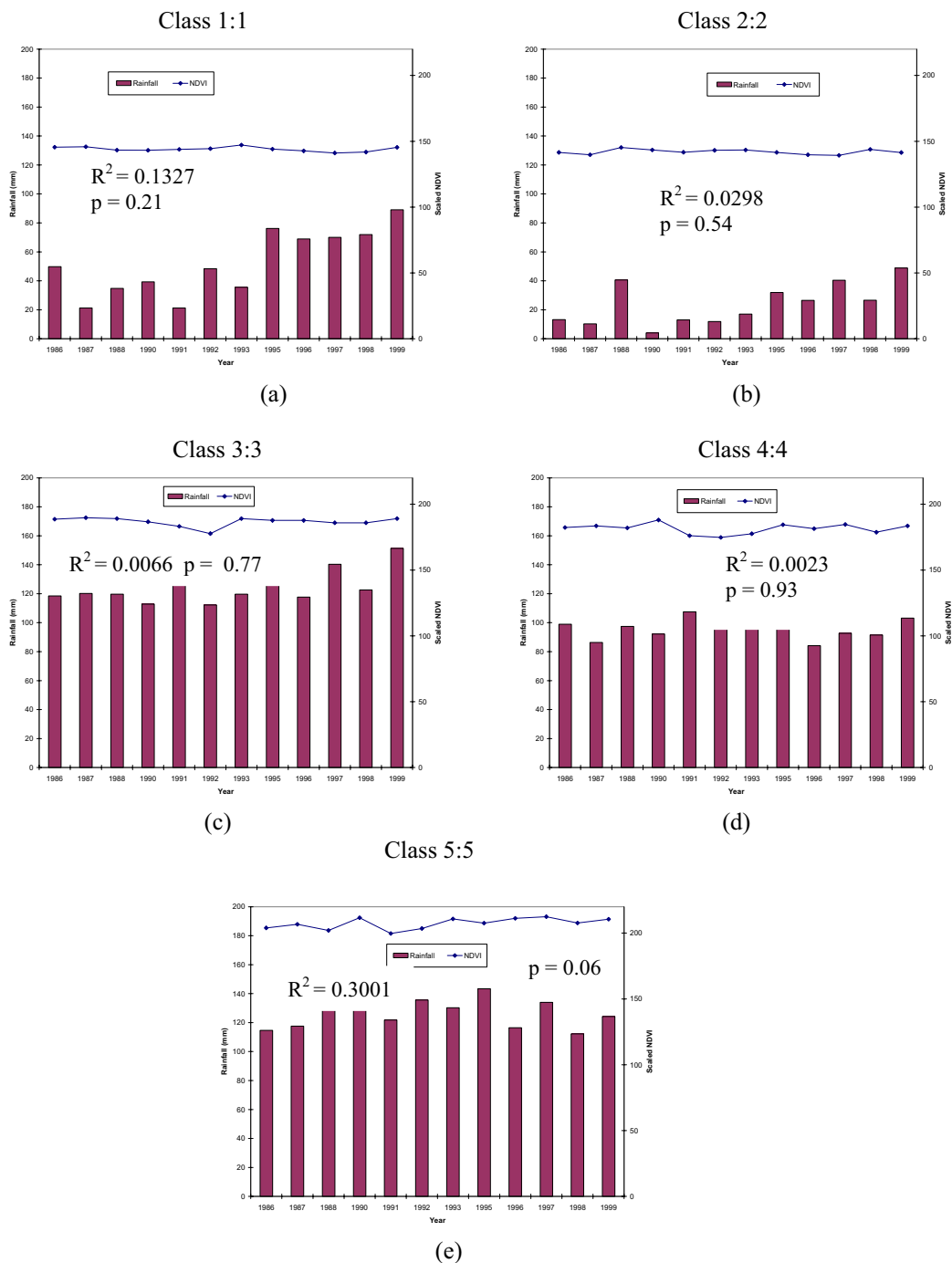
Figure 6.13 Temporal profiles of annual NDVI and rainfall data for the selected sites from areas of numerically comparable classes. Figure (a) shows the site in Class 1:1 in the Sudan savanna zone at the north-west corner (Niger-Nigeria border). (b) is part of change Class 2:2 representing a site falling in the northern sahel savanna in the north-eastern state of Yobe. Plot (c) is part of change Class 3:3 representing a site in the south-west forest zone of Nigeria. Plot (d) is part of change Class 4:4 representing a site in the montane area of Jos plateau in the central savanna zone. Plot (e) is part of change Class 5:5 representing a site in the dense tropical forest zone of Cameroon in the south-east. These selected sites show clear differences from the generalised profiles they individually belong in Figure 6.13. All the different sites showed indication of underlying change in NDVI which is not significant at $p < 0.05$ level except the forest site (e) which is almost significant. (Note that NDVI values as indicated were scaled from 0-255. To inter-convert, scaled_ndvi = float_ndvi*125+128).

In Figure 6.13, plot (a) representing the site in the Sudan savanna zone from class 1:1 shows sudden rises and falls in the NDVI profile. It shows major decrease in vegetation biomass from 1987 to 1988 and in 1997.

Plot (b) representing the sahel site in the north-east of the country from class 2:2, however, shows more rises and falls in temporal pattern of NDVI than class 1:1. The years with sharp falls (decrease in NDVI) in the profile despite increase in rainfall are 1987, 1991 and 1997.

Plot (c) representing a site in the forest region in the south-west of Nigeria chosen from class 3:3 shows a clear trend of decrease in vegetation biomass from 1987 to 1992. This however, changed with a rise in the NDVI profile in 1993 followed by a trend in decrease in NDVI up to 1997.

Plot (d) representing a site in the montane area of the central part of the country chosen from class 4:4 shows a different pattern in temporal profile with rises and falls. In this graph, the trend first showed a rise in NDVI between 1986 to 1987 with sudden fall in 1988. There was also a major fall (decrease) in the NDVI profile from 1990 to 1992.

Plot (e) representing a site in the humid dense forest area of the south-east chosen from class 5:5 also shows a pattern of rise and fall in the temporal profile. On this profile, there was a marked difference in high NDVI from the montane and the south-west forest sites in classes 3:3 and 4:4 respectively despite different degrees of increase in rainfall.

6.3.5 Comparison in the gradient of NDVI and rainfall in the savanna and forest areas

Two pairs of NDVI pixels on the 1986 base year in the time series were selected for comparison based on their rate of change and with corresponding rate of change in rainfall across the years. One pair of NDVI of the same heterogeneity was selected in the savanna and one pair of NDVI pixels of the same heterogeneity in the forest areas.

Their corresponding rainfall values were extracted from the annual rainfall datasets where both the gradients of the paired NDVI pixels and the rainfall values were determined (See Appendix 6). The final relationship between these changes in gradients is illustrated in Figure 6.14. This uses the same NDVI pixels (sites) on the main slope of change image in Figure 6.8a (showing both positive and negative changes in vegetation biomass) as those illustrated in Figure 6.7 as example. The gradient in Figure 6.14 shows that for given pairs of NDVI heterogeneity in the savanna and forest areas in the 1986 base image, there were no significant changes between changes in the gradient of NDVI for given change in rainfall in the time series. This suggest that there was more rapid change positively (increase in vegetation biomass) in the savanna than in the montane or forest areas given the rate of change in rainfall.

Gradient of NDVI and Rainfall
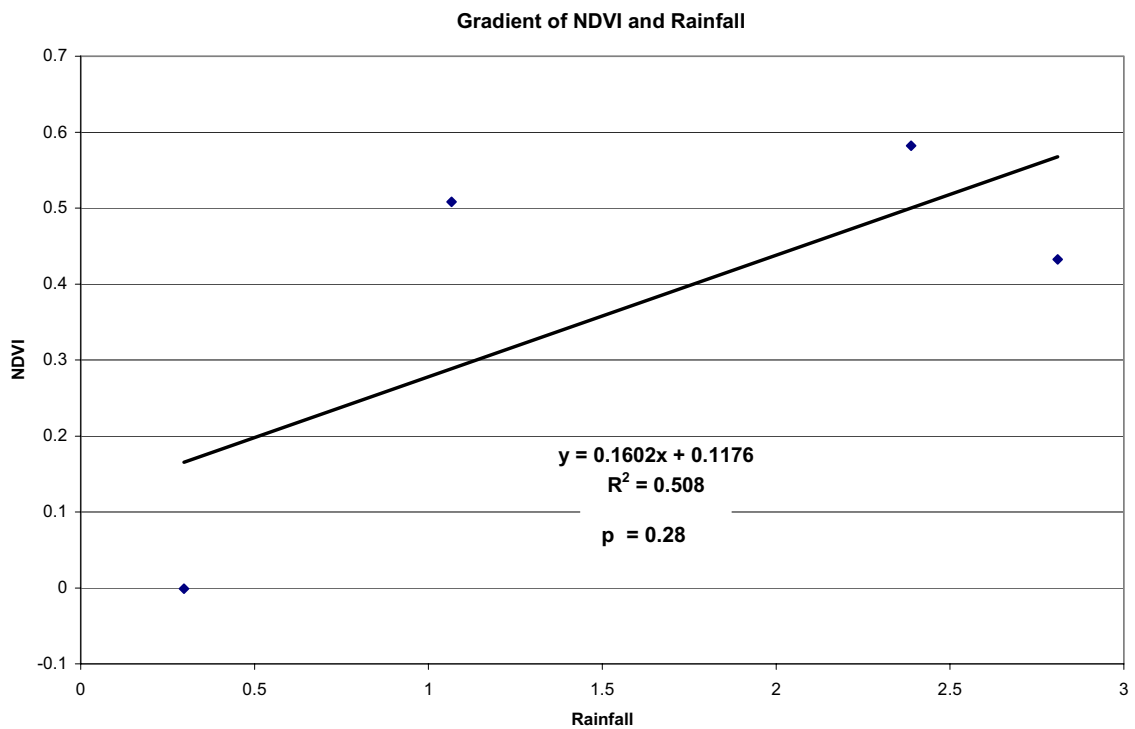
Figure 6.14 Gradient of NDVI and rainfall for selected pairs of pixels of same heterogeneity on the 1986 annual mean NDVI base image. The gradient of change shows that there is no good relationship between changes in the gradient of NDVI for given change in rainfall in the time series in those vegetation zones.

6.3.6 Relationship of NDVI and rainfall in the selected areas of numerically comparable change classes

To determine the relationship between the annual NDVI and rainfall for the selected sites monitored within areas of numerically comparable change classes, a correlation plot was illustrated in Figure 6.15. These plots show that no p-value is less than 0.05, suggesting no significant correlation between the changes observed in the inter-annual variations in NDVI and rainfall for the selected sites illustrated in Figure 6.13. Thus, such changes only occurred by chance. For example, in Figure 6.15(b) the correlation plot for the sahel site shows random distribution of points. Hence, the null hypothesis is accepted here as being true.

In general though, this investigation focused mainly on areas where there was decrease in biomass with increase in rainfall in order to highlight those areas affected either due deforestation, crop failure or related phenomena. On the other hand, areas where opposite changes are expected which is not the focus of this investigation suggest areas influenced in the positive way as result of reforestation or agricultural production.

(a)

(b)

(c)

(d)

(e)
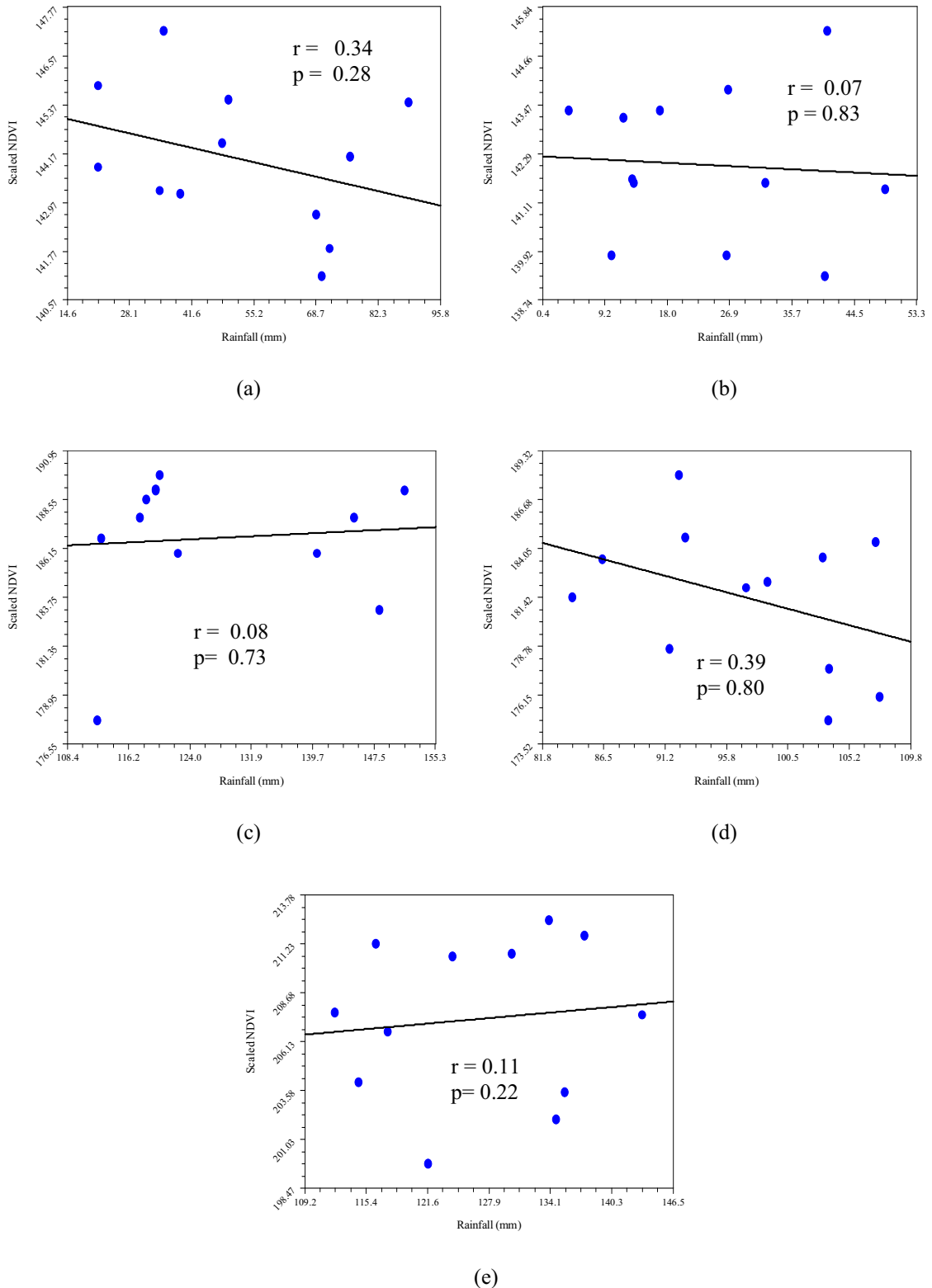
Figure 6.15 Correlation plots of NDVI and rainfall for the selected sites from changed areas of numerically comparable classes. Plot *(a)* represents the Sudan savanna site in north-west Nigeria from class 1:1, plot (b) represents the sahel site in the north-east of the country in class 2:2, plot (c) represents the forest site in the south-west of the country from class 3:3, plot (d) represents the site in the montane area around the central part of the country from class 4:4 and plot (e) represents the site in the humid dense forest in the south-east of the study area chosen from class 5:5. All these plots showed no significant correlation between NDVI and rainfall at *p < 0.05* level. (Note that NDVI values as indicated were scaled from 0-255. To inter-convert, scaled_ndvi = float_ndvi*125+128).

6.3.7   Discussion

Analysis of vegetation change across Nigeria using slope of change from regression technique with annual NDVI and rainfall datasets showed that it is feasible. However, there are some weaknesses in both the results obtained and in the technique as a method for detecting spatial changes. A number of studies using remotely sensed data have been conducted using linear regression techniques (eg Teillet, 1986; Hall *et al,* 1991; Yuan and Elvidge, 1993; Edvilge *et al,* 1995). But their aim tended to be data correction prior to change detection analysis rather than an application of a specific change detection technique such as the one applied in this investigation.

In comparison with the SID technique which uses selective annual mean NDVI data, the key advantage of the SCR over the SID technique is the ability to make direct comparison with other recorded temporal and spatial data, in this case rainfall. The second advantage over the SID technique is the ability to use all the available mean annual temporal dataset including NDVI and rainfall.

Although results from both the SID and SCR techniques are broad in nature, the negative results obtained from SID technique are highly generalised especially in the southern forested zones. As for the SCR technique, there was also an over-generalisation in the results across the whole country especially when data of the combined classes of change for NDVI and rainfall of changed areas were cross-classified (Figure 6.11) and also shown on temporal profiles in Figure 6.12. Spatial areas that were clearly detected by both techniques are the Lake Chad area and parts of the coastal areas.

With regard to where a threshold of change-no-change areas should be placed, both techniques have similar limitations. While in SID technique round number equal class interval was used to categorise spatially changed areas into different change classes, in the SCR technique quartiles were used. The disadvantage of using quartiles in the SCR technique is that some pixels with very close values may end up falling into different classes, especially if pixel values cluster. Hence this may exaggerate the differences between features (pixels) especially on the rainfall image on Figure 6.10b. On the other hand, some widely ranging adjacent pixel values may fall in the same class, minimising the differences between these pixels. However, though the slope of change from regression technique has such disadvantages, the use of quartiles may be better in the context of this investigation than using, for example, standard deviation. This is because two different variables datasets (NDVI and rainfall) of the same pixel number (quantity) are being compared. In the simple SID technique where many change classes were used, the grading of different change classes with, for example, high, medium and low will not be possible unless the class interval range is widened. This will further exaggerate the results. As for the SCR technique, though change classes were also not based on actual land cover classes, the grading of change classes into high moderate, slight and very slight in this approach is more appropriate because of the use of quartiles.

With regard to the overall results derived from the use of SCR technique, comparison between the slope of changes of these two variable datasets shown in Figures 6.11 to 6.13 suggested that the relationship of these changes are not linear even though many spatial changes in NDVI have been detected in different areas of change association. Many of these spatial changes in vegetation biomass detected would possibly have some elements of curvilinearity. However, changes either in vegetation biomass based

212

on NDVI and rainfall trajectory in the northern savanna and the southern forested areas of Nigeria may not necessarily be the same despite falling in the same category of cross-classified changes of these two variables. Hence, although some parts of the northern savanna and southern forest vegetation zones may fall into one particular category of change in both negative NDVI and positive rainfall based on the spatial changes observed in Figure 6.11 and represented on temporal profiles in Figure 6.12, this only gives an approximate average result. Firstly, many individual sites from different climatic and vegetation zones that are represented in one class of change could have, or possibly had, experienced different types of land use activities. Secondly, because the classification scheme was based on quartiles and the areas of different change class particularly for the rainfall change image vary greatly in size, this could have contributed in the skewed pattern of change classes on Figure 6.10(*b*). Hence since changes may have elements of curvilinearity, second or third order polynomials could be appropriate when using this approach of change detection particularly on vegetation cover.

6.3.8   Summary

- The use of slope of change from regression as a technique for assessing changes in vegetation cover across Nigeria from timeseries NDVI and rainfall data in a pairwise comparison have shown that it is feasible. However, it entails many procedures and it is time-consuming.

- With the SCR technique areas of decrease and increase in vegetation biomass as detected by NDVI despite decrease or increase in rainfall can broadly be detected and isolated.

- The rate of changes of the different areas broadly detected can also be determined.

- The main problem of the SCR approach is that there is an over-generalisation in terms of spatial changes from different vegetation zones falling in the same class of change in NDVI. This is because temporal profiles of the combined change classes do not reflect true representation of changes in a specific site (pixel).

- The relationship between annual mean NDVI and rainfall datasets for the selected sites within areas of numerically comparable change classes showed that there was no correlation between changes in NDVI and rainfall at $p < 0.05$ significant level. This suggest that the changes observed only occurred by chance. However, because the SCR technique utilised all the annual mean NDVI and rainfall datasets in the analysis, results of spatial negative changes in NDVI obtained could be more realistic than results obtained using the SID technique in which selective annual mean NDVI data were utilised.

6.4   Vegetation Change Detection using Principal Component Analysis (PCA)

6.4.1   Introduction

This section presents the results of the third approach to vegetation change assessment covering Nigeria using PCA. PCA is an attractive technique for change detection because it can decompose a timeseries of vegetation images into a sequence of spatial and temporal components. These spatial and temporal components from PCA are often interpreted as corresponding to particular environmental events (Eastman and Fulk, 1993). The first component typically indicates the characteristic value of the variable being studied (the average amount of green biomass in this case) while subsequent components represent change elements of decreasing magnitude. A technical issue that is still being debated is how many components to extract. PCA will extract as many components as variables entered but it has traditionally been argued that the low signal to noise ratio of later components renders them worthless. Indeed, one of the main uses of PCA is a data reduction or compression technique that retains a high proportion of the original variance on few derived components. The alternative argument is that PCA is a spatial technique being applied here in a spatial context and the normal rules for determining the useful end to analysis (eg using the eigenvalue) do not apply. PCA is 'unaware' of spatial pattern that may appear on components with only a tiny fraction of the original variance, percentage variance retained is not a useful indicator of whether a component has value or not. In this investigation, I decided to choose and concentrate on the most appropriate components that show probable patterns of temporal changes in green vegetation biomass across Nigeria.

6.4.2   Aim and objectives

The aim of this approach is to assess patterns of change in vegetation biomass derived from multi-temporal analysis of NDVI across Nigeria within the framework of PCA.

(i) To isolate the component or components that show a persistent decrease in NDVI over time.

(ii) To identify other patterns of change and interpret them in terms of probable environmental drivers.

6.4.3   Methodology

Simple reorganisation and recomposition of the NDVI dataset used in this study was explained in Section 4.4.2 and Section 5.4. In this approach, which uses standardised principal components from PCA, a total of 144 monthly NDVI-MVCs from 1986 to 1999 (excluding data for 1989 and 1994 which were not available) were used as input in the procedure.

Transformation of Time Series NDVI dataset into Standardised Component Images and Loading Scores

In order to process a dataset using PCA in IDRISI Time Series Analysis module (TSA), a time series file containing the data (in this case, the original monthly NDVI images) to be analysed have to be created after being converted to byte binary format. Hence, all the original 144 monthly NDVI-MVC images used in this analysis were first converted from real value format to byte binary format, lodged into a timeseries file created and then used

as input in the IDRISI-TSA procedure. The water bodies mask created and illustrated in Figure 4.3 was used to mask out all water bodies areas so that only land pixels are utilised in the analysis. The final result produced two forms of output: 84 component images and 144 standard scores (component loadings).

Temporal Profiles for highest anomaly NDVI pixels on Component Images

Temporal profiles of NDVI data for sites (pixels) that exhibit anomaly patterns are shown to provide additional clues of certain events in a locality or region where general vegetation cover was affected for example, during El-Niňo years (Bouma *et al*, 1997; Kogan and Wei, 2000). Hence, timeseries NDVI data within the warm ENSO (El Niňo) and the cold ENSO (La Niňa) periods were also used to monitor selected sites (pixels) in areas of strong anomaly change patterns on the derived component images. Firstly, the whole NDVI time series dataset for pixels with highest anomaly on the selected components that showed change patterns were provisionally monitored. Secondly, where the monthly NDVI data show serious trends, suggesting possible clues of events in a particular period, the NDVI data for that period was extracted and plotted on graphs to assist in the interpretation together with the graphs of loading scores.

6.4.4   Results from Principal Component Analysis (PCA)

Results of the first set of output from the PCA procedure gave 84 component images describing the change pattern in each respective residual image different from the first component and also from each other. Although PCA procedure is supposed to produce the same number of components as the variables (NDVI images in this case) entered, the TSA module in IDRISI-32 is capable of producing only 84 component images. However, all the 144 standard scores (component loadings) were obtained.

The Components and their respective graphs of loadings

Although there is no standard procedure or where to stop an analysis of derived component images from PCA (Eastman and Fulk, 1993), it is usually better to consider only few component images which together explain the bulk of the original variations in the dataset (Li and Kafatos, 2000) and also satisfy the primary purpose of the study. From the 84 component images derived from this procedure, a total of seven component images which exhibited patterns that can be attributed to vegetation or vegetation-related changes across Nigeria were chosen for assessment. These chosen component images, which together explained about 87% of the total variations in the 144 monthly NDVI dataset, are illustrated in different figures in the text. Commentary on each component image including its graph of loading scores are provided. Other component images not included in the text are illustrated in Appendix 7.

Component 1 Image

Component 1 image in Figure 6.16 explains about 72 % of the total variance in the 144 NDVI dataset used in the PCA procedure. It illustrates a representative vegetation pattern across Nigeria and surroundings. This image looks similar to the NDVI images in Figure 5.4. Areas that are less correlated with the loading scores are located in the northern savanna mostly in yellow, red and blue indicating less vegetation vigour. On the other hand, areas that are highly correlated with the loading scores are located in the southern forest zones which are in green colours indicating more vegetation vigour. The loadings scores show correlations between the component image and the NDVI dataset in positive

Component 1

(a)

(b)
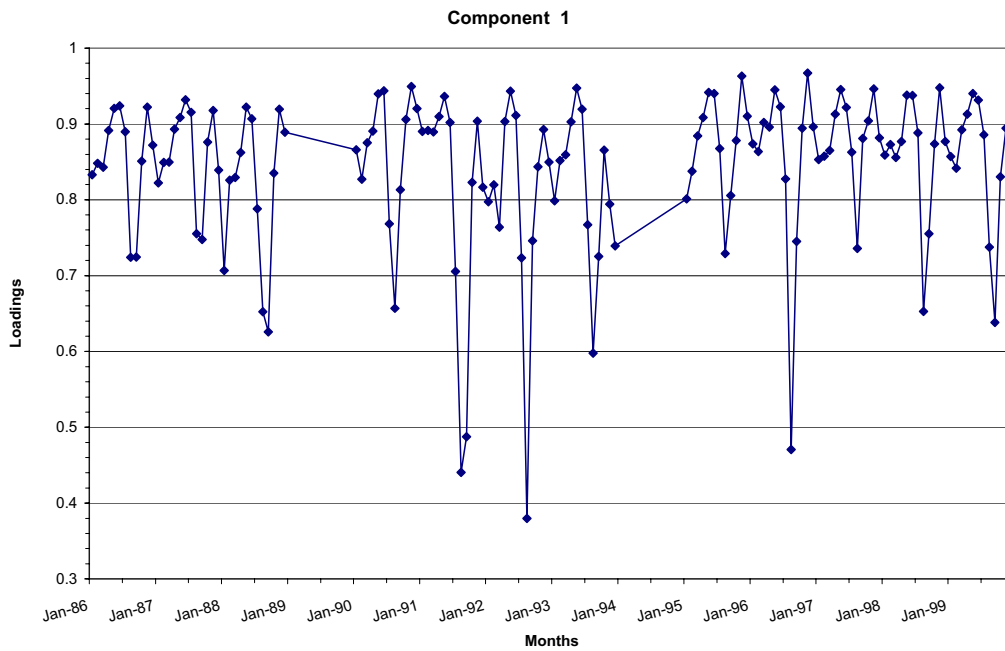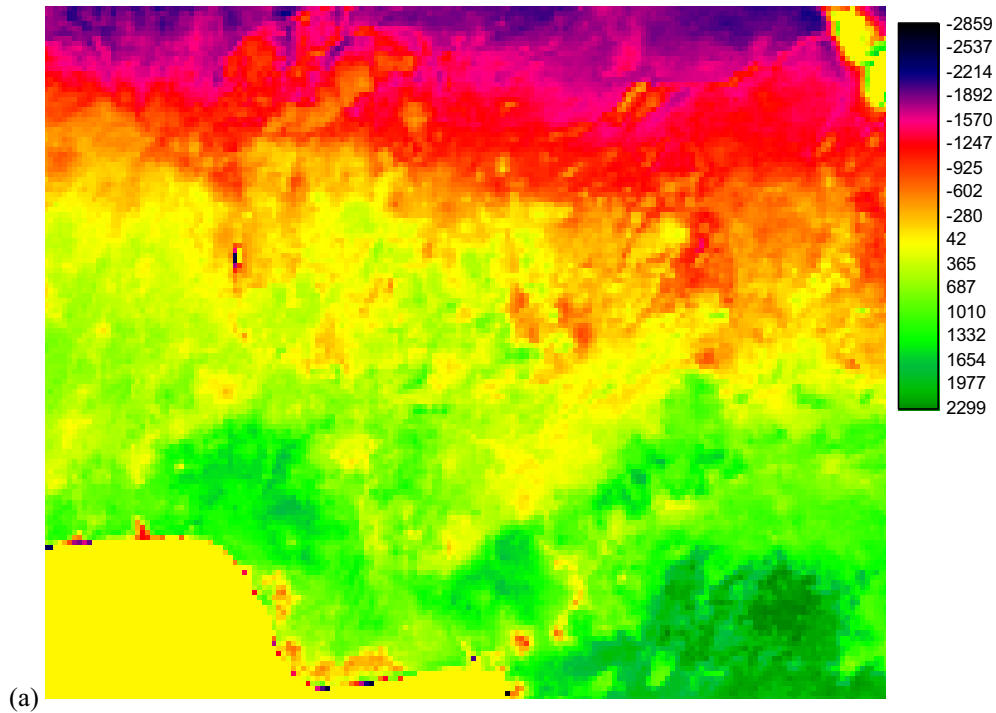
Figure 6.16. Component 1 image and its loading graph. The component image is shown above while its loading graph is shown below. This component image shows a typical characteristic of the average amount of vegetation biomass of the study area explaining about 72 % of the total variance of the whole 144 monthly NDVI dataset. On the graph, the $y-axis$ represents loading scores of the monthly NDVI image dataset and the $x-axis$ represents their respective months.

numbers. The two slidings dividing the profile into three sections (between 1988 and 1990 and between 1993 and 1995) are due to the missing NDVI data for 1989 and 1994. This can be noticed in all the profiles of the graph of loading scores. This image shows an average pattern of vegetation biomass as depicted by NDVI across the whole of Nigeria. The pattern on this component image shows a gradation of colours from blue in the northern fringes falling in the sahel region which extends from the southern part of the Niger Republic to dark green in the south falling in the forest region. The areas in red, yellow and light green colours mostly cover the savanna region while the dark green areas in the south-west is part of the forest region in Nigeria and that of the south-east falls in the forest region of Cameroon.

Component 2 Image

Component 2 image is an illustration of the first change component that differs from Component 1. This component image explains about 10 % of the total variance of the original dataset used as input in the TSA procedure. Its corresponding graph shows a pattern of cyclic trend showing positive scores and peaks mostly in August and September of each year while negative scores with lower peaks are mostly in February. The positive peaks correspond with the peaks of rainy seasons in most areas across Nigeria, while the negative peaks correspond with the dry seasons between January and March of each year. Component 2 image shows a clear distinctive pattern of changing season mostly across the west-east in the savanna zone. Apart from the northern areas, there are signs of high negative anomaly patterns in the south-west and south-east of the component image, particularly around the Niger Delta area. Hence, this component image shows an annual cycle of vegetation change across Nigeria. The temporal profile for the highest anomalous

Component 2

(a)

(b)
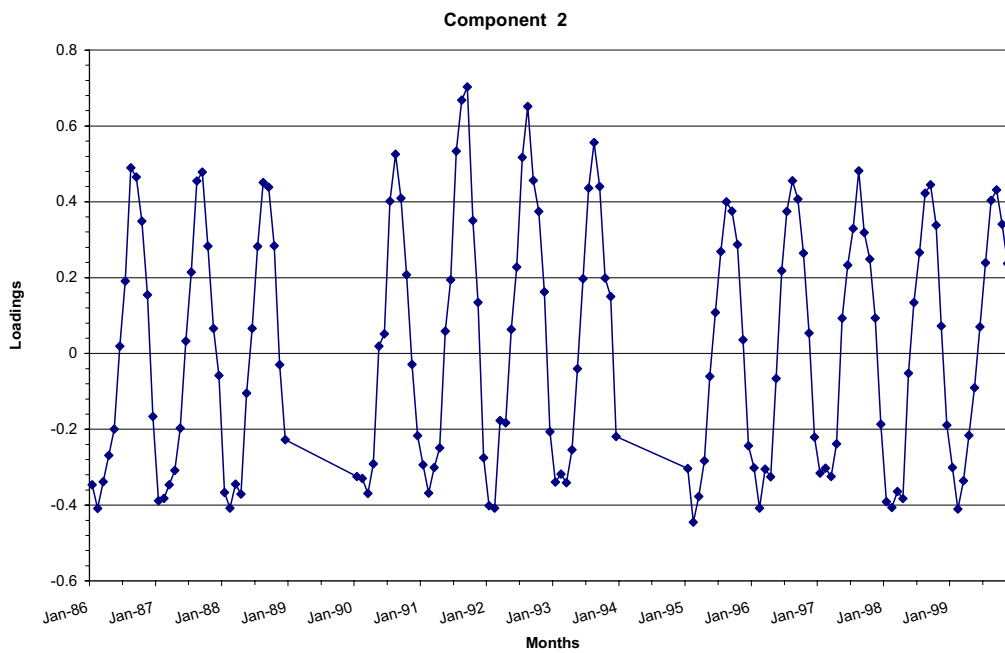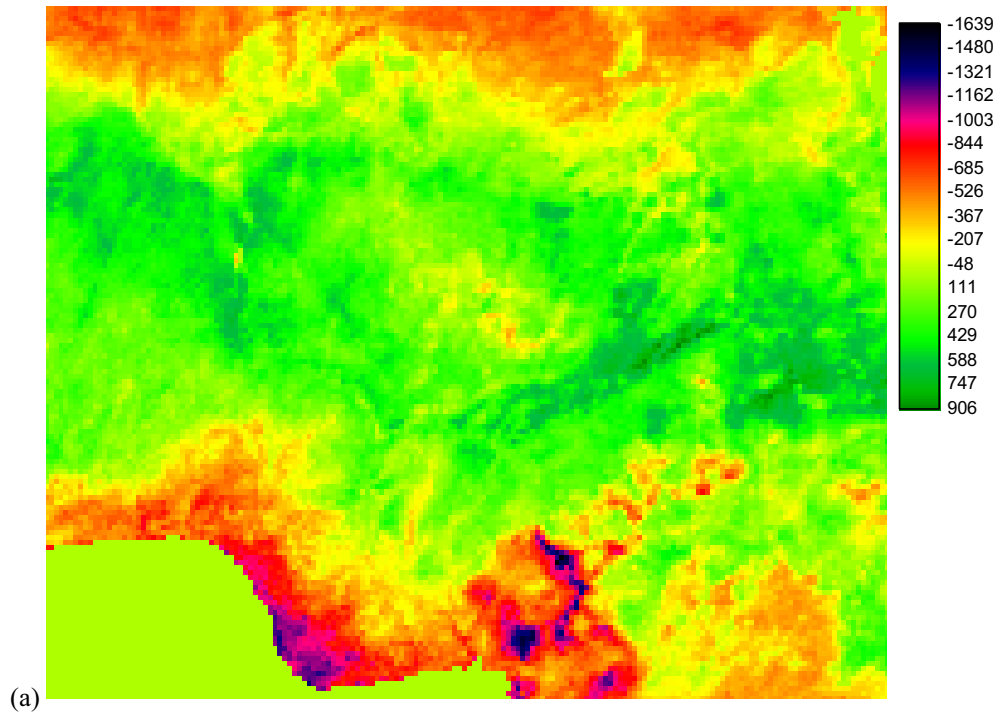
Figure 6.17. Component 2 image and its loading graph. The component image is shown in (a) while its graph of loading scores is shown in (b). This is the first change component image different from Component 1. It shows an annual cycle of vegetation change of the study area explaining about 10 % of the total variance of the whole 144 monthly NDVI dataset. On the graph, the $y – axis$ represents loading scores of the monthly NDVI image dataset and the $x – axis$ represents their respective months.
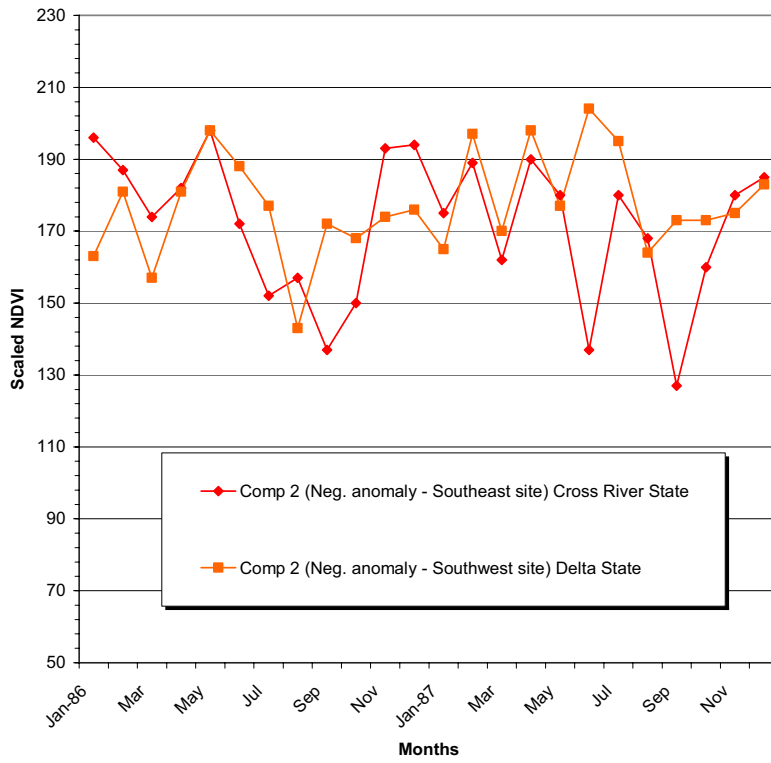
(a)
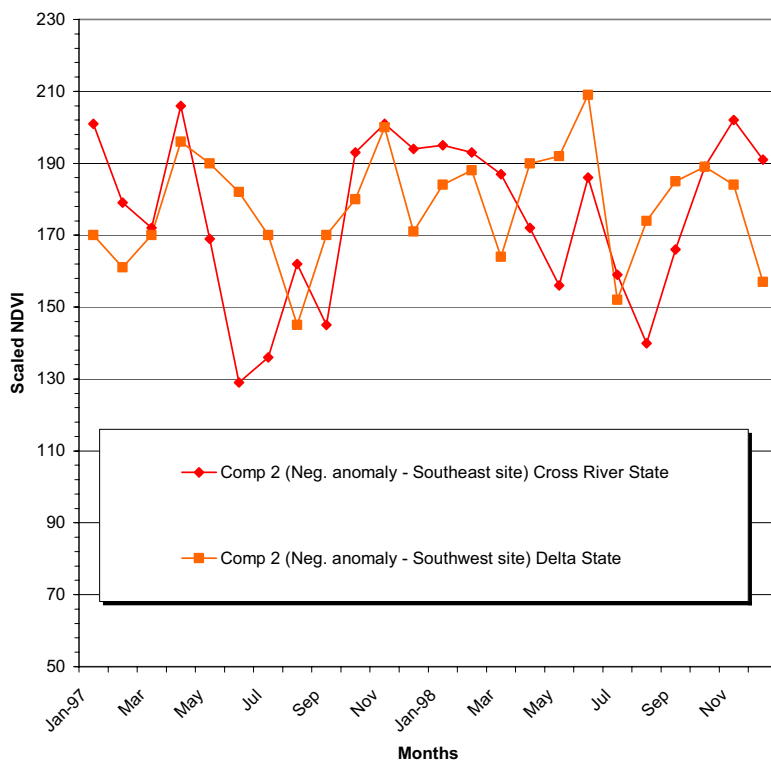
(b)

Figure 6.18 Temporal profile for highest anomalous NDVI pixels on Component 2 image. Plot (a) represents 1986/87 NDVI data while (b) represents the NDVI data for 1997/98 periods.

NDVI pixels (sites) illustrated in Figure 6.18 shows that NDVI values were very low mostly in August in the southern forest zone during the 1986/87 and the 1997/98 periods.

Component 3 Image

This image is the second change component exhibiting about 2.5 % of the variation in the NDVI dataset. The graph of this component image, though semi-circular, looks similar to Component 2 in terms of cyclic pattern of vegetation change as shown by the graph of its loading scores. However, the peak of the positive scores on the graph fall in January for most years while the negative (low) peaks fall in May/June. On this component image unlike Component 2 image, most of the positive anomaly patterns are located in the north-east (around Lake Chad and particularly Borno state), in the north-west (around Sokoto, Kebbi and Zamfara states) and in the south-east (mostly falling in the forest area in Cameroon). High negative anomaly patterns however, are located in the south-west and around the coastal areas. On the temporal profiles of pixels showing highest anomaly in Figure 6.20, two areas are very distinctive, the Niger Delta and Lake Chad. While Lake Chad site had high NDVI values during the 1986/86 period, the site in the Niger Delta area shows a fluctuated pattern in the profile during this period but shows a consistent low NDVI in the 1991/92 periods.

Component 4 Image

This is a change component image showing about 1.44 % of the total variation in the NDVI dataset. The graph of loading for this component image also shows some form of cyclic trend with all positive peak scores on the graph falling in December of all the years except 1993 when they fell in November. The negative score lower peaks, on the other hand, are

Component 3
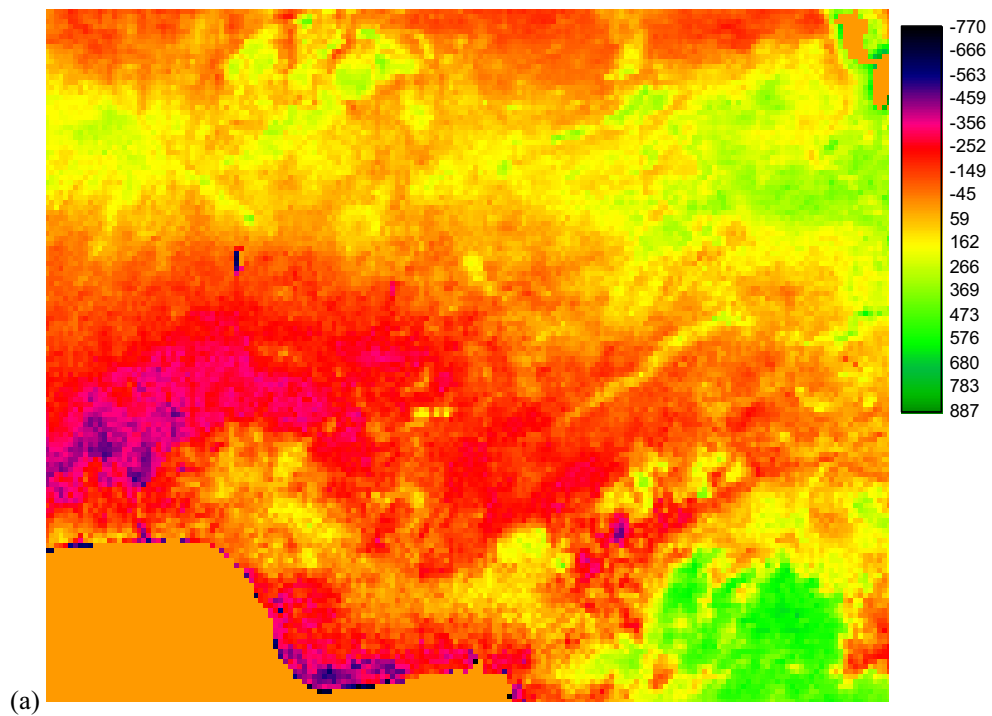
(a)

Component 3
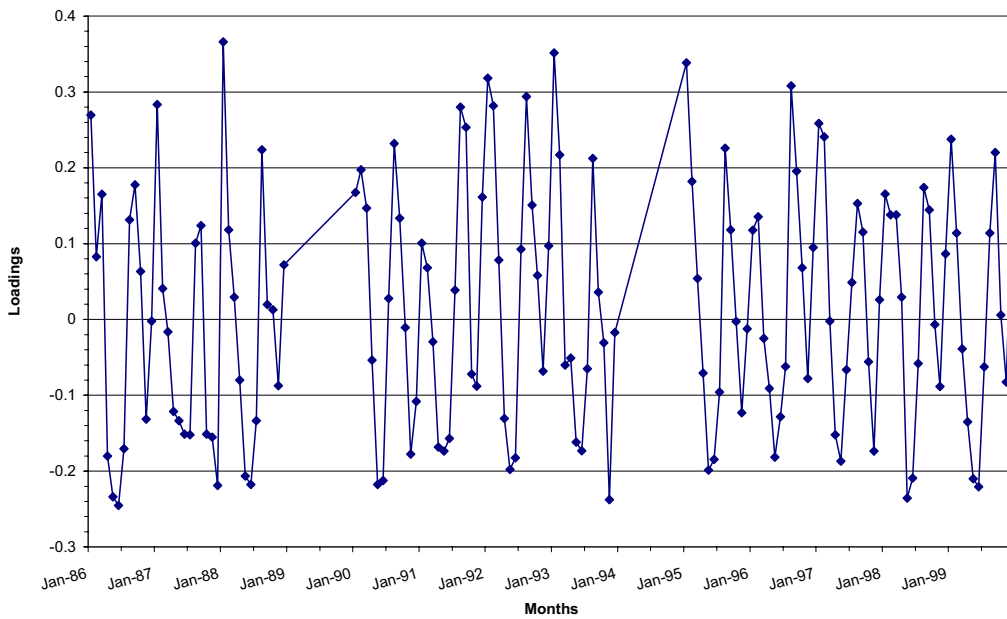
(b)

Figure 6.19. Component 3 image and its loading graph. The component image is shown in (a) while the graph of its loading scores is shown in (b). This is the second change component image. It also shows a semi- cyclic pattern of vegetation change close to the pattern on the graph of Component 2 image. It explains about 2.5 % of the total variance of the whole 144 monthly NDVI dataset. On the graph, the $y-axis$ represents loading scores of the monthly NDVI image dataset and the $x-axis$ represents their respective months.
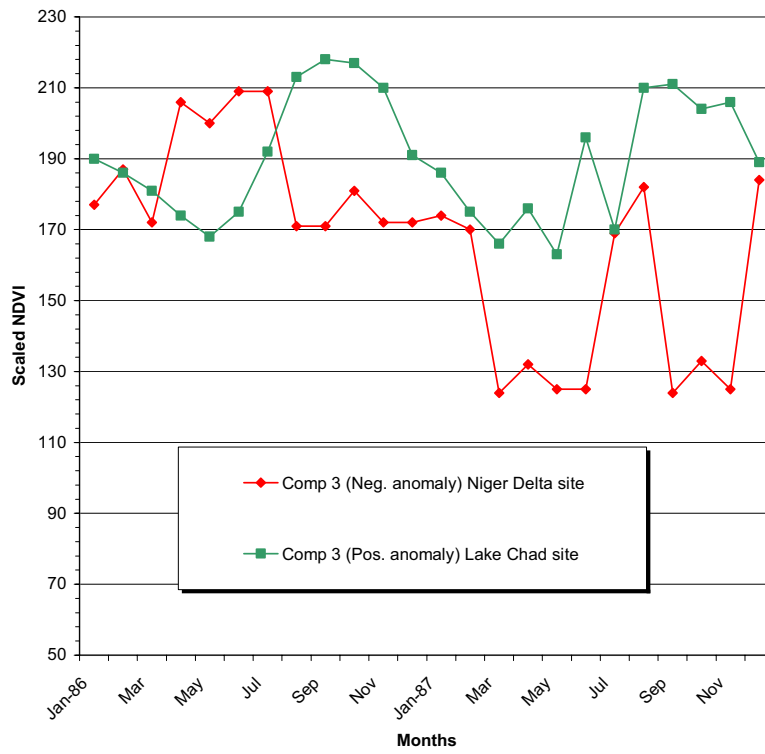
(a)
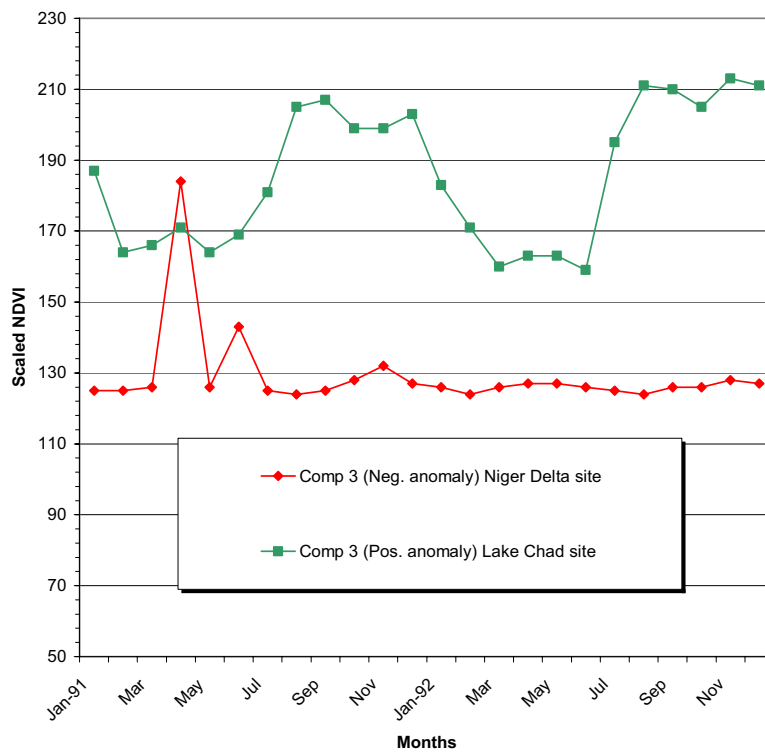
(b)

Figure 6.20. Temporal profile for highest anomalous NDVI pixels on Component 3 Image.
Plot (a) represents NDVI data for 1986/87 while (b) represents NDVI data for 1991/92 periods.

mostly in April and August. This component image shows a positive anomaly (mostly in green) around the Hadejia-Jama'are river and Chad basin areas with corresponding strong negatively anomalies in spot areas close by. The positive anomaly pattern on Component 4 image can also be seen around the Sokoto and Rima rivers basin area in the north-west, around Plateau, Bauchi and Gombe states in the east-central and in some states in the southern coastal areas of the country. There was also a very strong negative anomaly (in dark blue colour) around the forest area in the south-east mostly falling in the humid tropical forest area of Cameroon. The temporal profile on Figure 6.22 illustrates the pixels with highest anomaly on Component 4. From this plot it shows that an NDVI pixel from a sahel site south of Lake Chad had higher peaks than areas located in the tropical rain forest area located in Cameroon. This is unrealistic given the geographical and climatic locations of these different pixels.

Component 6 Image

This component image explains 0.6 % of the total variation in the NDVI dataset. The component image showed negative anomaly pattern affecting most parts of the country except spots of high positive anomaly along the coastal areas. The graph of the loading scores for this component image showed a curvilinear change pattern in NDVI. The highest spot of negative NDVI anomaly was located in the south-east falling around the Cross River state National Park. The highest spot of positive NDVI anomaly on the other hand was located in the coastal mangrove areas. The graph of loadings scores for this component image showed that the two highest positive peaks were in September 1986 and January 1988 while the highest negative peaks were in August 1992 and August 1993.

Component 4

(a)
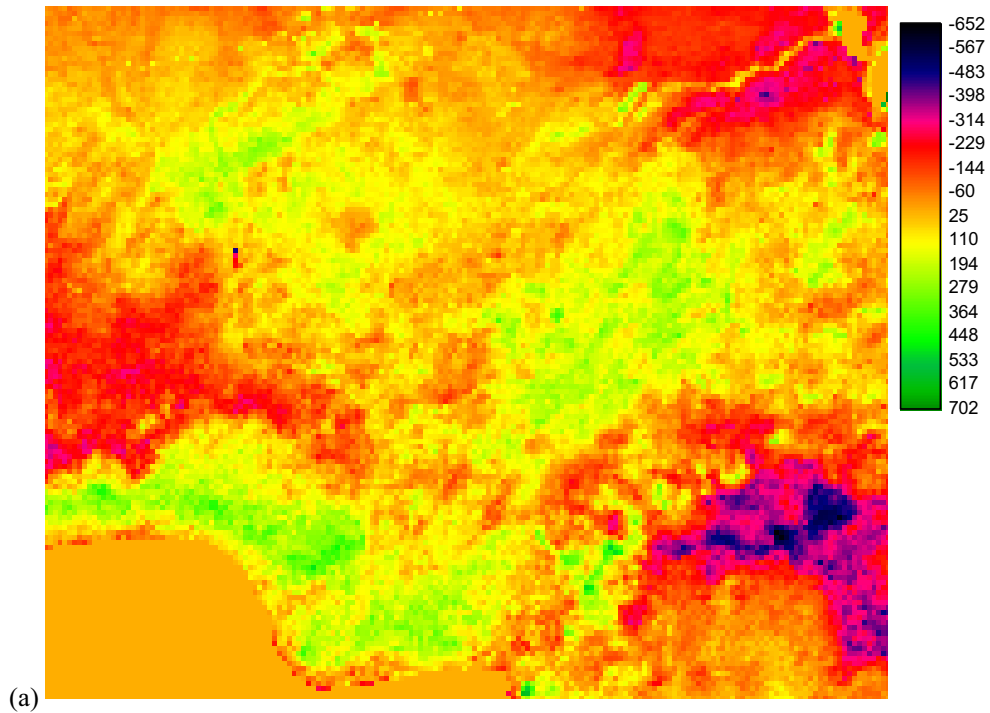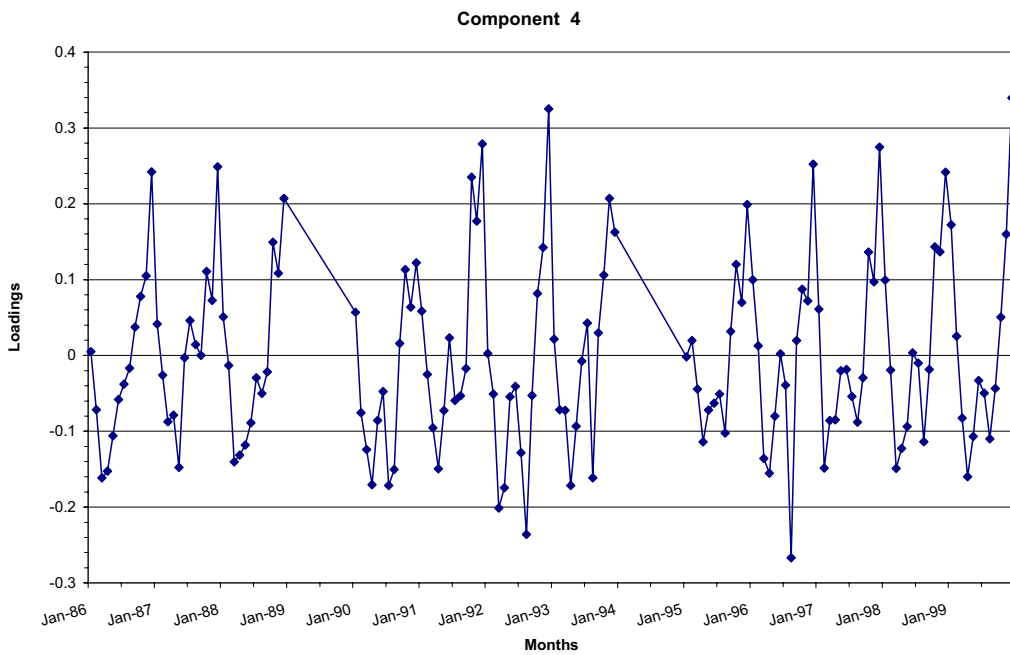
Component 4

(b)

Figure 6.21 Component 4 Image and its loading graph. The component image is shown in (a) while its graph of loading scores is shown in (b). This is the third change component image. It somewhat shows a semi- cyclic pattern of vegetation change close to the pattern on graph of Component 3 image. It explains about 1.44 % of the total variance of the whole 144 monthly NDVI dataset. On the graph, the $y-axis$ represents loading scores of the monthly NDVI image dataset and the $x-axis$ represents their respective months.
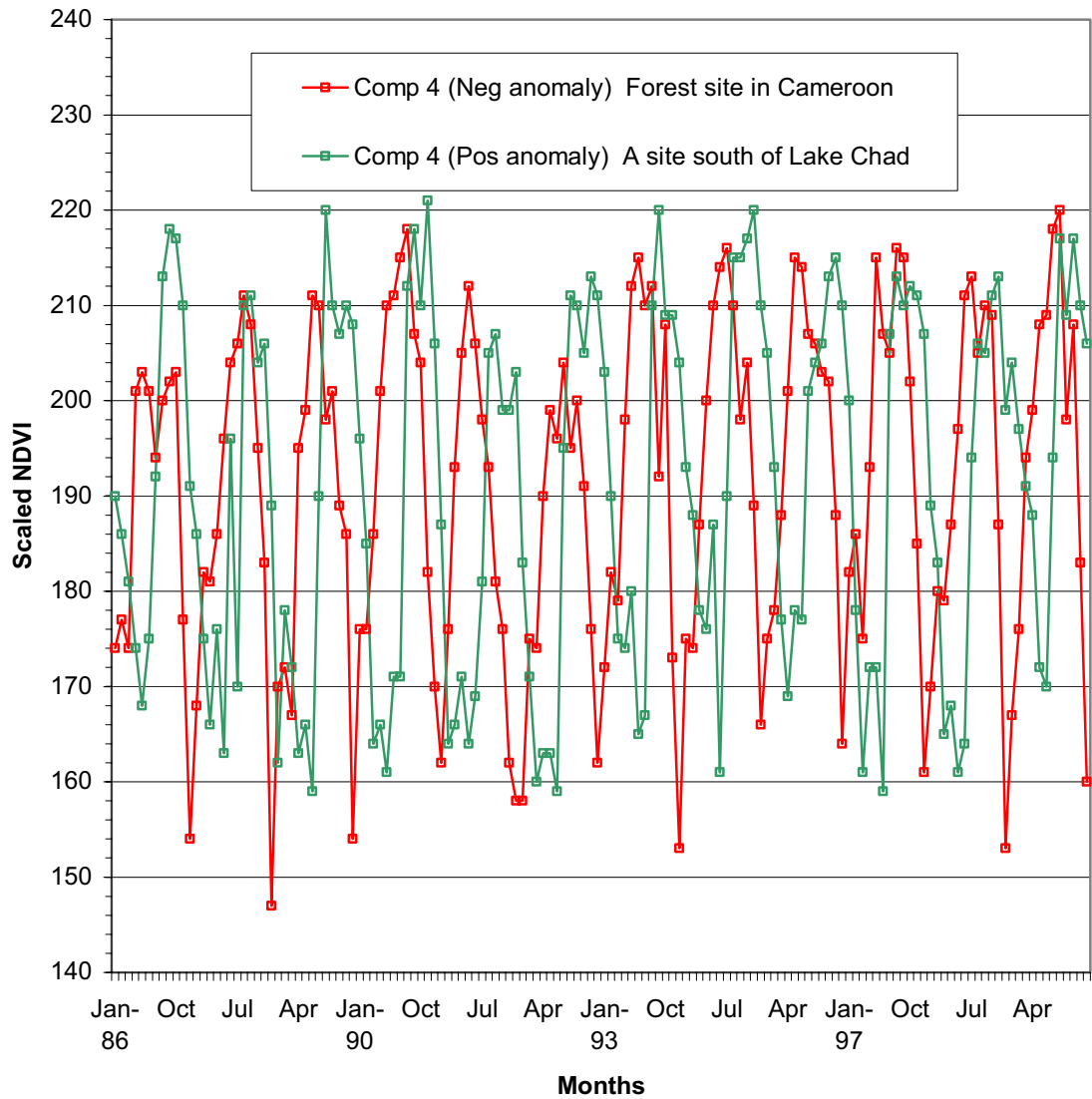
Figure 6.22 Temporal profile for highest anomalous NDVI pixels on Component 4 Image. The profiles cover the whole monthly NDVI dataset (1986-1999) used in the PCA analysis. The profile in green represents positive anomaly for sahel site while the one in red represents negative anomaly for the dense tropical forest area in the south-east falling in Cameroon.

Component 6

(a)

(b)
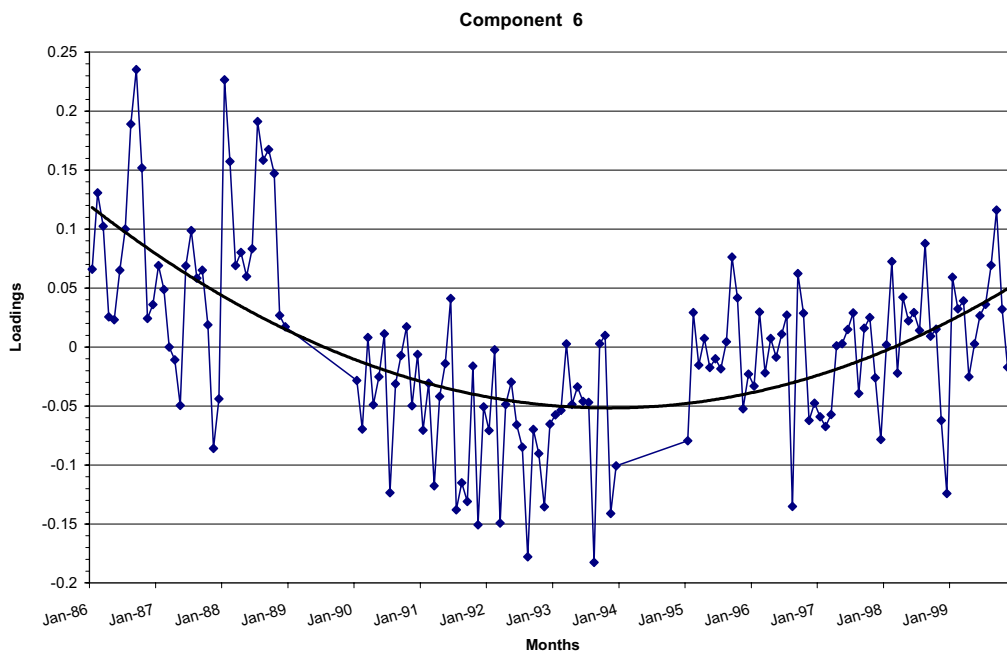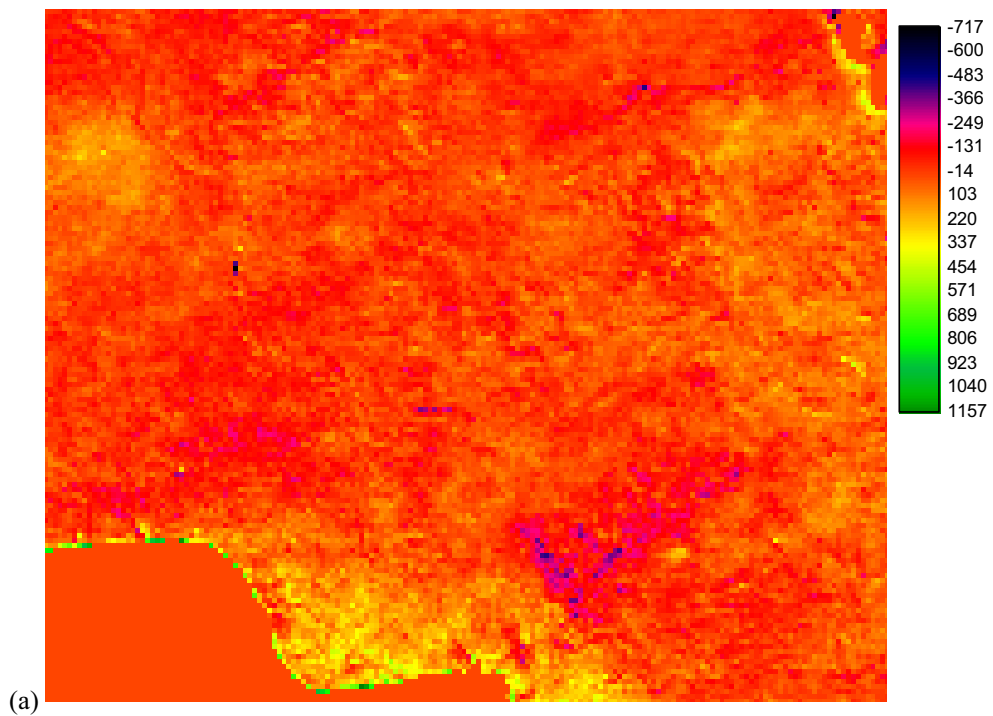
Figure 6.23. Component 6 Image and its loading graph. The component image is shown in (a) while its graph of loading scores is shown (b). This is one of the main change component images. The trend on the loading graph shows a mid series decline in NDVI. It explains only 0.6 % of the total variance of the whole 144 monthly NDVI dataset. On the graph, the $y - axis$ represents loading scores of the monthly NDVI image dataset and the $x - axis$ represents their respective months.
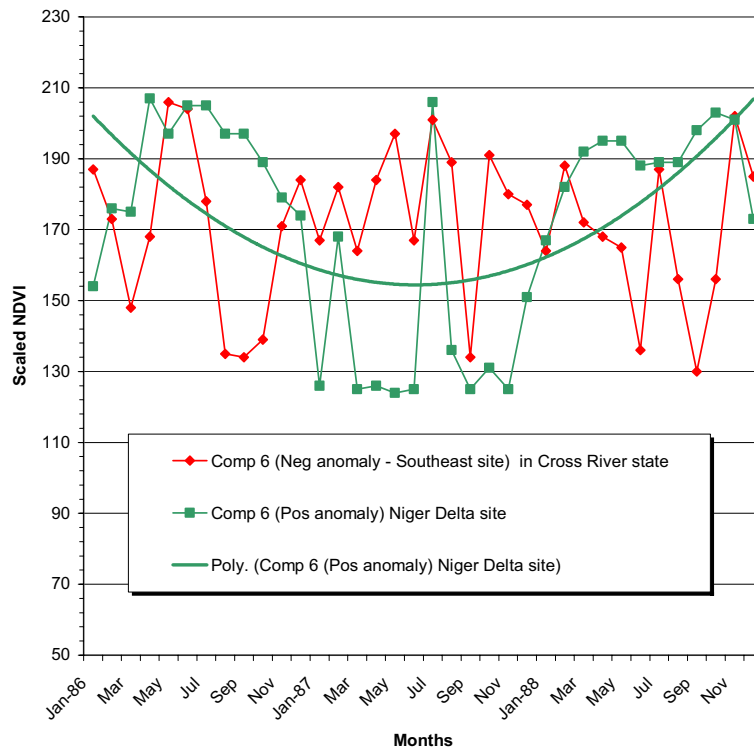
(a)
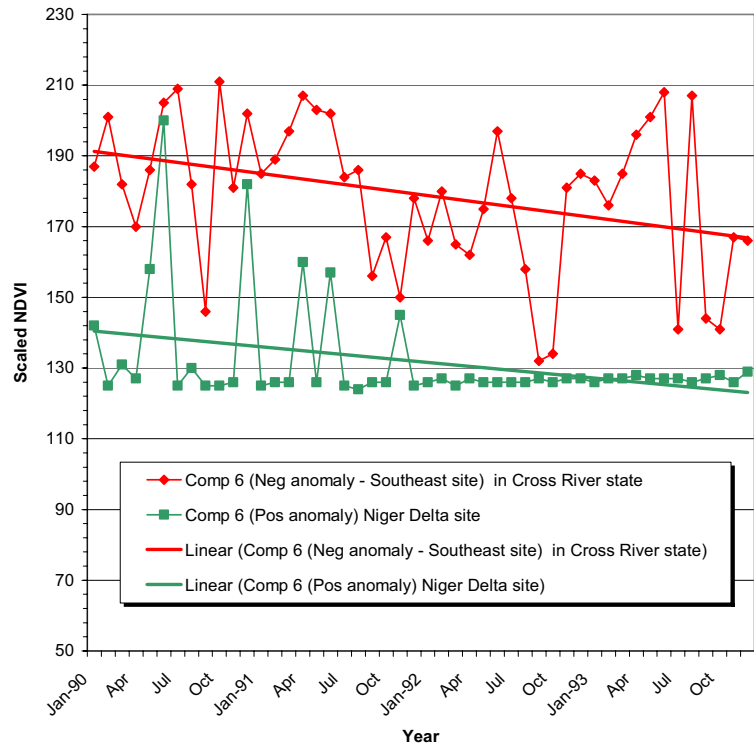
(b)

Figure 6.24 Temporal profile for highest anomalous NDVI pixels on Component 6. Plot (a) represents NDVI data for 1986 to 1988 while (b) represents NDVI data covering 1991 to 1993.
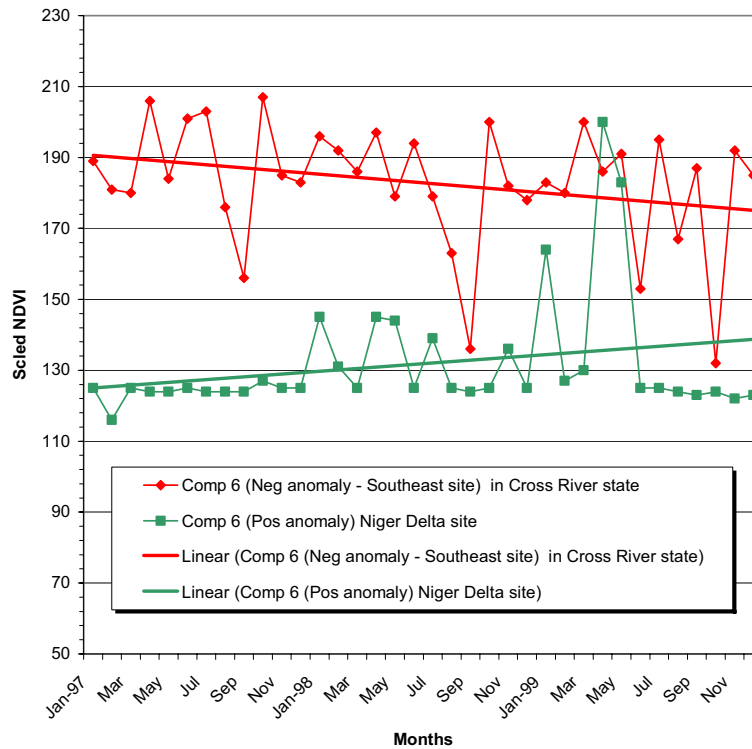
(c)

Figure 6.24 *(Cont.)* **Temporal profile for highest anomalous NDVI pixels on Component 6.** Plot (c) represents NDVI data covering 1997 to 1999.

Figure 6.24 shows the temporal profiles of highest anomalous NDVI pixels on Component 6 image. Both pixels of the highest negative and positive anomaly are located in the southern forest zone of Nigeria. On plot (a) The Niger Delta shows anomalous high NDVI peaks on the profile in 1986 and 1988 with a decline in 1987. On plot (b) showing the 1991 to 1993 periods and plot (c) showing the 1997 to 1999 periods, the site in the tropical forest area in the south-east shows troughs in the NDVI profiles mostly in August and September, the site in the Niger Delta shows anomalous high peaks in these months. There is a polynomial trend in plot (a) similar to the trend on the graph of the loading scores for Component 6 Image where there is an indication of a mid-term decline in NDVI in the

231

profile especially for the site in the Niger Delta. On plot (b) the trends for the two sites showed long term decline in NDVI. On plot (c) the site in the Niger Delta shows a positive (increase) trend in NDVI while the site in the tropical forest area in the south-east shows a long-term decline in NDVI.

Component 8 Image

This component image explains only 0.42 % variation of the whole NDVI dataset. The component image looks similar to Component 6 image in terms of showing change pattern of strong negative NDVI anomaly across the whole of Nigeria. The high negative anomaly patterns on this component image are prominently located along the coastal areas, but with high concentration spot at the northern part of Lake Chad in the north-east. In general, the anomaly shows a northwest-southwest and northeast-southeast pattern with less concentration of change in the south central and southeast of the country. The graph of loading scores for this component image indicated a positive correlation (> 0.1) between the component image and the NDVI dataset mostly in 1986 and 1988, 1991, 1992 and 1993. The highest positive correlation (~ 0.15) between the component image and the NDVI dataset was in September 1992. Negative correlations between the component and the dataset, generally, are from 1995 to 1999 with highest negative correlation (< -0.25) in August 1998. The trend shown on the graph of loading scores for this component image suggests that this component image shows a long term decline in NDVI across Nigeria. The two sites of anomalous NDVI pixels around Lake Chad and the Niger Delta are also illustrated in Figure 6.25.

Component 8

(a)

(b)
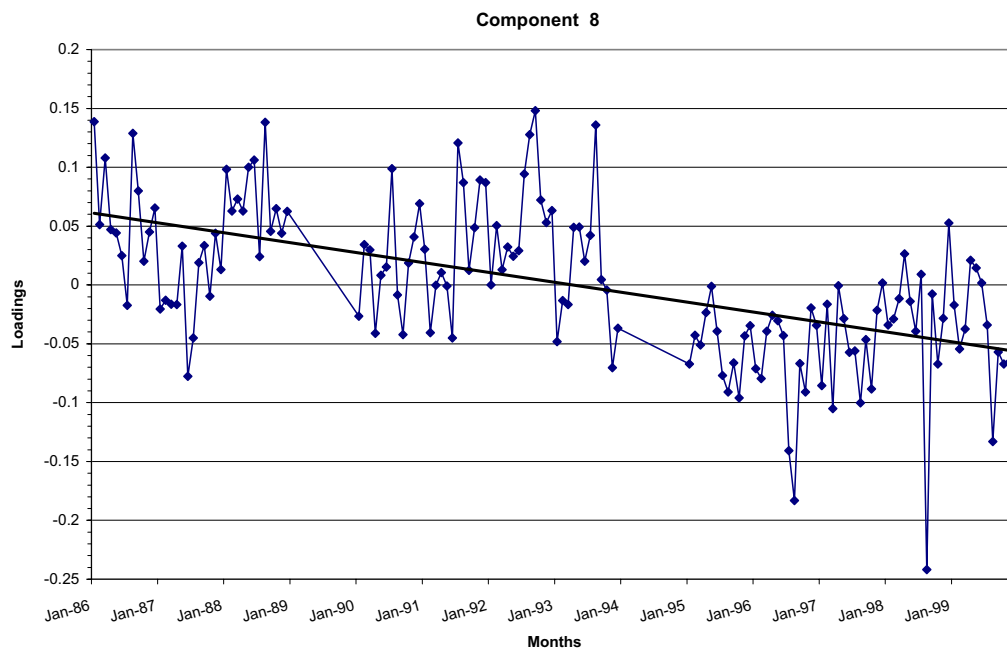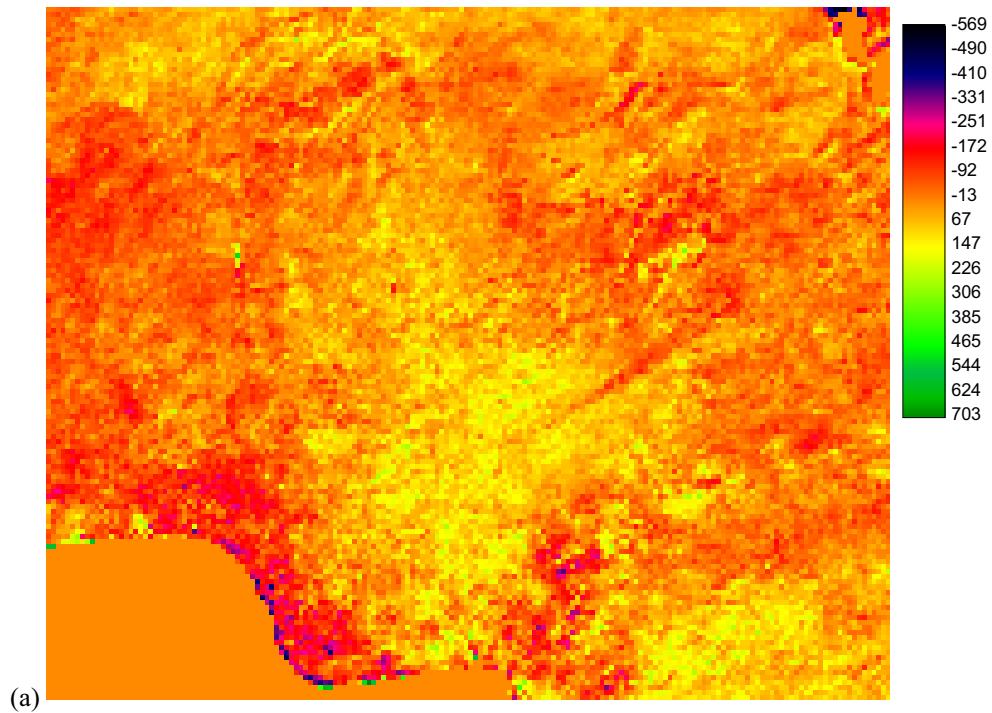
Figure 6.25. Component 8 Image and its loading graph. The component image is shown in (a) while its graph of loading scores is shown in (b). This is the main change component of all the images. The trend on the loading graph shows a long-term decline in NDVI. It explains only 0.42 % of the total variance of the whole 144 monthly NDVI dataset. On the graph, the $y – axis$ represents loading scores of the monthly NDVI image dataset and the $x – axis$ represents their respective months.

233
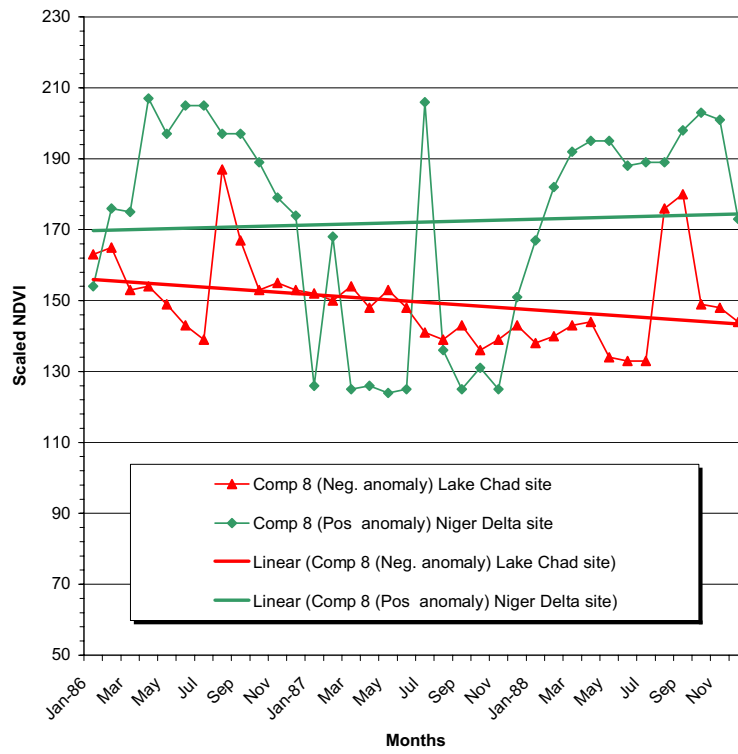
(a)
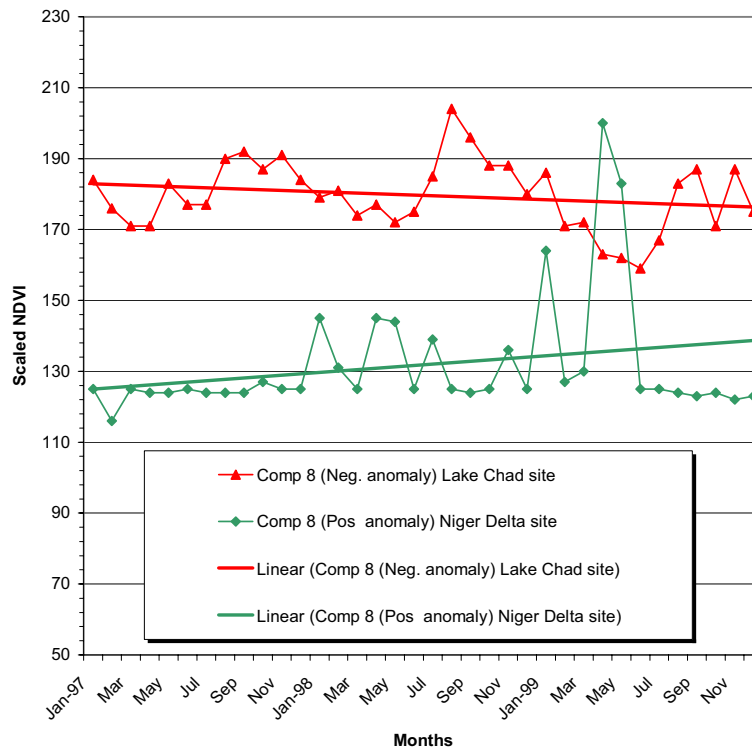
(b)

Figure 6.26.   Temporal profile for highest anomalous NDVI pixels on Component 8. Plot (a) represents NDVI data for 1986 to 1988 while plot (b) represents NDVI data covering 1997 to 1999.

Between 1986 and 1988 the temporal profile for the selected pixels on Component 8 image on Figure 6.26 (a) representing a site around Lake Chad shows a long-term decline in NDVI while the Niger Delta site shows a long-term positive trend. Plot (b) of the same figure shows opposite trends of what was on plot (a) where the site around Lake Chad shows an increase in NDVI while the Niger Delta site shows a long-term decline in NDVI according to these trends.

Component 80 Image

This is one of the low signal to noise ratio of the later component images. It explains a very tiny proportion (0.057 %) of the total variation in the whole 144 monthly NDVI data set used as input in the PCA procedure. The component image showed a somewhat negative anomaly pattern in pocket locations falling within certain reserve areas across the country (Figure 6.28) which can be attributed to very localised events related to changes in vegetation. The majority of change patterns cut across the country although a few spots of strong negative anomalies can be seen in smaller areas. The loading scores for this component image showed that its correlation with the NDVI dataset between January 1986 and November 1997 falls between -0.05 to 0.05 on the graph. However, the highest negative correlation (<-0.15) between this component image and the NDVI dataset on this graph of loading scores was in December 1998 while the highest positive correlation (< 0.15) was in December 1999. Because of the strong negative anomaly pattern on one of the last component images detected by PCA technique it was also chosen for interpretation. It suggests areas of possible localised change events that can be related to changes in vegetation. Temporal profiles of monthly NDVI and annual rainfall datasets for selected pixels in central areas of strong anomalous patterns are illustrated in Figure 6.29.

(a)

Component 80

(a)

Component 80

(b)
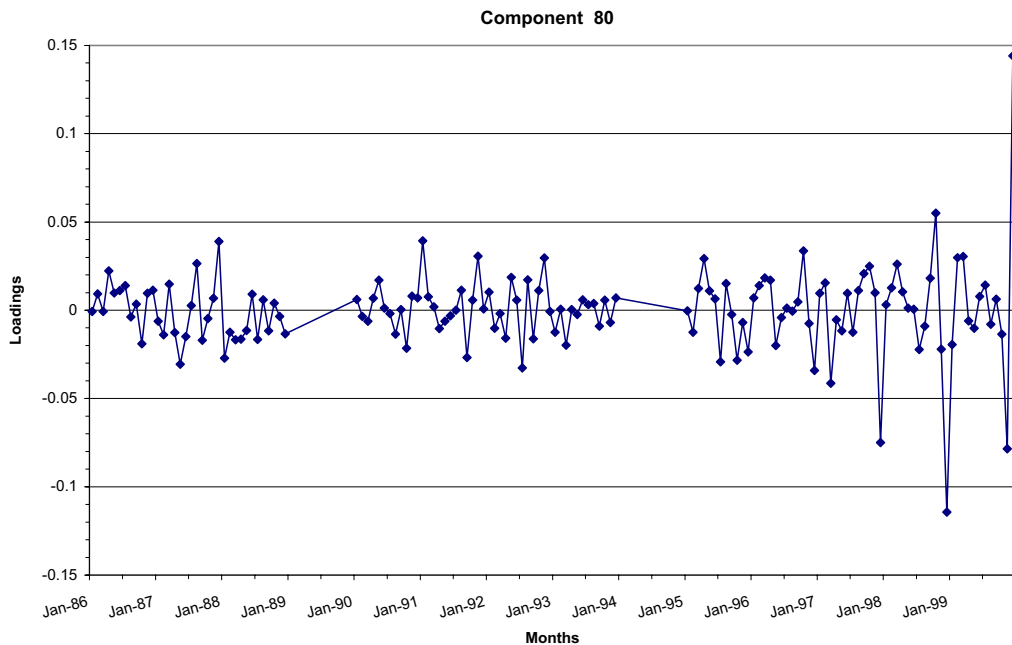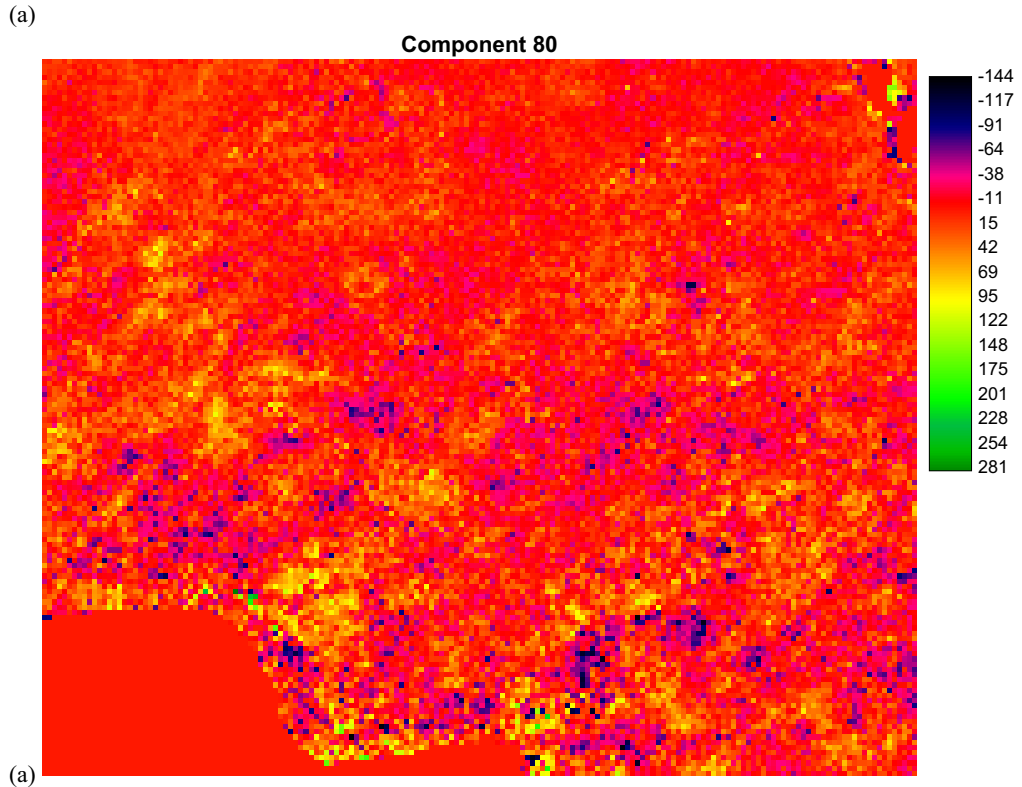
Figure 6.27. Component 80 Image and its loading graph. The component image is shown in (a) while its graph of loading scores is shown in (b). This is one of the last 'low signal-to-noise ratio' change component images. The image explains a very tiny proportion (0.057 %) of the total variance of the whole 144 monthly NDVI dataset, but exhibits an interesting change pattern. On the graph, the $y-axis$ represents loading scores of the monthly NDVI image dataset and the $x-axis$ represents their respective months.

236
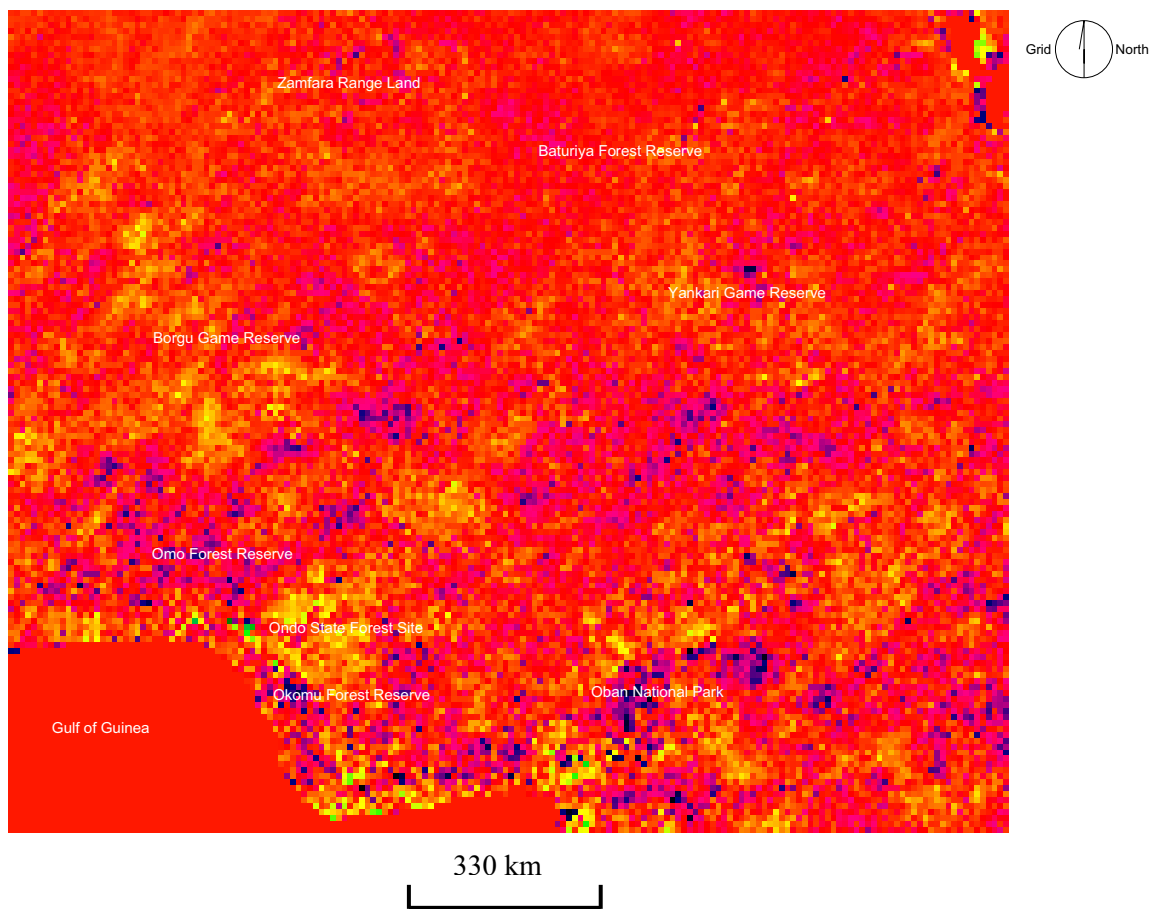
Figure 6.28 Approximate locations of certain reserve areas across Nigeria on Component 80 image.
These areas indicated pocket NDVI anomaly patterns suspected of changes related to localised events that can be linked to changes in vegetation within the northern savanna and the southern forest zones of Nigeria.

The corresponding pixels on the annual rainfall images covering the whole time series (1986 -1999) are also illustrated in Figure 6.30. The temporal profile in Figure 6.29 shows the monthly NDVI dataset for those pixels in the anomaly areas. These were selected in the northern savanna and southern forest zones covering the highest negative trend years (1997 - 1999) as indicated by the graph of loading scores for Component 80. This profile shows that most of these anomaly pixels falling approximately in reserve areas both in the northern and southern parts of the country have low NDVI values either in August, September or October. These are peak NDVI months in most of these areas.

(a)

(b)
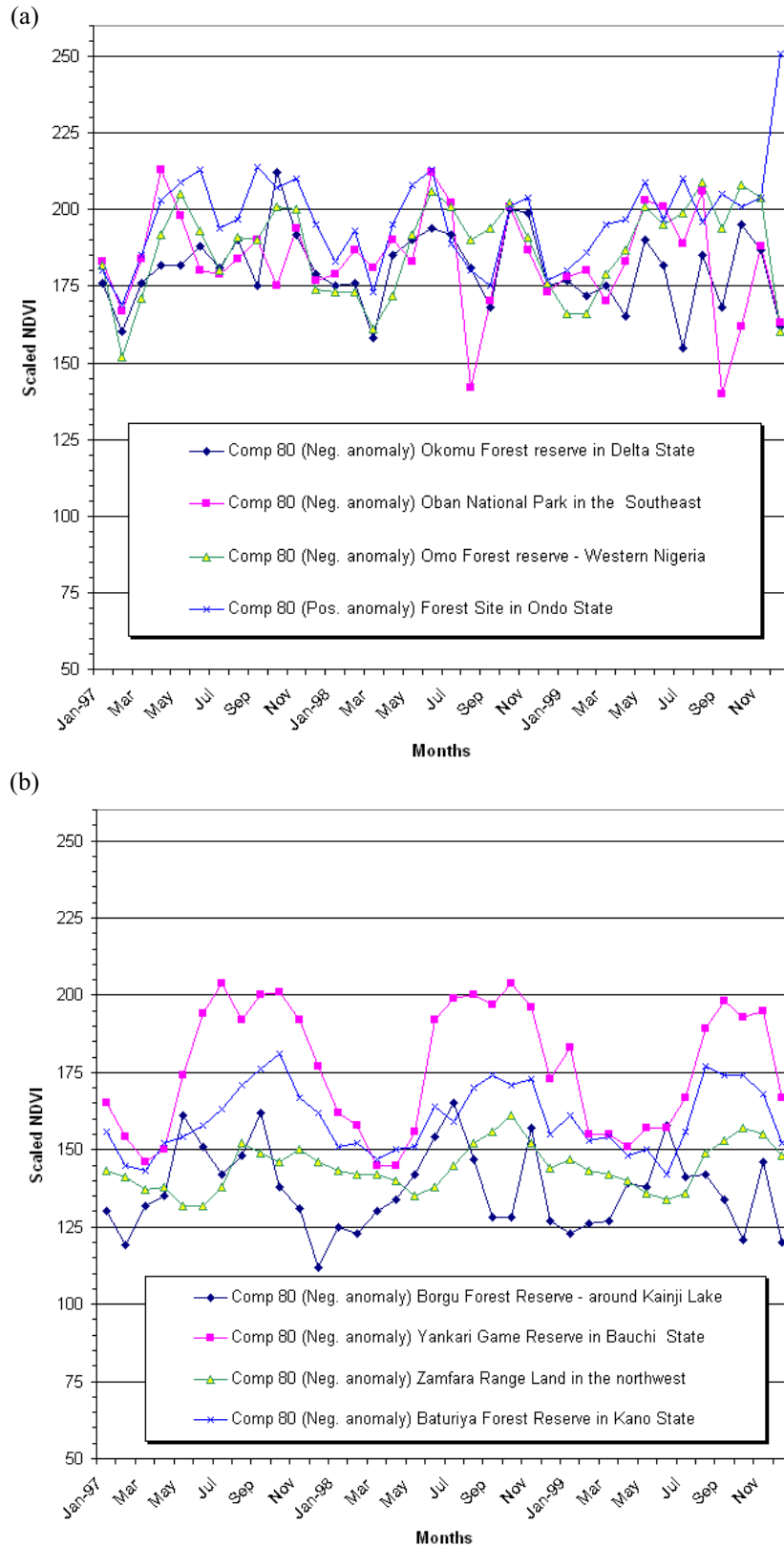
Figure 6.29 Temporal profile of NDVI for selected sites on Components 80 image within the 1997 to 1999 ENSO warm and cold   phases. Plot (a) represents sites in the reserve areas in the southern forest vegetation zone while plot (b) represents sites in reserve areas in the northern savanna vegetation zone.

(a)

(b)
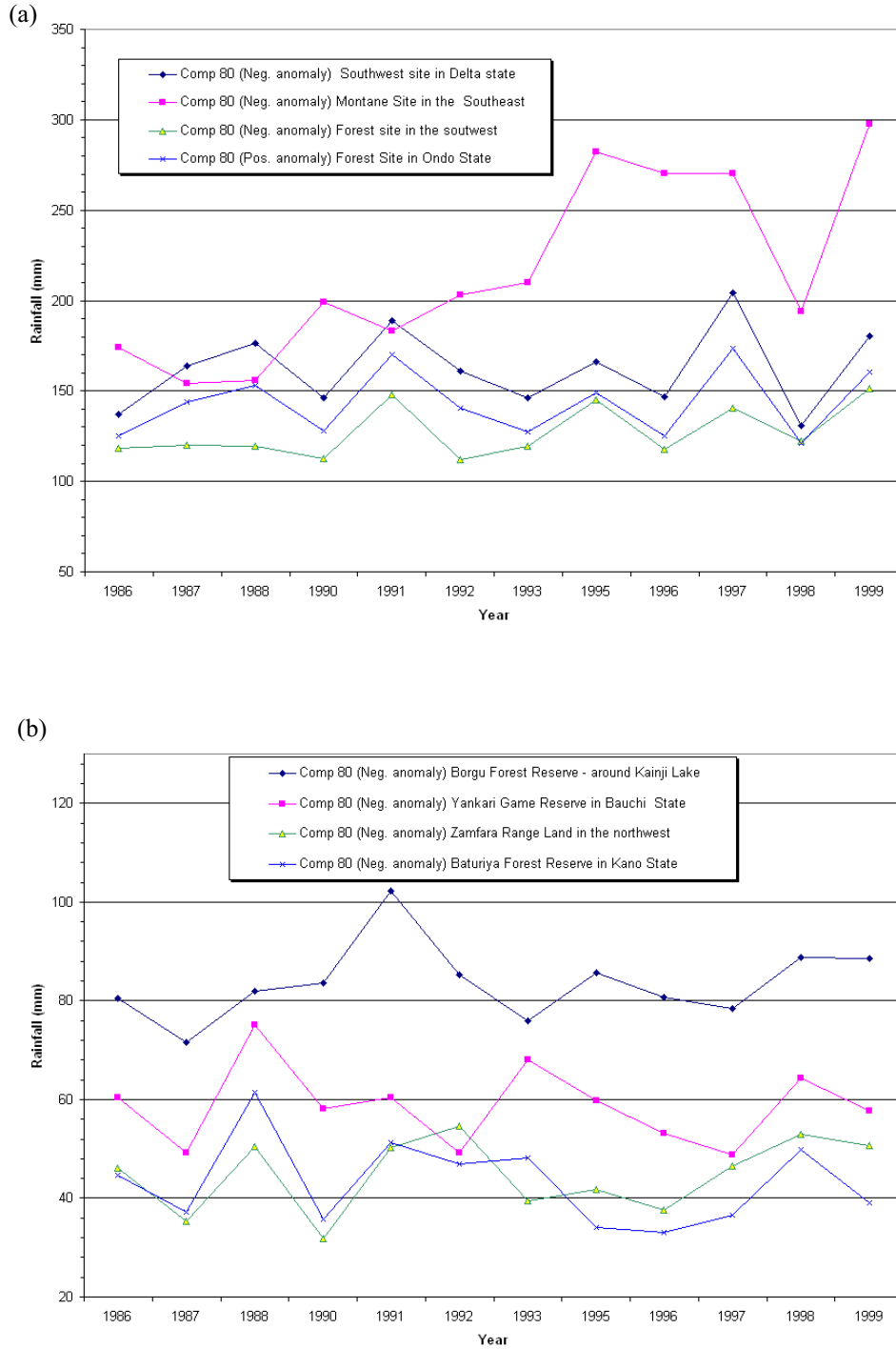
Figure 6.30. Temporal profile of annual mean rainfall for selected sites of NDVI anomalies on Component 80 image. Plot (a) represents sites in the southern forest vegetation zone of Nigeria while Plot (b) represents sites in the northern savanna zone.

On the profiles on Figure 6.30, showing annual rainfall data for the corresponding pixel positions of the monthly NDVI data illustrated in Figure 6.29, there were high peaks in 1997 and troughs in 1998 for the sites in the southern forest zone. On the other hand, there were troughs in 1997 and high peaks in 1998. There were also other peaks on this rainfall temporal profile in 1988, 1991 and 1995 for both these selected anomalous sites both in the savanna and forest zones.

6.4.5 Discussion

The use of standardised principal components in PCA change detection indicated clearly that the major element of variability is that which occurs spatially (Eastman and Fulk, 1993; Hirosawa *et al,* 1996). From the results of this investigation, Component 1 represents the characteristic pattern of vegetation across Nigeria between its two distinct wet and dry seasons.

As a technique for detecting spatial change, the PCA technique proved more efficient in isolating both short- and long-term changes in NDVI than the other two techniques (Image Differencing and Slope of Change from Regression) used in this investiagtion.

What is common to all the three change detection techniques employed in this investigation is that NDVI data is being assessed to determine spatial changes and location of such change areas across Nigeria. The NDVI data utilised here is not only a representation of green vegetation biomass but also an integration of other things like patterns and trends of climatic variables (Anyamba and Eastman, 1996). Thus, these patterns and trends are reflected in different degrees in the results of all the three different change detection techniques, but more specifically, in the results derived from PCA.

However, although each of the three techniques has its own unique methodology, image differencing approach adapted from Young and Wang (2001) and applied in this

investigation made use of selective NDVI data supplemented with climatic (rainfall) data of only specific sites from the two main vegetation zones across the country. In the slope of change from regression technique complete annual NDVI and rainfall datasets covering the time series were utilised across the country, and for specific sites. Most of the results from these two techniques hid certain patterns or trends where the final results showed either an under or over generalisation. In the PCA technique which utilised all the monthly NDVI dataset in the time series, the approach was able to extract both these climatic trends as well as true spatial changes in NDVI and false changes that relate to defects from AVHRR sensing mechanisms. For example, the detection of false positive change (increase in vegetation biomass) in the sahel area near Lake Chad, and false negative change (decrease vegetation biomass) in the dense forest area in Cameroon (see Figure 6.22). Furthermore, the PCA technique which utilised only monthly NDVI datasets without the use of rainfall data systematically isolated the first component image which shows a representative vegetation pattern across Nigeria that looks similar to the original NDVI images illustrated in Figures 5.2 and 6.2, while subsequent component images showed a pattern of varying changes in NDVI across the country.

In both the image differencing and slope of change from regression techniques, areas around Lake Chad in the northern savanna showed a mixture of negative (decline in vegetation) and positive (increase) changes while coastal areas and particularly areas around the Niger Delta showed a consistent decline in NDVI. On the other hand, results derived from PCA also showed these places with varying degrees of change depending on the component image, as successive components differ from each other in the type of change they detected.

Areas where both negative and positive change patterns are more prominent in most component images from the PCA but not on the change images derived from the other two

techniques can be seen in different locations across the country, and more specifically, in the forest areas of the south-west and the montane and forest areas of the south-east which fall both in Nigeria and Cameroon. This is one of the fundamental differences between the results obtained from PCA and the other two different techniques. However, what also seemed common in the general results derived from image differencing and PCA that is not common to the slope of change for regression technique is the spatial change patterns and trends on Component 6 and Component 8 images. The trend shown on the graph of loading scores for Component 6 image depicting a polynomial trend of mid term change across Nigeria can be compared with the results illustrated in Figure 6.2 derived from image differencing technique. This trend from the graph of loading of Component 6 showed a decline in NDVI from 1986 to 1993. More specifically is the decline in NDVI between 1990 and 1993 (see Figure 6.23b). This relates to the period when there was serious ENSO effects on world Net Primary Production (NPP) and crop production (see Figure 2.2). The period falls almost within the range of the two annual NDVI end-point years (1986 and 1992) used in image differencing to derive short- term changes in NDVI across Nigeria. Hence, although the changes derived from PCA on Component 6 image cut across the whole country, such negative (decline) changes in NDVI are more prominent in the southern areas, and specifically in the forests and coastal areas of the country.

As for the loading graph for Component 8 image which shows a long-term trend in vegetation changes across the whole of Nigeria, this also compares to a certain degree with the results derived from the image differencing technique showing long-term relative changes in NDVI as illustrated on Figure 6.4 (b) and (c). From these simple comparisons, PCA technique shows that it is more efficient as a technique for detecting spatial changes in vegetation biomass across the whole of Nigeria than the other two techniques even without supplementing the analysis with climatic (rainfall) data.

6.4.6 Summary

- The use of PCA as a technique for detecting spatial changes showed that vegetation change across Nigeria can be discerned in a more systematic way.

- The technique has the advantage of processing large amounts of dataset where it compresses them so as to show varying patterns of changes on component images as a percentage of the original data input.

- The first component image shows representative characteristics of vegetation across the whole of Nigeria while successive components represent changes which are uncorrelated with each other.

- Common areas where changes are detected as on the other two different change detection techniques are located around Lake Chad in the northern savanna and the coastal areas in the southern part of the country.

- Specific change areas that were detected and which relate to PCA are located around the south-west forest region as well as the forest and montane areas of the south-east which fall both in Nigeria and Cameroon.

- Other changes which the PCA technique was able to detect that differ from the other two techniques are evidence of inter-annual variability related to El Niňo and more specifically, artefacts that emanate from the AVHRR equipment used to acquire the NDVI data.

- One of the last component images considered less important in PCA still detected change patterns that can be related to very localised events which have links with changes in vegetation across Nigeria.

- Temporal profiles of anomalous NDVI pixels selected from areas that showed change patterns on component images gave further clues of possible long-term climatic events which the graph of loading scores highlighted.

CHAPTER SEVEN

GENERAL DISCUSSION AND CONCLUSIONS

7.1 Introduction

This chapter presents an overview of this study which utilised coarse spatial but high temporal resolution AVHRR-NDVI data from the PAL dataset to assess vegetation cover change across Nigeria. It briefly discusses issues related to the primary dataset and its preparation, the change detection techniques and then compares the techniques and results derived from this investigation with others. The implication and significance of the results in the Nigerian context is then highlighted and conclusions are summarised.

7.2 The Study Overview

The investigation assessed short- and long-term changes in vegetation cover across Nigeria. The study was built on the assumption, indicated by other published research on different parts of the country using high spatial resolution satellite data, that vegetation cover is changing qickly. A report on the implementation of Agenda 21 of the United Nations Commission Conference on Environment and Development (UNCED, 1997) that was based on studies which used a combination of high spatial resolution data and ancillary information showed that vegetation cover is persistently declining across Nigeria as a result of population pressure and continuous exploitation of vegetated areas. It therefore suggested that periodic monitoring and management of vegetation cover for ecological sustainability would be desirable. However, in those studies covering specific areas in Nigeria, the UNCED used high spatial resolution data which had low temporal resolution

and were also expensive. There is a need to develop a technique to test such results not only on those areas studied, but also across the whole of Nigeria, using coarse spatial resolution data which has high temporal resolution and is also obtainable free. This may therefore have benefits for countries with low economic standing like Nigeria.

Three change detection techniques were used in the assessment. A simple image differencing technique was first used with annual NDVI dataset so as to provide a quick and broad view of changes in short- and long-term periods. In the second technique, slope of change from regression of annual NDVI and rainfall datasets was used. In this technique, slope of change of NDVI and rainfall images were used in a pairwise comparison to detect areas that changed in vegetation cover for the entire period (1986 to 1999) under investigation, which resulted from non-climatic influences. This provides the opportunity to verify the UNCED (1997) report and also show vegetated areas vulnerable to population pressure across the country. The third technique employed PCA using standardised principal components. In the PCA, a multi-temporal analysis of monthly NDVI dataset across Nigeria was undertaken. The aim was to determine the spatio-temporal change pattern in vegetation cover across the whole of Nigeria.

The overall results from the three different techniques used in this investigation showed that there were specific locations characterised by increasing and decreasing vegetation cover over the study period. Long term decline in vegetation cover has implications and is perhaps of greater importance in the country's ecological sustainability. It therefore requires assessment for better management.

7.3   The AVHRR-NDVI data for vegetation change studies

Goward (1993) expressed concern about using the NDVI data from AVHRR for vegetation change studies that relates to non-climatic influences, particularly anthropogenic changes, because of atmospheric and climatic variations as well as sensor degradation. Other studies (eg Gutman and Ignatov, 1995; Prince and Goward, 1996) found a residual trend of increasing NDVI in the NOAA 11 period over the Sahara which was due to the calibrations of satellites carrying the AVHRR sensors (Rao and Chen, 1994). Smith *et al* (1997) highlighted some problems with the AVHRR data, particularly the PAL dataset and how the problems were later rectified. This was indicated in Section 2.4.3.

However, this investigation has shown that the AVHRR-NDVI data, particularly from the PAL dataset, when temporally averaged reduced most of the minor interannual climatic fluctuations in the data (Ehrlich and Lambin, 1996). It has therefore provided a very useful and more meaningful assessment of changes in vegetation cover. The results also gave clues to the cause of change which can be associated with man's influence on the land cover and those that relate to other factors associated with data quality. For example, during a check on data quality (Chapter 4), this investigation has identified one of the main problems of the PAL dataset. The whole data from 1995 to 1999 was affected by errors in calculating the calibration coefficients for Channels 1 and 2 of AVHRR onboard NOAA-14. Having identified the problem with NOAA/NASA, data covering that period had to be re-downloaded and re-analysed, had this not been undertaken, the results obtained with such data would have been highly misleading (see Appendix 4).

In the initial analysis and data preparation (Chapter 5) it was discovered that most of the peak NDVI periods in Nigeria are in September. However, the general trend indicated that the peak NDVI month is tending to get later in the year suggesting that the northern savannah is getting greener later and contributing to the overall blooming of the whole country.

7.4 Potential causes of changes in vegetation cover across Nigeria

Different causes of general land cover change enumerated by Lambin and Strahler (1994b) are indicated in Section 2.3.3. However, different studies that used remotely and non-remotely sensed data across Nigeria have shown that changes in vegetation cover are mostly as a result of changes in land use (Adeniyi, 1985; Thomas and Adams, 1997; Ite and Adams, 1998; Salami, 1999; Boele *et al,* 2001b). Other studies such as Osemeobo, (1988) showed that changes in vegetation cover in Nigeria were the result of population pressure on the environment while Ohamobi and Mohammed, (1999) showed that the collective effects of the causes are responsible for the encroaching desert from the Sahel region. Other socio-economic activities such as lumbering, mining, gathering of fuelwood that can affect plant growth and cause landcover variations especially in Nigeria, are highlighted in many articles (eg Siviconsult Ltd, 1991; Ite, 1995; Iliya and Mamman, 1996; Cline-Cole, 1997; Adamu, 2000; Ekanade, 2000b; Fadare, 2000; Falola, 2000; Iliya and Kwabe, 2000; Ijare and Daura, 2000).

7.5 The Generated Rainfall data and their validity

Raingauge data for much of Africa are very sparse, hence the efforts by international organisations such as NOAA, Climate Prediction Centre (CPC) and GPCC to provide satellite estimated rainfall (Thorne *et al,* 2001). However, rainfall is one of the most difficult variables to estimate accurately especially in a spatial context (Petty, 1995). While industrially developed countries of the world enjoy the benefit of raingauge networks across their countries, the construction of radar networks as well as satellite estimation of rainfall globally reduces the problems of ground observations of rainfall data for the developing nations like Nigeria. However, such satellite estimated data are mostly in gridded-point precipitation figures. This investigation provided a simple modelling technique for estimating spatial rainfall data from limited available precipitation data from such satellite estimated gridded-point rainfall for assessment of vegetation change. Validation of the estimated rainfall data with the originally acquired satellite estimated gridded-point precipitation data for all the years under study have shown a significant correlation at < 0.05 level. Although GPCC performed intercomparison studies for their gridded precipitation datasets from different sources (surface or satellite based observations) and has also applied its analysis for special studies, for example, the Oder river flooding in July 1997 and the El Niňo precipitation anomalies in winter 1997/98 (GPCC, 1998), the quality of the data is perhaps questionable. This is because data from different sources were initially merged together to create the gridded point dataset.

Many studies, based on the African sahel, suggest that the relationship between NDVI and rainfall can be described by a strong linear relationship, for example, (Malo and Nicholson 1990; Tucker *et al,* 1985; Justice *et al,* 1986; Tucker *et al,* 1991a; Milich and Weiss, 2000b).

This may not hold for all the African environments, and factors such as irrigation improve vegetation production. Thus, NDVI may be more important than rainfall (Millington *et al,* 1994), and it is these latter cases which are of primary interest here.

Although in this investigation annual rainfall data was utilised, such a relationship as shown by Millington *et al,* (1994) which used monthly rainfall data was also found to exist especially in the savanna areas of Nigeria, where NDVI profiles for irrigated and those for rainfed areas were markedly different (Figure 6.7). From what was derived in this investigation annual rather than monthly rainfall data should be used with caution especially if coarser spatial resolution dataset is to be used in an analysis with spatially estimated annual rainfall data. This is because firstly, the complete diurnal cycle of precipitation cannot be sampled with a single instrument such as those carried on meteorological satellites (Petty, 1995). Secondly, although the estimated annual rainfall data was derived at 1 km resolution and validated with the main satellite estimated data at < 0.05 level of significance, the data was first aggregated and resampled to 8 km spatial resolution before being used. Hence, the relationship between annual NDVI and rainfall datasets (Figure 6.15) for sites of numerically comparable change classes within the savanna and forest zones of the country have shown that there was no significant correlation at 95% level of confidence.

7.6   The Results from Image differencing technique

Simple subtractions of image datasets were performed in image differencing approach to detect changes caused by shifting cultivation in tropical moist forest (Singh, 1983), to monitor land-cover and land–use change (Green *et al,* 1994) and to detect general land

cover changes across China (Young and Wang, 2001). Results derived in this investigation using a similar approach showed that changes detected are highly generalised in some areas while in other areas there may be an underestimation of the results. This is because very serious events within a particular year when omitted in the procedure cannot be detected, and thus, can give an underestimation of changes detected. For example, there was a serious flood in 1988 along the Sokoto and Rima rivers in the northwest lowland areas of savanna region which destroyed many villages and farmlands. Although this investigation used a coarse spatial resolution data, if the base year data for the investigation was from 1988 and the averaging of these images included data for 1988 and 1989, it is most likely that such effects would be detected. Young and Wang, (2001) used a similar approach with similar coarse resolution data on a national scale investigation. The results from this investigation showed that it can only work in Nigeria if differencing of datasets are sequentially carried out, where data from the previous year is subtracted from the preceding year and so on. On the other, depending on what the investigation is aimed at, differencing of data should include all data for the specific period of study if the data for that year is available. For example, the trend of changes shown in Table 6.5 and Table 6.6 could be misleading. Hence, a useful development of this approach would be sequential differencing of complete data. This may show the correct magnitude of the effects for future plans due to recurring floods in those affected areas.

Studies that utilised high spatial resolution imagery such as aerial photos and Landsat MSS and TM (Kersten *et al,* 1998; Salami, 1999; Salami, *et al.,* 1999) have identified a high reduction of vegetation cover due to the incursion into the forest reserve areas in the south-western part of Nigeria, largely due to fuelwood gathering for domestic energy use and

agricultural activities such as burning and farm extensions by cocoa farmers. Results derived from this investigation with coarse resolution data using a simple differencing technique (Figure 6.2) also showed decline in NDVI. The overall results between the absolute and relative changed areas showed a significant correlation (R^2 = 99.3%) with decline in vegetation cover particularly in the southern forest zone.

Ite and Adams (1998) and Boele *et al* (2001a) used aerial photographs to detect land cover changes and linked the observed changes in the coastal areas and the south-east forest zones, in particular the Niger Delta area, to the activities of the Shell petroleum companies and other forms of land-use such as forest conversions. This also showed some correspondence with results obtained in this investigation using coarse spatial resolution imagery. For example, the preliminary assessment in Chapter 5 (Figure 5.6) indicated negative trends in the two southern forest sites. Secondly, not only the absolute change results in Figure 6.2a indicated strong signs of decline in NDVI, but even selected sites within the southern forest zone in Figure 6.7 also showed negative trends in the NDVI profile, suggesting that there was a decline in vegetation cover around those areas.

Such changes in the forests areas will have serious implications for the general ecosystems of the area. For example, Ite and Adams (1998) have shown that there are rare species, especially gorillas, around the south-east forest zone of Nigeria. Intensive agricultural activities and fuelwood gathering was shown to reduced the forest areas into pockets of unsustainable habitat for many plant and wildlife species (Ite, 1998). Boele *et al* (2001a) have shown that the Niger Delta is one of the world's largest wetlands covering over 20,000 square km. This area was said to contain enormous biodiversity including rare

species (Boele *et al* (2001a). Hence, without strict conservation and management of these different habitats, extinction becomes a serious threat to many species of plants and animals.

Based on the overall positive changes (Figure 6.2b and c) obtained in this investigation, image differencing approach has shown a strong correlation between the absolute (R^2 = 98.3), and the relative changes (R^2 = 97.4) in the lowland areas in the north-western and north-eastern savanna zones respectively, where there are some agreements with studies obtained from studies like Adams (1985), Adeniyi (1985) and Thomas and Adams (1997). However, the longer term change periods (ie the ten-year period covering 1986 to 1996 in Figure 6.2c and the 14-year period covering 1986 to 1999) showed more positive (increase in vegetation cover) changes in NDVI than the short-term change period covering 1986 to 1991. One reason that can be associated with the high negative changes in the first five-year period (Figure 6.2a) would be the application of this approach of change detection where selective end-point year images were merely subtracted or divided from one another and a simple round number class interval applied to the change images to indicate different change classes. On the other hand, three reasons could be liked to the high negative (decrease in vegetation cover) changes during the first 5-year period in the time series in the southern forested zone, particularly the coastal areas. Firstly, the effect of the ENSO phenomenon which was reflected in both the 1986/87 and 1991/92 annual mean images used in the differencing procedure. This is because there are similarities in troughs in the temporal NDVI profiles for those years affected by the World Net Primary Production (NPP) and Crop Production during the El-Niňo/Southern Oscillation periods. The results obtained by Ochi *et al,* (2000) which used 8 km NDVI data from PAL dataset have

indicated such effects (see Figure 2.2). Secondly, because of the location of this part of the country very close to the sea, both aerosol and atmospheric water vapour could be a contributing factor for such negative changes resulting to low NDVI values. Such atmospheric water vapour affecting NDVI especially in the coastal regions are also difficult to eliminate completely (Justice *et al,* 1991a). Thirdly, because NDVI from the PAL dataset were derived from the original 1 km LAC and 4 km GAC and resampled to 8 km resolution, it is most likely to suffer from misregistration of pixels. This could be another reason for such low NDVI values along the coastal regions of Nigeria as Figure 6.2a have shown.

The Image differencing approach used by Young and Wang (2001) was shown to reduce the skewing effect of abnormal climatic conditions. However, the results obtained in this investigation using a similar approach showed that despite further recomposition and averaging of the NDVI datasets, there were still troughs in the temporal profiles of NDVI data for the forest areas. This confirmed the view that there is high concentration of water vapour in the atmosphere around forest areas which can seriously affect NDVI data in such zones (Laporte *et al,* 1995; Lucas *et al,* 2000), and it is very difficult of correct (Justice *et al,* 1991). This suggests that very low peaks in NDVI temporal profiles observed in ENSO years may not necessarily be as a result of a general decline in biomass, but may also be as a result of persistent water vapour in the atmosphere especially in areas of dense forest cover.

7.7 The Results from Slope of change from Regression Technique

Because the whole annual mean NDVI dataset covering the time-series was utilised, results of long term positive (increase) and negative (decline) changes in vegetation cover across the whole of Nigeria from this approach gave a clearer view of areas where such changes occurred than the approach that used image differencing. However, though there are no similar studies that used slope of change approach from regression of time series NDVI for vegetation studies, pairwise comparison of individually classified NDVI and rainfall slope of change images (Figure 6.11) indicated that most of the combined areas of different associations in spatially changed areas are highly generalised. Hence, temporal profiles in Figure 6.12 demonstrated that spatial changes which fell in the same class in different vegetation zones across the country and represented on the same profile in Figure 6.12 may not necessarily be the case.

Although the temporal profiles (Figures 6.12 and 6.13) showed shallow gradients in NDVI due to the smoothing of the 8 km resolution data used in this investigation compared to what may be obtainable from studies with high spatial resolution data, they still indicated underlying changes in NDVI in different areas and for specific sites in different vegetation zones across Nigeria. Thus, total destruction of forest cover in small areas, for example, may result in gradual change in the 8 km resolution pixel, and the magnitude of the effect may depend on the size of the areas detected. On the other hand, gradual large-scale effects as a result of climatic change may be more representative within the 8 km pixel. The combination of such gradual and large-scale effects can therefore lead to a bigger change than anticipated.

Tucker *et al,* (1991) used mean annual NDVI from AVHRR and rainfall dataset covering the northern savanna areas of Nigeria and showed that annual variations in rainfall correspond to changes in vegetation cover. From this investigation individual sites from different climatic and vegetation zones across the country falling in the same numerically comparable change classes were selected and plotted on graphs (Figure 6.13). The general relationship between changes in NDVI (vegetation cover) and rainfall for those selected sites (Figure 6.15) showed no significant correlation between the decline in vegetation cover and increase in rainfall at $p < 0.05$ level. This suggest that factors other than climatic (rainfall) as shown by Millington *et al,* (1994) may be responsible for such long term decline in vegetation cover (See Table 7.1). By implication from such results, land mismanagement generally would seriously affect biodiversity across the country. This was reported by UNCED (1997). Hence, such results reflect, possibly, the different types of land-use in operation in such locations rather than what prevails generally in the broad area where a collective of individual pixels (sites) were represented in temporal profiles in Figure 6.12. As a result, unless mismanagement of the resources (vegetation) and the growing number of population checked this would continue to be an environmental issue in Nigeria.

Studies with high resolution data (Ekanade, 1987; Justice *et al,* 1997; Salami *et al,* 1999; Salami, 1999) observed that despite very little or no variation in rainfall within the south-west forest zone of Nigeria, there was evidence to suggest that the general decline in vegetation cover is not totally due to climatic influence, but mostly due to anthropogenic factors. In Chapter 3, examples of such anthropogenic influences on the general vegetation

Table 7.1 Some environmental and socio-economic factors which can affect plant growth and cause land-cover variations around the study area

Main ecological zones and other environmental divisions (including type of agroecosytems)	Causal factors
Sahel, Sudan and Guinea savanna zones (including rain-fed and irrigated cultivation around the river basins)	Rainfall variations Land degradation processes (including soil erosion, sand-dune encroachment, waterlogging and flooding) Woodland clearance, plant cover destruction (especially due to expansion of settlements and farmlands as well as fuelwood collection) Impact of agricultural projects (especially the expansion of the river basin irrigation systems) Crop pests Crop diseases
Forest savanna mosaic and montane zones (including rain-fed and irrigated cultivation around the river basins)	Land degradation processes (including soil erosion, water-logging and secondary salinisation and flooding) Deforestation (due to timber logging, fuel wood collection, farmland extension and construction) Impact of agricultural projects (especially the expansion of the river basin irrigation systems) Crop pests Crop diseases
Forest, coastal forest and mangrove zones (including incursions into forest reserve areas for agricultural and other purposes)	Land degradation processes (including soil erosion, water-logging and flooding, construction and oil exploration) Deforestation (due to timber logging, fuelwood collection, farmland extension and construction) Crop pests Crop diseases

Adapted and modified from Millington, *et al* (1994)

cover across Nigeria were shown. These include factors such as logging (see Figure 3.13), bush fires (see Figure 3.19), fuelwood gathering (see Figure 3.23), overgrazing and farmland extensions especially in the savanna zones (see Figure 3.10), soil erosion and flooding (see Figure 3.6) as well as construction and other land clearance (see Figure 3.20). When these types of different land-use activities are persistent over the years the regeneration of vegetation cover will seriously be affected. This can even affect the micro-climate of the area and this will in turn reflect on the general land-cover in the form of soil, rain and wind erosions (Indrabudi *et al,* 1998; Jaiyeoba, 1998; Osemeoba, 1988) (see Figure 3.6, Figure 3.7, and Figure 3.21). In the context of the 8 km resolution data, while individual small events may not be detected, cumulative effects may be detected.

From the results of both the image differencing and the regression techniques the general spatio-temporal changes suggest that there are more areas where vegetation cover has declined over the years than where there has been an increase. However, the overall changed areas where vegetation cover declined across the whole study area, particularly in areas of non-climatic influences is only about 7 % (1,544 land pixels) of the total land cover area (22,272 land pixels) at 8 km resolution under investigation. This is a very large area considering the spatial scale of the dataset used. These results, though of non-climatic influences, should not be related totally to anthropogenic influences because studies with NDVI data from AVHRR (Heute and Tucker, 1991) have shown that changes of vegetation cover detected from NDVI can be affected by soil conditions. Nicholson and Farrar (1994) and Farrar *et al,* (1994) on the other hand, have shown that the total productivity of vegetation as assessed by NDVI from AVHRR varies with location of vegetation and soil

type. A summary of both the inter-annual and inter-seasonal coefficients of variation in NDVI for selected areas monitored across Nigeria from the three different change detection approaches used in this investigation are given in able 7.2. However, the inter-annual coefficient of variation image in Figure 5.5 demonstrated clearly the different variations in vegetation cover across Nigeria. Different soil types of different moisture conditions within the northern savanna and the southern forest zones across Nigeria were clearly shown (Areola, 1982). Such variations in soil moisture condition may well affect changes in specific locations across different vegetation zones.

7.8 The results from Principal Component Analysis (PCA)

PCA was successful in isolating spatial change patterns. Results derived from spatio-temporal change patterns in NDVI covered seven component images which are relevant to the original objectives of this investigation and were chosen for interpretation.

The study around the lowland areas of the north-eastern part of Nigeria (Adams and Thomas, 1996) who used ancillary and field data has shown that the construction of dams within that region has improved the socio-economic status of the people in that area over the years. Adeniyi (1985) on the other hand, using Landsat MSS data has shown that, as a result of the construction of the Bakalori dam and the intensification of dryland irrigation farming in the north-western part of the country, there was an increase in vegetation cover around this savanna zone. This investigation with coarse resolution NDVI data from AVHRR has shown that there is a level of agreement with the results obtained by studies that utilised high spatial resolution dataset.

However, there are implications in the positive changes (increase in vegetation cover) from results derived using both the image differencing and PCA in areas like Lake Chad and the lowland areas in the savanna zone, and in particular, the Hadejia-Jama'are river basin in the north-east and possibly Sokoto Rima basin in the northwest. The savanna wetland areas in the northern part of Nigeria was reported to be a wetland area that serve as passage and wintering grounds for significant number of Palaearctic migrant birds such as waterfowl. The areas also serve as an important habitat for Afrotropical species (Stowe and Coulthard, 1990). Hence, any overuse or misuse of such vegetated lowland areas by the increasing population ignoring the need for planning and conservation of river basin ecology would consequently have an impact on the ecology of these savanna wetland areas.

Previous studies using PCA (Eastman and Fulk, 1993; Anyamba and Eastman, 1996; Hirosawa *et al,* 1996; Young and Wang, 2001) have shown that the first component image always shows a spatial pattern that indicates the characteristic value of vegetation biomass cover as represented by NDVI. Subsequent component images normally represent changes of decreasing magnitude. Although Anyamba and Eastman, (1996) and Young and Wang (2001) used data of similar spatial and temporal resolution, results derived from this investigation confirms this view because Component 1 image indicated a representative pattern which is typical of vegetation cover across Nigeria where the northern savanna vegetation is distinguished from the southern forest vegetation. On the other hand, the Component 2 image detected a cyclic pattern as indicated by the loading score, suggesting alternating dry and wet seasons across the country. This type of cyclic change pattern has previously been shown in an analysis on a continental scale with much coarser spatial resolution NDVI data from AVHRR (Eastman and Fulk, 1993).

Although the results shown on Component 3 image has similarities of cyclic change pattern it clearly differs from Component 2 image. The changes on Component 3 image suggests firstly, that the changes in the southerly location of the normal position (close to the sea) of the ITCZ in Nigeria from the southern forest zone to the semi-arid north (Ilesanmi, 1971) could have some variations in rainfall that can have positive impacts on the savanna vegetation. Secondly, different land use in operation across the country could also be the likely causes those spatial change patterns because there is more intensive dryland irrigation farming in the northern savanna than in the southern forest zone. This is in line with results obtained from the image differencing technique shown in Figure 6.2(a) and (b) in some areas. For example, pervious studies across Nigeria for example, have shown that different dryland agricultural activities in the northwestern lowland of the Savanna region (Adams, 1985; Adeniyi, 1985) and the lowland areas in the northeast (Thomas and Adams, 1996) was intensive. The results shown by this change pattern reflect such changes in vegetation cover from the northwest across to the northeast of the country because of the signs of positive (increase) in vegetation biomass cover. The graph in Figure 6.20 showing a site in the northeast, close to Lake Chad also indicates high NDVI values compared with the site in the Niger Delta. On the other hand, studies have also shown that there was serious destruction of vegetation cover in the southwest are of Nigeria (Adeniyi, 1980; Adejuwun and Adesina; Salami, 1999; Salami *et al.,* 1999) as a result of logging (see Figure 3.13) forest incursion for farm land extensions and fuel wood gathering. Most of these results corresponds with the results derived from image differencing (Figure 6.2) for example, the southern swamp forest (Boele, *et al.,* 2001a; Boele, *et al.,* 2001b), the moist tropical forest area (Ite, 1998; Ite and Adams, 1998). Hence, the high negative NDVI

anomaly patterns mostly in the southern forest zones and the Niger Delta area on Component 3 image. The trend in Figure 6.20b in particular, further confirms this decline in NDVI using the 1991- 1992 NDVI dataset for a site around this region close to Niger Delta.

The use Standardised principal components from PCA (Eastman and Fulk, 1993; Hirowasa *et al.,* 1996; Young and Wang, 2001) have also shown that some component images are likely to indicate trends that reflects NDVI anomaly due to artefacts of sensing mechanisms and the satellite itself. Although results from this investigation was also able indicate such trends, they do not correspond from component to component as in those results for different reasons. Firstly, Eastman and Fulk, (1993) analysed only three years monthly NDVI data of 10 minute spatial resolution acquired by AVHRR through NOAA-9 and NOAA-11 covering the whole of African Continent. Hirowasa *et al.,* 1996 analysed six years monthly NDVI data of about 1 km resolution acquired by AVHRR through NOAA-9 and NOAA-11 covering a limited geographic area in the State of Arizona, USA, while Young and Wang, (2001) analysed ten years annual mean NDVI data from the PAL dataset of 8 km resolution acquired by AVHRR through NOAA-7, NOAA-9 and NOAA-11 covering the whole of China. In this investigation covering Nigeria, monthly NDVI data for twelve years from the PAL dataset was used. The data has a spatial resolution of 8km and was acquired from NOAA-9, NOAA-11 and NOAA-14. Hence, even if the differences in other factors did not affect results from those studies, the fact that data used in the different investigations came from different satellites, certainly, this will affect the results of the different investigations. Thus, the spatial change patterns on Component 4, 6 and 8 images derived for this investigation showed different change patterns across the country which

suggest three distinct spatial changes as represented by a complex NDVI analysis covering Nigeria. In this investigation what the change pattern in Component 4 image suggests is that atmospheric dust is falsely represented with high NDVI values in specific locations in the northeast and low NDVI values in the southeast as a result of possible degradation of the AVHRR sensors. The floodland along rivers Gana and Hadejia which both flow into Lake Chad are very distinct from the intensively grazed and irrigated areas of the Chad Basin on Component 4 image. The spatial change patterns on this Component image for example, indicated more positive anomaly patterns in the northern Savanna than in the southern forest zones. However, although there are signs of positive anomalies in some areas in the southwest forest zone the area mostly affected with highest negative anomaly pattern is the dense forest area of Cameroon in the southeast of the component image. The graph of loading scores shows very high positive correlation with the image in the month of December of every year throughout the NDVI time series under investigation. Temporal profiles of NDVI data covering the period 1986 to 1999 for two sites, one in the Sahel and one in the tropical forest shown in Figure 6.22. suggest that the Sahel area and particularly around Lake Chad had two high NDVI peaks alternating in September and December or August and November of most of the years, while the tropical forest site had lower NDVI peaks in December than the Sahel site every year in the time series.

Although other data would be required to confirm this view, but the evidence in the NDVI data suggest that in December when almost all parts of the country is affected by the atmospheric hamattan dust of the Sahara, it is unrealistic to see that most areas across the country have high NDVI values in the month of December.

On the other hand, the dense tropical forest zone has less NDVI values than the Sahel site even in March or April. The high negative correlation in December for each year in the time series between the NDVI dataset and the Component 4 image as its graph of loading scores have shown points to strong negative NDVI anomaly in both the Savanna and the forest zones. But such effects from hamattan dust in the NDVI data leads to high NDVI values in the Sahel, while in the tropical dense forest area, the effect of the dust leads to lower NDVI values during this month. This type of anomaly pattern as a result of the effect of atmospheric dust corresponds with the view that the high reduction of the shorter red wavelengths of AVHRR sensor compared with the infrared wavelengths leads to a high vegetation index values in some areas (Eastman and Fulk, 1993; Cracknell, 1997).

Both Component 6 and 8 images generally, indicated a decline in vegetation biomass across the whole country as shown by NDVI. On the graph of loading scores of Component 6 image for example, it shows a curvelinear trend where NDVI across the country declined between 1986 and 1990 and then shows an increase between 1995 and 1999. However, there are signs of positive NDVI anomaly patterns around the Delta region generally including the coastal areas. The curvelinear trend on the whole component image (Figure 6.23) is reflected on the positive anomaly pattern in this region on the temporal profile covering NDVI data from 1986 to 1999 shown in Figure 6.24. It shows that from 1991 to 1993 the trend changed from decline in vegetation to increase between the 1995 to 1999 periods. However, the area with highest negative anomaly pattern in vegetation cover is located in the southeast forest zone which consistently shows a trend of decline in vegetation cover (Figure 6.24). Thus, most of the forest areas in the southeast and southwest were more affected with a decline in NDVI than other parts of the country.

The trend on Component 8 image shows a long term decline in vegetation biomass than Component 6 image, the graph of loading scores for Component 8 image indicated an opposite trend in the decline of vegetation biomass compared to Component 6 image across the country between 1990 and 1993. From the trend indicated by the loading scores, the correlation between the NDVI dataset and Component 8 image suggests that there was more vegetation vigour across the country between 1990 and 1993 and, particularly in the south central part of the country. There was less vegetation vigour on Component 6 image around these areas during the same period. On the other hand, there was more decline in vegetation biomass between 1995 and 1999 as Component 8 image has shown than there was on Component 6 image during this period. The areas most affected in the decline in vegetation cover on Component 8 image are located in the coastal regions. These are also reflected on the temporal NDVI profile covering these years (Figure 6.26).

The curvelinear trend as shown on Component 6 image may also be indicative of small anomaly as a result of the switch between NOAA-9, NOAA-11 and NOAA-14 which acquired the data used in this investigation because small magnitude of spatial changes in NDVI are shown to affect large areas (Eastaman and Fulk, 1993). However, although the switch in the dataset between satellites that carries the AVHRR sensors may have little effects with drops in NDVI values for most areas generally, this will not be dramatic ([1]Smith, 2001, personal communication, see Appendix 4). Large effects of spatial changes in most cases appear on the last component images if such effects cover small places on the spatial area being analysed in PCA (Eastman and Fulk, 1993).

---

[1] Peter Smith is with NASA and he is part of the NOAA/NASA Pathfinder Land Dataset processing team.

With regards to Component 80 image, this explains less that 0.1 per cent of the total variation in the 144 monthly NDVI dataset used in the PCA procedure.

Studies with time series NDVI data using standardized PCA showed that what remains in the much later component images are very localized events and random noise (Eastman and Fulk,1993; Anyamba and Eastman, 1996; Li and Kafatos, 2000). Based on the concentration of negative anomaly patterns in pocket locations on component 80 image, it is possible to suggest that such anomaly patterns are likely to be related to very localized events rather than random noise. Although it is not very clear what caused these anomalies, the graph of loadings for this component image shows that most of the significant anomalies are during the strong 1997/98 El Niño and cold 1998/999 La Niña periods. However, certain vector diseases such as animal trypanasomiasis and malaria for example, are said to be linked with anomalies in time-series NDVI due to very high or very low rainfall (Linthicum *et al.,* 1999).

Although there are few locations in the northern savanna areas affected with the pockets of negative anomaly on component 80 image, most of the areas affected with both negative and positive anomaly are located in the southern Guinea savanna and the southern forested areas (see Figure 6.28). The temporal profile of NDVI data of areas with strong anomalies covering the ENSO periods between 1997 to 1999 for selected sites representing the southern forest areas in Figure 6.29 *(a)* and the Northern Savanna sites in *(b)* suggest that most of the reserve areas in the northern and southern parts of the country are alternately affected both during the warm ENSO period of 1997/98 and the cold ENSO phase of 1998/99. Although there are other parts in the northern savanna reserve areas affected by

some positive NDVI anomalies on this component image, the area that had the highest positive NDVI anomaly especially during the ENSO cold phase of 1998/99 periods is located in the southern part of Ondo state in the southwest. The concentration of locally affected areas suggest that most of the pockets of negative anomaly patterns are either around Montane, reserve or agriculturally productive areas of the country which are affected during the ENSO phenomenon.

Varying climatic conditions related to ENSO events are now becoming risks to both humans and animals based on recent health studies linked to climate variability, landuse and global climatic change (Sutherst, 1998; Linthicum, *et al.,* 1999; Patz *et al.,* 2000; Anyamba *et al.,* 2002). For example, the habitat of parasites of most human and animal diseases are said to be located in vegetated areas (Patz *et al.,* 2000; Patz, 2001). It was also shown that the world's most prevalent and serious vector-borne diseases, malaria, clearly responds to climatic fluctuations (Patz and Reisen, 2001). Hence, dense forest areas and forest edges can be associated with habitat of both animal and human vector diseases.

In Nigeria, the outbreaks of most animal related diseases are reported to have occurred in areas dominated by savanna, montane and rain forest vegetation zones as well as seasonally flooded areas such as water courses, ponds, reservoirs and lakes (Kalu. 1995; Anene *et al.,* 1991). This also suggest that such outbreaks must have occurred following periods of above or below normal rainfall.

The temporal profile of annual mean rainfall of the selected anomaly sites on component 80 in illustrated in Figure 6.30 further suggest that, relative to the location of the selected sites

in two distinct vegetation zones of Nigeria, the northern savanna sites had low rainfall during the warm ENSO phase in 1987 followed by high rainfall in the cold ENSO phase of 1988. During these periods, high mortality of animals were reported in the northeastern part of Nigeria (Alaku and Moruppa, 1993) due to prevalence of animal tuberculosis between the rainy and Harmattan seasons. Furthermore, a study across the Sudano-sahelina vegetation zone (White, 1983) of Nigeria covering the northern states of Sokoto (which included Zamfara state at that time), Bauchi, Borno and Adamawa showed that in 1997 there was an outbreak of a contagious bovine pleuroneumonia (CBPP) diseases with a serious outbreak and high mortality in cattle in the 1990 outbreaks (Aliyu *et al.* 2000). Hence, the same selected sites in the northern savanna vegetation zone had less rainfall during the Cold ENSO period in 1990 and the warn ENSO phase of 1997 but experienced high rainfall in the 1998 cold phase. In the southern forest vegetation zone of what the profile suggest in Figure 6.30(a) is that during the warm phase of 1997/98 ENSO period, these forest sites had high rainfall followed by some form of drought during the cold ENSO phase in 1998.

Most animals especially cattle are concentrated in the northern part of the country and mostly owned by the Fulani nomadic herders (Bourn *et al,* 1994). These nomadic herders move for long distances from the northern part of the country in the dry season to the southern forest areas in search of greener pastures. During this movement periods they enhance the spread of most animal related diseases in Nigeria (Aliyu *et al.,* 2000). Matola *et al*, (1987) on the other hand have shown that there is a link between malaria transmission and the montane vegetated areas while Patz et al, (2000) have shown that when there is deforestation and vegetation is replaced by tall crops such as cocoa, coffee, oil palms,

rubber plantations and other agricultural crops, it provides comfortable habitats for tsetse-flies colonization. Hence, many of the pockets anomaly change patterns around Omo forest reserve in the south-west forest region on Nigeria can be seen on Figure 6.28. These are areas where cases of deforestation due to agricultural activities and fuelwood gathering was reported (eg Kersten *et al,* 1998; Salami *et al*, 1999). Hence, it is most likely to suggest that the anomalies on component 80 image may have certain links with disease related events due to changing weather conditions which can have impact on vegetation cover. However, further localised environmental data particularly from those affected areas would be required to ascertain the causes of such negative change patterns in vegetation and land-cover.

Vegetation is generally shown to be the most representative of ecosystems on this planet (Mather *et al,* 1998; Meyer and Turner, 1992) because they are essential resources for the sustainable development of human society and also due to their economic and environmental value. However, according to this investigation PCA has shown that the areas with high negative long term change (decline) in vegetation cover are located in the south-east forest zone. This area showed a trend of more consistent decline in vegetation cover (see Figure 6.23 and Figure 6.24) than other parts of the country.

One other efficiency of PCA as an approach for detecting spatial change patterns compared to the other two approaches (image differencing and slope of change from regression) used in this investigation is that even the last component image that has a legacy of noise detected meaningful information. For example, some pockets of negative spatial change patterns located approximately in reserve areas both in the savanna and forest zones were detected by the PCA (see Figure 6.28). This is not possible using the SID and SCR

techniques for change detection. Such negative change patterns are likely to be related to very localised events which could have links with changes in vegetation across Nigeria. Although it is not very clear what caused such negative change patterns, studies with time-series NDVI data (Linthicum *et al,* 1999) have shown that as a result of very high or very low rainfall certain habitats of animals and other species can be affected.

In most of the sites selected for examination from all the three change detection techniques used, areas around the coastal swamp forest, particularly the Niger Delta, showed a consistent decline in NDVI over the years. Similar changes were also observed using the special UN/FAO 8 km coarse resolution AVHRR data. However, the negative and positive changes in general vegetation cover across Nigeria identified by this investigation with similar coarse resolution NDVI data cannot be conclusive and ascribed totally to anthropogenic influences without further verifications using ground truth and other published information as Justice *et al,* (1985) have shown. However, inference can still be drawn that the negative changes (decline in vegetation cover) result from non-climatic influences and can be linked to deforestation or crop failure. On the other hand, the positive changes resulting from increase in vegetation cover can be linked to climatic influences and inference can be made that such changes may be as result of man's positive influence on the land cover as result of reforestation or agricultural production etc.

From the summary of the inter-seasonal and inter-annual coefficient variation of NDVI of the selected and monitored sites from the three different change detection approaches, shown in Table 7.2., it appeared that some locations (sites) in the northern savanna vegetation zones across the country have lower inter-annual/seasonal coefficient of

variation in NDVI than the south-west or south-east forested zones of the country. Although the inter-annual coefficient of variation image in Figure 5.5(b) showed that majority of this variations are concentrated in the south forest zone, the majority of high variations in the inter-seasonal coefficient of variation in NDVI (see Appendix 8) are concentrated in the northern savanna zone. The most conclusive evidence, however, regarding ecological impacts in those selected sites and in particular, the Niger Delta and Lake Chad areas, are reflected in Figure 5.5(*b*) and indicated in Table 7.2. The results summarised in Table 7.2 showed that Niger Delta area has the highest values of inter-seasonal and inter-annual coefficient variation in NDVI, followed by the south-west forest zone around Lagos area. A particular site in the Niger Delta area that was monitored both in the simple image differencing (SID) and PCA techniques had a 19% and 16% inter-seasonal and inter-annual coefficient of variations in NDVI respectively. On the other hand, sites monitored on component 80 image from the vegetated or reserved areas in the northern savanna and southern forest zones suspected to have links with environmental change events which can be related to changes in vegetation cover showed that the two sites (Borgu forest reserve in the north-west and Yankari game reserve in the north-east) in the northern savanna zone, have higher inter-seasonal and inter-annual coefficient of variations than the sites in the southern forest zones (Table 7.2).

When changes in landuse seen to affect vegetation cover are checked using strict management and conservation policies, the issue of population growth should equally be addressed very carefully otherwise the persistent decline in vegetation cover will continue to be an environmental issue for Nigeria.

Table 7.2 Summary of Inter-annual and Inter-seasonal Coefficient of Variation in NDVI of selected sites monitored using the different change detection techniques

Change Detection Approach Utilised	Selected assessed areas	Inter Annual Coefficient of Variation (%)	Inter-Seasonal Coefficient of Variation (%)
Simple Image Differencing (SID)	Site in Niger Delta area (< -31 Class)	16	19
	Site around Lagos area (< -31 Class)	14	17
	Site in the Cocoa Belt of South-west Forest area (Class -11 to -6)	3	8
	Montane site around Jos Plateau (Class -6 to -1)	2	8
	Hadejia-Jama'are site in the North-east savanna (Class -1 to 4)	5	8
	Site north of Lake Chad in the sahel (Class >34)	10	11
Slope of Change from Regression (SCR)	Sudan Savanna site in the north-west (Class1:1)	1	5
	Sahel site in the north-east (Class 2:2)	1	3
	Forest site in the south-west (3:3)	2	8
	Montane site in the central area (Class 4:4)	2	9
	Dense Humid Forest site in the south-east (Class 5:5)	2	5

Table 7.2 (*Cont.*) Summary of Inter annual and Inter-seasonal Coefficient of Variation in NDVI of selected sites monitored using the different change detection techniques

Change Detection Approach Utilised	Selected assessed areas	Inter Annual Coefficient of Variation (%)	Inter-Seasonal Coefficient of Variation (%)
Principal Component Analysis (PCA)	**Comp 2 Image** (Neg. anomaly – south-east site) Cross River State	4	12
	(Neg. anomaly – south-west site) Delta state	4	10
	Comp 3 Image (Pos. anomaly) Lake Chad site	2	10
	(Neg. anomaly) Niger Delta site	13	19
	Comp 4 Image (Pos. anomaly) A site south of Lake Chad in Borno state	2	10
	(Neg. anomaly) A forest site in the south-east site in Cameroon	2	9
	Comp 6 Image (Neg. anomaly - Southeast site) in Cross River state	5	11
	(Pos. anomaly) Niger Delta site	16	19
	Comp 8 Image (Pos. anomaly) Niger Delta site	16	19
	(Neg. anomaly) Lake Chad site	10	11

Table 7.2 (*Cont.*) Summary of Inter-annual and Inter-seasonal Coefficient of Variation in NDVI of selected sites monitored using the different change detection techniques

Change Detection Approach Utilised	Selected assessed areas	Inter Annual Coefficient of Variation (%)	Inter-Seasonal Coefficient of Variation (%)
Principal Component Analysis (PCA)	**Comp 80 Image Southern Forest Zone** (Neg. anomaly) Okomu Forest reserve in Delta State	4	8
	(Neg. anomaly) Oban National Park in the South-east	4	10
	(Neg. anomaly) Omo Forest reserve - western Nigeria	2	8
	(Pos. anomaly) Forest Site in Ondo State	4	8
	Northern Savanna Zone (Neg. anomaly) Borgu Forest Reserve - around Kainji Lake	10	14
	(Neg. anomaly) Yankari Game Reserve in Bauchi State	3	11
	(Neg. anomaly) Zamfara Range Land in the north-west	1	5
	(Neg. anomaly) Baturiya Forest Reserve in Kano State	1	7

In Chapter Eight the final conclusions are presented with a summary and recommendations based on the findings from the study.

CHAPTER EIGHT

CONCLUSIONS AND RECOMMENDATIONS

8.1   Introduction

This chapter presents the conclusions arising from the investigation and assessment of vegetation and land cover change across Nigeria using coarse spatial but high temporal resolution AVHRR-NDVI data from the PAL dataset. The first section outline the conclusions that emerged from the investigation. In the second section of the chapter recommendations for further work are outlined.

8.2   Conclusions

This investigation set out on three main objectives:

1.   Assess temporal changes in vegetation cover in absolute and relative terms across Nigeria from multi-temporal NDVI data.

2.   Develop a spatial model of precipitation for Nigeria based on coarse resolution rainfall estimates and other environmental variables.

3.   Use the modelled rainfall data and the NDVI data-set to identify and explain areas of change in vegetation and land-cover across Nigeria.

From these objectives conclusions were that :

a). The PAL dataset has the capability of mapping NDVI change.

b). It is sufficiently sensitive to pick out major changes that could influence an 8 km pixel or general slight large scale changes related to climatic change.

c). It is not generally possible to identify the causes and spatial scales within an 8 km pixel though spatial context may aid interpretation.

The first objective was to assess temporal changes in vegetation cover in absolute and relative terms across Nigeria with coarse resolution AVHRR-NDVI data. The simple image differencing technique was first attempted to tackle the first hypothesis where selective annual mean NDVI dataset were utilised. Potential areas of change in vegetation cover within short- and long-term periods across the whole of Nigeria were derived. The investigation demonstrated that it is a quick and simple approach of obtaining information about changes in vegetation cover that are potentially at risk, particularly if the objective is not to classify specific types of land-cover which have changed. However, results from this approach should be used with caution because it gives a highly generalised picture of areas that have changed in vegetation cover.

On the other hand, the use of selective annual mean dataset to derive absolute and relative change information across Nigeria had implications. For example, because the start and end- point dates of the annual mean images used in simple image differencing fall within ENSO warm and cold phases most of the positive changes (increase in vegetation biomass) are prominent in the northern savanna zones, more particularly along the river basins than

in the southern forest zones for the long-term assessment period. Most of the negative changes (decrease in vegetation biomass) in the short-term period, on the other hand, are prominent in the southern forest zones than in the northern savanna zones. This relates to the fact that intensive irrigation farming in the lowland savanna zones contributed to the overall vegetation biomass cover in those areas. On the other hand, the southern forest zone is more sensitive to climatic change that is connected to the ENSO phenomenon at the spatial scale of the PAL-NDVI data. Although the approach used for assessing the short- and long-term absolute changes utilised annual mean datasets which captured average productivity over a single year and end-point years, it reduced the problem of capturing vegetation at different phenological cycles.

The second objective was to develop a spatial model for estimating rainfall across Nigeria from coarse resolution precipitation data. Because raingauges across developing countries like Nigeria are rare, rainfall data from Nigeria in particular are difficult to obtain and sometimes very unreliable due to administrative lapses. As satellite estimated precipitation data covering the globe are now being made available on a grid-point format, this investigation demonstrated an approach where polynomials could be applied to create simple models for generating spatial rainfall data from coarse resolution satellite estimated gridded-point precipitation data. The spatially derived data can be validated with the original data obtained from the satellite estimated data or rainfall data obtained directly from raingauge stations across a country or locality.

The third objective was to use the modelled rainfall data and the NDVI data-set to identify and explain areas of change in vegetation and land-cover across Nigeria Achieving these

objectives entailed many procedures and was time-consuming. However, the investigation has shown that long-term changes (increase or decrease) in vegetation cover can be detected and isolated in areas of increase or decrease in rainfall. The investigation further revealed that cross-classified areas of long- term changes of individually classified annual NDVI and rainfall dataset would give a highly generalised picture of specific areas within the savanna and forest vegetation zones. This is because, firstly, the rate of change of rainfall within the savanna and forest areas are shown to be significantly different over the time period under investigation. Secondly, there are different types of landuse in operation in specific areas within these different vegetation zones despite changes in rainfall. In general there was more rapid increase in vegetation biomass cover in the savanna than in the forest vegetation zones given the rate of change in rainfall.

Spatial change patterns which were derived as a result of multi-temporal NDVI analysis revealed that they relate to both climatic and non-climatic induced changes across the whole of Nigeria. The investigation indicated that even in the absence of climatic data such as rainfall, monthly MVC-NDVI data from AVHRR can be utilised to assess spatio-temporal changes in vegetation cover within the framework of PCA using principal standardised components. Temporal profiles of monthly NDVI-MVCs or a combination of annual mean NDVI and rainfall datasets have shown that climatic effects that can be linked to the ENSO phenomenon are much easier identified within the southern forest zones which contains evergreen vegetation than in the northern savanna zones. Furthermore, substantial areas with high coefficient of variation in NDVI are concentrated in the southern forest zones while the majority of areas with high inter-seasonal NDVI are located in the northern sananna area.

The investigation further demonstrated that from spatio-temporal analysis of monthly MVC-NDVI undertaken within the framework of PCA one of the low signal-to-noise ratio component images was able to identify spatial change patterns around specific reserve areas across Nigeria which can be linked to localised changes in vegetation cover. However, because the spatial scale of the data used in this investigation was able to capture broad areas of change, high spatial resolution data and ancillary information are required to investigate those specific areas in order to ascertain the causes of the localised changes detected.

The overall results demonstrated that AVHRR-NDVI data has the potential of being used periodically to detect changes in vegetation cover across a whole nation particularly for countries with very low economic status like Nigeria. The changes detected particularly from PCA can be used as a provisional working document for further studies on vulnerable areas and for better management of the ecological sustainability of the country concerned.

Although the general results derived from this investigation are not validated or incorporated in any systematic procedure such as inclusion of ground truth and ancillary information within a GIS, it demonstrated further the potential of AVHRR-NDVI data from AVHRR for monitoring vegetation across Nigeria in particular, and for other countries that cannot afford expensive high spatial resolution satellite data.

8.3   Recommendations for Further Work

This investigation provided a provisional result that can be used for specific purposes or for further investigation with high spatial resolution satellite data in order to assess temporal changes in vegetation and land cover across Nigeria. The following suggestions can be taken on board for future studies across the country.

For better results to be derived from using dekadal NDVI data acquired from the PAL dataset, they should be recomposed into monthly and annual mean datasets before analysis commences. Since the problems of AVHRR data have not been completely solved, periodic checks on the data source or archives should be made at regular intervals during the use of the data for any information related to data revision due to changes in calibrations and computations.

Since the overall aim of this investigation was to obtain a broad picture of changes in vegetation cover across Nigeria, what was obtained particularly with the slope of change from regression technique using pairwise comparison of NDVI and rainfall cannot be conclusive. This is because not only actual climatic (rainfall) data directly from raingauge stations within the study area were not utilised to validate the derived rainfall datasets, but other environmental data like soil information and temperature were not incorporated into the GIS analysis. Later studies should consider these factors and also incorporate the use of current available vegetation maps together with other ancillary information. Data for several years should also be utilised in order to overcome yearly climatic variations.

Analysis of the rainfall data across the country would also provide information on areas where rainfall is changing.

Results derived from SCR emphasised the negative (decline) aspect of changes in vegetation cover and positive (increase) changes in rainfall across Nigeria. Later studies should focus on the opposite side of this assessment so that the two ways can be compared in order to arrive at more conclusive results.

Where local climatic data (rainfall) have to be spatially estimated using regression models, mean monthly climatic data should be derived using similar simple or more complex models, rather than mean annual. This is because estimated monthly mean rainfall data will enable a more efficient assessment of inter-seasonal changes in vegetation when used together with the monthly NDVI-MVCs. It is also possible to obtain better correlations between monthly NDVI-MVCs and the mean rainfall figures.

Given the cost of other remotely sensed imagery used for studies in specific areas in Nigeria, the value of the approach using AVHRR-NDVI from the PAL dataset to assess vegetation cover change across the whole country has been demonstrated from this investigation. This could be a useful approach to identify those areas at risk. Vulnerable areas which changed from one particular period to another could further be investigated first using a 1 km AVHRR data which has better spatial resolution and is also very cheap. For more detailed information on the vulnerable areas very little of such expensive imagery, and particularly, the new very high spatial IKONOS imagery could then be used.

It would also be desirable if a broad map of general vegetation cover of the country could be produced periodically using coarse resolution AVHRR-NDVI from the PAL dataset.

For both the economic and ecological sustainability of the country, a sustainable land management system should be established where there would be a collective effort between authorities and local people, and in particular, the peasant farmers and community leaders in rural areas. Strict policies on land use generally could be formulated, with monitoring and activities such as environmental awareness for the rural sector on the consequences of overuse/misuse of land resources and in particular woodlands and forests. The country should explore the feasibility of utilising its petroleum resources to provide accessible and affordable energy such as gas for domestic and other use. This will go a long way in reducing pressure on the vegetated surfaces by the growing population particularly in forest areas for fuelwood.

APPENDICES

APPENDIX 1a

Sample Macro command written in IDRISI-32 GIS Software for converting the original 1995 AVHRR-NDVI data in Band Interleaved-by-Line (BIL) format from the PAL Dataset archive into separate raster images.

```
BILIDRIS  x avhrrpf.ndvi.1ntfaf.950101.27017059*Jan
951*1*174*138*latlong.ref*deg*1.995833*14.00416*4.145873*14.00417*1.0*1*0*8
CONVERT x Jan 9511.rst*Jan 951.rst*I*2*2*2

BILIDRIS  x avhrrpf.ndvi.1ntfaf.950111.27017059*Jan
952*1*174*138*latlong.ref*deg*1.995833*14.00416*4.145873*14.00417*1.0*1*0*8
CONVERT x Jan 9521.rst*Jan 952.rst*I*2*2*2

BILIDRIS  x avhrrpf.ndvi.1ntfaf.950121.27017059*Jan
953*1*174*138*latlong.ref*deg*1.995833*14.00416*4.145873*14.00417*1.0*1*0*8
CONVERT x Jan 9531.rst*Jan 953.rst*I*2*2*2

BILIDRIS  x avhrrpf.ndvi.1ntfaf.950201.27017059*Feb
951*1*174*138*latlong.ref*deg*1.995833*14.00416*4.145873*14.00417*1.0*1*0*8
CONVERT x Feb 9511.rst*Feb 951.rst*I*2*2*2

BILIDRIS  x avhrrpf.ndvi.1ntfaf.950211.27017059*Feb
952*1*174*138*latlong.ref*deg*1.995833*14.00416*4.145873*14.00417*1.0*1*0*8
CONVERT x Feb 9521.rst*Feb 952.rst*I*2*2*2

BILIDRIS  x avhrrpf.ndvi.1ntfaf.950221.27017059*Feb
953*1*174*138*latlong.ref*deg*1.995833*14.00416*4.145873*14.00417*1.0*1*0*8
CONVERT x Feb 9531.rst*Feb 953.rst*I*2*2*2

BILIDRIS  x avhrrpf.ndvi.1ntfaf.950301.27017059*Mar
951*1*174*138*latlong.ref*deg*1.995833*14.00416*4.145873*14.00417*1.0*1*0*8
CONVERT x Mar 9511.rst*Mar 951.rst*I*2*2*2

BILIDRIS  x avhrrpf.ndvi.1ntfaf.950311.27017059*Mar
952*1*174*138*latlong.ref*deg*1.995833*14.00416*4.145873*14.00417*1.0*1*0*8
CONVERT x Mar 9521.rst*Mar 952.rst*I*2*2*2

BILIDRIS  x avhrrpf.ndvi.1ntfaf.950321.27017059*Mar
953*1*174*138*latlong.ref*deg*1.995833*14.00416*4.145873*14.00417*1.0*1*0*8
CONVERT x Mar 9531.rst*Mar 953.rst*I*2*2*2

BILIDRIS  x avhrrpf.ndvi.1ntfaf.950401.27017059*Apr
951*1*174*138*latlong.ref*deg*1.995833*14.00416*4.145873*14.00417*1.0*1*0*8
CONVERT x Apr 9511.rst*Apr 951.rst*I*2*2*2

BILIDRIS  x avhrrpf.ndvi.1ntfaf.950411.27017059*Apr
952*1*174*138*latlong.ref*deg*1.995833*14.00416*4.145873*14.00417*1.0*1*0*8
CONVERT x Apr 9521.rst*Apr 952.rst*I*2*2*2

BILIDRIS  x avhrrpf.ndvi.1ntfaf.950421.27017059*Apr
953*1*174*138*latlong.ref*deg*1.995833*14.00416*4.145873*14.00417*1.0*1*0*8
CONVERT x Apr 9531.rst*Apr 953.rst*I*2*2*2
```

APPENDIX 1a (Cont.)

Sample Macro command for converting Band Interleaved-by-Line (BIL) data format into separate raster images

```
BILIDRIS  x avhrrpf.ndvi.1ntfaf.950501.27017059*May
951*1*174*138*latlong.ref*deg*1.995833*14.00416*4.145873*14.00417*1.0*1*0*8
CONVERT x May 9511.rst*May 951.rst*I*2*2*2

BILIDRIS  x avhrrpf.ndvi.1ntfaf.950511.27017059*May
952*1*174*138*latlong.ref*deg*1.995833*14.00416*4.145873*14.00417*1.0*1*0*8
CONVERT x May 9521.rst*May 952.rst*I*2*2*2

BILIDRIS  x avhrrpf.ndvi.1ntfaf.950521.27017059*May
953*1*174*138*latlong.ref*deg*1.995833*14.00416*4.145873*14.00417*1.0*1*0*8
CONVERT x May 9531.rst*May 953.rst*I*2*2*2

BILIDRIS  x avhrrpf.ndvi.1ntfaf.950601.27017059*Jun
951*1*174*138*latlong.ref*deg*1.995833*14.00416*4.145873*14.00417*1.0*1*0*8
CONVERT x Jun 9511.rst*Jun 951.rst*I*2*2*2

BILIDRIS  x avhrrpf.ndvi.1ntfaf.950611.27017059*Jun
952*1*174*138*latlong.ref*deg*1.995833*14.00416*4.145873*14.00417*1.0*1*0*8
CONVERT x Jun 9521.rst*Jun 952.rst*I*2*2*2

BILIDRIS  x avhrrpf.ndvi.1ntfaf.950621.27017059*Jun
953*1*174*138*latlong.ref*deg*1.995833*14.00416*4.145873*14.00417*1.0*1*0*8
CONVERT x Jun 9531.rst*Jun 953.rst*I*2*2*2

BILIDRIS  x avhrrpf.ndvi.1ntfaf.950701.27017059*Jul
951*1*174*138*latlong.ref*deg*1.995833*14.00416*4.145873*14.00417*1.0*1*0*8
CONVERT x Jul 9511.rst*Jul 951.rst*I*2*2*2

BILIDRIS  x avhrrpf.ndvi.1ntfaf.950711.27017059*Jul
952*1*174*138*latlong.ref*deg*1.995833*14.00416*4.145873*14.00417*1.0*1*0*8
CONVERT x Jul 9521.rst*Jul 952.rst*I*2*2*2

BILIDRIS  x avhrrpf.ndvi.1ntfaf.950721.27017059*Jul
953*1*174*138*latlong.ref*deg*1.995833*14.00416*4.145873*14.00417*1.0*1*0*8
CONVERT x Jul 9531.rst*Jul 953.rst*I*2*2*2

BILIDRIS  x avhrrpf.ndvi.1ntfaf.950801.27017059*Aug
951*1*174*138*latlong.ref*deg*1.995833*14.00416*4.145873*14.00417*1.0*1*0*8
CONVERT x Aug 9511.rst*Aug 951.rst*I*2*2*2

BILIDRIS  x avhrrpf.ndvi.1ntfaf.950811.27017059*Aug
952*1*174*138*latlong.ref*deg*1.995833*14.00416*4.145873*14.00417*1.0*1*0*8
CONVERT x Aug 9521.rst*Aug 952.rst*I*2*2*2

BILIDRIS  x avhrrpf.ndvi.1ntfaf.950821.27017059*Aug
953*1*174*138*latlong.ref*deg*1.995833*14.00416*4.145873*14.00417*1.0*1*0*8
CONVERT x Aug 9531.rst*Aug 953.rst*I*2*2*2
```

APPENDIX 1a (Cont.)
Sample Macro command for converting Band Interleaved-by-Line (BIL) data format into separate raster images

```
BILIDRIS  x avhrrpf.ndvi.1ntfaf.950901.27017059*Sept
951*1*174*138*latlong.ref*deg*1.995833*14.00416*4.145873*14.00417*1.0*1*0*8
CONVERT x Sept 9511.rst*Sept 951.rst*I*2*2*2

BILIDRIS  x avhrrpf.ndvi.1ntfaf.950911.27017059*Sept
952*1*174*138*latlong.ref*deg*1.995833*14.00416*4.145873*14.00417*1.0*1*0*8
CONVERT x Sept 9521.rst*Sept 952.rst*I*2*2*2

BILIDRIS  x avhrrpf.ndvi.1ntfaf.950921.27017059*Sept
953*1*174*138*latlong.ref*deg*1.995833*14.00416*4.145873*14.00417*1.0*1*0*8
CONVERT x Sept 9531.rst*Sept 953.rst*I*2*2*2

BILIDRIS  x avhrrpf.ndvi.1ntfaf.951001.27017059*Oct
951*1*174*138*latlong.ref*deg*1.995833*14.00416*4.145873*14.00417*1.0*1*0*8
CONVERT x Oct 9511.rst*Oct 951.rst*I*2*2*2

BILIDRIS  x avhrrpf.ndvi.1ntfaf.951011.27017059*Oct
952*1*174*138*latlong.ref*deg*1.995833*14.00416*4.145873*14.00417*1.0*1*0*8
CONVERT x Oct 9521.rst*Oct 952.rst*I*2*2*2

BILIDRIS  x avhrrpf.ndvi.1ntfaf.951021.27017059*Oct
953*1*174*138*latlong.ref*deg*1.995833*14.00416*4.145873*14.00417*1.0*1*0*8
CONVERT x Oct 9531.rst*Oct 953.rst*I*2*2*2

BILIDRIS  x avhrrpf.ndvi.1ntfaf.951101.27017059*Nov
951*1*174*138*latlong.ref*deg*1.995833*14.00416*4.145873*14.00417*1.0*1*0*8
CONVERT x Nov 9511.rst*Nov 951.rst*I*2*2*2

BILIDRIS  x avhrrpf.ndvi.1ntfaf.951111.27017059*Nov
952*1*174*138*latlong.ref*deg*1.995833*14.00416*4.145873*14.00417*1.0*1*0*8
CONVERT x Nov 9521.rst*Nov 952.rst*I*2*2*2

BILIDRIS  x avhrrpf.ndvi.1ntfaf.951121.27017059*Nov
953*1*174*138*latlong.ref*deg*1.995833*14.00416*4.145873*14.00417*1.0*1*0*8
CONVERT x Nov 9531.rst*Nov 953.rst*I*2*2*2

BILIDRIS  x avhrrpf.ndvi.1ntfaf.951201.27017059*Dec
951*1*174*138*latlong.ref*deg*1.995833*14.00416*4.145873*14.00417*1.0*1*0*8
CONVERT x Dec 9511.rst*Dec 951.rst*I*2*2*2

BILIDRIS  x avhrrpf.ndvi.1ntfaf.951211.27017059*Dec
952*1*174*138*latlong.ref*deg*1.995833*14.00416*4.145873*14.00417*1.0*1*0*8
CONVERT x Dec 9521.rst*Dec 951.rst*I*2*2*2

BILIDRIS  x avhrrpf.ndvi.1ntfaf.951221.27017059*Dec
953*1*174*138*latlong.ref*deg*1.995833*14.00416*4.145873*14.00417*1.0*1*0*8
CONVERT x Dec 9531.rst*Dec 953.rst*I*2*2*2
```

APPENDIX 1b

Sample Macro command written in IDRISI-32 GIS Software   to converting the original 1995 AVHRR-NDVI raster images into ASCII format.

```
CONVERT  x Jan 951.rst*Jan 951.rst*I*1*1*2
CONVERT  x Jan 952.rst*Jan 952.rst*I*1*1*2
CONVERT  x Jan 953.rst*Jan 953.rst*I*1*1*2
CONVERT  x Feb 951.rst*Feb 951.rst*I*1*1*2
CONVERT  x Feb 952.rst*Feb 952.rst*I*1*1*2
CONVERT  x Feb 953.rst*Feb 953.rst*I*1*1*2
CONVERT  x Mar 951.rst*Mar 951.rst*I*1*1*2
CONVERT  x Mar 952.rst*Mar 952.rst*I*1*1*2
CONVERT  x Mar 953.rst*Mar 953.rst*I*1*1*2
CONVERT  x apr 951.rst*apr 951.rst*I*1*1*2
CONVERT  x apr 952.rst*apr 952.rst*I*1*1*2
CONVERT  x apr 953.rst*apr 953.rst*I*1*1*2
CONVERT  x May 951.rst*May 951.rst*I*1*1*2
CONVERT  x May 952.rst*May 952.rst*I*1*1*2
CONVERT  x May 953.rst*May 953.rst*I*1*1*2
CONVERT  x Jun 951.rst*Jun 951.rst*I*1*1*2
CONVERT  x Jun 952.rst*Jun 952.rst*I*1*1*2
CONVERT  x Jun 953.rst*Jun 953.rst*I*1*1*2
CONVERT  x Jul 951.rst*Jul 951.rst*I*1*1*2
CONVERT  x Jul 952.rst*Jul 952.rst*I*1*1*2
CONVERT  x Jul 953.rst*Jul 953.rst*I*1*1*2
CONVERT  x Aug 951.rst*Aug 951.rst*I*1*1*2
CONVERT  x Aug 952.rst*Aug 952.rst*I*1*1*2
CONVERT  x Aug 953.rst*Aug 953.rst*I*1*1*2
CONVERT  x Sept 951.rst*Sept 951.rst*I*1*1*2
CONVERT  x Sept 952.rst*Sept 952.rst*I*1*1*2
CONVERT  x Sept 953.rst*Sept 953.rst*I*1*1*2
CONVERT  x Oct 951.rst*Oct 951.rst*I*1*1*2
CONVERT  x Oct 952.rst*Oct 952.rst*I*1*1*2
CONVERT  x Oct 953.rst*Oct 953.rst*I*1*1*2
CONVERT  x Nov 951.rst*Nov 951.rst*I*1*1*2
CONVERT  x Nov 952.rst*Nov 952.rst*I*1*1*2
CONVERT  x Nov 953.rst*Nov 953.rst*I*1*1*2
CONVERT  x Dec 951.rst*Dec 951.rst*I*1*1*2
CONVERT  x Dec 952.rst*Dec 952.rst*I*1*1*2
CONVERT  x Dec 953.rst*Dec 953.rst*I*1*1*2
```

APPENDIX 1c

Sample Macro command written in IDRISI-32 GIS Software   used to convert the AVHRR-NDVI ASCII format data to raster data.

```
SSTIDRIS x apr 1995.prn*apr
1995.rst*2*138*174*latlong.ref*deg*1.0*1.995833*14.00416*1.145873*14.00417
OVERLAY x 3*apr 1995.rst*mask for ndvi.rst*Masked Apr 1995.rst

SSTIDRIS x apr 1996.prn*apr
1996.rst*2*138*174*latlong.ref*deg*1.0*1.995833*14.00416*1.145873*14.00417
OVERLAY x 3*apr 1996.rst*mask for ndvi.rst*Masked Apr 1996.rst

SSTIDRIS x apr 1997.prn*apr
1997.rst*2*138*174*latlong.ref*deg*1.0*1.995833*14.00416*1.145873*14.00417
OVERLAY x 3*apr 1997.rst*mask for ndvi.rst*Masked Apr 1997.rst

SSTIDRIS x apr 1998.prn*apr
1998.rst*2*138*174*latlong.ref*deg*1.0*1.995833*14.00416*1.145873*14.00417
OVERLAY x 3*apr 1998.rst*mask for ndvi.rst*Masked Apr 1998.rst

SSTIDRIS x apr 1999.prn*apr
1999.rst*2*138*174*latlong.ref*deg*1.0*1.995833*14.00416*1.145873*14.00417
OVERLAY x 3*apr 1999.rst*mask for ndvi.rst*Masked Apr 1999.rst

SSTIDRIS x aug 1995.prn*aug
1995.rst*2*138*174*latlong.ref*deg*1.0*1.995833*14.00416*1.145873*14.00417
OVERLAY x 3*aug 1995.rst*mask for ndvi.rst*Masked Aug 1995.rst

SSTIDRIS x aug 1996.prn*aug
1996.rst*2*138*174*latlong.ref*deg*1.0*1.995833*14.00416*1.145873*14.00417
OVERLAY x 3*aug 1996.rst*mask for ndvi.rst*Masked Aug 1996.rst

SSTIDRIS x aug 1997.prn*aug
1997.rst*2*138*174*latlong.ref*deg*1.0*1.995833*14.00416*1.145873*14.00417
OVERLAY x 3*aug 1997.rst*mask for ndvi.rst*Masked Aug 1997.rst

SSTIDRIS x aug 1998.prn*aug
1998.rst*2*138*174*latlong.ref*deg*1.0*1.995833*14.00416*1.145873*14.00417
OVERLAY x 3*aug 1998.rst*mask for ndvi.rst*Masked Aug 1998.rst

SSTIDRIS x aug 1999.prn*aug
1999.rst*2*138*174*latlong.ref*deg*1.0*1.995833*14.00416*1.145873*14.00417
OVERLAY x 3*aug 1999.rst*mask for ndvi.rst*Masked Aug 1999.rst

SSTIDRIS x dec 1995.prn*dec
1995.rst*2*138*174*latlong.ref*deg*1.0*1.995833*14.00416*1.145873*14.00417
OVERLAY x 3*dec 1995.rst*mask for ndvi.rst*Masked Dec 1995.rst

SSTIDRIS x dec 1996.prn*dec
1996.rst*2*138*174*latlong.ref*deg*1.0*1.995833*14.00416*1.145873*14.00417
OVERLAY x 3*dec 1996.rst*mask for ndvi.rst*Masked Dec 1996.rst
```

APPENDIX 1c *(Cont.)*

Sample Macro command to convert the AVHRR-NDVI ASCII format to raster data

```
SSTIDRIS x dec 1997.prn*dec
1997.rst*2*138*174*latlong.ref*deg*1.0*1.995833*14.00416*1.145873*14.00417
OVERLAY x 3*dec 1997.rst*mask for ndvi.rst*Masked Dec 1997.rst


SSTIDRIS x dec 1998.prn*dec
1998.rst*2*138*174*latlong.ref*deg*1.0*1.995833*14.00416*1.145873*14.00417
OVERLAY x 3*dec 1998.rst*mask for ndvi.rst*Masked Dec 1998.rst


SSTIDRIS x dec 1999.prn*dec
1999.rst*2*138*174*latlong.ref*deg*1.0*1.995833*14.00416*1.145873*14.00417
OVERLAY x 3*dec 1999.rst*mask for ndvi.rst*Masked Dec 1999.rst

SSTIDRIS x feb 1995.prn*feb
1995.rst*2*138*174*latlong.ref*deg*1.0*1.995833*14.00416*1.145873*14.00417
OVERLAY x 3*feb 1995.rst*mask for ndvi.rst*Masked Feb 1995.rst

SSTIDRIS x feb 1996.prn*feb
1996.rst*2*138*174*latlong.ref*deg*1.0*1.995833*14.00416*1.145873*14.00417
OVERLAY x 3*feb 1996.rst*mask for ndvi.rst*Masked Feb 1996.rst

SSTIDRIS x feb 1997.prn*feb
1997.rst*2*138*174*latlong.ref*deg*1.0*1.995833*14.00416*1.145873*14.00417
OVERLAY x 3*feb 1997.rst*mask for ndvi.rst*Masked Feb 1997.rst

SSTIDRIS x feb 1998.prn*feb
1998.rst*2*138*174*latlong.ref*deg*1.0*1.995833*14.00416*1.145873*14.00417
OVERLAY x 3*feb 1998.rst*mask for ndvi.rst*Masked Feb 1998.rst

SSTIDRIS x feb 1999.prn*feb
1999.rst*2*138*174*latlong.ref*deg*1.0*1.995833*14.00416*1.145873*14.00417
OVERLAY x 3*feb 1999.rst*mask for ndvi.rst*Masked Feb 1999.rst

SSTIDRIS x jan 1995.prn*jan
1995.rst*2*138*174*latlong.ref*deg*1.0*1.995833*14.00416*1.145873*14.00417
OVERLAY x 3*jan 1995.rst*mask for ndvi.rst*Masked Jan 1995.rst

SSTIDRIS x jan 1996.prn*jan
1996.rst*2*138*174*latlong.ref*deg*1.0*1.995833*14.00416*1.145873*14.00417
OVERLAY x 3*jan 1996.rst*mask for ndvi.rst*Masked Jan 1996.rst

SSTIDRIS x jan 1997.prn*jan
1997.rst*2*138*174*latlong.ref*deg*1.0*1.995833*14.00416*1.145873*14.00417
OVERLAY x 3*jan 1997.rst*mask for ndvi.rst*Masked Jan 1997.rst

SSTIDRIS x jan 1998.prn*jan
1998.rst*2*138*174*latlong.ref*deg*1.0*1.995833*14.00416*1.145873*14.00417
OVERLAY x 3*jan 1998.rst*mask for ndvi.rst*Masked Jan 1998.rst
```

APPENDIX 1c *(Cont.)*

Sample Macro command to convert the AVHRR-NDVI ASCII format to raster data

```
SSTIDRIS x jan 1999.prn*jan
1999.rst*2*138*174*latlong.ref*deg*1.0*1.995833*14.00416*1.145873*14.00417
OVERLAY x 3*jan 1999.rst*mask for ndvi.rst*Masked Jan 1999.rst

SSTIDRIS x jul 1995.prn*jul
1995.rst*2*138*174*latlong.ref*deg*1.0*1.995833*14.00416*1.145873*14.00417
OVERLAY x 3*jul 1995.rst*mask for ndvi.rst*Masked Jul 1995.rst

SSTIDRIS x jul 1996.prn*jul
1996.rst*2*138*174*latlong.ref*deg*1.0*1.995833*14.00416*1.145873*14.00417
OVERLAY x 3*jul 1996.rst*mask for ndvi.rst*Masked Jul 1996.rst

SSTIDRIS x jul 1997.prn*jul
1997.rst*2*138*174*latlong.ref*deg*1.0*1.995833*14.00416*1.145873*14.00417
OVERLAY x 3*jul 1997.rst*mask for ndvi.rst*Masked Jul 1997.rst

SSTIDRIS x jul 1998.prn*jul
1998.rst*2*138*174*latlong.ref*deg*1.0*1.995833*14.00416*1.145873*14.00417
OVERLAY x 3*jul 1998.rst*mask for ndvi.rst*Masked Jul 1998.rst

SSTIDRIS x jul 1999.prn*jul
1999.rst*2*138*174*latlong.ref*deg*1.0*1.995833*14.00416*1.145873*14.00417
OVERLAY x 3*jul 1999.rst*mask for ndvi.rst*Masked Jul 1999.rst

SSTIDRIS x jun 1995.prn*jun
1995.rst*2*138*174*latlong.ref*deg*1.0*1.995833*14.00416*1.145873*14.00417
OVERLAY x 3*jun 1995.rst*mask for ndvi.rst*Masked Jun 1995.rst

SSTIDRIS x jun 1996.prn*jun
1996.rst*2*138*174*latlong.ref*deg*1.0*1.995833*14.00416*1.145873*14.00417
OVERLAY x 3*jun 1996.rst*mask for ndvi.rst*Masked Jun 1996.rst

SSTIDRIS x jun 1997.prn*jun
1997.rst*2*138*174*latlong.ref*deg*1.0*1.995833*14.00416*1.145873*14.00417
OVERLAY x 3*jun 1997.rst*mask for ndvi.rst*Masked Jun 1997.rst

SSTIDRIS x jun 1998.prn*jun
1998.rst*2*138*174*latlong.ref*deg*1.0*1.995833*14.00416*1.145873*14.00417
OVERLAY x 3*jun 1998.rst*mask for ndvi.rst*Masked Jun 1998.rst

SSTIDRIS x jun 1999.prn*jun
1999.rst*2*138*174*latlong.ref*deg*1.0*1.995833*14.00416*1.145873*14.00417
OVERLAY x 3*jun 1999.rst*mask for ndvi.rst*Masked Jun 1999.rst

SSTIDRIS x mar 1995.prn*mar
1995.rst*2*138*174*latlong.ref*deg*1.0*1.995833*14.00416*1.145873*14.00417
OVERLAY x 3*mar 1995.rst*mask for ndvi.rst*Masked Mar 1995.rst
```

APPENDIX 1c *(Cont.)*

Sample Macro command to convert the AVHRR-NDVI ASCII format to raster data

```
SSTIDRIS x mar 1996.prn*mar
1996.rst*2*138*174*latlong.ref*deg*1.0*1.995833*14.00416*1.145873*14.00417
OVERLAY x 3*mar 1996.rst*mask for ndvi.rst*Masked Mar 1996.rst

SSTIDRIS x mar 1997.prn*mar
1997.rst*2*138*174*latlong.ref*deg*1.0*1.995833*14.00416*1.145873*14.00417
OVERLAY x 3*mar 1997.rst*mask for ndvi.rst*Masked Mar 1997.rst

SSTIDRIS x mar 1998.prn*mar
1998.rst*2*138*174*latlong.ref*deg*1.0*1.995833*14.00416*1.145873*14.00417
OVERLAY x 3*mar 1998.rst*mask for ndvi.rst*Masked Mar 1998.rst

SSTIDRIS x mar 1999.prn*mar
1999.rst*2*138*174*latlong.ref*deg*1.0*1.995833*14.00416*1.145873*14.00417
OVERLAY x 3*mar 1999.rst*mask for ndvi.rst*Masked Mar 1999.rst

SSTIDRIS x may 1995.prn*may
1995.rst*2*138*174*latlong.ref*deg*1.0*1.995833*14.00416*1.145873*14.00417
OVERLAY x 3*may 1995.rst*mask for ndvi.rst*Masked May 1995.rst

SSTIDRIS x may 1996.prn*may
1996.rst*2*138*174*latlong.ref*deg*1.0*1.995833*14.00416*1.145873*14.00417
OVERLAY x 3*may 1996.rst*mask for ndvi.rst*Masked May 1996.rst

SSTIDRIS x may 1997.prn*may
1997.rst*2*138*174*latlong.ref*deg*1.0*1.995833*14.00416*1.145873*14.00417
OVERLAY x 3*may 1997.rst*mask for ndvi.rst*Masked May 1997.rst

SSTIDRIS x may 1998.prn*may
1998.rst*2*138*174*latlong.ref*deg*1.0*1.995833*14.00416*1.145873*14.00417
OVERLAY x 3*may 1998.rst*mask for ndvi.rst*Masked May 1998.rst

SSTIDRIS x may 1999.prn*may
1999.rst*2*138*174*latlong.ref*deg*1.0*1.995833*14.00416*1.145873*14.00417
OVERLAY x 3*may 1999.rst*mask for ndvi.rst*Masked May 1999.rst

SSTIDRIS x nov 1995.prn*nov
1995.rst*2*138*174*latlong.ref*deg*1.0*1.995833*14.00416*1.145873*14.00417
OVERLAY x 3*nov 1995.rst*mask for ndvi.rst*Masked Nov 1995.rst

SSTIDRIS x nov 1996.prn*nov
1996.rst*2*138*174*latlong.ref*deg*1.0*1.995833*14.00416*1.145873*14.00417
OVERLAY x 3*nov 1996.rst*mask for ndvi.rst*Masked Nov 1996.rst

SSTIDRIS x nov 1997.prn*nov
1997.rst*2*138*174*latlong.ref*deg*1.0*1.995833*14.00416*1.145873*14.00417
OVERLAY x 3*nov 1997.rst*mask for ndvi.rst*Masked Nov 1997.rst
```

APPENDIX 1c *(Cont.)*

Sample Macro command to convert the AVHRR-NDVI ASCII format to raster data

```
SSTIDRIS x nov 1998.prn*nov
1998.rst*2*138*174*latlong.ref*deg*1.0*1.995833*14.00416*1.145873*14.00417
OVERLAY x 3*nov 1998.rst*mask for ndvi.rst*Masked Nov 1998.rst

SSTIDRIS x nov 1999.prn*nov
1999.rst*2*138*174*latlong.ref*deg*1.0*1.995833*14.00416*1.145873*14.00417
OVERLAY x 3*nov 1999.rst*mask for ndvi.rst*Masked Nov 1999.rst

SSTIDRIS x oct 1995.prn*oct
1995.rst*2*138*174*latlong.ref*deg*1.0*1.995833*14.00416*1.145873*14.00417
OVERLAY x 3*oct 1995.rst*mask for ndvi.rst*Masked Oct 1995.rst

SSTIDRIS x oct 1996.prn*oct
1996.rst*2*138*174*latlong.ref*deg*1.0*1.995833*14.00416*1.145873*14.00417
OVERLAY x 3*oct 1996.rst*mask for ndvi.rst*Masked Oct 1996.rst

SSTIDRIS x oct
1997.prn*oct1997.rst*2*138*174*latlong.ref*deg*1.0*1.995833*14.00416*1.145873*
14.00417
OVERLAY x 3*oct 1997.rst*mask for ndvi.rst*Masked Oct 1997.rst

SSTIDRIS x oct 1998.prn*oct
1998.rst*2*138*174*latlong.ref*deg*1.0*1.995833*14.00416*1.145873*14.00417
OVERLAY x 3*oct 1998.rst*mask for ndvi.rst*Masked Oct 1998.rst

SSTIDRIS x oct 1999.prn*oct
1999.rst*2*138*174*latlong.ref*deg*1.0*1.995833*14.00416*1.145873*14.00417
OVERLAY x 3*oct 1999.rst*mask for ndvi.rst*Masked Oct 1999.rst

SSTIDRIS x sept 1995.prn*sept
1995.rst*2*138*174*latlong.ref*deg*1.0*1.995833*14.00416*1.145873*14.00417
OVERLAY x 3*sept 1995.rst*mask for ndvi.rst*Masked Sept 1995.rst

SSTIDRIS x sept 1996.prn*sept
1996.rst*2*138*174*latlong.ref*deg*1.0*1.995833*14.00416*1.145873*14.00417
OVERLAY x 3*sept 1996.rst*mask for ndvi.rst*Masked Sept 1996.rst

SSTIDRIS x sept 1997.prn*sept
1997.rst*2*138*174*latlong.ref*deg*1.0*1.995833*14.00416*1.145873*14.00417
OVERLAY x 3*sept 1997.rst*mask for ndvi.rst*Masked Sept 1997.rst

SSTIDRIS x sept 1998.prn*sept
1998.rst*2*138*174*latlong.ref*deg*1.0*1.995833*14.00416*1.145873*14.00417
OVERLAY x 3*sept 1998.rst*mask for ndvi.rst*Masked Sept 1998.rst

SSTIDRIS x sept 1999.prn*sept
1999.rst*2*138*174*latlong.ref*deg*1.0*1.995833*14.00416*1.145873*14.00417
OVERLAY x 3*sept 1999.rst*mask for ndvi.rst*Masked Sept 1999.rst
```

APPENDIX 2a

Univariate Statistics for the **Dekadal** AVHRR-NDVI Image data used for the Study

Dekadal NDVI Images	1986				1987			
	Min	Max	Mean	SD	Min	Max	Mean	SD
Jan 1 -10	91	201	155.4	12.9	111	204	150.9	10.4
Jan 11 -20	91	201	155.4	12.9	82	205	154.6	13.4
Jan 21 - 31	108	235	153.2	13.0	111	206	153.2	11.4
Feb 1 - 10	108	201	152.1	12.3	102	252	151.2	11.4
Feb 11 - 20	121	205	153.3	13.4	97	194	146.7	9.8
Feb 21 - 29	92	202	153.7	13.1	93	228	156.7	15.6
Mar 1 - 10	103	212	152.5	16.6	110	203	149.6	11.2
Mar 11 - 20	108	199	146.5	12.2	121	193	150.4	12.9
Mar 21 - 31	108	199	146.5	12.2	123	213	154.5	18.1
Apr 1 - 10	113	252	156.9	18.8	115	217	162.1	19.8
Apr 11 - 20	118	214	161.6	21.4	105	214	161.4	18.3
Apr 21 - 30	119	212	157.5	21.0	113	202	151.1	13.5
May 1 - 10	120	252	159.2	21.3	108	213	161.0	21.1
May 11 - 20	116	221	166.1	25.8	122	222	160.2	23.1
May 21 - 31	125	219	167.1	26.4	121	227	163.2	23.9
Jun 1 - 10	122	252	167.1	23.3	114	225	166.1	24.7
Jun 11 - 20	97	216	169.6	24.3	113	252	170.2	21.4
Jun 21 - 30	121	225	170.4	24.4	122	220	171.2	22.6
Jul 1 - 10	120	234	167.6	22.1	122	220	171.2	22.6
Jul 11 - 20	121	249	168.1	20.6	109	224	178.2	24.6
Jul 21 - 31	121	225	170.4	24.4	123	225	177.1	23.4
Aug 1 - 10	123	220	182.5	18.0	123	225	180.7	22.2
Aug 11 - 20	119	252	176.0	19.1	121	218	177.6	21.7
Aug 21 - 31	122	221	183.5	17.4	101	225	181.9	21.8
Sep 1 - 10	123	220	182.5	18.0	123	232	186.6	19.2
Sep 11 - 20	123	221	184.2	17.3	123	252	180.4	19.0
Sep 21 - 30	123	221	184.2	17.3	107	223	173.8	20.5
Oct 1 - 10	109	224	181.0	18.2	110	252	177.5	22.7
Oct 11 - 20	121	224	180.3	19.4	93	252	168.8	25.1
Oct 21 - 31	122	244	181.0	18.0	117	217	178.1	21.2
Nov 1 - 10	111	217	174.4	18.1	116	230	170.9	17.1
Nov 11 - 20	117	211	170.5	16.4	113	210	166.4	16.8
Nov 21 - 30	98	208	164.1	15.4	113	210	166.4	16.8
Dec 1 - 10	118	206	158.1	12.9	107	205	158.2	13.1
Dec 11 - 20	99	252	161.0	13.4	97	199	156.9	11.8
Dec 21 - 31	108	198	149.8	9.3	109	208	166.0	15.2

APPENDIX 2a *(Cont.)*

Univariate Statistics for the **Dekadal** AVHRR-NDVI Image data used for the Study

Dekadal NDVI Images	1988				1990			
	Min	Max	Mean	SD	Min	Max	Mean	SD
Jan 1 -10	115	199	144.4	11.3	123	213	158.2	13.2
Jan 11 -20	110	183	146.6	8.4	120	220	157.1	13.3
Jan 21 - 31	118	224	149.7	11.0	121	207	155.3	12.5
Feb 1 - 10	123	209	153.6	14.1	114	205	155.0	13.1
Feb 11 - 20	124	200	152.3	11.7	122	252	154.2	13.1
Feb 21 - 29	117	226	148.2	10.6	111	205	155.4	13.9
Mar 1 - 10	126	211	149.0	12.8	119	202	156.2	14.3
Mar 11 - 20	115	196	150.6	12.0	120	211	157.2	14.3
Mar 21 - 31	124	207	152.7	15.2	118	202	151.9	11.9
Apr 1 - 10	99	211	151.7	15.2	124	214	156.1	16.2
Apr 11 - 20	124	231	157.0	22.9	123	213	156.4	16.5
Apr 21 - 30	124	227	156.9	22.9	122	217	159.8	20.4
May 1 - 10	126	220	161.2	23.9	119	223	163.2	21.6
May 11 - 20	125	226	166.5	24.1	124	223	169.4	24.6
May 21 - 31	117	252	167.9	26.2	123	226	175.3	24.8
Jun 1 - 10	125	252	165.8	26.9	123	227	176.8	25.9
Jun 11 - 20	125	252	168.0	26.1	123	220	174.9	24.1
Jun 21 - 30	124	249	159.2	22.0	122	220	173.7	24.2
Jul 1 - 10	125	230	174.7	24.4	124	223	174.1	24.5
Jul 11 - 20	123	252	165.0	22.3	121	222	170.4	23.1
Jul 21 - 31	119	224	176.6	23.1	121	252	176.0	20.1
Aug 1 - 10	121	218	176.6	19.4	121	223	179.0	20.9
Aug 11 - 20	122	252	177.8	20.3	117	223	176.9	19.7
Aug 21 - 31	122	252	185.9	19.3	117	223	183.4	17.7
Sep 1 - 10	123	252	177.9	20.5	122	228	185.8	17.8
Sep 11 - 20	119	252	175.9	18.2	123	227	180.2	19.6
Sep 21 - 30	111	252	172.3	19.9	123	226	181.5	18.4
Oct 1 - 10	97	252	183.0	19.2	124	226	183.8	20.6
Oct 11 - 20	118	252	181.0	18.1	122	226	179.5	19.9
Oct 21 - 31	113	252	177.2	18.4	108	217	174.9	18.2
Nov 1 - 10	119	252	178.4	18.4	109	221	176.8	19.0
Nov 11 - 20	106	215	176.3	17.0	115	222	172.3	20.2
Nov 21 - 30	125	218	172.6	16.7	98	212	170.3	16.9
Dec 1 - 10	120	214	165.8	14.6	118	211	170.1	17.3
Dec 11 - 20	104	209	163.6	14.0	117	216	166.1	17.7
Dec 21 - 31	125	207	158.9	13.1	111	252	162.6	15.4

APPENDIX 2a *(Cont.)*

Univariate Statistics for the **Dekadal** AVHRR-NDVI Image data used for the Study

Dekadal NDVI Images	1991				1992			
	Min	Max	Mean	SD	Min	Max	Mean	SD
Jan 1 -10	111	198	156.5	12.4	116	194	148.9	11.0
Jan 11 -20	119	252	151.2	10.6	117	190	147.0	9.5
Jan 21 - 31	110	203	158.8	14.6	119	186	147.2	9.2
Feb 1 - 10	113	207	159.0	15.1	117	199	154.1	12.8
Feb 11 - 20	120	213	157.9	15.5	114	201	153.9	12.7
Feb 21 - 29	122	206	156.2	14.7	119	197	149.1	11.1
Mar 1 - 10	121	208	155.5	15.2	111	194	149.2	10.7
Mar 11 - 20	122	209	157.1	15.6	123	252	139.7	9.0
Mar 21 - 31	117	215	159.7	16.8	123	193	149.9	11.4
Apr 1 - 10	122	223	162.9	21.0	117	204	157.0	16.4
Apr 11 - 20	122	218	159.8	19.5	123	203	155.6	17.1
Apr 21 - 30	123	225	165.7	24.0	122	203	155.4	14.0
May 1 - 10	125	221	165.8	25.4	124	210	163.1	21.0
May 11 - 20	124	247	170.6	26.4	125	218	165.2	21.8
May 21 - 31	123	248	175.2	25.5	124	218	173.9	23.9
Jun 1 - 10	123	221	173.0	19.7	119	252	172.4	21.0
Jun 11 - 20	125	224	179.4	21.9	123	213	168.8	20.8
Jun 21 - 30	123	217	174.0	19.6	119	211	166.5	19.1
Jul 1 - 10	124	216	171.8	20.7	124	216	171.8	20.7
Jul 11 - 20	122	212	172.6	18.5	124	215	174.4	18.9
Jul 21 - 31	120	203	165.7	14.8	118	214	170.7	20.7
Aug 1 - 10	118	209	163.5	16.3	117	252	171.9	17.1
Aug 11 - 20	122	201	167.6	14.1	120	207	165.3	17.6
Aug 21 - 31	121	234	170.7	15.9	120	246	170.7	17.6
Sep 1 - 10	119	212	174.2	13.6	118	218	173.7	18.6
Sep 11 - 20	120	204	170.8	12.3	121	252	176.2	17.0
Sep 21 - 30	120	200	167.8	14.3	125	223	184.9	18.2
Oct 1 - 10	125	199	167.2	13.8	121	224	179.7	16.2
Oct 11 - 20	124	202	168.3	13.7	118	225	180.0	17.5
Oct 21 - 31	124	203	163.9	12.0	120	214	176.8	15.0
Nov 1 - 10	123	200	165.8	12.6	126	222	176.3	17.0
Nov 11 - 20	115	199	159.8	11.3	120	252	169.1	14.7
Nov 21 - 30	107	196	160.8	11.5	114	203	159.2	14.6
Dec 1 - 10	115	198	156.2	9.4	92	211	161.9	12.3
Dec 11 - 20	119	225	152.0	10.3	116	230	166.6	13.5
Dec 21 - 31	120	252	155.8	11.6	119	220	160.9	12.4

APPENDIX 2a   *(Cont.)*

Univariate Statistics for the **Dekadal** AVHRR-NDVI Image data used for the Study

Dekadal NDVI Images	1993				1995			
	Min	Max	Mean	SD	Min	Max	Mean	SD
Jan 1 -10	110	203	153.8	10.7	75	203	160.5	11.0
Jan 11 -20	112	203	146.3	12.3	89	207	157.1	11.8
Jan 21 - 31	115	241	155.1	12.8	116	209	156.8	14.3
Feb 1 - 10	119	242	153.5	12.0	115	205	155.7	11.4
Feb 11 - 20	120	205	154.9	12.2	89	206	157.1	13.5
Feb 21 - 29	125	206	155.2	13.2	86	208	158.8	14.9
Mar 1 - 10	125	252	150.6	11.4	116	215	160.2	15.7
Mar 11 - 20	126	213	158.3	17.3	117	218	157.8	16.8
Mar 21 - 31	119	203	157.5	13.3	120	209	158.1	16.1
Apr 1 - 10	123	223	163.2	17.8	111	219	161.9	20.2
Apr 11 - 20	119	220	155.9	18.6	121	214	160.6	19.8
Apr 21 - 30	123	252	161.4	22.5	120	219	162.2	21.3
May 1 - 10	126	252	166.6	23.7	116	229	171.0	25.9
May 11 - 20	125	250	171.3	24.7	121	252	174.7	25.3
May 21 - 31	125	244	171.4	25.3	122	232	173.7	25.3
Jun 1 - 10	125	230	172.1	25.8	121	225	174.8	25.8
Jun 11 - 20	112	252	178.4	24.8	122	252	172.9	24.3
Jun 21 - 30	126	225	175.2	24.8	120	219	171.0	23.1
Jul 1 - 10	124	249	170.8	22.4	119	220	172.2	21.4
Jul 11 - 20	123	252	174.2	22.7	121	223	176.3	22.4
Jul 21 - 31	124	241	178.7	21.5	121	224	176.4	20.5
Aug 1 - 10	123	237	178.8	20.9	121	252	170.4	19.8
Aug 11 - 20	120	227	180.0	20.3	121	225	183.2	18.7
Aug 21 - 31	123	252	180.9	21.0	117	223	182.5	17.8
Sep 1 - 10	120	252	188.5	17.7	120	222	181.9	16.6
Sep 11 - 20	123	252	184.8	20.3	120	224	182.4	18.9
Sep 21 - 30	125	252	188.3	18.9	109	252	183.9	17.3
Oct 1 - 10	124	252	183.3	20.9	118	226	178.1	19.0
Oct 11 - 20	117	252	179.2	18.9	122	222	181.6	18.0
Oct 21 - 31	117	252	181.1	20.4	113	225	180.9	18.9
Nov 1 - 10	114	252	178.0	17.3	115	223	176.9	19.1
Nov 11 - 20	124	252	168.0	18.3	109	220	177.4	18.8
Nov 21 - 30	121	252	163.3	13.5	110	211	173.2	16.9
Dec 1 - 10	111	252	159.2	18.0	110	210	164.6	15.1
Dec 11 - 20	114	208	152.7	10.7	110	210	164.6	15.1
Dec 21 - 31	123	208	152.3	9.0	107	212	163.4	15.9

APPENDIX 2a *(Cont.)*

Univariate Statistics for the **Dekadal** AVHRR-NDVI Image data used for the Study

Dekadal NDVI Images	1996				1997			
	Min	Max	Mean	SD	Min	Max	Mean	SD
Jan 1 -10	98	252	164.2	15.5	84	209	159.0	12.4
Jan 11 -20	120	215	157.5	13.7	115	210	158.8	13.8
Jan 21 - 31	115	240	158.6	14.6	100	200	152.8	10.9
Feb 1 - 10	90	210	159.0	14.9	100	203	152.0	11.8
Feb 11 - 20	114	208	156.3	15.9	96	207	155.7	13.3
Feb 21 - 29	119	206	152.2	12.4	112	203	148.7	12.2
Mar 1 - 10	113	220	156.0	17.6	118	197	146.9	11.7
Mar 11 - 20	116	218	157.7	18.6	119	204	150.9	12.7
Mar 21 - 31	114	216	160.8	18.1	121	202	152.8	14.1
Apr 1 - 10	120	220	164.1	22.2	112	225	165.0	22.0
Apr 11 - 20	120	219	158.3	21.3	112	225	162.4	20.8
Apr 21 - 30	123	220	160.5	22.3	118	224	164.8	23.4
May 1 - 10	119	226	169.0	25.3	123	219	167.4	22.7
May 11 - 20	119	221	170.4	26.0	115	228	176.3	24.7
May 21 - 31	121	229	172.4	25.2	122	226	177.6	26.3
Jun 1 - 10	121	224	172.1	24.3	121	226	174.6	25.1
Jun 11 - 20	113	226	177.1	23.1	122	224	174.5	23.1
Jun 21 - 30	122	222	175.3	21.4	120	230	178.2	23.4
Jul 1 - 10	121	252	178.1	20.5	118	222	177.5	21.3
Jul 11 - 20	119	252	172.4	20.6	114	224	175.8	22.8
Jul 21 - 31	120	221	168.5	19.0	109	222	178.7	20.8
Aug 1 - 10	115	222	173.4	21.4	118	223	175.6	21.1
Aug 11 - 20	121	222	171.9	19.4	117	221	171.9	20.4
Aug 21 - 31	120	221	179.0	17.7	120	224	185.1	18.3
Sep 1 - 10	117	220	177.3	16.0	120	225	185.2	18.6
Sep 11 - 20	119	223	179.0	18.9	122	230	185.9	19.7
Sep 21 - 30	121	221	184.3	19.4	123	228	186.3	19.6
Oct 1 - 10	120	222	180.1	18.2	117	221	185.3	18.9
Oct 11 - 20	112	227	179.4	19.3	116	240	183.2	21.2
Oct 21 - 31	115	220	178.7	18.1	109	223	180.9	21.3
Nov 1 - 10	94	219	179.0	18.2	106	225	180.6	21.1
Nov 11 - 20	84	215	173.9	17.2	119	218	177.6	19.6
Nov 21 - 30	107	215	170.3	14.5	111	216	174.9	19.4
Dec 1 - 10	74	210	166.7	14.2	112	207	164.3	13.3
Dec 11 - 20	74	210	166.7	14.2	112	207	164.3	13.3
Dec 21 - 31	96	239	163.5	13.6	94	208	162.7	13.0

APPENDIX 2a   *(Cont.)*

Univariate Statistics for the **Dekadal** AVHRR-NDVI Image data used for the Study

Dekadal NDVI Images	1998				1999			
	Min	Max	Mean	SD	Min	Max	Mean	SD
Jan 1 -10	121	205	153.2	13.0	87	201	160.7	12.5
Jan 11 -20	119	206	156.3	13.0	102	209	158.5	11.9
Jan 21 - 31	88	204	158.6	12.8	122	202	156.8	11.2
Feb 1 - 10	89	215	161.7	16.9	124	200	156.1	12.9
Feb 11 - 20	116	206	155.3	14.7	123	201	154.0	12.5
Feb 21 - 29	98	205	154.8	14.8	110	214	155.4	12.1
Mar 1 - 10	111	192	151.5	11.2	108	207	156.8	12.8
Mar 11 - 20	113	205	150.5	11.9	116	219	163.8	19.8
Mar 21 - 31	123	206	154.7	15.2	115	215	162.2	17.8
Apr 1 - 10	120	209	154.6	16.0	122	210	157.7	17.6
Apr 11 - 20	116	225	160.3	20.2	122	212	162.8	18.5
Apr 21 - 30	124	217	156.3	21.7	122	217	164.6	21.6
May 1 - 10	122	217	162.6	21.8	124	227	169.7	24.9
May 11 - 20	115	223	169.2	24.1	122	228	169.9	25.5
May 21 - 31	121	221	173.2	25.7	120	225	172.5	26.5
Jun 1 - 10	123	220	175.6	25.6	121	223	172.9	25.0
Jun 11 - 20	122	228	178.0	25.3	123	252	177.4	26.3
Jun 21 - 30	124	225	178.7	24.7	123	248	173.4	25.3
Jul 1 - 10	123	224	177.8	24.2	123	231	177.0	24.7
Jul 11 - 20	122	252	167.2	23.6	122	226	177.1	24.9
Jul 21 - 31	124	226	176.6	20.7	121	245	168.9	20.2
Aug 1 - 10	119	224	174.1	20.1	114	221	177.2	19.7
Aug 11 - 20	118	215	169.8	19.0	121	224	183.0	19.2
Aug 21 - 31	117	223	180.7	17.3	123	223	185.8	18.7
Sep 1 - 10	119	226	184.5	19.1	121	250	175.3	21.3
Sep 11 - 20	116	223	181.1	19.3	121	250	175.3	21.3
Sep 21 - 30	119	252	185.7	18.5	121	225	186.7	18.4
Oct 1 - 10	101	226	189.3	17.0	104	252	180.0	21.9
Oct 11 - 20	117	225	187.1	18.6	116	252	182.3	18.2
Oct 21 - 31	123	238	186.3	18.5	112	235	180.6	17.0
Nov 1 - 10	94	216	178.5	17.0	81	252	181.9	17.6
Nov 11 - 20	123	217	178.1	18.1	83	252	177.9	16.9
Nov 21 - 30	114	252	173.1	16.1	108	252	168.9	17.4
Dec 1 - 10	117	199	155.9	10.3	87	211	164.2	12.7
Dec 11 - 20	117	199	155.9	10.3	87	211	164.2	12.7
Dec 21 - 31	95	207	161.4	12.5	112	252	160.9	12.6

APPENDIX 2b

Univariate Statistics for the **Monthly** Maximum Value Composites AVHRR-NDVI Image data used for the Study

NDVI Image	1986				1987				1988			
	Min	Max	Mean	SD	Min	Max	Mean	SD	Min	Max	Mean	SD
Jan	121.2	209.3	171.6	16.2	111	206	156.6	13.2	126	224	151.9	11.4
Feb	125.4	210.9	172.7	16.6	105	252	157.8	15.4	124	226	156.6	13.5
Mar	135.2	210.9	173.0	15.6	124	213	157.3	16.9	126	211	156.6	14.9
Apr	126.1	213.8	175.2	16.8	117	217	165.3	19.9	125	231	162.5	22.4
May	130.5	202.0	170.7	13.9	124	227	167.4	23.9	126	252	171.7	25.8
Jun	126.0	205.3	171.4	13.3	123	252	177.7	24.4	128	252	173.9	27.7
Jul	126.8	214.4	176.0	15.7	125	225	183.4	24.5	128	252	185.6	21.5
Aug	125.3	213.1	175.9	16.9	124	225	190.6	18.6	126	252	191.8	16.2
Sep	123.0	212.1	175.2	16.6	124	252	190.6	17.5	124	252	188.3	16.3
Oct	121.8	214.4	176.2	17.0	122	252	185.3	20.9	120	252	188.7	18.0
Nov	124.0	211.6	175.2	16.1	123	230	173.1	17.0	125	252	180.8	18.4
Dec	123.7	212.0	177.0	16.2	121	208	167.0	14.8	125	214	168.2	15.1

NDVI Image	1990				1991				1992			
	Min	Max	Mean	SD	Min	Max	Mean	SD	Min	Max	Mean	SD
Jan	124	220	161.5	14.3	120	252	160.7	14.4	120	194	151.8	10.5
Feb	122	252	158.8	14.9	125	213	161.8	16.9	124	201	156.7	13.1
Mar	125	211	158.7	14.9	124	215	162.9	18.4	125	252	154.2	12.5
Apr	125	217	163.1	20.0	126	225	168.9	23.8	127	204	161.7	17.7
May	125	226	177.3	25.5	126	248	179.9	26.0	126	218	175.1	23.9
Jun	125	227	180.9	26.3	133	224	183.3	21.7	125	252	175.6	21.1
Jul	124	252	183.7	20.7	125	216	179.7	17.0	125	216	181.8	17.1
Aug	123	223	189.5	16.7	122	234	176.1	13.4	124	252	179.9	14.9
Sep	124	228	190.6	17.4	120	212	177.0	12.1	125	252	188.7	16.0
Oct	125	226	187.3	20.3	125	203	172.2	13.1	126	225	185.1	16.0
Nov	120	222	179.0	20.1	125	200	167.0	12.4	126	252	178.3	15.7
Dec	125	252	171.6	18.2	122	252	159.2	10.9	127	230	168.2	13.7

APPENDIX 2b *(Cont.)*

Univariate Statistics for the **Monthly** Maximum Value Composites AVHRR-
NDVI Image data used for the Study

NDVI Image	1993				1995				1996			
	Min	Max	Mean	SD	Min	Max	Mean	SD	Min	Max	Mean	SD
Jan	120	241	157.8	12.8	117	209	163.1	12.8	122	252	165.2	16.1
Feb	125	242	158.7	13.7	115	208	160.4	15.0	120	210	160.6	16.1
Mar	126	252	162.2	16.7	123	218	163.3	17.5	123	220	164.0	19.8
Apr	126	252	167.3	20.9	121	219	166.9	22.4	124	220	167.1	24.0
May	127	252	176.3	26.1	124	252	178.7	27.0	123	229	177.1	26.1
Jun	126	252	182.8	25.7	122	252	179.5	26.0	122	226	182.3	23.3
Jul	126	252	186.0	20.2	123	224	184.3	20.7	122	252	182.6	19.5
Aug	125	252	190.5	17.2	123	252	189.4	16.6	120	221	179.0	17.7
Sep	126	252	196.0	16.7	123	252	190.8	15.8	123	223	189.7	16.4
Oct	126	252	189.8	20.0	122	226	187.6	18.3	122	227	186.9	17.8
Nov	126	252	180.5	17.5	122	223	180.1	19.2	107	219	179.9	18.3
Dec	125	252	163.5	16.3	116	212	166.5	16.3	101	239	167.6	14.4

NDVI Image	1997				1998				1999			
	Min	Max	Mean	SD	Min	Max	Mean	SD	Min	Max	Mean	SD
Jan	115	210	161.3	13.7	121	206	160.7	14.1	122	209	163.4	13.0
Feb	113	207	156.3	13.3	123	215	162.6	17.2	124	214	159.1	13.7
Mar	121	204	155.3	14.9	123	206	156.8	14.6	120	219	166.7	20.1
Apr	118	225	170.8	24.1	124	225	162.7	21.2	123	217	167.5	21.4
May	124	228	181.1	26.1	123	223	175.0	26.2	124	228	177.1	26.7
Jun	123	230	183.1	24.4	125	228	183.6	25.9	125	252	181.2	26.8
Jul	121	224	186.0	20.1	125	252	184.9	21.8	123	245	185.9	22.0
Aug	122	224	188.4	17.5	124	224	186.3	16.1	123	224	192.5	15.9
Sep	124	230	192.4	18.2	119	252	193.0	16.6	122	250	189.8	16.8
Oct	125	240	189.8	20.0	124	238	193.6	17.0	118	252	190.1	16.8
Nov	120	225	183.4	20.8	125	252	181.4	17.5	108	252	184.6	17.1
Dec	112	208	166.4	13.9	117	207	162.1	12.4	112	252	165.9	12.9

APPENDIX 2c

Univariate Statistics for the **Annual Mean** of the Monthly Maximum Value Composites AVHRR-NDVI Image data used for the Study

Annual Mean NDVI Image	Statistics			
	Min	Max	Mean	SD
1986	121.2	209.3	171.6	16.2
1987	125.4	210.9	172.7	16.6
1988	135.2	210.9	173.0	15.6
1990	126.1	213.8	175.2	16.8
1991	130.5	202.0	170.7	13.9
1992	126.0	205.3	171.4	13.3
1993	126.8	214.4	176.0	15.7
1995	125.3	213.1	175.9	16.9
1996	123.0	212.1	175.2	16.6
1997	121.8	214.4	176.2	17.0
1998	124.0	211.6	175.2	16.1
1999	123.7	212.0	177.0	16.2

APPENDIX 3

Sample of the 13 Variables used in creating Rainfall Models
(1986 Gridded Rainfall from GPCC)

1986

Rainfall	Longitude	Latitude	Altitude	Long**	Lat**	Alt**	Long***	Lat***	AltCub	Long*Lat	Long*Alt	Lat*Alt	Long*Lat*Alt
38.71	2.5	13.5	248	6.25	182.25	61504	15.63	2460.38	15252992	33.75	620	3348	8370
42.74	3.5	13.5	241	12.25	182.25	58081	42.88	2460.38	13997521	47.25	843.5	3253.5	11387
41.99	4.5	13.5	304	20.25	182.25	92416	91.13	2460.38	28094464	60.75	1368	4104	18468
34.79	5.5	13.5	336	30.25	182.25	112896	166.38	2460.38	37933056	74.25	1848	4536	24948
40.4	6.5	13.5	339	42.25	182.25	114921	274.63	2460.38	38958219	87.75	2203.5	4576.5	29747
41.09	7.5	13.5	432	56.25	182.25	186624	421.88	2460.38	80621568	101.25	3240	5832	43740
37.49	8.5	13.5	418	72.25	182.25	174724	614.13	2460.38	73034632	114.75	3553	5643	47966
31.77	9.5	13.5	380	90.25	182.25	144400	857.38	2460.38	54872000	128.25	3610	5130	48735
23.97	10.5	13.5	361	110.25	182.25	130321	1157.63	2460.38	47045881	141.75	3790.5	4873.5	51172
19.12	11.5	13.5	387	132.25	182.25	149769	1520.88	2460.38	57960603	155.25	4450.5	5224.5	60082
20.31	12.5	13.5	298	156.25	182.25	88804	1953.13	2460.38	26463592	168.75	3725	4023	50288
20.87	13.5	13.5	280	182.25	182.25	78400	2460.38	2460.38	21952000	182.25	3780	3780	51030
52.95	2.5	12.5	228	6.25	156.25	51984	15.63	1953.13	11852352	31.25	570	2850	7125
60.1	3.5	12.5	221	12.25	156.25	48841	42.88	1953.13	10793861	43.75	773.5	2762.5	9669
56.13	4.5	12.5	305	20.25	156.25	93025	91.13	1953.13	28372625	56.25	1372.5	3812.5	17156
54.2	5.5	12.5	291	30.25	156.25	84681	166.38	1953.13	24642171	68.75	1600.5	3637.5	20006
59.56	6.5	12.5	445	42.25	156.25	198025	274.63	1953.13	88121125	81.25	2892.5	5562.5	36156
51.51	7.5	12.5	610	56.25	156.25	372100	421.88	1953.13	2.27E+08	93.75	4575	7625	57188
40.75	8.5	12.5	437	72.25	156.25	190969	614.13	1953.13	83453453	106.25	3714.5	5462.5	46431
34.88	9.5	12.5	362	90.25	156.25	131044	857.38	1953.13	47437928	118.75	3439	4525	42988
24.92	10.5	12.5	315	110.25	156.25	99225	1157.63	1953.13	31255875	131.25	3307.5	3937.5	41344
21.51	11.5	12.5	299	132.25	156.25	89401	1520.88	1953.13	26730899	143.75	3438.5	3737.5	42981
24.75	12.5	12.5	306	156.25	156.25	93636	1953.13	1953.13	28652616	156.25	3825	3825	47813
29.46	13.5	12.5	283	182.25	156.25	80089	2460.38	1953.13	22665187	168.75	3820.5	3537.5	47756
74.62	2.5	11.5	304	6.25	132.25	92416	15.63	1520.88	28094464	28.75	760	3496	8740
75.4	3.5	11.5	230	12.25	132.25	52900	42.88	1520.88	12167000	40.25	805	2645	9258

73.07	4.5	11.5	229	20.25	132.25	52441	91.13	1520.88	12008989	51.75	1030.5	2633.5	11851
70.92	5.5	11.5	308	30.25	132.25	94864	166.38	1520.88	29218112	63.25	1694	3542	19481
74.35	6.5	11.5	609	42.25	132.25	370881	274.63	1520.88	2.26E+08	74.75	3958.5	7003.5	45523
71.04	7.5	11.5	612	56.25	132.25	374544	421.88	1520.88	2.29E+08	86.25	4590	7038	52785
57.64	8.5	11.5	518	72.25	132.25	268324	614.13	1520.88	1.39E+08	97.75	4403	5957	50635
52.37	9.5	11.5	449	90.25	132.25	201601	857.38	1520.88	90518849	109.25	4265.5	5163.5	49053
40.19	10.5	11.5	392	110.25	132.25	153664	1157.63	1520.88	60236288	120.75	4116	4508	47334
30.83	11.5	11.5	458	132.25	132.25	209764	1520.88	1520.88	96071912	132.25	5267	5267	60571
32.62	12.5	11.5	414	156.25	132.25	171396	1953.13	1520.88	70957944	143.75	5175	4761	59513
36.59	13.5	11.5	327	182.25	132.25	106929	2460.38	1520.88	34965783	155.25	4414.5	3760.5	50767
83.73	2.5	10.5	306	6.25	110.25	93636	15.63	1157.63	28652616	26.25	765	3213	8033
76.74	3.5	10.5	304	12.25	110.25	92416	42.88	1157.63	28094464	36.75	1064	3192	11172
77.09	4.5	10.5	78	20.25	110.25	6084	91.13	1157.63	474552	47.25	351	819	3686
79.52	5.5	10.5	352	30.25	110.25	123904	166.38	1157.63	43614208	57.75	1936	3696	20328
82.67	6.5	10.5	457	42.25	110.25	208849	274.63	1157.63	95443993	68.25	2970.5	4798.5	31190
81.8	7.5	10.5	631	56.25	110.25	398161	421.88	1157.63	2.51E+08	78.75	4732.5	6625.5	49691
81.58	8.5	10.5	760	72.25	110.25	577600	614.13	1157.63	4.39E+08	89.25	6460	7980	67830
82.83	9.5	10.5	567	90.25	110.25	321489	857.38	1157.63	1.82E+08	99.75	5386.5	5953.5	56558
80.01	10.5	10.5	484	110.25	110.25	234256	1157.63	1157.63	1.13E+08	110.25	5082	5082	53361
67.27	11.5	10.5	264	132.25	110.25	69696	1520.88	1157.63	18399744	120.75	3036	2772	31878
62.19	12.5	10.5	391	156.25	110.25	152881	1953.13	1157.63	59776471	131.25	4887.5	4105.5	51319
60.14	13.5	10.5	894	182.25	110.25	799236	2460.38	1157.63	7.15E+08	141.75	12069	9387	126725
86.42	2.5	9.5	304	6.25	90.25	92416	15.63	857.38	28094464	23.75	760	2888	7220
83.65	3.5	9.5	353	12.25	90.25	124609	42.88	857.38	43986977	33.25	1235.5	3353.5	11737
90.35	4.5	9.5	146	20.25	90.25	21316	91.13	857.38	3112136	42.75	657	1387	6242
92.72	5.5	9.5	217	30.25	90.25	47089	166.38	857.38	10218313	52.25	1193.5	2061.5	11338
91.68	6.5	9.5	196	42.25	90.25	38416	274.63	857.38	7529536	61.75	1274	1862	12103
90.35	7.5	9.5	594	56.25	90.25	352836	421.88	857.38	2.1E+08	71.25	4455	5643	42323
91.16	8.5	9.5	564	72.25	90.25	318096	614.13	857.38	1.79E+08	80.75	4794	5358	45543
96.08	9.5	9.5	696	90.25	90.25	484416	857.38	857.38	3.37E+08	90.25	6612	6612	62814
95.09	10.5	9.5	259	110.25	90.25	67081	1157.63	857.38	17373979	99.75	2719.5	2460.5	25835
84.08	11.5	9.5	242	132.25	90.25	58564	1520.88	857.38	14172488	109.25	2783	2299	26439
80.66	12.5	9.5	203	156.25	90.25	41209	1953.13	857.38	8365427	118.75	2537.5	1928.5	24106

55404	4104	5832	128.25	80621568	857.38	2460.38	186624	90.25	182.25	432	9.5	13.5	74.83
4973	1989	585	21.25	12812904	614.13	15.63	54756	72.25	6.25	234	8.5	2.5	80.92
12614	3604	1484	29.75	76225024	614.13	42.88	179776	72.25	12.25	424	8.5	3.5	103.83
11666	2592.5	1372.5	38.25	28372625	614.13	91.13	93025	72.25	20.25	305	8.5	4.5	126.14
12342	2244	1452	46.75	18399744	614.13	166.38	69696	72.25	30.25	264	8.5	5.5	114.49
6575	1011.5	773.5	55.25	1685159	614.13	274.63	14161	72.25	42.25	119	8.5	6.5	110.64
19380	2584	2280	63.75	28094464	614.13	421.88	92416	72.25	56.25	304	8.5	7.5	111.22
21458	2524.5	2524.5	72.25	26198073	614.13	614.13	88209	72.25	72.25	297	8.5	8.5	109.31
19299	2031.5	2270.5	80.75	13651919	614.13	857.38	57121	72.25	90.25	239	8.5	9.5	117.36
15173	1445	1785	89.25	4913000	614.13	1157.63	28900	72.25	110.25	170	8.5	10.5	118.72
42717	3714.5	5025.5	97.75	83453453	614.13	1520.88	190969	72.25	132.25	437	8.5	11.5	106.37
32300	2584	3800	106.25	28094464	614.13	1953.13	92416	72.25	156.25	304	8.5	12.5	100.07
40507	3000.5	4765.5	114.75	43986977	614.13	2460.38	124609	72.25	182.25	353	8.5	13.5	96.31
3169	1267.5	422.5	18.75	4826809	421.88	15.63	28561	56.25	6.25	169	7.5	2.5	82.98
3806	1087.5	507.5	26.25	3048625	421.88	42.88	21025	56.25	12.25	145	7.5	3.5	119.89
8303	1845	1107	33.75	14886936	421.88	91.13	60516	56.25	20.25	246	7.5	4.5	138.35
15098	2745	2013	41.25	49027896	421.88	166.38	133956	56.25	30.25	366	7.5	5.5	131.13
12236	1882.5	1631.5	48.75	15813251	421.88	274.63	63001	56.25	42.25	251	7.5	6.5	130.1
8494	1132.5	1132.5	56.25	3442951	421.88	421.88	22801	56.25	56.25	151	7.5	7.5	129.96
9116	1072.5	1215.5	63.75	2924207	421.88	614.13	20449	56.25	72.25	143	7.5	8.5	132.79
11044	1162.5	1472.5	71.25	3723875	421.88	857.38	24025	56.25	90.25	155	7.5	9.5	151.53
19688	1875	2625	78.75	15625000	421.88	1157.63	62500	56.25	110.25	250	7.5	10.5	149.8
52785	4590	7038	86.25	2.29E+08	421.88	1520.88	374544	56.25	132.25	612	7.5	11.5	143.31
76969	6157.5	10263	93.75	5.53E+08	421.88	1953.13	674041	56.25	156.25	821	7.5	12.5	131.85
115324	8542.5	15377	101.25	1.48E+09	421.88	2460.38	1E+06	56.25	182.25	1139	7.5	13.5	131.98
731	292.5	112.5	16.25	91125	274.63	15.63	2025	42.25	6.25	45	6.5	2.5	79.31
865	247	133	22.75	54872	274.63	42.88	1444	42.25	12.25	38	6.5	3.5	100.21
2048	455	315	29.25	343000	274.63	91.13	4900	42.25	20.25	70	6.5	4.5	123.43
2717	494	418	35.75	438976	274.63	166.38	5776	42.25	30.25	76	6.5	5.5	122.85
5239	806	806	42.25	1906624	274.63	274.63	15376	42.25	42.25	124	6.5	6.5	132.96
10920	1456	1680	48.75	11239424	274.63	421.88	50176	42.25	56.25	224	6.5	7.5	132.35
6243	734.5	960.5	55.25	1442897	274.63	614.13	12769	42.25	72.25	113	6.5	8.5	140.67
21921	2307.5	3372.5	61.75	44738875	274.63	857.38	126025	42.25	90.25	355	6.5	9.5	163.7

152.37	10.5	6.5	1141	110.25	42.25	1E+06	1157.63	274.63	1.49E+09	68.25	11981	7416.5	77873
151.94	11.5	6.5	1211	132.25	42.25	1E+06	1520.88	274.63	1.78E+09	74.75	13927	7871.5	90522
132.52	12.5	6.5	872	156.25	42.25	760384	1953.13	274.63	6.63E+08	81.25	10900	5668	70850
122.83	13.5	6.5	914	182.25	42.25	835396	2460.38	274.63	7.64E+08	87.75	12339	5941	80204
*	2.5	5.5	0	6.25	30.25	0	15.63	166.38	0	13.75	0	0	0
*	3.5	5.5	0	12.25	30.25	0	42.88	166.38	0	19.25	0	0	0
114.43	4.5	5.5	0	20.25	30.25	0	91.13	166.38	0	24.75	0	0	0
130	5.5	5.5	10	30.25	30.25	100	166.38	166.38	1000	30.25	55	55	303
152.2	6.5	5.5	77	42.25	30.25	5929	274.63	166.38	456533	35.75	500.5	423.5	2753
157.66	7.5	5.5	152	56.25	30.25	23104	421.88	166.38	3511808	41.25	1140	836	6270
162.22	8.5	5.5	147	72.25	30.25	21609	614.13	166.38	3176523	46.75	1249.5	808.5	6872
164.49	9.5	5.5	1037	90.25	30.25	1E+06	857.38	166.38	1.12E+09	52.25	9851.5	5703.5	54183
140.89	10.5	5.5	1178	110.25	30.25	1E+06	1157.63	166.38	1.63E+09	57.75	12369	6479	68030
123.52	11.5	5.5	740	132.25	30.25	547600	1520.88	166.38	4.05E+08	63.25	8510	4070	46805
113.14	12.5	5.5	758	156.25	30.25	574564	1953.13	166.38	4.36E+08	68.75	9475	4169	52113
110.04	13.5	5.5	757	182.25	30.25	573049	2460.38	166.38	4.34E+08	74.25	10220	4163.5	56207
*	2.5	4.5	0	6.25	20.25	0	15.63	91.13	0	11.25	0	0	0
*	3.5	4.5	0	12.25	20.25	0	42.88	91.13	0	15.75	0	0	0
*	4.5	4.5	0	20.25	20.25	0	91.13	91.13	0	20.25	0	0	0
146.46	5.5	4.5	0	30.25	20.25	0	166.38	91.13	0	24.75	0	0	0
162.84	6.5	4.5	97	42.25	20.25	9409	274.63	91.13	912673	29.25	630.5	436.5	2837
173.47	7.5	4.5	250	56.25	20.25	62500	421.88	91.13	15625000	33.75	1875	1125	8438
209.58	8.5	4.5	0	72.25	20.25	0	614.13	91.13	0	38.25	0	0	0
225.36	9.5	4.5	94	90.25	20.25	8836	857.38	91.13	830584	42.75	893	423	4019
155.98	10.5	4.5	132	110.25	20.25	17424	1157.63	91.13	2299968	47.25	1386	594	6237
115.02	11.5	4.5	442	132.25	20.25	195364	1520.88	91.13	86350888	51.75	5083	1989	22874
121.8	12.5	4.5	622	156.25	20.25	386884	1953.13	91.13	2.41E+08	56.25	7775	2799	34988
116.18	13.5	4.5	687	182.25	20.25	471969	2460.38	91.13	3.24E+08	60.75	9274.5	3091.5	41735

APPENDIX 4

Correspondence with NOAA-NASA regarding PAL dataset

From: daacuso@eosdata.gsfc.nasa.gov[SMTP:daacuso@eosdata.gsfc.nasa.gov]
Sent: Tuesday, March 26, 2002 10:25 PM
To: s.a.yelwa@stir.ac.uk
Cc: psmith@eosdata.gsfc.nasa.gov
Subject: Re: Mean NDVI Plot form PAL data.xls

Your message has been received by the AVHRR Land Science User Support Team at the NASA GSFC DAAC. We will investigate your query and contact you as soon as possible. Meanwhile, if you have additional questions, please contact us at psmith@daac.gsfc.nasa.gov. Thank you.

AVHRR Land Science User Support Team

Your tracking number:

AVHRR00162

This message is in MIME format. Since your mail reader does not understand this format, some or all of this message may not be legible.

------_=_NextPart_000_01C1D4FD.251C2360
Content-Type: text/plain

Dear Dr. Smith,

I write seek your assistance and clarification please.
I refer to your highlighted article in the Photogrammetric Engineering and Remote Sensing Journal (1997) Vol. 63 No.1 pp 12 - 37 as I am not sure if the problem with the attached Mean NDVI plot below from 1986 to 1999 of a subset from the AVHRR 8-km PAL dataset covering Long 2.00 to 14.00degress and Lat 4.15 to 14.00 degrees is due to processing errors because of the big differences in the means.

The NDVI data I am using at present in my research was originally downloaded in June 2000 from the Pathfinder dataset. I am wondering whether the data in the Pathfinder archive has undergone another correction since then or the changes in the means observed here are true surface changes.

I masked the water areas (Bight of Benin in the South of Nigeria, Lake Chad and Kainji Lake in Nigeria) out before calculating the means. The plot is below

 <<Univariate Statistics for Masked NDVI Images.xls>>

Sadiq Yelwa
Department of Environmental Science
University of Stirling
FK9 4LA
U.K.
Tel. +(44) (0)1786 467862
Fax. +(44) (0)1786 467843

E-mail   s.a.yelwa@stir.ac.uk

From: Peter Smith[SMTP:psmith@eosdata.gsfc.nasa.gov]
Sent: Tuesday, March 26, 2002 11:52 PM
To: s.a.yelwa@stir.ac.uk
Subject: Re: Mean NDVI Plot form PAL data.xls

ndvi.gif

Hi Sadiq,

I thought you might be interested in some preliminary results. The
enclosed gif image shows a time-series plot for the area of interest.
We have a tool here that calculates the average ndvi for the area
selected and plots out each 10-day value for the computed average.

We will calculate yearly means tomorrow. But in the interim, the plot
shows as expected a gap for September- December for 1994 when we have a
missing data gap. Your computed yearly mean for 1994 would thus not be
very reliable for comparing with the other years.

We are on a scale of -1.0 to +1.0 for our ndvi and your ndvi is scaled
and is on a range of 0-255. To inter-convert

scaled_ndvi = float_ndvi*125 + 128

In January of 1995 the dataset switches satellites form NOAA-11 to
NOAA-14. There does seem to be a bit of a drop in the ndvi, but nothing
too dramatic.

I am also curious about your statement of masking out certain water
covered regions. You should be able to use the mask included with our
ndvi data to remove any water covered region of 8 * 8 km areas or more.
Thus the only ndvi values you should allow into your calculations are
land pixels which have scaled ndvi values in the 3-253 range.

ndvi values of 0-2 are special values with
ndvi =0 ... missing data
    =1 ... ocean/ inland lake data
    =2 ... non-physical space

Regards
Peter Smith

Org.   Goddard DAAC http://daac.gsfc.nasa.gov Work Phone 301-614-5325

===

The GIF Image above
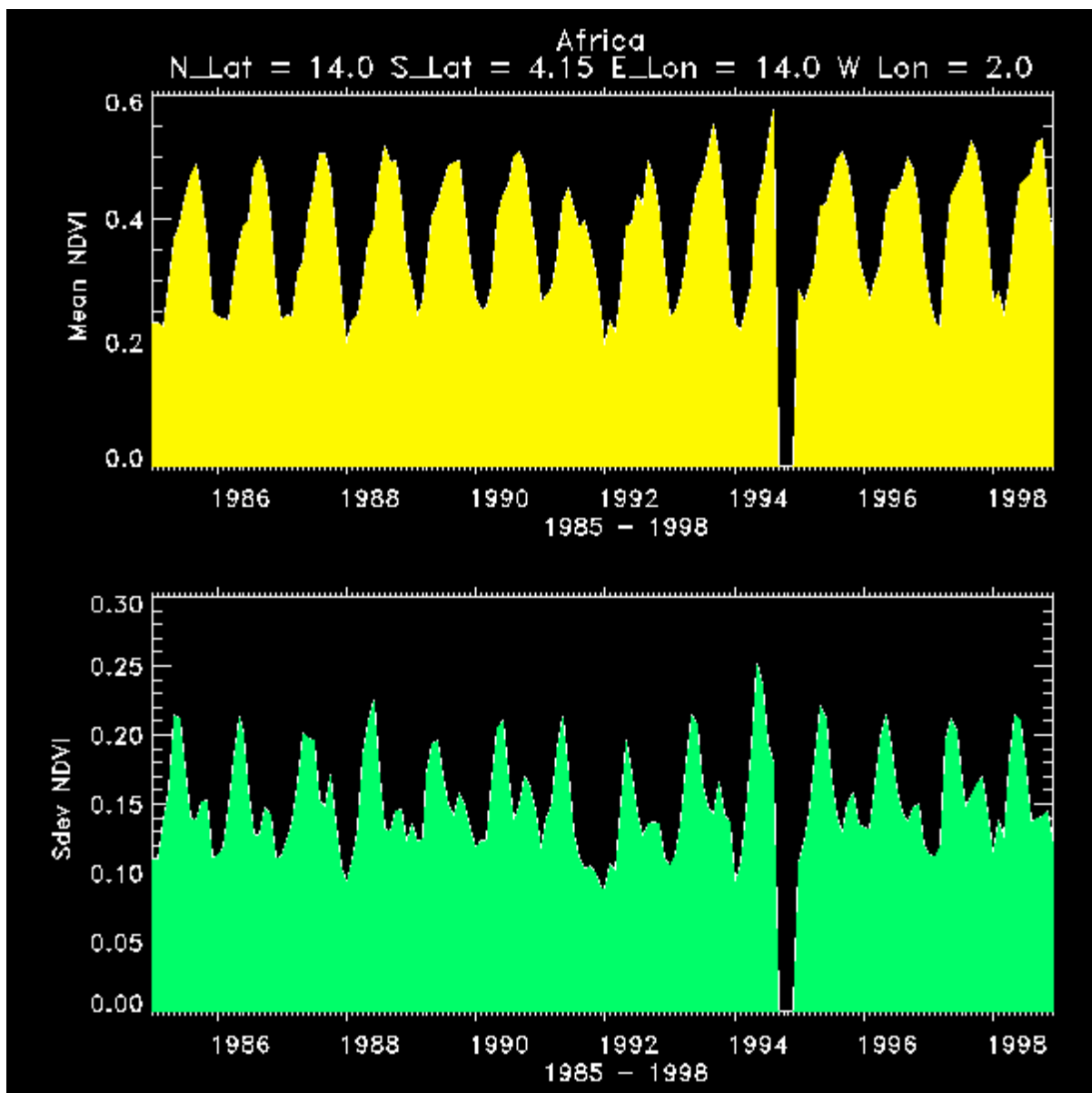
From: psmith@eosdata.gsfc.nasa.gov[SMTP:psmith@eosdata.gsfc.nasa.gov]
Sent: Wednesday, March 27, 2002 5:55 PM
To: s.a.yelwa@stir.ac.uk
Cc: daacuso@eosdata.gsfc.nasa.gov; psmith@eosdata.gsfc.nasa.gov;
tzhu@eosdata.gsfc.nasa.gov
Subject: (AVHRR00162) Re: Mean NDVI Plot form PAL data.xls

GDAAC User Assistance System -- Tracking Number: AVHRR00162
The above tracking number has been updated.
===

Hi Sadiq,

The tool, to which I referred in my earlier email, actually calculates statistics for our monthly data. I suspect you were using our 10-day data. The monthly statistics based on a maximum value monthly will have slightly higher ndvi values than the 10-day product. We calculated yearly means for our monthly data and reproduce your values very closely for time periods prior to 1995, but for periods later than 1994 we disagree. Here are the results of our calculations using the same regional area in Africa for which your data was produced.

```
n_month     168
year   1985   mean    0.348719   count   171
year   1986   mean    0.358737   co
unt   172
year   1987   mean    0.362278   count   173
year   1988   mean    0.371277   count   174
year   1989   mean    0.385215   count   176
year   1990   mean    0.386375   count   176
year   1991   mean    0.347542   count   171
year   1992   mean    0.354463   count   172
year   1993   mean    0.392049   count   177
year   1994   mean    0.248975   count   159
year   1995   mean    0.393147   count   177
year   1996   mean    0.390732   count   176
year   1997   mean    0.399027   count   177
year   1998   mean    0.392961   count   177
```

1994 is of course not a reliable year.

Thus our yearly means are relatively constant. These means were calculated for your geographic area, monthly data and land pixels only.

We checked our production records and note our 1995-1999 data was corrected and replaced on April 6, 2000. I suspect that maybe you downloaded prior to this date and not June 2000 as you say.

Please download again and verify you can repeat your original results. If you can then that would indicate a difference between our monthly and 10-day products.

Please keep us informed on your progress.

Regards
Peter M. Smith

From:	psmith@eosdata.gsfc.nasa.gov[SMTP:psmith@eosdata.gsfc.nasa.gov]
Sent:	Thursday, March 28, 2002 5:32 PM
To:	s.a.yelwa@stir.ac.uk
Cc:	daacuso@eosdata.gsfc.nasa.gov; psmith@eosdata.gsfc.nasa.gov; tzhu@eosdata.gsfc.nasa.gov
Subject:	(AVHRR00162) Re: Mean NDVI Plot form PAL data.xls

GDAAC User Assistance System -- Tracking Number: AVHRR00162
The above tracking number has been updated.
===

The status for AVHRR00162 has been changed to: closed.

Hi Sadiq,

I am glad we have been able to straighten out your problem. We do not have any plans for updating the PAL ndvi archive data.

Good luck with your research and sorry for any delay we might have caused you!

Regards,

Peter Smith

===

```
----------
```
From: Peter M. Smith[SMTP:psmith@eosdata.gsfc.nasa.gov]
Sent: Monday, September 11, 2000 2:19 PM
To: Sadiq Yelwa {PG}
Cc: tzhu@eosdata.gsfc.nasa.gov
Subject: Fwd: Rao calibration for channel 1,2 NOAA 7,9,11,14

Hi Sadiq,

Here is the requested information. The corrections were applied to the
radiances for channels 1,2. If you require further background information
on how these coefficients were used in the s/w code please contact my
programmer Ms. Tong Zhu.

The following coefficients were supplied by Dr. N. Rao of NOAA to the PAL
processing task to remove the degradation of Channel 1,2 radiance
measurements and normalize the channel 1,2 radiances to that of NOAA 9.

They were used in the following equations.

channel_gain = A1 * exp(A2 * post-launch)
channel_offset = C0

post_launch = days from launch_date

channel_calibrated_flux = (channel_count _ offset)* gain

a.   NOAA-7 was launched on June 23, 1981.

b.   Channels 1 and 2
      Channel 1:   A1 = 0.5753
               A2 = 1.01e-4
               C0 = 36.0

      Channel 2:   A1 = 0.3914
               A2 = 1.2e-4
               C0 = 37.0

a.   NOAA-9 was launched on December 12, 1984.

b.   Channels 1 and 2
      Channel 1:   A1 = 0.5406
               A2 = 1.66e-4
               C0 = 37.0

      Channel 2:   A1 = 0.3808
               A2 = 0.98e-4
               C0 = 39.6

a.   NOAA-11 was launched on September 24, 1988.

b.   Channels 1 and 2
       Channel 1:   A1 = 0.5496
                          A2 = 0.33e-4
                          C0 = 40.0

       Channel 2:   A1 = 0.3680
                          A2 = 0.55e-4
                          C0 = 40.0

a.   NOAA-14 was launched on December 30, 1994.

b.   Channels 1 and 2
       Channel 1:   A1 = 0.566
                          A2 = 0.0001219
                          C0 = 41.0

       Channel 2:   A1 = 0.440
                          A2 = 0.0000989
                          C0 = 41.0

Regards,
Peter Smith

Appendix 5 : Residual images for the annual mean NDVI images derived from Image Deviations

The images were contrast stretched for visual purposes so as to highlight potential pixels that deviate from the overall mean image of the time-series dataset.
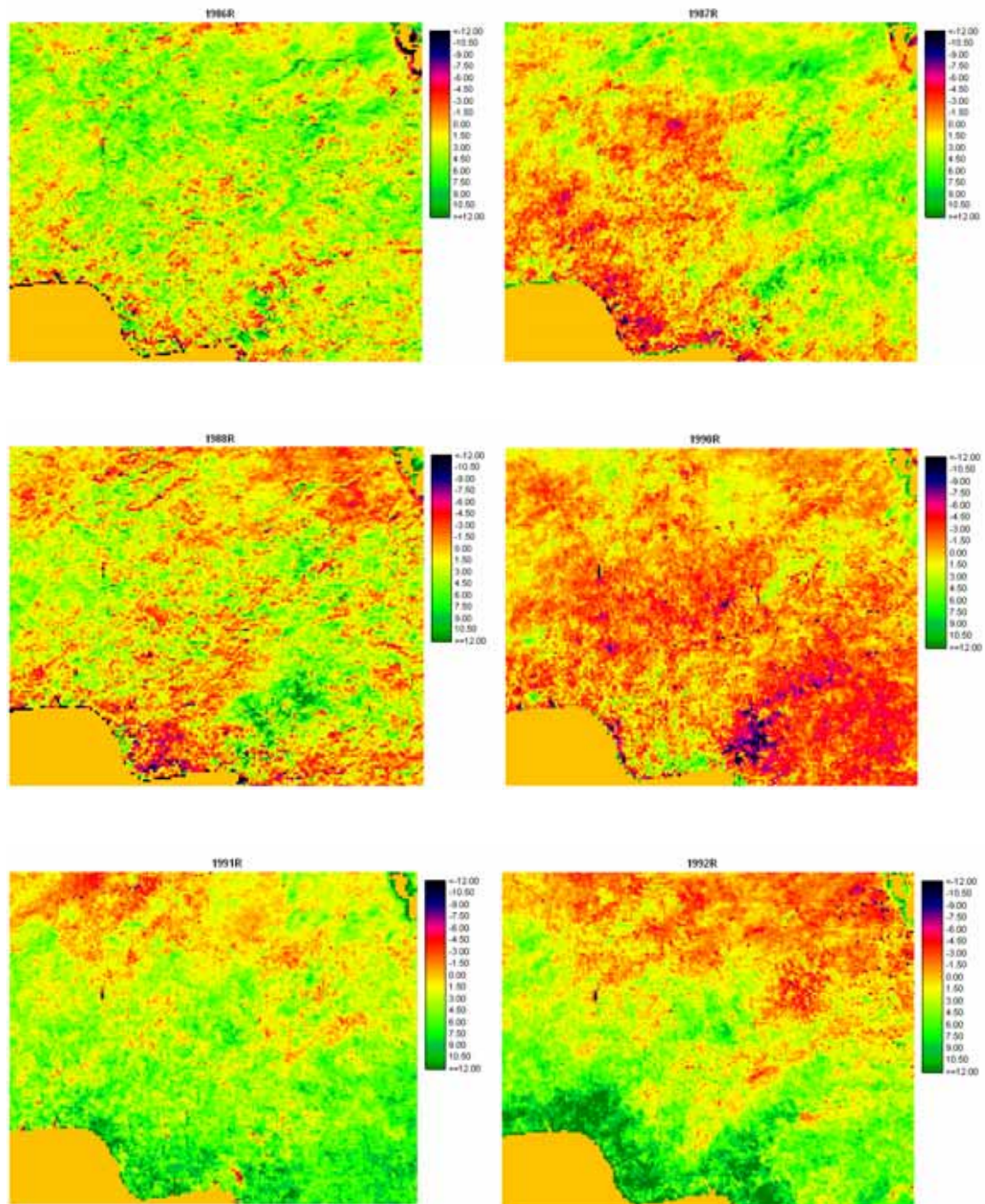
Appendix 5 *(Cont.)* : *Residual images for the annual Mean NDVI images derived from Image Deviations*

The images were contrast stretched for visual purposes so as to highlight potential pixels that deviate from the overall mean image of the time-series dataset.
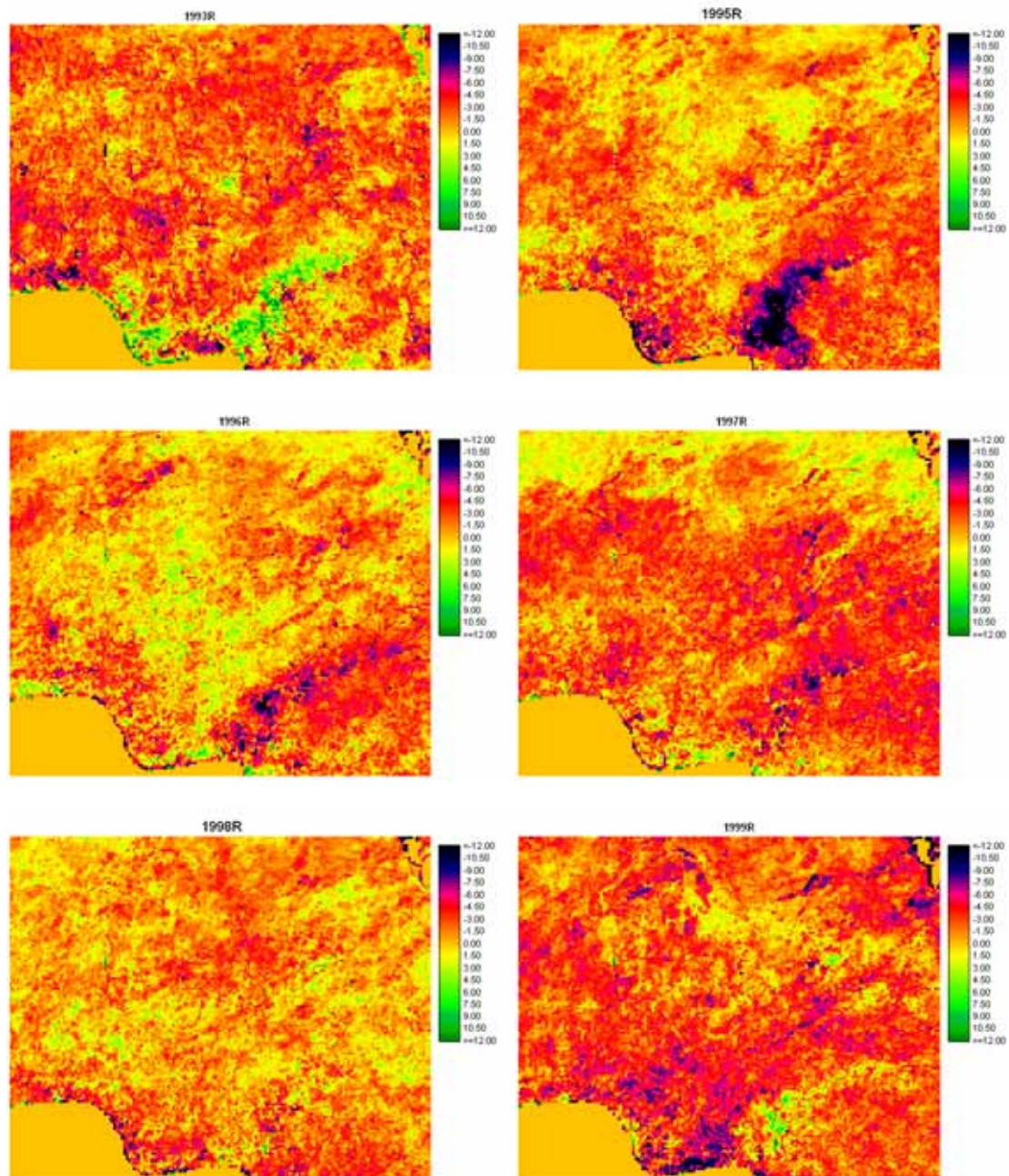
Appendix 6 : Gradients of NDVI and Rainfall for selected Pixel pairs of NDVI heterogeneity in the Savanna and Forest Areas on the 1986 Base image
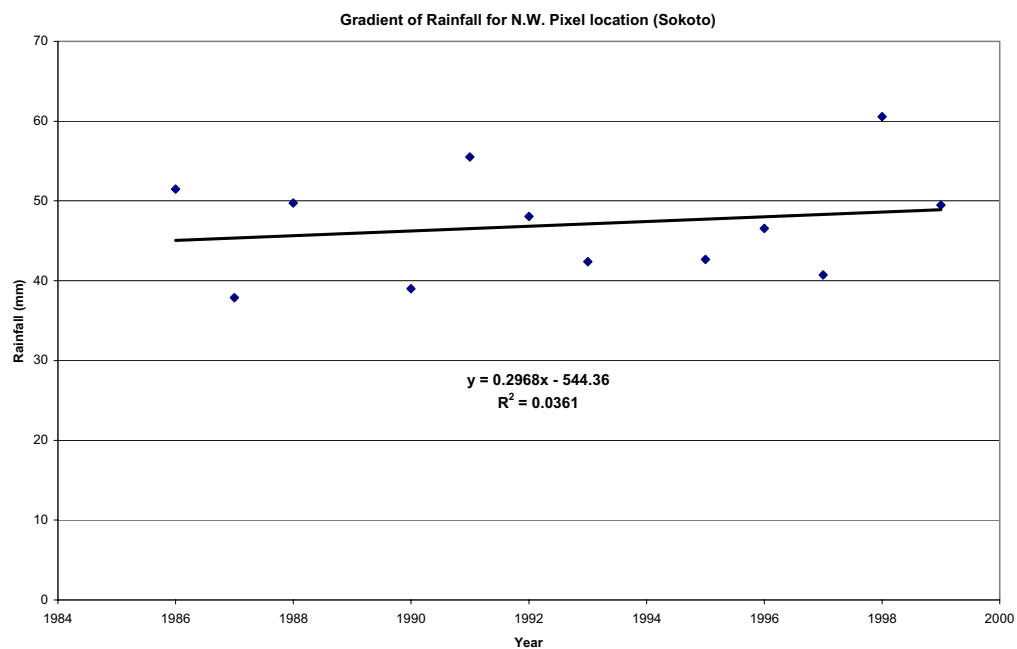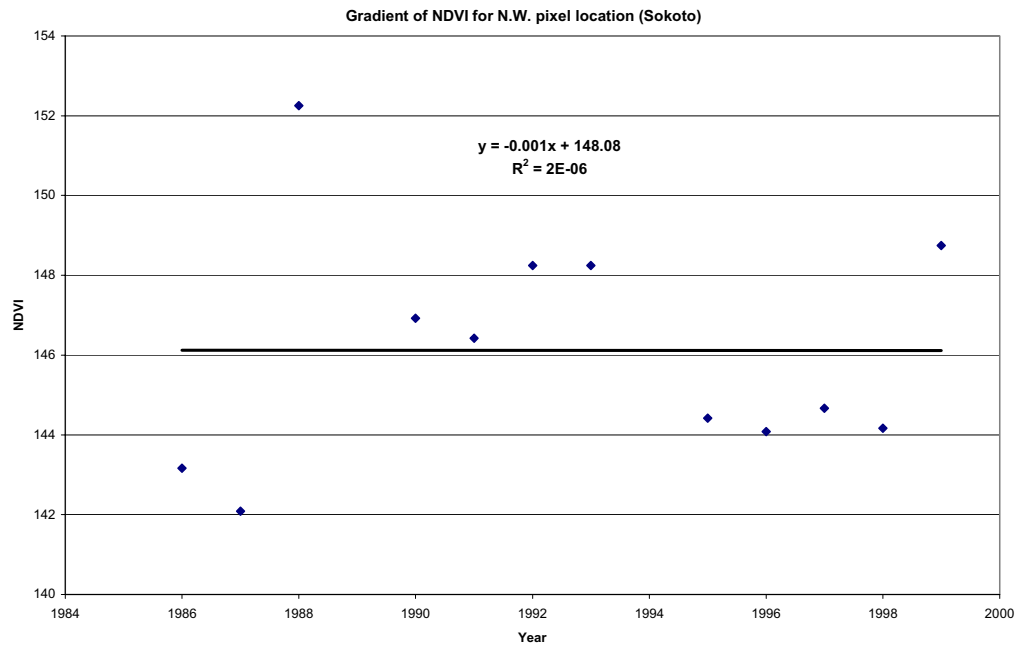
Gradient of NDVI for N.W. pixel location (Sokoto)

$y = -0.001x + 148.08$
$R^2 = 2E\text{-}06$

Gradient of Rainfall for N.W. Pixel location (Sokoto)

$y = 0.2968x - 544.36$
$R^2 = 0.0361$

Appendix 6 (Cont.) Gradients of NDVI and Rainfall for selected Pixel pairs

Gradient of NDVI for N.E. pixel location (Hadejia)

$y = 0.5081x - 864.37$
$R^2 = 0.6836$

Gradient of Rainfall for N.E. pixel location (Hadejia)

$y = 1.0668x - 2090.7$
$R^2 = 0.2685$

316

Appendix 6 (Cont.) Gradients of NDVI and Rainfall for selected Pixel pairs

Gradient of NDVI for S.W. Forest pixel location

$y = 0.582x - 965.85$
$R^2 = 0.2549$

Gradient of Rainfall for S.W. Forest pixel location

$y = 2.3881x - 4616.4$
$R^2 = 0.3545$

Appendix 6 (Cont.) Gradients of NDVI and Rainfall for selected Pixel pairs

Gradient of Rainfall for S.E. pixel Location (Cameroon)

y = 2.8101x - 5450.1
$R^2 = 0.3926$

Gradient of NDVI and Rainfall

y = 0.1602x + 0.1176
$R^2 = 0.508$
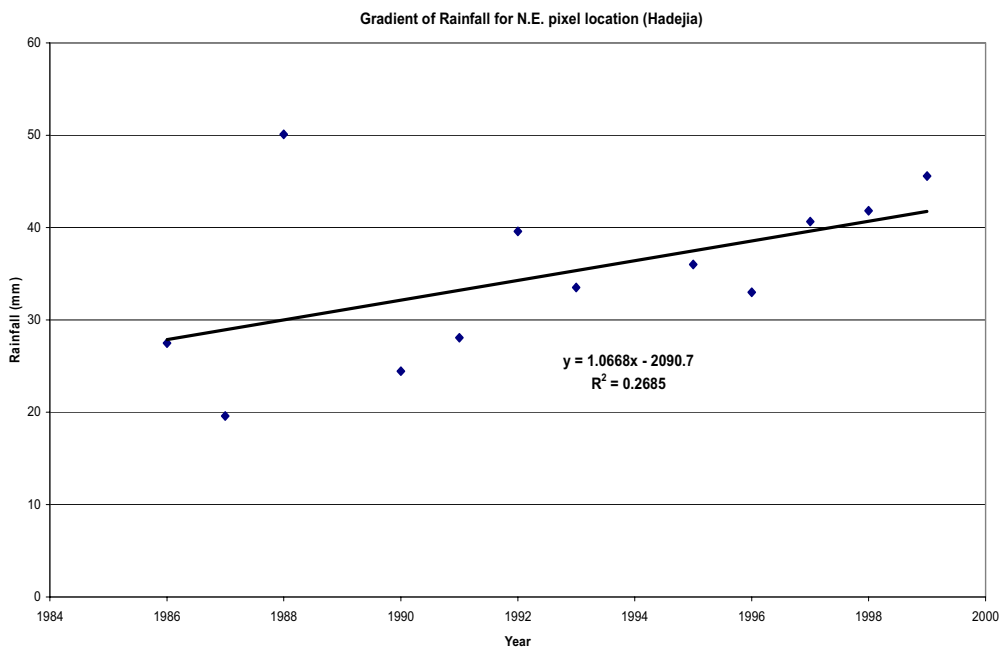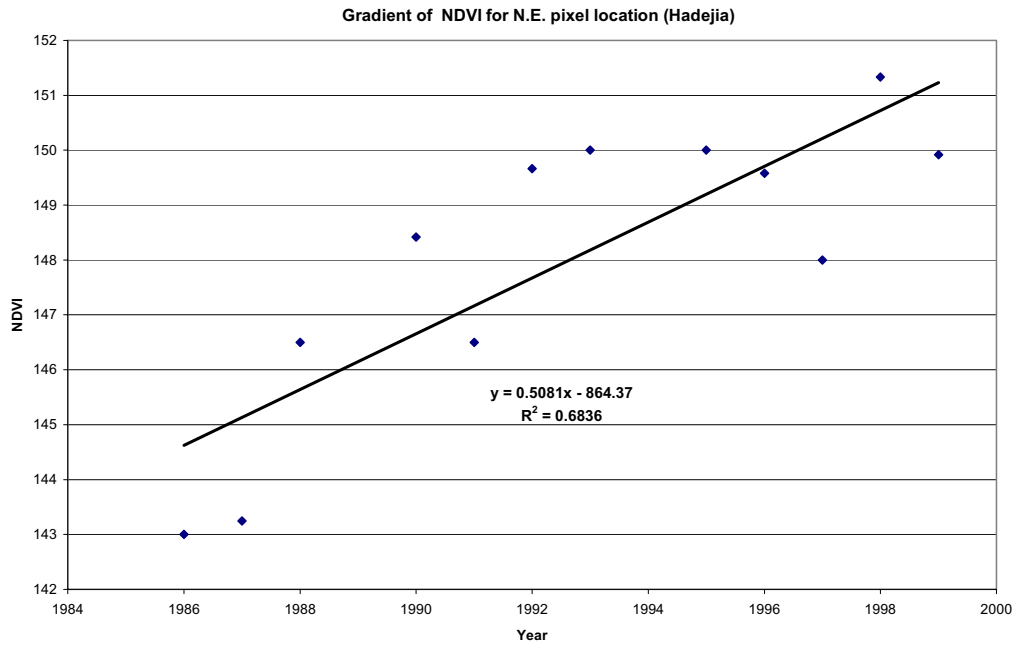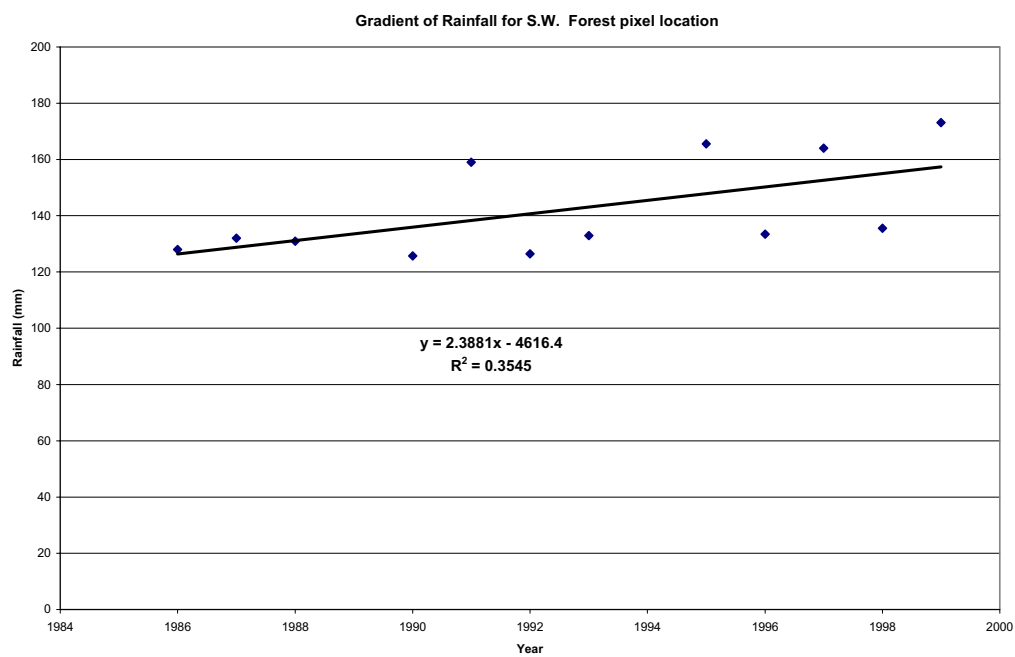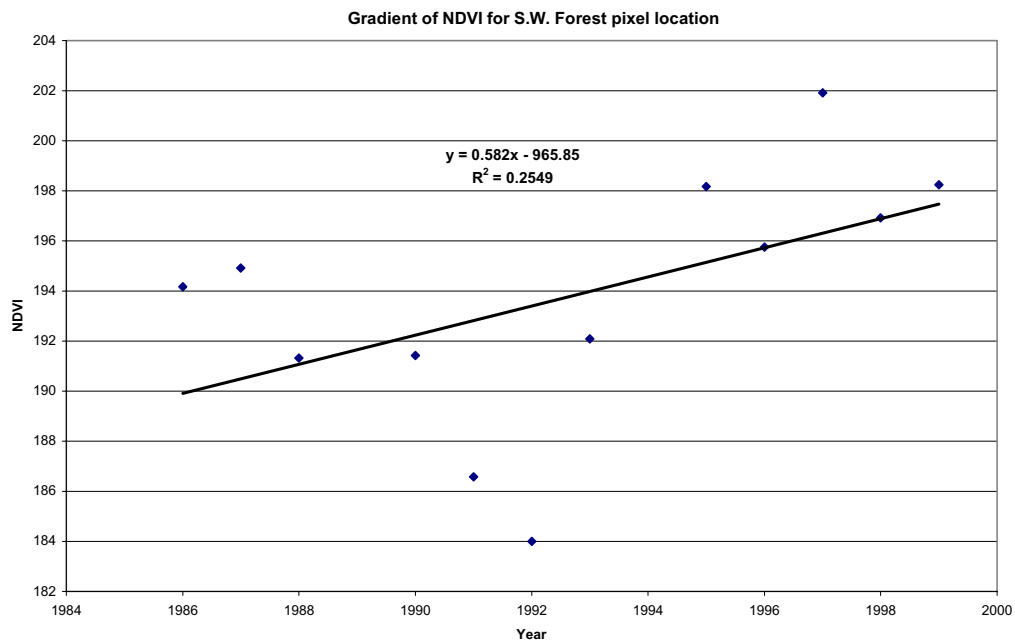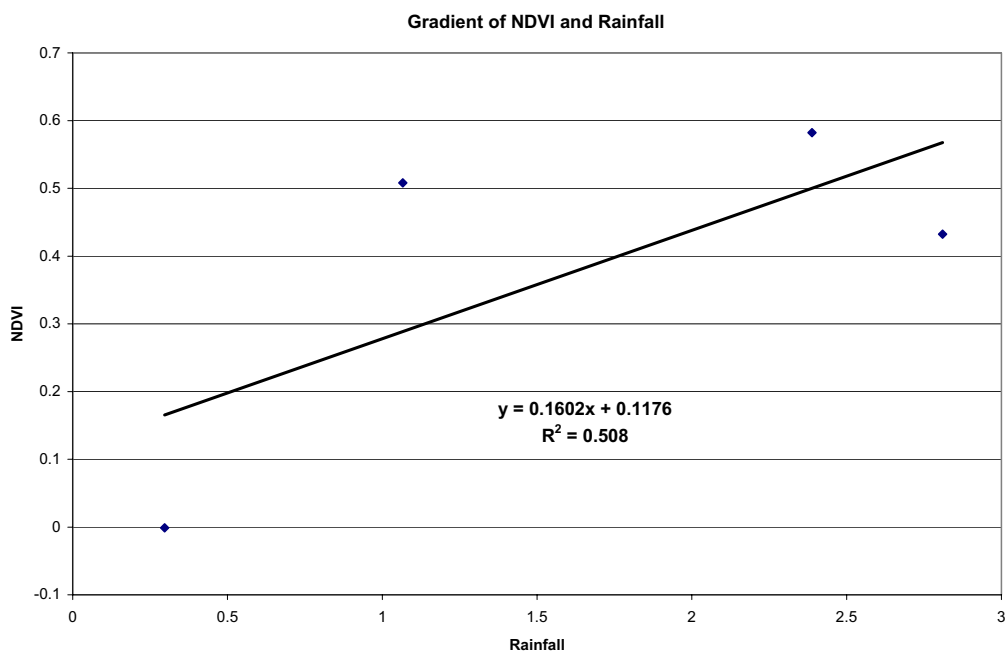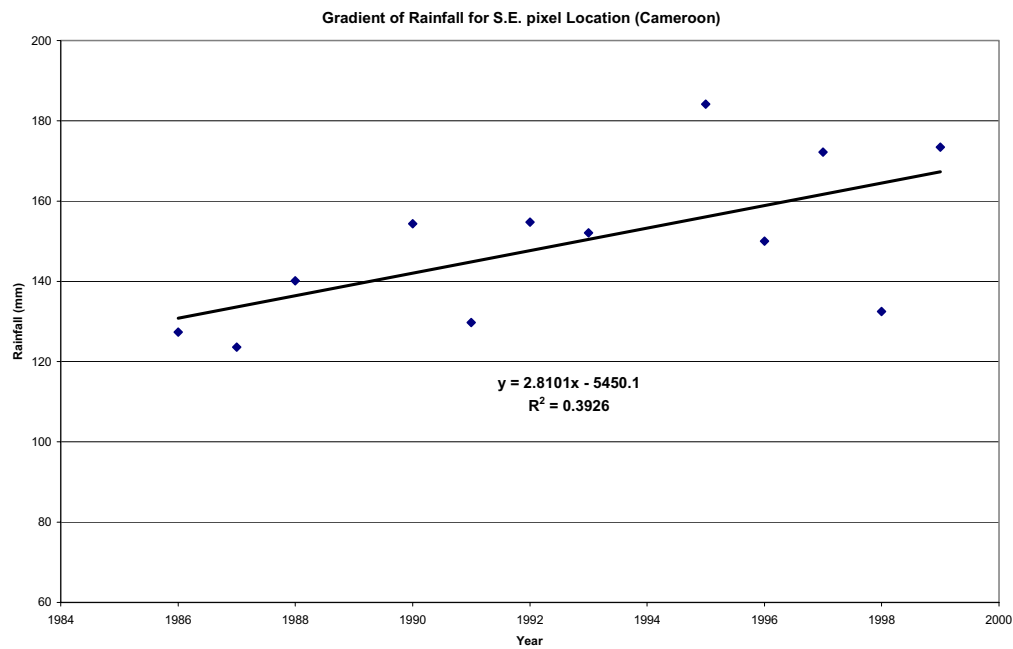
APPENDIX 7 - Some of the Standardised Principal Component Images from PCA Analysis
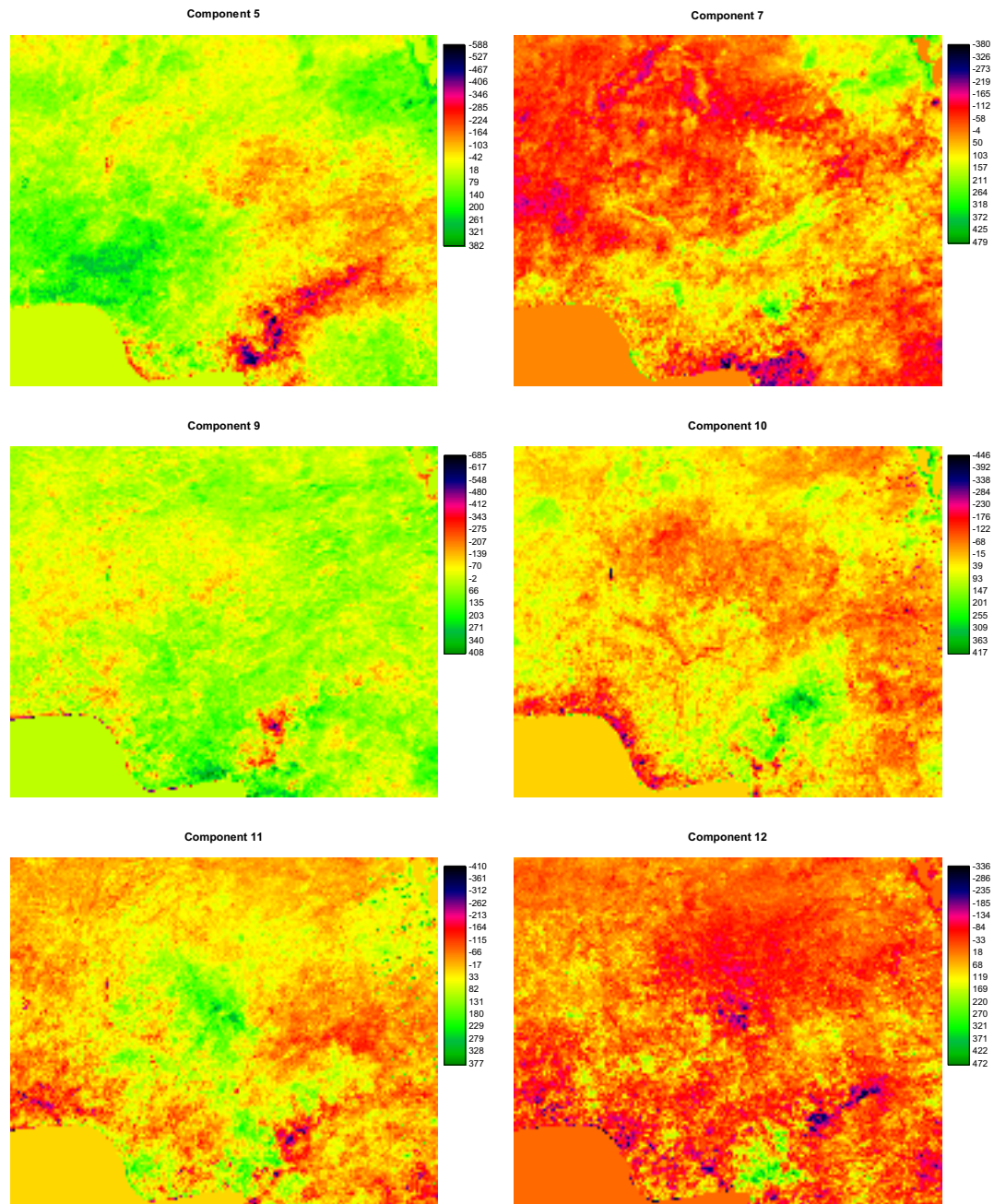
APPENDIX 7 (Cont.) - Some of the Standardised Principal Component Images from PCA Analysis
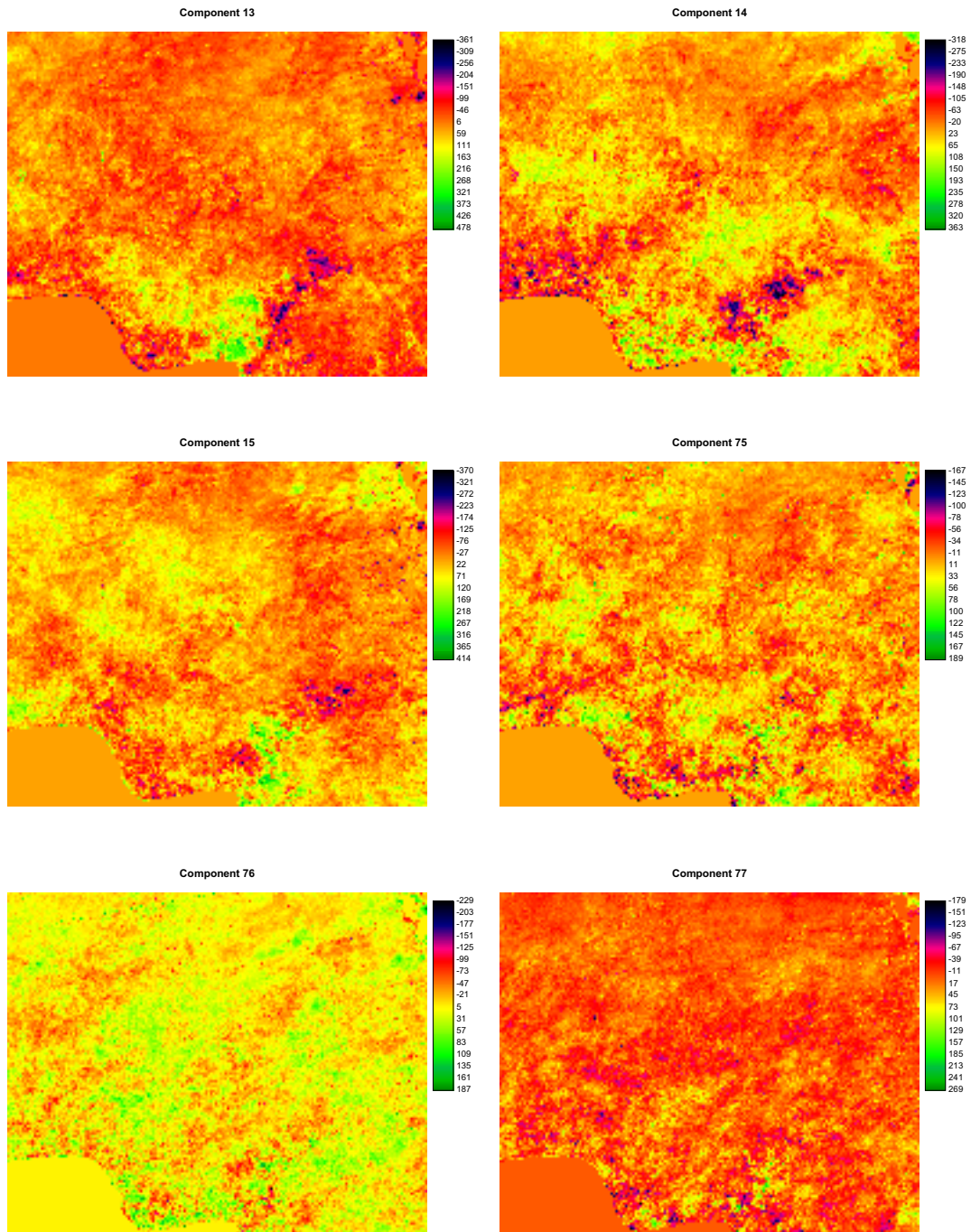
Component 13

Component 14

Component 15

Component 75

Component 76

Component 77

APPENDIX 7 (Cont.) - Some of the Standardised Principal Component Images from PCA Analysis
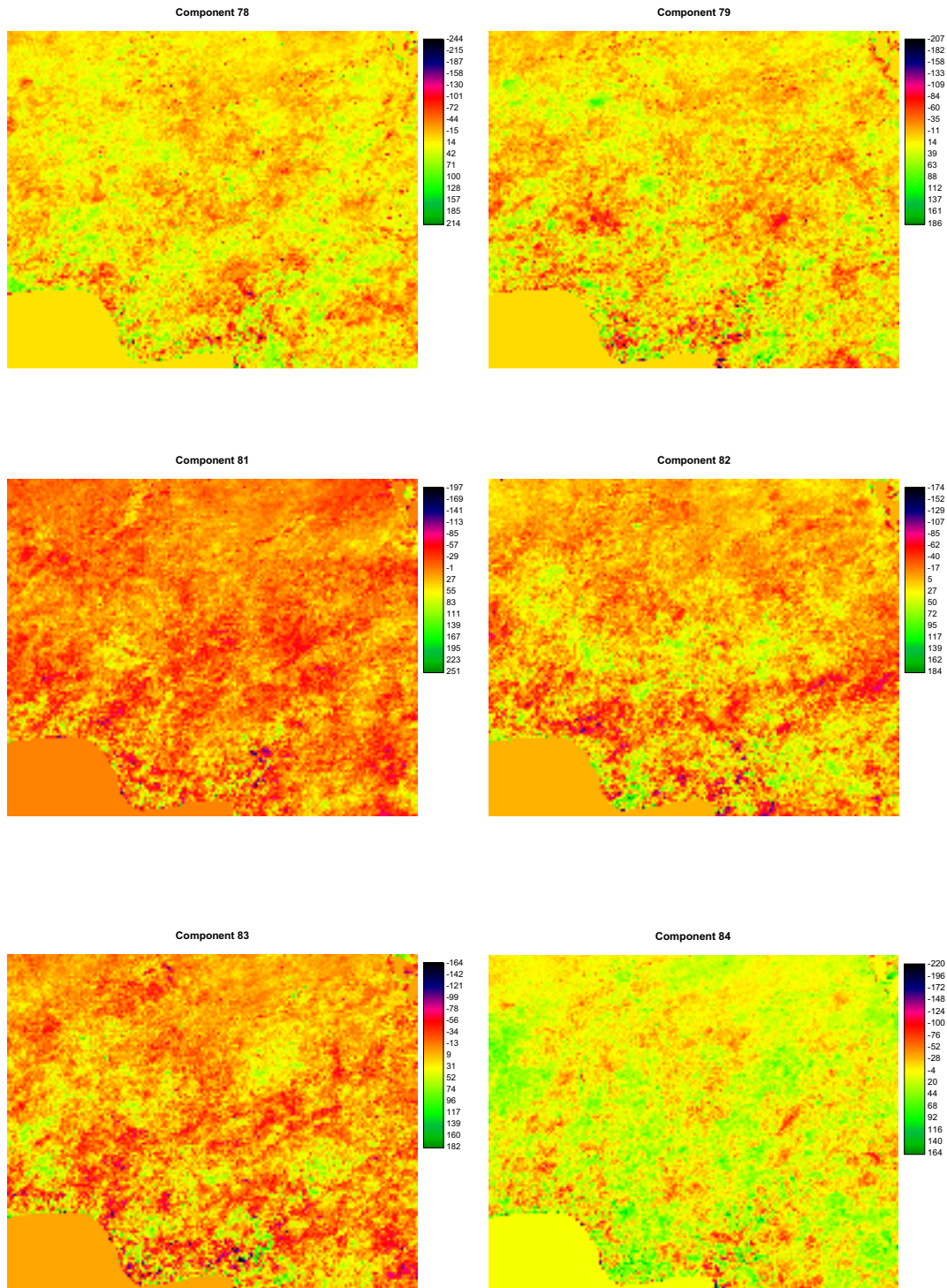
Appendix 8 – **Inter-seasonal Coefficient of Variation Image Covering the Study
Area centred on Nigeria**
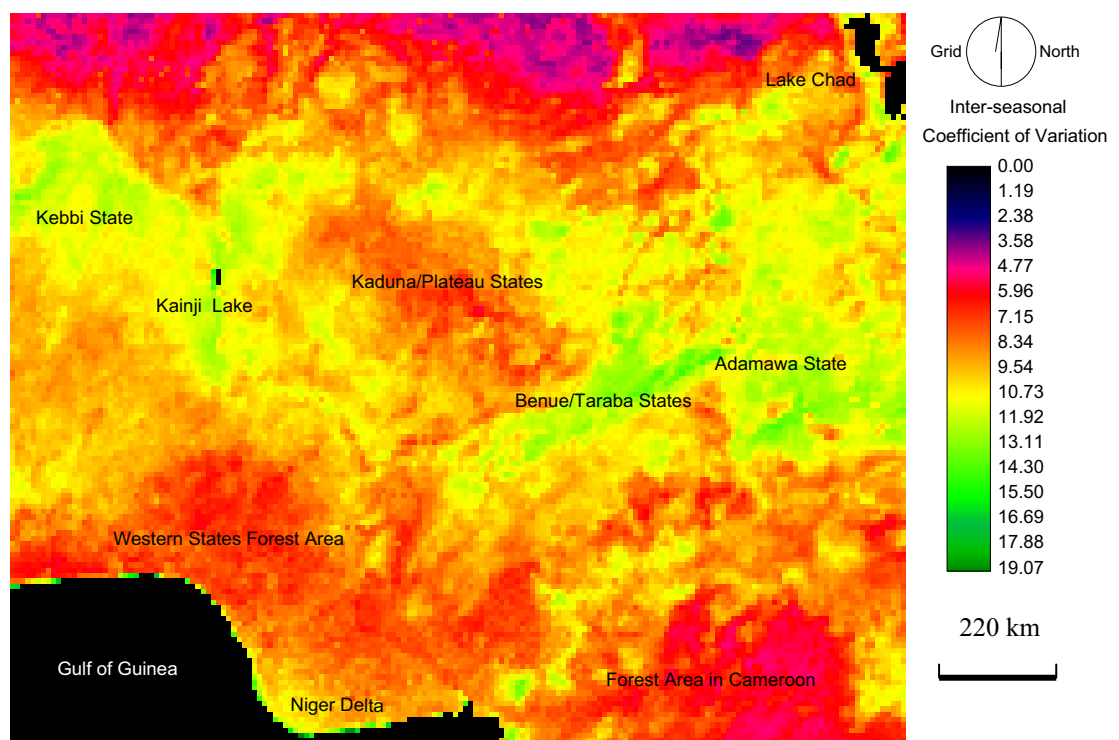
This image was derived from the 144 monthly NDVI-MVCs. It highlights areas with maximum inter-monthly (inter-seasonal) variability. Areas of high seasonal variability are located in the coastal areas and Niger Delta, around Kainji Lake and Kebbi state in the north-west (around Nigeria-Benin boarder), around Lake Chad as well as parts of Benue, Taraba and Adamawa states. Places with less inter-seasonal coefficient of variation in NDVI are located around parts of Kaduna and Plateau states in the central savanna zone, the south-west forest zone and the humid tropical forest area of Cameroon in the southeast. Areas around the coastal region and particularly in the Niger Delta area still show signs of very high inter-seasonal coefficient of variation in NDVI.

REFERENCES

Abubakar, S. M. and Mundi, R. (2000). The Federal Capital Territory (Abuja). In Mamman A.B., Oyebanji, J.O. and Petters, S.W. (Editors.), *Nigeria : A People United, A Future Assured, Volume 2,* Federal Ministry of Information, Abuja, Nigeria, Gabumo Publishing Company Ltd Calabar, Nigeria pp. 562 – 578.

Adalemo, I. A. and Baba, J. M. (1993). Rural Development. In Adalemo, I. A. and Baba, J. M. (Editors.), *Nigeria : Giant in the Tropics, Volume 1,* Federal Ministry of Information, Abuja, Nigeria, Gabumo Publishing Company Ltd Lagos, Nigeria pp. 331 – 336.

Adams, J. M. (1999). A suggestion for an improved vegetation scheme for local and global mapping and monitoring. *Environmental Management*, **23**, 1 -13.

Adams, W. M. (1985). The downstream impacts of dam construction : a case study from Nigeria. *Transactions, Institute of British Geographers, N. S.*, **10**, 292 - 302.

Adams, W. M. and Thomas, D. H. L. (1996). Conservation and sustainable resource use in Hadejia-Jama'are Valley, Nigeria. *ORYX*, **30**, 131 - 142.

Adamu, I. A. (2000). Katsina State. In Mamman A.B., Oyebanji, J.O. and Petters, S.W. (Editors.), *Nigeria : A People United, A Future Assured, Volume 2* pp. 290 – 302, Federal Ministry of Information, Abuja, Nigeria, Gabumo Publishing Company Ltd Calabar, Nigeria.

Adejuwon, J. O. and Adesina, F. A. (1988). Vegetation patterns along the forest savanna boundary in Nigeria. *Singapore Journal of Tropical Geography*, **9,** 18 – 32.

Adejuwon, J. O. (1974). Savanna in the forest areas of western Nigeria : distribution and vegetation characteristics. *Journal of Tropical Geography, 39,* 1 – 10.

Adeniyi, P. O. (1980). Land-Use Change Analysis Using Sequential Aerial Photography and Computer Techniques. *Photogrammetric Engineering and Remote Sensing*, **46**, 1447-1464.

Adeniyi, P. O. (1985). Digital Analysis of Multi-temporal Landsat Data for Land use/Land-cover Classification in a Semi-Arid Area of Nigeria. *Photogrammetric Engineering and Remote Sensing*, **46**, 1447-1464.

Adepetu, J. A. (1994). Soil fertility Management and Sustainable Farming Systems. *National Development Authority (NALDA) Workshop*, Minna, Nigeria.

Adeyemo, A. M. (2000). Rivers State. In Mamman A.B., Oyebanji, J.O. and Petters, S.W. (Eds.), *Nigeria : A People United, A Future Assured, Volume 2* pp. 485 – 496, Federal Ministry of Information, Abuja, Nigeria, Gabumo Publishing Company Ltd Calabar, Nigeria.

Afeti, G. M. and Resch, F. J. (2000). Physical Characteristics of Saharan Dust near the Gulf of the Gulf of Guinea. *Atmospheric Environment, 34,* 1273 - 1279.

Akintola, F. O. (1982). Nigeria : Relief and Drainage. In Barbour, K.M., Oguntoyinbo, J. S., Onyemelukwe, J. O. C. and Nwafor, J. C. (Editors) *Nigeria in Maps* pp 8 – 9, Hodder and Stoughton Ltd London.

Alaku, S. O. and Moruppa, S. M. (1993). Tuberculosis condemnations in livestock slaughtered for meat in northeastern Nigeria. *Preventive Veterinary Medicine* **15,** 67 - 72.

Aliyu, M. M., Obi, T. U. and Egwu, G. O. (2000). Prevalence of contagious bovine pleuropneumonia (CBPP) in northern Nigeria. *Preventive Veterinary Medicine,* **47,** 263 - 269.

Ameh, J. A., Egwu, G. O. and Tijjani, A. N. (2000). Mortality in Sahelian goats in Nigeria. *Preventive Veterinary Medicine.* **44,** 107 - 111.

Andrew, K. S., Wietske B., Karin, S., and Lalit, K. (1997). Use of Remote Sensing and GIS for sustainable land management. *ITC Journal*, **3/4,** 302 - 315.

Anene, B. M., Chime, A. B., Jibike, G.I. and Anika, S. M. (1991). Prevalence of trypanosomiasis in Zebu cattle at Obiudu ranch – a tsetse-free zone in Nigeria. *Preventive Veterinary Medicine,* **10,** 257 - 260.

Anyamba, A. (1994). Retrieval of the ENSO Signal from Vegetation Index Data. *The Earth Observer*, **6,** 24 - 26.

Anyamba, A. and Eastman, J. R. (1996). Interannual variability of NDVI over Africa and its relation to El-Nino/Southern Oscillation. *International Journal of Remote Sensing*, **17,** 2533-2548.

Anyamba, A., Tucker, C. J. and Eastman, J.R. (2001). NDVI anomaly patterns over Africa during the 1997/98 ENSO warm event. *International Journal of Remote Sensing*, **22,** 1847 - 1859.

Anyamba, A., Linthicum, J., Mahoney, R., Tucker, C.J. and Kelley, P.W. (2002). Mapping potential risk of Rift Valley fever outbreaks in African Savanna using Vegetation Index Time Series Data. *Photogrammetric Engineering and Remote Sensing*, **68,** 137 - 145.

Apan, A. A. (1997). Land Cover Mapping for Tropical Forest Rehabilitation Planning using Remotely - Sensed Data. *International Journal of Remote Sensing*, **18,** 1029-1049.

Areaola, O. (1982a). Nigeria : Vegetation. In Barbour, K.M., Oguntoyinbo, J. S., Onyemelukwe, J. O. C. and Nwafor, J. C. (Editors) *Nigeria in Maps*. Hodder and Stoughton Ltd. London, pp 24 – 25.

Areaola, O. (1982b). Nigeria : Soils. In Barbour, K.M., Oguntoyinbo, J. S., Onyemelukwe, J. O. C. and Nwafor, J. C. (Editors) *Nigeria in Maps*. Hodder and Stoughton Ltd. London, pp 22 – 23.

Areola, O. (1982c). Nigeria : Land use. In Barbour, K.M., Oguntoyinbo, J. S., Onyemelukwe, J. O. C. and Nwafor, J. C. (Editors) *Nigeria in Maps*. Hodder and Stoughton Ltd London. pp 28 – 29.

Asangwe, C. K. A. (1993). Land, Climate and Vegetation. In Adalemo, I. A. and Baba, J. M. (Editors) *Nigeria - Giant in the Tropics, Volume 1*. Gabumo Publishing Company Ltd, Lagos pp 45 – 52.

Ash, J. H. and Sharland, R. E. (1986). Nigeria: Assessment of bird conservation Priorities. International Council for Bird Preservation, Cambridge University Press.

Augenstein, E., Stow, D. and Hope, A. (1991). Evaluation of SPOT HRV-XS Data for Kelp Resource Inventories. *Photogrammetric Engineering and Remote Sensing,* **57,** 501 – 509.

Aweto, A. O. (1993). Biotic Resources. In Adalemo, I. A. and Baba, J. M., (Editors) *Nigeria : Giant in the Tropics, Volume 1*. Gabumo Publishing Company Limited, Lagos, Nigeria pp 71 – 75.

Ayoade, J. O. (1982). Nigeria : Climate I : ITD movements and Winds. In Barbour, K.M., Oguntoyinbo, J. S., Onyemelukwe, J. O. C. and Nwafor, J. C. (Editors) *Nigeria in Maps*. Hodder and Stoughton Ltd. London pp 14 – 15.

Badejo, M. A. (1998). Agroecological restoration of savanna ecosystems. *Ecological Engineering,* **10,** 209 – 219.

Bailey, R. G. (1983). Delineation of ecosystem regions. *Environmental Management*. 7, 365 – 373.

Ball, G. H., and Hall, D. J. (1965). A Novel Method of Data Analysis and Pattern Classification. *Menlo Park, CA: Stanford Research Institute*.

Balogun, O. Y. (1985). Topographic Mapping in Nigeria : Revision or New Series. *Technical Papers of the 12th Conference of the International Cartographic Association, Perth, Australia, August 6 – 13* pp 75 – 85.

Balogun, O. Y. and Uluocha, N.O. (1998). Fundamental issues in sustainable GIS implementation in Nigeria. In Balogun and Uluocha (Editors), *Cartography and challenges of the 21st century in Nigeria*. Nigerian Cartographic Association.

Batista, G. T., Shimabukuro, Y.E. and Lawrence, W. T. (1997). The long-term monitoring of Vegetation in the Amazonian region on Northern Brazil using NOAA-AVHRR data. *International Journal of Remote Sensing*, **18**, 3195-3210.

Boahene, K. (1998). The Challenges of Deforestation in Tropical Africa : Reflections on its Principal Causes, Consequences and Solutions. *Land Degradation and Development* **9,** 247 - 258.

Boele, R., Fabig, H. and Wheeler, D. (2001a). Shell, Nigeria and the Ogoni. A study in Unsustainable Development I. The Story of Shell, Nigeria and the Ogoni People – Environment, Economy, Relationships : Conflict and Prospects for Resolution. *Sustainable Development,* **9,** 74 – 86.

Boele, R., Fabig, H. and Wheeler, D. (2001b). Shell, Nigeria and the Ogoni. A study in Unsustainable Development II. Corporate social responsibility and Stakeholder Management versus a right-based approach to sustainable development. *Sustainable Development,* **9,** 121 – 135.

Bourn, D., Wint, W., Blench, R. and Wolley, E. (1994). Nigerian livestock resources surveys. *World Bank Animal Review,* **78,** 49 - 58.

Briggs, J. M. and Nellis, M. D. (1991). Seasonal Variation of Heterogeneity in Tallgrass Prairie : A quantitative Measure using Remote Sensing. *Photogrammetric Engineering and Remote Sensing*, **57**, 407- 411.

Burgess, D. W., Lewis, P. and Muller, J.-P. A. L. (1995). Topographic Effects in AVHRR NDVI data. *Remote Sensing of Environment,* **54,** 223 - 232.

Byrne, G. F., Crapper, P. F and Mayo, K. K. (1980). Monitoring Land cover change by PCA of multi temporal Landsat data. *Remote Sensing of the Environment,* **10,** 175-184.

Campbell, J. B. (1996). Introduction to Remote Sensing. Second Edition. Taylor and Francis, London.

Che, L. and Lee, L. (1992). Progressive Generation of Control Frameworks for Image Registration. *Photogrammetric Engineering and Remote Sensing*, **58**, 1321-1328.

Che, N. and Price, J. C. (1992). Survey of Radiometric Calibration Results and Methods for Visible and Near Infrared Channels of NOAA-7, -9 and -11 AVHRRs. *Remote Sensing of Environment,* **41,** 19 - 27.

Chopping, M. J. (1999). Comment on 'A simple method to account for off-nadir-scattering in the NOAA/NASA Pathfinder AVHRR Land Data Set' by Seaquist and Olsson (1998). *International Journal of Remote Sensing*, **20**, 815-821.

Chuvieco, E (1999). Measuring changes in landscape pattern from satellite images short-term effects of fire on spatial diversity. *International Journal of Remote Sensing*, **20**, 2331-2346.

Climate Prediction Center (CPC), (2001). Ten-Day ITCZ Position. *http://www.cpc.ncep.noaa.gov/products/african_desk/ITCZ/ITCZ.html*.

Cline-Cole, R. (1997). Promoting (anti-) social forestry in Northern Nigeria. *Reviews of African Political Economy,* **74,** 515-536.

Cline-Cole, R. (1998). Knowledge claims and landscape: alternative views of the fuelwood-degradation nexus in Northern Nigeria. *Journal of Environment and Planning D-Society & Space,* **16**, 311-346.

Cracknell, A. P. (1997). The Advanced Very High Resolution Radiometer (AVHRR), (Taylor and Francis, London).

Cross, A. M., Seatle, J. J., Drake, N. A. and Paivinen, R. T. M. (1991). Sub-pixel measurement of tropical forest cover using AVHRR data. *Remote Sensing Letters,* **12**, 1119 - 1129.

Curran, P.C and Foody, G.M. (1994). Environmental Issues at Regional to Global Scales. In Giles Foody and Paul Curran (Editors), *Environmental Issues at Regional to Global Scales*. John Wiley and Sons Ltd, Chichester.

Curran, P.C and Foody, G.M. (1994). The Use of Remote Sensing to Characterise the Regenerative States of Tropical Forests. In Giles Foody and Paul Curran (Editors), *Environmental Issues at Regional to Global*. John Wiley and Sons Ltd, Chichester.

Dabrowska-Zielinska, K., Kogan, F., Ciolkosz, A. Gruszczynska, M. and Kowalik, W. (2002). Modelling of Crop growth conditions and crop yield in Poland using AVHRR-based indices. *International Journal of Remote Sensing,* **23**, 1109 – 1123.

Dada, F. O. A. (1998). Population growth and Land-use Mapping in Nigeria. In Balogun, O. Y. and Uluocha, N .O.(Editors), *Cartography and the challenges of the 21st Century in Nigeria*. Nigerian Cartographic Association, pp 51 – 63.

D'amato, N. and Lebel, T. (1998). On the Characteristics of the Rainfall Events in the Sahel with a view to the Analysis of Climatic Variability. *International Journal of Climatology,* **18,** 955-974.

Danielson, J. J. (1996). Delineation of drainage basins from 1 km African digital elevation data. In : Pecora Thirteen, Human Interactions with the Environment – Perspectives from Space, Sioux Falls, South Dakota, August 20-22, 1996.

Davenport, M. L. and Nicholson, S.E. (1993). On the relationship between rainfall and the Normalised Difference Vegetation Index for diverse vegetation types in East Africa. *International Journal of Remote Sensing,* **14,** 2369 - 2389.

Deering, D. W. and Eck, T. F. (1987). Atmospheric optical depth effects on angular anisotrophy of plant canopy reflectance. *International Journal of Remote Sensing,* **8,** 893 – 916.

De Fries, R. S. and Townshend, J. R. G. (1994). NDVI-derived land cover classifications at global scale. *International Journal of Remote Sensing*, **15**, 3567 - 3586.

De Fries, R., Hansen, M. and Townshend, J. (1995). Global Discrimination of Land Cover Types from Metrics derived from AVHRR Pathfinder Data. *Remote Sensing of Environment*, **54**, 209 - 222.

De Fries, R. S., Hansen, M.C., Steininger, M., Dubayah, R., Sohlberg, R. and Townshend, J. R. G. (1997). Sub-pixel Forest Cover in Central Africa from Multisensor, Multitemporal Data. *Remote Sensing of Environment*, **60**, 228 – 246.

De Fries, R. S., Hansen, M.C., Townshend, J. R. G. and Sohlberg, R. (1998). Global land cover classifications at 8 km spatial resolution : the use of training data derived from Landsat imagery in decision tree classifiers. *International Journal of Remote Sensing*, **19**, 3141 - 3168.

De Fries, R. S., Hansen, M.C. and Townshend, J. R. G. (2000). Global continuous field of vegetation characteristics : a linear mixture model applied to multi-year 8km AVHRR data. *International Journal of Remote Sensing*, **21**, 1389 - 1414.

Diallo, O., Diouf, A., Hanan, N. P., Ndiaye, A. and Prevost, Y. (1991). AVHRR monitoring of savanna primary production in Senegal, West Africa : 1987 – 1988. *International Journal of Remote Sensing*, **12**, 1259 - 1279.

Duchemin, B., Guyon, D. and Lagouarde, J. P. (1999). Potential and limits of NOAA-AVHRR temporal composite data for phenology and water stress monitoring of temperate forest ecosystems. *International Journal of Remote Sensing,* **20,** 895 - 917.

Duggin, M. J. and Robinove, C. J. (1990). Assumptions implicit in Remote Sensing Data Acquisition and Analysis. *International Journal of Remote Sensing,* **11,** 1669 - 1694.

Eastman, J. R. (1999a). Idrisi-32 Guide to GIS and Image Processing Volume 1. *Clark Labs., Clark University, 950 Main Street Worcester MA, U.S.A.*

Eastman, J. R. (1999b). Idrisi-32 Guide to GIS and Image Processing Volume 2. *Clark Labs., Clark University, 950 Main Street, Worcester MA, U.S.A.*

Eastman, J. R. (2000). Change and Time Series Analysis Techniques : A review. *In Eastman, J.R., McKendry, J. E. and Fulk, M.A. (Editors) Explorations in Geographical Information Systems Technology, Volume 1. Change and Time Series Analysis Second Edition.* United Nations Institute for Training and Research, pp 1 -28.

Eastman, J. R. and Fulk, M., (1993). Long sequence time series evaluation using standardised principal components. *Photogrammetric Engineering and Remote Sensing*, **59**, 991-996.

Eck, T.F. and Kalb, V.L. (1991). Cloud-screening for Africa using a geometrically and seasonally variable infrared threshold. *International Journal of Climatology,* **12,** 1205 - 1221.

Egbu, A. U. (2000). Ebonyi State. In Mamman A.B., Oyebanji, J.O. and Petters, S.W. (Editors.), *Nigeria : A People United, A Future Assured, Volume 2* pp. 150 – 158*,* Federal Ministry of Information, Abuja, Nigeria, Gabumo Publishing Company Ltd, Calabar, Nigeria.

Ehrlich, D. and Lambin, E.F. (1996). Broadscale land-cover classification and interannual climatic variability. *International Journal of Remote Sensing,* **17**, 845-862.

Eidenshink, J.C. (1992). The 1990 Conterminous U.S. AVHRR data set. *Photogrammetric Engineering and Remote Sensing*, **58**, 809 - 813.

Ekanade, O. (1987). Small-scale cocoa farmers and environmental change in the tropical rainforest region of south-western Nigeria*. Journal of Environmental Management,* **25,** 61 – 70.

Ekanade, O. (2000a). Ekiti State*.* In Mamman A.B., Oyebanji, J.O. and Petters, S.W. (Eds.), *Nigeria : A people United, A Future Assured, Volume 2*. pp. 171 – 182*,* Federal Ministry of Information, Abuja, Nigeria, Gabumo Publishing Company Ltd. Calabar, Nigeria.

Ekanade, O. (2000b). Ondo State*.* In Mamman A.B., Oyebanji, J.O. and Petters, S.W. (Editors), *Nigeria : A People United, A Future Assured, Volume 2*. pp. 433 – 444*,* Federal Ministry of Information, Abuja, Nigeria, Gabumo Publishing Company Ltd, Calabar, Nigeria.

Eklundh, L. (1998). Estimating relations between AVHRR NDVI and Rainfall in East Africa at 10-day and monthly time scales. *International Journal of Remote Sensing*, **19**, 563 - 569.

El-Raey, M., Nasr, S. M., El-Hattab, M. M. and Frihy, O. E. (1995). Change detection of Rosetta promontory over the last forty years, *International Journal of Remote Sensing*, **16**, 825 - 834.

Eltahir, E.A.B, and. Humphries, E.J. (1998). The role of clouds in the surface energy balance over the Amazon forest, *International Journal of Climatology,* **18**, 1575-1591.

Elvidge, C. D., Yuan, D., Ridgeway, D. W. and Lunetta, R. S. (1995). Relative radiometric normalisation of Landsat Multispectral Scanner (MSS) data using automatic scattergram-controlled regression. *Photogrammetric Engineering and Remote Sensing*, **61**, 1255 - 1260.

Encarta Encyclopedia (2002). Microsoft Corporation, Inc.

Engvall, J. L., Tubbs, J. D. and Holmes, Q. A. (1977). Pattern Recognition of Landsat data based upon temporal trend analysis. *Remote Sensing of Environment*, **6**, 303 - 314.

ERDAS, (1997). *ERDAS Imagine Version 8.3.1,* Earth Resources Data Analysis Systems Inc., Atlanta, Georgia.

Fadare, S. O. (2000). Osun State. In Mamman A.B., Oyebanji, J.O. and Petters, S.W. (Editors), *Nigeria : A People United, A Future Assured, Volume 2*. pp. 446 – 455*,* Federal Ministry of Information, Abuja, Nigeria, Gabumo Publishing Company Ltd, Calabar, Nigeria.

Falola, J. A. (2000). Kano State. In Mamman A.B., Oyebanji, J.O. and Petters, S.W. (Editors), *Nigeria : A People United, A Future Assured, Volume 2* pp. 265 – 287, Federal Ministry of Information, Abuja, Nigeria, Gabumo Publishing Company Ltd, Calabar, Nigeria.

Farrar, T.J., Nicholson, S.E and Lare, A. R. (1994). The Influence of Soil Type on the Relations between NDVI, Rainfall and Soil Moisture in Semiarid Botswana. II. NDVI Response to Soil Moisture. *Remote Sensing of Environment,* **50,** 121 - 133.

Flitcroft, I. D., Miford, J. R. and Dugdale, G. (1989). Relating point average rainfall in semi-arid West Africa and the implications for rainfall estimates derived from satellite data. *Journal of Applied Meteorology*, **28**, 252 – 266.

Finch, J.W. (1997). Monitoring small dams in semi-arid regions using remote sensing and GIS. *Journal of Hydrology*, **195**, 335-351

Fung, T. and LeDrew, E. (1988). The determination of Optical threshold levels for changes detection using various accuracy indices. *Photogrammetric Engineering and Remote Sensing,* **10,** 1449-1454.

Gallo, K. P. and Eidenshink, J. C. (1988). Differences in the visible and near-infrared responses, and derived vegetation indices, for the NOAA-9 and NOAA-10 AVHRRs : A case study. *Photogrammetric Engineering and Remote Sensing,* **54,** 485 - 490.

Gallup, J. L. and Sachs, J. D. (2001). The Economic Burden of Malaria. *American Journal of Tropical Medicine and Hygiene,* **64,** 85 - 96.

Gaston, G.G., Bradley, P.M., Vinson, T.S and Kolchugina, T.P. (1997). Forest Ecosystem Modelling in the Russian Far East Using Vegetation and Land-Cover Regions Identified by Classification of Global Vegetation Index (GIV). *Photogrammetric Engineering and Remote Sensing,* **63,** 51-58.

Gonima, L. (1993). Simple algorithm for the atmospheric correction of reflectance images. *International Journal of Remote Sensing*, **14**, 1179 - 1187.

Goward, S. N., Dye, D. G., Turner, S. and Yang, J. (1993). Objective Assessment of the NOAA Global Vegetation Index data product. *International Journal of Remote Sensing*, **14**, 3365-3394.

GPCC, (1998). The Global Precipitation Climatology Centre. Information on World Wide Web under *http://www.dwd.de/research/gpcc*

Grainger, A. (1993). Rates of Deforestation in the humid tropics: estimates and measurements. *The Geographical Journal*. **159,** 33 – 44.

Green, K., Kempka, D. and Lackey, L. (1994). Using Remote Sensing to detect and Monitor Land Cover and Land Use Change. *Photogrammetric Engineering and Remote Sensing,* **60,** 331- 337.

Green, R.M. and Hay, S.I. (2002). The Potential of Pathfinder AVHRR data for providing surrogate climatic variables across Africa and Europe for Epidemological applications. *Remote Sensing of Environment, 79,* 166 - 175.

Gupta, R. K. (1992).   Processing error reduction factors in the generation of geometrically corrected NOAA/AVHRR vegetation index images. *International Journal of Remote Sensing*, **13**, 515 - 526.

Gutman, G. G. (1991). Vegetation Indices from AVHRR : An Update and Future Prospects. *Remote Sensing of Environment*, **35** 121 - 236.

Gutman, G. and Ignatov, A. (1995).   Global land monitoring from AVHRR : Potentials and Limitations. *International Journal of Remote Sensing*, **16**, 2301 - 2309.

Gutman, G. and Ignatov, A. (1996). The Relative merit of cloud/clear identification in the NOAA/NASA Pathfinder AVHRR Land 10-day composites. *International Journal of Remote Sensing*, **17**, 3295 - 3304.

Hall, F.G., Strebel, D.E., Nickerson, J. E. and Goetz, S.J. (1991). Radiometric rectification : Towards a common radiometric response among multidate, multisensor images. *Remote Sensing of Environment,* **35,** 11 - 27.

Hall, F.G., Townshend, J. R. G. and Engman, E. T. (1995). Status of Remote Sensing algorithms for estimation of land surface state parameters. *Remote Sensing of Environment,,* **51,** 138 - 156.

Hanan, N. P., Prince, S. D. and Holben, B.N. (1995). Atmospheric Correction of AVHRR Data for Biophysical Remote Sensing of the Sahel. *Remote Sensing of Environment,,* **51,** 306 - 316.

Hansen, M. C., Dubayah, R. and DeFries, R. (1996).   Classification trees : an alternative to traditional land cover classifiers. *International Journal of Remote Sensing*, **17**, 1075 - 1081.

Hansen, M. C., DeFries, R. S., Townshend, J. R. G. and Sohlberg, R. (2000). Globala land cover classification at 1 km resolution using a classification tree approach. *International Journal of Remote Sensing*, **21**, 1331 - 1364.

Hay, S. I., Packer, M. J. and Rogers, D. J. (1997). The impact of remote sensing on the study and control of invertebrate intermediate hosts and vectors for disease. *International Journal of Remote Sensing*, **18**, 2899 - 2930.

Hayes, M. J. and Decker, W. L. (1996). Using NOAA AVHRR data to estimate maize production in the United States Corn Belt. *International Journal of Remote Sensing*, **13**, 515 - 526.

He, H. S., Mladenoff, D. J., Radeloff, V. C. and Crow, T. R., (1998). Integration of GIS data and classified satellite imagery for regional forest assessment. *Ecological Applications*, **18**, 1072-1083.

Hielkema, J. U., Prince, S. D. and Astle, W. L. (1986a). Rainfall and Vegetation monitoring in the Savanna Zone of the Democratic Republic of Sudan using NOAA Advanced Very High Resolution Radiometer. *International Journal of Remote Sensing,* **7,** 1499 – 1513.

Hielkema, J. U., Roffey, J. and Tucker, C. J. (1986b). Assessment of Ecological conditions associated with the 1980/1981 – desert locust plague upsurge in West Africa using environmental satellite data. *International Journal of Remote Sensing,* **7,** 1609 – 1622.

Henrickson, B. L. (1986a). Reflections on drought : Ethiopia 1983 - 1984. *International Journal of Remote Sensing,* **7,** 1447 – 1451.

Henrickson, B. L. (1986b). Rainfall and Vegetation monitoring in the Savanna Zone of the Democratic Republic of Sudan using NOAA Advanced Very High Resolution Radiometer. *International Journal of Remote Sensing.* **7,** 1499 – 1513.

Hill, M. J., Vickery, P. J., Furnival, E..P., Donald, G. E., (1999). Pasture land cover in eastern Australia from NOAA-AVHRR NDVI and classified Landsat TM. *Remote Sensing of Environment,* **67**, 32-50

Himiyama, Y. (1998). Land use/cover changes in Japan : from the past to the future, *Hydrological Process,* **12,** 1995 - 2001.

Hixson, M.D., Scholz, D., Fuhs, N. and Akiyama, T. (1980). Evaluation of Several Schemes for Classification of remotely sensed data. *Photogrammetric Engineering and Remote Sensing,* **46,** 1547-1553.

Holben, B. N. (1986). Characteristics of maximum-value composite images from temporal AVHRR data. *International Journal of Remote Sensing*, **7,** 1417-1434.

Holben, B. N., Kimes, D. S. and Fraser, R. S. (1986). Directional Reflectance in AVHRR red and near-IR bands for three types of cover types and varying atmospheric conditions. *Remote Sensing of Environment,* **19,** 213 – 236.

Holben, B. N., Kaufman, Y. J. and Kendall, J. D. (1990). NOAA-11 AVHRR Visible and Near-IR Inflight Calibration. *International Journal of Remote Sensing*, **11,** 1511 – 1519.

Hulme, M. and Kelly, M. (1993). Exploring the links between desertification and Climate change. *Environment,* **35,** 39-45.

Huete, A. R. and Tucker, C. J. (1991). Investigation of soil influences in AVHRR red and near-infrared vegetation index imagery. *International Journal of Remote Sensing,* **12,** 1223 - 1242.

Hutchinson, C.F. (1991). Uses of Satellite Data for Famine early Warnings in Sub-Saharan Africa. *International Journal of Remote Sensing,* **12,** 1405-1421.

IDRISI-32 (1998). A Raster-based Geographical Information Systems Analysis Software. *Clarks Lab., Clark University, 950 Main Street, Worcester, U.S.A.*

Ijagbemi, E. A. (1982). Nigeria : Historical Development I: Pre-colonial and Colonial Nigeria. In Barbour, K.M., Oguntoyinbo, J. S., Onyemelukwe, J. O. C. and Nwafor, J. C. (Editors) *Nigeria in Maps,* pp 36 – 37, Hodder and Stoughton Ltd, London.

Ijere, A. and Daura, M. M. (2000). Borno State. In Mamman A.B., Oyebanji, J.O. and Petters, S.W. (Editors.), *Nigeria : A People United, A Future Assured, Volume 2,* pp. 103 – 119, Federal Ministry of Information, Abuja, Nigeria, Gabumo Publishing Company Ltd, Calabar, Nigeria.

Ilesanmi, O. O. (1971). An Empirical Formulation of an ITD Rainfall Model for the Tropics : A Case Study of Nigeria**.** *Journal of Applied Meteorology,* **10,** 882 - 891.

Iliya, M. A. and Kwabe, S. A. (2000). Kebbi State. In Mamman A.B., Oyebanji, J.O. and Petters, S.W. (Editors), *Nigeria : A People United, A Future Assured, Volume 2*, pp. 303 – 320, Federal Ministry of Information, Abuja, Nigeria, Gabumo Publishing Company Ltd, Calabar, Nigeria.

Imoroa, N. O. (2000). Delta State. In Mamman A.B., Oyebanji, J.O. and Petters, S.W. (Editors), *Nigeria : A People United, A Future Assured, Volume 2*, pp. 171 – 182*,* Federal Ministry of Information, Abuja, Nigeria, Gabumo Publishing Company Ltd. Calabar, Nigeria.

Indrabudi, H., De Gier, A. and Fresco, L.O. (1998). Deforestation and its driving forces : A Case Study of River Kanan Watershed, Indonesia. *Land Degradation and Development,* **9,** 311 - 322.

Ite, U. E. (1998). New wine in an old skin: the reality of moist tropical forest conversion in Nigeria. *Landuse Policy, .* **15,** 135 – 147.

Ite, U. E., and Adams, W. M. (1998). Forest conservation and forestry in Cross River State, Nigeria. *Applied Geography,* **18,** 301 - 314.

Jaiyeoba, I.A. (1998). Changes in Soil Properties related to Conversion of Savannah Woodlands into Pine and Eucalyptus Plantations, Northern Nigeria. *Land Degradation and Development,* **9,** 207 - 215.

James, M.E. and Kalluri, S. (1994). The Pathfinder AVHRR Land data set : an improved coarse resolution data set for terrestrial monitoring. *International Journal of Remote Sensing,* **15,** 3347-3364.

Jensen, J. R. (1979). Spectral and Textual features to classify Elusive Landcover at the Urban Fringe. *The Professional Geographer,* **31,** 400 - 409.

Jensen, J.R., Cowen, D. J., Althausen, J. D., Narumalani, S. and Weatherbee, O. (1993). An Evaluation of the CoastWatch Change Detection Protocol in South Carolina. *Photogrammetric Engineering and Remote Sensing,* **59,** 1039 – 1046.

Jensen, J.R. (1996). Introductory Digital Image Processing : A Remote Sensing Perspective, Prentice Hall, Eagle Wood Cliffs, New Jersey, USA.

Johnston, R. J. (1978). Multivariate Statistical Analysis in Geography. Longman Group Ltd, London.

Johnson, L . B. (1990). Analyzing spatial and temporal phenomena using geographical Information Systems. *Landscape Ecology,* **4,** 31-430.

Johnston, C. (1998). Geographical Information Systems in Ecology. Blackwell Science, Ltd.

Justice, C.O. and Townshend, J. R. G., Holben, B. N. and Tucker, C. J. (1985). Analysis of the Phenology of global vegetation using meteorological satellite data. *International Journal of Remote Sensing,* **6,** 1271-1318.

Justice, C.O. and Hienaux, P.H.Y. (1986). Monitoring the grasslands of the Sahel using NOAA AVHRR data : Niger 1983. *International Journal of Remote Sensing,* **7,** 1475 - 1497.

Justice, C. O., Eck, T. F., Tanre, D. and Holben, B. N. (1991a). The effect of water vapour on the normalised difference vegetation index derived for the sahelian region from NOAA AVHRR data**.** *International Journal of Remote Sensing,* **12,** 1165 – 1187.

Justice, C. O., Dugdale, G., Townshend, J. R. G., Narracott, A. S. and Kumar, M. (1991b). Synergism between NOAA-AVHRR and Meteosat data for studying vegetation development in semi-arid West Africa. *International Journal of Remote Sensing,* **12,** 1349 – 1368.

Justice, C. O. and Townshend, J. R. G. (1994). Data sets for global remote sensing : lesson learned. *International Journal of Remote Sensing,* **15,** 3621 – 3639.

Justice, C. O. Bailey, G. B., Maiden, M. E., Rasool, S. I., Strebel, D.E. and Tarpley, J. D. (1995). Recent Data and Information System initiatives for Remotely Sensed Measurements of the Land Surface. *Remote Sensing of Environment,* **51,** 235 – 244.

Kahn, J. R. and McDonald, J. A. (1995). Third-world dept and tropical deforestation. *Ecological Economics.* **12,** 107 – 123.

Kajirawa, K. and Tateishi, R. (1990). Integration of Satellite data and Geographic Data for Global ad Cover Analysis. *Proceedings, ISPRS Commission IV, Tsukuba Japan,* 221 – 229.

Kalu, A. U. (1995). Prevalence of trypanosomiasis among Trypanotolerant cattle at the lower Benue River area of Nigeria. *Preventive Veterinary Medicine,* **24,** 97 – 103.

Kalu, A. U. (1996). Current status of tsetse fly and animal trypanosomiasis on the Jos Plateau, Nigeria. *Preventive Veterinary Medicine,* **27,** 107 – 113.

Kasischke, E. S. and French, N. H. F. (1995). Locating and Estimating the Areal extent of Wildfires in Alaskan Boreal Forests using Multi-Season AVHRR NDVI Composite Data. *Remote Sensing of Environment,* **51,** 263 - 275.

Kasischke, E. S. and French, N. H. F. (1997). Constraints on using AVHRR composite index imagery to study patterns of vegetation cover in boreal forests. *International Journal of Remote Sensing,* **18,** 2403 - 2426.

Kaufman, Y. J. and Holben, B. N. (1993). Calibration of the AVHRR visible and near-IR bands by atmospheric scattering, ocean glint and desert reflection. *International Journal of Remote Sensing,* **14,** 21 - 52.

Kersten, I., Baumbach, G., Oluwole, A. F. , Obioh, I. B. and Ogunsola, O. J. (1998). Urban and Rural Fuelwood situation in the tropical rain-forests area of south-west Nigeria. *Energy,* **23,** 887 - 898.

Kindwell, K. B. (1991). NOAA polar orbiter data (TIROS-N, NOAA-6, NOAA-7, NOAA-8, NOAA-9, NOAA-10, NOAA-11 and NOAA-12) user's guide. National Oceanic and Atmospheric Administration, *National Environmental Satellite Data, and Information Service, Washington, DC.*

Kite, G. (1988). Integration of Forest Ecosystem and Climatic models with a hydrologic model. *Journal of the American Water Resources Association,* **34,** 743-753.

Kogan, F. N. (1990).   Remote Sensing of weather impacts on vegetation in non-homogeneous areas. *International Journal of Remote Sensing,* **11,** 1405 - 1419.

Kogan, F. N. (1997). Global Drought Watch from Space. *Bulletin of American Meteorological Society,* **78,** 621 - 636.

Kogan, F. N. and Wei, G. (2000). Using AHVRR data for the Detection of EL Niňo/La Niňa impacts on Land Ecosystems. *Advanced Space Research,* **26,** 1165 - 1168.

Koop, G. and Tole, L. (2001). Deforestation, Distribution and Development. *Global Environmental Change*, **11**, 193 - 202.

Kummer, D.M. (1992). Remote Sensing and Tropical Deforestation : a cautionary note from the Phillipines. *Photogrammetric Engineering and Remote Sensing*, **58**, 1469-1471.

Kushwaha, S.P.S., Subramanian, S. K., Chennaiah, G. C., Murthy, J. R., Rao, S.V.C.K., Perumal, A. and Behera, G. (1996). Interfacing remote sensing and GIS methods for sustainable rural development. *International Journal of Remote Sensing,* **17**, 3055-3069.

Lambin, E.F. and Strahler, A. H. (1994a). Change-vector Analysis in multispectral space : A tool to detect and categorise landcover changes processes using high temporal-resolution satellite data. *Remote Sensing of Environment,* **48,** 231 – 244.

Lambin, E. F. and Strahler, A. H. (1994b). Indicators of land-cover change for change-vector analysis in multitemporal space at coarse spatial scales. *International Journal of Remote Sensing,* **15,** 2099 – 2119.

Lambin, E. F. and Ehrlich, D. (1995). Combining Vegetation Indices and Surface Temperature for Land-cover mapping at broad spatial scales. *International Journal of Remote Sensing*, **16,** 573-579.

Lambin, E. F. and Ehrlich, D. (1996). The Surface Temperature-Vegetation Index space for land-cover and land-cover change analysis. *International Journal of Remote Sensing*, **17,** 1-15.

Lambin, E. F. and Ehrlich, D. (1997a). Landscape changes in Sub-Saharan Africa (1982-1991) : Application of change Index based on Remotely Sensed Surface Temperature and Vegetation Index at Continental Scale. *Remote Sensing of Environment,* **61**, 181- 200.

Lambin, E.F. and Ehrlich, D. (1997b). The identification of tropical deforestation fronts at broad spectral scales. *International Journal of Remote Sensing*, **18,** 3551-3568.

Laporte, N., Justice, C. O. and Kendall, J. (1995). Mapping the dense humid forest of Cameroon and Zaire using AVHRR satellite data. *International Journal of Remote Sensing,* **16,** 1127 – 1145.

Laporte, N. T., Goetz, S. J., Justice, C. O., and Heinickel, M. (1998). A new land cover map of central Africa derived from multi-resolution, nulti-temporal AVHRR data. *International Journal of Remote Sensing,* **16,** 3537 – 3550.

Leblon, B., Alexander, M., Chen, J. and White, S. (2001). Monitoring fire danger of northern boreal forests with NOAA-AVHRR NDVI images. *International Journal of Remote Sensing,* **22,** 2839 - 2846.

Lee, R., Yu, F., Price, K. P., Ellis, J. and Shi, P. (2002). Evaluating vegetation phonological patterns in Inner Mongolia using NDVI time-series analysis. *International Journal of Remote Sensing,* **23,** 2505 - 2512.

Leprieur, C., Kerr, Y. H. and Pichon J. M. (1996). Critical assessment of vegetation indices from AVHRR in a semi-arid environment. *International Journal of Remote Sensing*, **16,** 2549-2563.

Leprieur, C., Kerr, Y.H., Mastorchio, S. and Meunier, J. C. (2000). Monitoring Vegetation Cover across Semi-arid regions : Comparison of Remote Observations from various scales. *International Journal of Remote Sensing,* **21,** 281 - 300.

Li, B., Tao, S. and Dawson, R.W. (2002). Relations between AVHRR-NDVI and ecoclimatic parameters in China. *International Journal of Remote Sensing,* **23,** 989 - 999.

Li, Z. and Kafatos, M. (2000). Interannual Variability of Vegetation in the United States and Its Relation to El-Niṅo/Southern Oscillation. *Remote Sensing of Environment,* **71,** 239 - 247.

Liang, S. (2001). Landcover classification methods for multi-year AVHRRR data. *International Journal of Remote Sensing,* **22,** 1479 - 1493.

Lillesand, T. M. and Kiefer, R. W. (1994). Remote Sensing and Image Interpretation, Third Edition, John Wiley and Son, Inc.

Linthicum, K. J., Anyamba, A., Tucker, C.J., Kelley, P.W., Myers, M. F. and Peters, C. J. (1999). Southern Oscillation Index, sea surface temperature and satellite vegetation index indicators to forecast Rift Valley fever epizootics/epidemics in Kenya. *Science,* **285,** 397 - 400.

Liu, W. T. and Kogan, F. N. (1996). Monitoring regional drought using the Vegetation Condition Index. *International Journal of Remote Sensing,* **17,** 2761 - 2782.

Lobo, A., Ibanez-Marti, J. J. and Gimenez-Cassina, C. C. (1997). Regional Scale Hierarchical Classification of Temporal Series of AVHRR Vegetation Index. *International Journal of Remote Sensing*, **18**, 3167-3193.

Los, S. O., Justice, C. O. and Tucker, C. J. (1994). A 1^0 by 1^0 NDVI data set for climatic studies derived from the GIMMS continental NDVI data. *International Journal of Remote Sensing*, **15**, 3493 - 3518.

Loveland, T. R., Merchant, J. W., Ohlen, D. O. and Brown, J. F. (1991). Development of a land cover characteristics database for the conterminous US. *Photogrammetric Engineering and Remote Sensing*, **57**, 1453 - 1463.

Loveland, T. R., Reed, B. C., Brown, J. F., Ohlen, D. O., Zhu, Z., Yang, L. and Merchant, J. W. (2000). Development of a land cover characteristics database and IGBP DISCover from 1 km AVHRR data. *International Journal of Remote Sensing*, **21**, 1303 - 1330.

Lovell, J. L. and Graetz, R. D. (2001). Filtering Pathfinder AVHRR Land NDVI data for Australia**.** *International Journal of Remote Sensing*, **22**, 3167-3193.

Lowe, M.S. and Bowlby, S. R. (1992). Population and Environment. In Mannion, A.M. and Bowlby S.R (Editors), *Environmental Issues in the 1990s*. John Wiley and Sons Ltd.

Lucas, R.M., Honzak, M., Curran, P.J., Foody, G.M. and Nguele, D.T. (2000). Characterizing tropical forest regeneration in Cameroon using NOAA AVHRR data. *International Journal of Remote Sensing,* **21,** 2831- 2854.

Lunetta, R. S., Congalton, R. G., Fenstermaker, L. K., Jensen, J. R., McGwire, K. C. and Tinney, L. R. (1991), Remote Sensing and Geographical Information Systems

Data Integration : Error Sources and Research Issues. *Photogrammetric Engineering and Remote Sensing*, **57**, 677- 687.

Lunetta R. S. (1998), Applications Project Formulation, and Analytical Approach. In Lunetta, R.S. and Elvidge, C.D. (Editors.), *Remote Sensing Change Detection - Environmental Monitoring Methods and Applications,* pp. 1 – 19.

Lupo, F., Reginster, I. and Lambin, E.F. (2001). Monitoring land-cover changes in West Africa with SPOT Vegetation : impact of natural disasters in 1998-1999. *International Journal of Remote Sensing*, **22**, 2633 – 2639.

Lyon, J.D., Yuan, D., Lunetta, R. S. and Elvidge, C. D. (1998). A Change Detection Experiment Using Vegetation Indices. *Photogrammetric Engineering and Remote Sensing*, **64**, 143-150.

Maclean, A.L., Reed, D.D., Mroz, G.D., Lyon, G.W. and Edison, T. (1991). Using GIS to Estimate Forest Resource Changes. *Forestry Chronicle,* **67,** 151-155.

Maiden, M. E. and Greco, S. (1994). NASA's Pathfinder dataset programme : land surface parameters. *International Journal of Remote Sensing,* **15,** 3333 - 3342.

Makarov, V. I., Ankilov, A. N., Koutsenogii, K . P. , Borodulin, A. I. and Samsonov, Y. N. (1996). Efficiency of the Inertial Wind Capture of Pesticide Aerosols by Vegetation Species. *Journal of Aerosol Science,* **27,** 67 – 68.

Malingreau, J. P. and Belward, A. S. (1994). Recent activities in the European Community for the creation and analysis of global AVHRR data sets. *International Journal of Remote Sensing,* **15,** 3397 – 3416.

Malo, A. R. and Nicholson, S.E. (1990). A study of rainfall and vegetation dynamics in the African Sahel using normalised difference vegetation index. *Journal of Arid Environments,* **19,** 1 – 24.

Mamman, A. B. (2000). Sokoto State. In Mamman A.B., Oyebanji, J.O. and Petters, S.W. (Editors), *Nigeria : A People United, A Future Assured, Volume 2,* pp. 497 – 514*,* Federal Ministry of Information, Abuja, Nigeria, Gabumo Publishing Company Ltd, Calabar, Nigeria.

Mas, J. F. (1999). Monitoring Land-cover Changes : A Comparison of Detection Techniques. *International Journal of Remote Sensing,* **20,** 139-152.

Maselli, F., Conese, C., Petkov, L. and Gilabert, M.A. (1992). Use of NOAA-AVHRR NDVI data for environmental monitoring and crop forecasting in the Sahel. Preliminary results. *International Journal of Remote Sensing,* **13,** 2743 - 2749.

Massart, M., Petillion, M. and Wolff, E. (1995). The impact of an Agricultural Development Project on a Tropical Forest Environment : The case of Shaba (Zaire). *Photogrammetric Engineering and Remote Sensing*, **61**, 1153-1158.

Mather, A.S., Needle, C.L., and Fairbairn, J. (1998). The Human Drivers of Global Land Cover Change : the case of forests. *Hydrological Process,* **12**, 1983 - 1994.

Mather, P.M. (1999a). Computer Processing of Remotely Sensed images : An Introduction. John Wiley, Chincester.

Mather, P.M. (1999b). Land Cover Classification Revisited. In Atkinson, P.M and Tate, N.J. (Editors) *Advances in Remote Sensing and GIS Analysis.* John Wiley and Sons.

Matola, Y. G., White, G. B. and Magayuka, S. A. (1987). The changed pattern of Malaria endemicity and transmission at Amani in the eastern Usumbara mountains, north-eastern Tanzania. *Journal of Tropical Medical Hygiene.* **90,** 127 – 134.

Mayaux, P. and Lambin, E. (1995). Estimating of tropical forest area from coarse spatial resolution data: A two-step correction function for proportional errors due to spatial aggregation. *Remote Sensing of Environment,* **53,** 1 - 15.

Mbagwu, T. C. (2000). Enugu State. In Mamman A.B., Oyebanji, J.O. and Petters, S.W. (Editors), *Nigeria : A People United, A Future Assured, Volume 2*, pp. 184 – 196, Federal Ministry of Information, Abuja, Nigeria, Gabumo Publishing Company Ltd, Calabar, Nigeria.

McPhaden, M. (1999). Genesis and Evolution of the 1997- 98 El Nińo. *Science.* **283,** 950 – 954.

McVicar, T. R. and Bierwirth, P. N. (2001). Rapidly assessing the 1997 drought in Papua New Guinea using composite AVHRR imagery. *International Journal of Remote Sensing,* **22,** 2109 – 2128.

Meyer, W. B. and Turner, B. L. (1992). Human Population growth and Global Landuse/Landcover change. *Annual Review of Ecology and Systematics,* **23,** 39 – 61.

Meyer, D., Verstraete, M. and Pinty, B. (1995). The effect of surface anisotropy and viewing geometry on the estimation of NDVI from AVHRR. *Remote Sensing Review.* **12,** 3 – 27.

Michaleck, J. L., Wagner, T. W., Luczkovich, J. J. and Stoffle, R. W. (1993). Multispectral Change Vector Analysis for Monitoring Coastal Marine Environments. *Photogrammetric Engineering and Remote Sensing,* **59,** 381 – 384.

Miliaresis, G. Ch. and Argialas, D. P. (2002). Quantitative representation of mountain objects extracted from the global digital elevation model (GTOPO30). *International Journal of Remote Sensing,* **23,** 949 - 964.

Milich, L. and Weiss, E. (1997). Characterization of the Sahel: implications of correctly calculating inter-annual coefficient of variation (COVs) from GAC NDVI values. *International Journal of Remote Sensing,* **18,** 3749 - 3759.

Milich, L. and Weiss, E. (2000a). GAC NDVI Interannual coefficient of variation (CoV) images : ground truth sampling of the Sahel along north-south transects. *International Journal of Remote Sensing.* **21,** 235 - 260.

Milich, L. and Weiss, E. (2000b). GAC NDVI Images : Relationship to rainfall and potential evaporation in the grazing lands of The Gourma (Northern Sahel) in the croplands of the Niger-Nigeria boarder (Southern Sahel). *International Journal of Remote Sensing,* **21,** 261 - 280.

Millington, A. C., Styles, P.J. and Critchley, R. W. (1992). Mapping Forests and Savannas in sub-saharan Africa from Advanced Very High Resolution Radiometer (AVHRR) imagery. In *Forest-Savanna Boundaries,* edited by P.A. Furley, J Proctor and J.A. Ratter, Chapman & Hall, London. pp. 37 – 62.

Millington, A. C., Wellens, J., Settle, J. J. and Saull, R. J. (1994). Explaining and Monitoring Land cover dynamic in drylands using Multi-temporal Analysis of NOAA AVHRR Imagery. In *Environmental Remote Sensing from Regional to Global Scales,* edited by Foody, G. and Curran, P., pp16 – 43, John Wiley and Sons Ltd.

Milne, A.K. (1986). The use of Remote Sensing in mapping and monitoring vegetational change associated with bushfire events in Eastern Australia. *GeoCarto International,* **1,** 25-57.

Mitchell, C.W. (1991), Terrain Evaluation. Longman, London.

Mohammed, S.O., Farshad, A. and Farifteh, J.(1996). Evaluating land degradation for assessment of land vulnerability to desert conditions in the Sokoto Area, Nigeria. *Land Degradation and Development,* **7,** 205 - 215.

Monmonier, M. S. (1982). Flat Laxity Optimisation and rounding in the selection of class interval. Cartographica, **9**, 19 – 27.

Moody, A. and Strahler, A.H. (1994). Characteristics of composited AVHRR data and problems in their classification. *International Journal of Remote Sensing*, **15**, 3473-3491.

Morgan, W.B. and Moss, R.P. (1965). Savanna and Forest in Western Nigeria. *Africa.* **35,** 286-295.

Moser, G. G. (1995). The Main Determinants of Inflation in Nigeria. *IMF Staff Papers, International Monetary Fund,* **42,** 270 – 289.

Muchoney, D.M. and Haack, B.N. (1994), Change detection for monitoring forest defoliation. *Photogrammetric Engineering and Remote Sensing,* **60,** 1243-1251.

Myneni, R. B. and Asrar, G. (1994). Atmospheric effects and spectral vegetation indices. *Remote Sensing of Environment,* **47,** 390 – 402.

NCDC (2000). National Climatic Data Center, 151 Patton Avenue, Asheville, NC 28801-5001, USA. *http://www5.ncdc.noaa.gov/cgi-bin/cdo/cdoprod.pl*

NCSA (1990). Hierarchical Data Format (HDF) User's Guide, National Centre for Supercomputing Applications, University of Illinois at Urbana-Champaign, Urbana-Champaign, Illinois.

Nicholson, S. E., Davenport, M. L. and Malo, A. R. (1994). A comparison of the vegetation response to rainfall in the Sahel and East Africa using NDVI from NOAA AVHRR. *Climatic Change,* **17,** 207 – 241.

Nicholson, S.E and Farrar, T.J. (1994). The Influence of Soil Type on the Relations between NDVI, Rainfall and Soil Moisture in Semiarid Botswana. I. NDVI Response to Rainfall. *Remote Sensing of Environment,* **50,** 107-120.

Nelson, R. F. (1989). Regression and ratio estimates to integrate AVHRR and MSS data. *Remote Sensing of Environment,* **30,** 201 **-** 206.

Nelson, R. F. and Holben, B.N. (1986). Identifying deforestation in Brazil using multi resolution Satellite data. *International Journal of Remote Sensing,* **7,** 429-448.

Norwine, J. and Greegor, D.H. (1983). Vegetation classification based on AVHRR satellite imagery. *Remote Sensing of Environment*, **13**, 69 - 87.

Nsofor, N. (1998). Topographic Mapping of Nigeria in the Computer Age. In Balogun, O. Y. and Uluocha, N .O.(Editors), *Cartography and the challenges of the 21st Century in Nigeria*. Nigerian Cartographic Association, pp 51 – 63.

Ochi, S., Shibasaki, R. and Murai, S. (2000). Modelling and assessment of NPP/Crop productivity in Asia by GIS combined with remote sensing data. Conference Proceedings on GIS for Developing Countries International Rice Research Institute (IRRI), Los Banos, The Philippines. November, 2000. *www.geo.uu.nl/gisdeco/gisdeco.html*

Ogunjumo, A. (2000). Kogi State. In Mamman A.B., Oyebanji, J.O. and Petters, S.W. (Editorts), *Nigeria : A People United, A Future Assured, Volume 2,* Federal Ministry of Information, Abuja, Nigeria, Gabumo Publishing Company Ltd, Calabar, Nigeria. . pp. 322 – 332.

Oguntoyinbo, J. S. (1982). Climate 2 : Precipitation (1). In Barbour, K. M., Oguntoyinbo, J. S., Onyemelukwe, J. O. C. and Nwafor, J. C. (Editors) *Nigeria in Maps,* pp 16 – 17. Hodder and Stoughton Ltd, London.

Ohamobi, S.I. and Mohammed S.O. (1999). Desertification in Northern Nigeria Using Remote Sensing and Geographical Information Systems. *Proceedings of the Fourth International Airborne Remote Sensing Conference and Exhibition/21st Canadian Symposium on Remote Sensing, 12 - 24 June 1999, Ottawa, Canada,* pp 743 - 750.

Oindo, B. O. and Skidmore, A. K. (2002). Interannual variability of NDVI and species richness in Kenya. *International Journal of Remote Sensing,* **23,** 285 - 298.

Okoye, T. O. (2000). Anambra State. In Mamman A.B., Oyebanji, J.O. and Petters, S.W. (Editors), *Nigeria : A People United, A Future Assured, Volume 2,* Federal Ministry of Information, Abuja, Nigeria, Gabumo Publishing Company Ltd, Calabar, Nigeria, pp. 46 - 56.

Olomo, O., Ufuah, M.E. and Akpan, D. U. (1998). An appraisal of the Federal Survey Department of Nigeria. In Balogun and Uluocha (Eds), *Cartography and challenges of the 21st century in Nigeria.* Nigerian Cartographic Association. pp7 - 23

Osemeobo, G. J. (1988). The human causes of forest depletion in Nigeria. *Environmental Conservation,* **15,** 18 – 28.

Patz, J. A., Graczyk, T. K., Geller, N. and Vittor, A. Y. (2000). Effects of Environmental change on emerging parasitic diseases. *International Journal for Parasitology,* **30,** 1395 – 1405.

Patz, J. A. (2001). Public Health Risk Assessment Linked to Climatic and Ecological Change. *Human and Ecological Risk Assessment,* **7,** 1317 – 1327.

Patz, J. A. and Reisen, W. K. (2001). Immunology, Climate change and vector-borne diseases. *Trends in Immunology,* **22**, 171 - 172

Petty, G. W. (1995). The Status of Satellite-Based Rainfall Estimation over Land. *Remote Sensing of Environment,* **51,** 125 – 137.

Pilon, P. G., Howarth, P. J., Bullock, R. A. and Adeniyi P.O. (1988). An enhanced classification approach to change detection in semi-arid environments. *Photogrammetric Engineering and Remote Sensing,* **54,** 1709-1716.

Price, K. P., Pike, D. A and Mendes, L. (1992). Shrub die back in a semiarid ecosystem: the integration of remote sensing and geographic information systems for detecting vegetation change. *Photogrammetric Engineering and Remote Sensing,* **58,** 455-463.

Prince, S. D. (1991a). Satellite remote sensing of primary production : comparison of results for Sahelian grasslands. *International Journal of Remote Sensing*, **12,** 13-30.

Prince, S. D. (1991b). A model of regional primary production for use with coarse-resolution satellite data. *International Journal of Remote Sensing*, **12,** 1313-1330.

Prince, S. D. and Justice, C. O. (1991). Coarse resolution remote sensing of the Sahelian Environments. Editorial, *International Journal of Remote Sensing*, **12,** 1137-1146.

Prince, S.D. and Goward, S. N. (1995). Global Primary Production : A remote Sensing Approach. *Journal of Biogeography*, **22**, 815 - 835.

Purevdorj, T. S., Tateishi, R., Ishiyama, T. and Honda, Y. (1998). Relationship between percentage vegetation cover and vegetation indices. *International Journal of Remote Sensing*, **19**, 3519-3535.

Quarmby, N. A., Townshend, J. R. G. and Millington, A. C. (1987). Change detection algorithms for monitoring sediment transport in south-central Tunisia. In *Advances in Digital Image Processing,* Remote Sensing Society, University of Nottingham, U.K., pp. 174 – 183.

Quarmby, N. A., Milnes, M., Hindle, T. and Silleos, N. (1993). The use of multi-temporal NDVI measurements from AVHRR data from crop yield estimation and prediction. *International Journal of Remote Sensing*, **14**, 199 - 210.

Rasmussen, M. S. (1998). Developing simple, operational, consistent NDVI-vegetation models by applying environmental and climatic information : Part I. Assessment of net primary production. *International Journal of Remote Sensing*, **19**, 97 - 117.

Rasmussen, M. S. (1998). Developing simple, operational, consistent NDVI-vegetation models by applying environmental and climatic information : Part II. Crop yield assessment. *International Journal of Remote Sensing*, **19**, 119 - 139.

Rao, C. R . N. (1993). Non-Linearity corrections for the thermal infrared of the Advance Very High Resolution Radiometer : assessment and recommendations, *NOAA Technical Report NESDIS-69,* NOAA/NEDIS, Washington D.C., Dept. of Commerce.

Rao, C. R. N. and Chen, J. (1994). Post-launch calibration of the visible and near-infrared channels of the Advance Very High Resolution Radiometer on NOAA-7, -9, and -11 spacecraft. *NOAA Technical Report NESDIS-78,* NOAA/NEDIS, Washington D.C., Dept. of Commerce.

Rao, C. R. N. and Chen, J. (1995). Inter-satellite calibration linkages for the visible and near-infrared channels of the Advance Very High Resolution Radiometer on the NOAA-7, -9, and -11 spacecraft. *International Journal of Remote Sensing,* **16,** 1931 - 1942.

Rao, C. R. N. and Chen, J. (1996). Post-launch calibration of the visible and near-infrared channels of the Advance Very High Resolution Radiometer on the NOAA-14 spacecraft. *International Journal of Remote Sensing,* **17,** 2743 - 2747.

Rao, C. R. N. and Chen, J. (1999). Revised post-launch calibration of the visible and near-infrared channels of the Advance Very High Resolution Radiometer (AVHRR) on the NOAA-14 spacecraft. *International Journal of Remote Sensing,* **20,** 3485 - 3491.

Reed, B. C. (1993). Using Remote Sensing and Geographic Information Systems for analysing landscape/drought interaction. *International Journal of Remote Sensing,* **18,** 3489 - 3503.

Reed, B. C., Brown, J. F., Vanderzee, D., Loveland, T. R., Merchant, J. W. and Ohlen, D. O. (1994). Measuring Phenological variability from satellite imagery. *Journal of Vegetation Science,* **5,** 703 - 714.

Reich, P. B., Turner, D. P. and Bolstad, P. (1999). An Approach to Spatially Distributed Modelling of Net Primary Production (NPP) at the Landscape Scale and Its Application in Validation of EOS NPP Products. *Remote Sensing of Environment,* **70,** 69 - 81.

Rembold, F., Maselli, F. and Rossini, P. (2001). Effects of environmental spatial variatiability on the differences between NOAA-AVHRR LAC and GAC NDVI data. *International Journal of Remote Sensing,* **22,** 895 - 900.

Remmel, T. K., and Parera, A. H. (2001). Pre-mapping in northern boreal forest : assessing AVHRR/NDVI methods of change detection. *Forest Ecology and Management ,* **152,** 119 - 129.

Richards, J. A. (1986). Remote Sensing Digital Image Analysis. : An Introduction. Springer- Verlag, New York.

Richards, Y. and Poccard, I. (1998). A Statistical study of NDVI Sensitivity to seasonal and inter-annual rainfall variation in Southern Africa. *International Journal of Remote Sensing,* **19,** 2907 - 2920.

Ricotta, C., Avena, G. C., and Ferri, F. (1996). Analysis of human Impact on a forested landscape of central Italy with simplified NDVI texture descriptor. *International Journal of Remote Sensing,* **17,** 2869 - 2874.

Ripple, W. (1994). Determining Coniferous Forest Cover and Forest Fragmentation with NOAA-9 Advance Very High Resolution Radiometer data. *Photogrammetric Engineering and Remote Sensing*, **60**, 533 - 540.

Robinson, T. P. (1996). Spatial and Temporal accuracy of coarse resolution products of NOAAA-AVHRR NDVI data. *International Journal of Remote Sensing*, **17**, 2303-2321.

Roderick, M., Smith, R. and Cridland, S. (1996a). The Precision of the NDVI Derived from AVHRR Observations. *Remote Sensing of Environment*, **56**, 57- 65.

Roderick, M., Smith, R. and Lodwick, G. (1996b). Calibrating long-term AVHRR-Derived NDVI Imagery. *Remote Sensing of Environment*, **58**, 1- 12.

Roerink, G. J., Menenti, M. and Verhoef, W. (2000). Reconstructing cloud free NDVI Composites using Fourier Analysis of time-series. *International Journal of Remote Sensing*, **14**, 1911 - 1917.

Rogers, D. J. and Randolph, S. E. (1991). Mortality rates and Population density of tsetse flies correlated with satellite imagery. *Nature,* **351,** 739 – 741.

Rogers, D. J., Hay, S. I. and Packer, M. J. (1996). Predicting the distribution of tsetse-flies in West Africa using temporal Fourier processed Meteorological Satellite Data. *Annals of Tropical Medicine and Parasitology,* **90,** 225 – 241.

Rogers, D. J., Hay, S. I., Packer, M. J. and Wint, G. R. W. (1997). Mapping Land-cover over large areas using Multispectral data derived from the NOAA-AVHRR : A case Study of Nigeria. *International Journal of Remote Sensing*, **18**, 3297-3303.

Russell, R.W., Hunt Jr. G. L., Coyle, K. O. and Ted Cooney, R. (1992). Foraging in Fractal environment : Spatial patterns in a marine predator-prey system. *Landscape Ecology,* **7,** 195-209.

Salami, A. T., Ekanade, O. and Oyinloye, R. O. (1999). Detection of Forest Reserve Incursion in south-west Nigeria from a combination of Multi-date Aerial photographs and High resolution Satellite Imagery. *International Journal of Remote Sensing,* **20,** 1487-1497.

Salami, A. T. (1999). Vegetation Dynamics on the fringes of lowland humid tropical rainforest of the south-western Nigeria - An assessment of environmental change with air photos and Landsat TM. *International Journal of Remote Sensing,* **20,** 1169-1181.

Samson, S. (1993). Two indices to characterise temporal patterns in spectral response of vegetation. *Photogrammetric Engineering and Remote Sensing*, **59**, 39- 48.

Schmidt, H. and Gitelson, A. (2000). Temporal and spatial vegetation cover changes in Israel transition zone: AVHRR-based assessment of rainfall impact. *International Journal of Remote Sensing,* **21,** 997 - 1010.

Schneider, S., McGinnis, Jr. D. F. and Stephens, G. (1985). Monitoring Africa's Lake Chad basin with Landsat and NOAA satellite data. *International Journal of Remote Sensing,* **6,** 59-73.

Schott, J. R., Salvaggio, C. and Volchok, W. (1988). Radiometric scene normalisation using pseudoinvariant features. *Remote Sensing of Environment,* **26,** 1 – 6.

Schweik, C. M. and Green, G. M. (1999). The use of spectral mixture analysis to study human incentives, actions and environmental outcomes. *Social Science Computer Review,* **17**, 40-63**.**

Seaquist, J. W. and Olsson, L. (1998). A simple method to account for off-nadir-scattering in the NOAA/NASA Pathfinder AVHRR Land Data set. *International Journal of Remote Sensing,* **19,** 1425 - 1431.

Sellers, P. J., Tucker, C. J., Collatz, J. A., Los, S. O., Justice, C. O., Dazlich, D. A. and Randall, D. A. (1994). A global 1^0 by 1^0 NDVI data set for climate Studies. Part 2 : The generation of global fields of terrestrial biophysical parameters from NDVI. *International Journal of R emote Sensing,* **15,** 3519 – 3545.

Sellers, P. J., Meeson, B. W., Hall, F. G., Asrar, G., Murphy, R. E., Schiffer, R. A., Bretherton, F. P., Dickenson, R. E., Ellingson, R. G., Field, C. B., Huemmrich, K.

F., Justice, C. O., Melack, J. M., Roulet, N. T., Schimel, D. S. and Try, P. D. (1995). Remote Sensing of the Land Surface for Studies of Global Change :   Models-Algorithms-Experiments. *Remote Sensing of Environment,* **51,** 3 – 26.

Senay, G. B. and Elliott, R. L. (2000). Combining AVHRR-NDVI and Landuse data to describe temporal and spatial dynamics of vegetation. *Forest Ecology and Management,* **128**, 83-91.

Serneels, S., Said, M. Y. and Lambin, E. F. (2001).   Land cover changes around a major east African wildlife reserve : the Mara Ecosystem (Kenya). *International Journal of Remote Sensing.* **22,** 3397 – 3420.

Shoshany, M., Kutiel, P. and Lavee, H. (1996).   Monitoring temporal vegetation cover changes in Mediterranean and arid ecosystems using a remote sensing technique : case study of the Judean Mountain and the Judean Desert. *Journal of Arid Environment,* **33,** 9-21.

Silviconsult Ltd. (1991).** Northern Nigeria Household energy study, *Silviconsult,* Bjarred, Sweden.

Singh, A. (1983).** Univariate Image Differencing for Forest change detection with Landsat. In *Remote Sensing for Rangeland Monitoring and Management.* Proceedings of an International conference in Silsoe, UK. 1983, Remote Sensing Society**,** 154-160.

Singh, A. and Harrison, A. (1985).** Standardized Principal Components. *International Journal of Remote Sensing,* **6,** 883- 896.

Singh, A. (1989).** Review article : Digital Change detection techniques using remotely-sensed data. *International Journal of Remote Sensing,* **10,** 989-1003.

Smith, P. M.,   Kalluri, S. N. V.,   Prince, S. D. and DeFries, R. (1997).   The NOAA/NASA Pathfinder AVHRR 8-Km Land Data set. *Photogrammetric Engineering and Remote Sensing,* **63,**   12 -13 and 27 - 32.

Soufflet, V., Tanré, D., Bégué, A., Podaire, A. and Deschamps, P. Y. (1991). Atmospheric effects on NOAA AVHRR data over Sahelian regions. *International Journal of Remote Sensing,* **12,** 1189 - 1203.

Soussan, J. G. and Millington, A. C. (1992). Forest, Woodlands and Deforestation. In Mannion A.M. and Bowlby S.R (Editors), *Environmental Issues in the 1990s*. John Wiley and Sons Ltd.

Srivastava, S. K., Jayaraman, V., Rao, N. P. P., Manikiam, B.   and Chandrasekhar, M. G. (1997).** Interlinkages of NOAA/AVHRR derived integrated NDVI to seasonal precipitation and transpiration in drylands tropics. *International Journal of Remote Sensing,* **18,** 2931- 2952.

Stone, T. A., Schlesinger, P., Houton, R. A. and Woodwell, G. M. (1994). A Map of the Vegetation of South America based on Satellite Imagery. *Photogrammetric Engineering and Remote Sensing,* **60,** 541 - 551.

Stowe, T. and Coulthard, N. (1990). The conservation of a Nigerian Wetlands : The Hadejia-Nguru Wetland Project. RSPB *Conservation Review,* **4,** 880 – 85.

Strahler, A. H., Woodcock C.E. and Smith, J.A (1986). On the Nature of Models in Remote Sensing. *Remote Sensing of the Environment,* **20,** 121-139.

Sutherst, R, W. (1998). Implications of global change and climatic variability for vector-borne diseases : generic approaches to impact assessments. *International Journal for Parasitology,* **28,** 935 - 945.

Tanré, D., Holben, B. N. and Kaufman, Y. J. (1992). Atmospheric correction algorithm for NOAA-AVHRR products : Theory and Application**.** *IEEE Transactions in GeoSciences and Remote Sensing,* **30**, 231 - 248.

Teillet, P. M. (1986). Image Correction for Radiometric effects in Remote Sensing**.** *International Journal of Remote Sensing*, **7**, 1637 - 1651.

Teillet, P. M., Slater, P. N., Ding, Y., Santer, R. P., Jackson, R. D. and Moran, M. S. (1990). Three methods for the absolute Calibration of the NOAA AVHRR Sensors In-Flight. *Remote Sensing of the Environment,* **31,** 105-120.

Teillet, P.M. and Staenz, K. (1992). Atmospheric effects due to topography on MODIS vegetation index data simulation from AVIRIS imagery over mountainous terrain. *Canadian Journal of Remote Sensing,* **18**, 283 – 291.

Teillet, P.M. and Holben, B.N. (1993). Towards operational radiometric calibration of NOAAA AVHRR imagery in the visible and infrared channels. *Canadian Journal of Remote Sensing,* **20**, 1 – 10.

Teillet, P.M., Staenz, K. and Williams, D. J. (1997). Effects of spectral, spatial and radiometric characteristics on remote sensing vegetation indices. *Remote Sensing of the Environment,* **61,** 139 - 149.

Thomas, D. H. L. and Adams, W. M. (1997). Space, Time and Sustainability in the Hadejia-Jama're Wetlands and the Komodugu Yobe Basin, Nigeria. *Transactions Institute of British Geographers,* **22,** 430-449.

Thorne, V., Coakeley, P., Grimes, D. and Dugdale, G. (2001). Comparison of TAMSAT and CPC rainfall estimates with raingauges, for Southern Africa. *International Journal of Remote Sensing,* **22**, 1951-1974.

Townshend, J. R. G. and Tucker, C. J. (1984). Objective Assessment of Advanced Very High Resolution Radiometer data for land cover mapping. *International Journal of Remote Sensing*, **5**, 497 – 504.

Townshend, J. R. G., Justice, C. O. and Kalb, V. T. (1987). Characterization and classification of South American Landcover types using Satellite data. *International Journal of Remote Sensing*, **8**, 1189 - 1207.

Townshend, J. R.G. and Tucker, C. J. (1990). The spatial variation of vegetation changes at very coarse scales. *International Journal of Remote Sensing*, **11**, 149-157.

Townshend, J. R.G., Justice, C. O., Li, W., Gurney, C. and McManus, J. (1991). Global Landcover Classification by Remote Sensing: Present Capabilities and Future Possibilities. *Remote Sensing of Environment*, **35**, 243 - 256.

Trevett, J.W. (1978). Vegetation Mapping of Nigeria from Radar. *Remote Sensing of the Environment,* **3,** 1919-1935.

Tucker, C.J., Holben, B. N. and Goff, T.E. (1984). Intensive Forest Clearing in Randonia, Brazil as detected by satellite remote sensing. *Remote Sensing of Environment*, **15**, 255 - 261.

Tucker, C.J., Galtin, J. A. and Schneider, S. R. (1984b). Monitoring Vegetation in the Nile Delta with NOAA-6 and NOAA-7 AVHRR Imagery. *Photogrammetric Engineering and Remote Sensing*, **50**, 53 - 61.

Tucker, C.J., Townshend, J.R.G. and Goff, T.E. (1985). African Land-cover classification using Satellite data. *Science,* **227,** 369-375.

Tucker, C.J., and Sellers, P. (1986). Satellite remote sensing of primary production. *International Journal of Remote Sensing*, **7**, 1395 - 1416.

Tucker, C.J., Newcomb, W.W., Los, S.O. and Prince, S.D. (1991a). Mean and Inter-Year Variation of growing-season Normalised Difference Vegetation Index for the Sahel 1981 - 1989. *International Journal of Remote Sensing*, **12**, 1133-1155.

Tucker, C. J., Dregne, H. E. and Newcomb, W. W. (1991b). Expansion and Contraction of the Sahara desert from 1980 to 1990. *Science,* **253,** 299-301.

Tucker, C. J., Newcomb, W. W. and Dregne, H. E. (1994). AVHRR data sets for determination of desert spatial extent. *International Journal of Remote Sensing*, **15**, 3547- 3565.

Turner, M. G. (1990). Spatial and Temporal analysis of landscape patterns. *Landscape Ecology*, **4,** 21 – 30.

Turner II, B. L. (1994). Local faces, Global flows : The role of land use and land cover in Global Environmental change. *Land Degradation and Rehabilitation,* **5,** 71-78.

UNCED (1992). Agenda 21 – Report of the United Nations Conference on Environment and Development, Rio de Janeiro, Brazil, 3 – 14 June 1992.

UNCED (1997). Report on the implementation of Agenda 21: Review and progress for Nigeria. *United Nations Commission on Sustainable Development, Fifth Session, New York, 7-25 April 1997. http:/www.un.org/dpcsd/earthsummit.html*

USGS (1998). United States Geological Survey**,** GTOPO30: Global 30 Arc-seconds digital elevation model. USGS EROS Data Centre, http://edcwww.cr.usgs.gov/landdaac/gotopo30/gotopo30.html.

Usoro, E. J. (2000). Akwa-Ibom State. In Mamman A.B., Oyebanji, J.O. and Petters, S.W. (Editors), *Nigeria : A People United, A Future Assured, Volume 2*, pp. 30 – 43*,* Federal Ministry of Information, Abuja, Nigeria, Gabumo Publishing Company Ltd, Calabar, Nigeria.

Vanderzee, D. and Ehrlich, D. (1995). Sensitivity to changes in sampling procedures and processing parameters when applied to AVHRR time-series NDVI data. *International Journal of Remote Sensing,* **16,** 673 - 686.

Verdin, J. P. (1996). Remote sensing of ephemeral water bodies in western Niger. *International Journal of Remote Sensing,* **17,** 733 - 748.

Vermote, E., Santer, R., Dechamps, P. Y. and Herman, M. (1992). In-Flight Calibration of large Field of View Sensors at Short Wavelengths Using Rayleigh Scattering. *International Journal of Remote Sensing,* **13,** 3409 - 3429.

Vermote, E. and Kaufman, Y. J. (1995). Absolute calibration of visible and near-infrared channels using ocean and cloud views. *International Journal of Remote Sensing,* **16,** 2317 – 2340

Vijayakumar, G., Parameswaran, K. and Rajan, R. (1998). Aerosols in the Atmospheric Boundary layer and its Association with surface wind speed at Coastal Site. *Journal of Atmospheric and Solar-Terrestrial Physics,* **60,** 1531 – 1542.

Viovy, N., Arono, O. and Belward, A. S. (1992). The Best Index Slope Extraction (BISE) : A method for reducing noise in NDVI time-series. *International Journal of Remote Sensing,* **13,** 1585 – 1590.

Wang, J., Price, K. P. and Rich, P. M. (2001). Spatial patterns of NDVI in response to precipitation and temperature in the central Great Plains. *International Journal of Remote Sensing,* **22,** 2827-3844.

Walker, R. and Homma, A. K. O. (1996). Land use and Land Cover dynamics in the Brazilian Amazon : An Overview, *Ecological Economics,* **18,** 67-80*.*

Weiler, R. A. and Stow, D. A. (1991). Spatial analysis of landcover patterns and corresponding remotely-sensed image brightness. *International Journal of Remote Sensing,* **12,** 2237-2257.

Weiss, E. Marsh, S. E. and Pfirman, E. S. (2001). Application of NOAA-AVHRR NDVI time-series data to assess changes in Saudi Arabia's rangelands. *International Journal of Remote Sensing,* **22,** 1005 - 1027.

Wen, C. G. and Tateishi, R. (2001). 30-Second degree grid land cover classification of Asia. *International Journal of Remote Sensing,* **22,** 3845 - 3854.

White, F. (1983). The Vegetation of Africa (Natural Resources Research Series, 20), Paris, UNESCO.

Wilkie, D. S. and Finn, J. T. (1996). Remote Sensing Imagery for Natural Resources Monitoring - A guide to First-time users. Columbia University Press, Chinchester.

Wood, W. B. (1990). Tropical deforestation : balancing regional development demands and global environmental concerns. *Global Environmental Change,* **1,** 23 – 41.

World Conservation Centre. (1992). Global Diversity *:Status of the Earth's Living Resources*. Chapman and Hall, London.

Yang, J. and Prince S. D. (2000). Remote sensing of Savanna vegetation changes in Eastern Zambia 1972-1989. *International Journal of Remote Sensing,* **21,** 301-322.

Yin, Z. and Williams, T. H. L. (1997). Obtaining Spatial and Temporal Vegetation Data from Landsat MSS and AVHRR/NOAA Satellite Images for a Hydrological Model. *Photogrammetric Engineering and Remote Sensing,* **63,** 69-77.

Young, S. S., and Wang, C. Y. (2001). Land-cover change analysis of China suing global-scale Pathfinder AVHRR Landcover (PAL) data, 1982-92. *International Journal of Remote Sensing.* **22,** 1457 – 1477.

Yuan, D. and Elvidge, C. D. (1993). Application of relative radiometric rectification procedure to Landsat data for use in change detection. *Proceedings of the Workshop on Atmospheric Correction of Landsat Imagery.* The Defence Landsat Program Office, Torrance, California, 29 June – 1 July, pp 162 – 166.

CURRICULUM VITAE

18th January, 1955	Born in Yelwa-Yauri, Kebbi State, Nigeria
1962-1964	Junior Primary School Sabon Gari Yelwa-Yauri
1965-1968	Senior Primary School Yelwa-Yauri
1969-1973	Government Secondary School Birnin-Kebbi (WASC)
1973-1974	Kaduna Polytechnic, Kaduna (Certificate in Cartography)
1974-1976	Assistant Cartographer, Ministry of Lands and Survey, Survey Division, North-Western State, Sokoto.
1976-1980	Kaduna Polytechnic, Kaduna (OND and HND)
1980/1981	National Youth Service (NYSC) at Ministry of Education Rivers State, Port Harcourt and Ministry of Education Kaduna State, Kaduna (GCSS Nkoro and GDSS Rigachikun)
1981-1982	Lecturer, Sokoto State Polytechnic, Birnin-Kebbi
1982-1984	Instructor/Cartographer, University of Sokoto
1984-1985	Postgraduate Diploma, University College Swansea, UK.
1985-1988	Instructor/Cartographer, Usmanu Danfodiyo University, Sokoto
1989-1992	BSc. Combine Honours (Geography/Cartography) Oxford Brookes University, Oxford, UK.
1992-1994	Postgraduate Studies in GIS, University of Leicester, UK.
1995-1998	Lecturer, Usmanu Danfodiyo University, Sokoto
1999-2003	PhD. in Environmental Science (Application of Remote Sensing and GIS to Vegetation Change Assessment), University of Stirling, Scotland, UK.
2004-	Lecturer in Applied Biogeography, Cartography, Remote Sensing and GIS, Usmanu Danfodiyo University, Sokoto